



**HAL**  
open science

# Role of DNA polymerase $\alpha$ phosphorylation in homologous recombination-related mechanisms in Mitosis and Meiosis

Juan de Dios Barba Tena

► **To cite this version:**

Juan de Dios Barba Tena. Role of DNA polymerase  $\alpha$  phosphorylation in homologous recombination-related mechanisms in Mitosis and Meiosis. Human health and pathology. Université de Montpellier, 2022. English. NNT : 2022UMONT079 . tel-04698653

**HAL Id: tel-04698653**

**<https://theses.hal.science/tel-04698653v1>**

Submitted on 16 Sep 2024

**HAL** is a multi-disciplinary open access archive for the deposit and dissemination of scientific research documents, whether they are published or not. The documents may come from teaching and research institutions in France or abroad, or from public or private research centers.

L'archive ouverte pluridisciplinaire **HAL**, est destinée au dépôt et à la diffusion de documents scientifiques de niveau recherche, publiés ou non, émanant des établissements d'enseignement et de recherche français ou étrangers, des laboratoires publics ou privés.

# THÈSE POUR OBTENIR LE GRADE DE DOCTEUR DE L'UNIVERSITÉ DE MONTPELLIER

En Biologie-Santé

École doctorale Sciences Chimique et Biologiques pour la Santé (CBS2)  
Unité de recherche Institut de Génétique Moléculaire de Montpellier (IGMM)

## Role of DNA Polymerase $\alpha$ phosphorylation in homologous recombination-related mechanisms in Mitosis and Meiosis

Présentée par Juan de Dios BARBA TENA  
Le 13 Décembre 2022

Sous la direction de Etienne SCHWOB

Devant le jury composé de

Dr. Armelle LENGRONNE, Institut de Génétique Humaine, Montpellier

Dr. Sarah LAMBERT, Institut Curie, Paris

Dr. Jose Antonio TERCERO ORDUÑA, Centro de Biología Molecular Severo Ochoa, Madrid

Dr. Aurèle PIAZZA, Laboratory of Biology and Modeling of the Cell, Lyon

Dr. Nicolas TALAREK, Institut de Génétique Moléculaire de Montpellier, Montpellier

Dr. Etienne SCHWOB, Institut de Génétique Moléculaire de Montpellier, Montpellier

Présidente/Examinatrice

Rapportrice

Rapporteur

Examineur

Co-Encadrant de thèse

Directeur de thèse



UNIVERSITÉ  
DE MONTPELLIER





## **Acknowledgments**

First, I would like to thank my thesis jury members: Armelle Lengronne, Sarah Lambert, José Antonio Tercero and Aurèle Piazza for accepting to evaluate this work. Importantly, I would also like to thank Gerard Mazòn and Thomas Robert for being part of my Thesis Committee for 3 years, especially for the suggestions and comments, both scientific and personal.

For my thesis directors: Etienne Schwob and Nicolas Talarek. Thank you both giving me the opportunity to perform this Ph.D. and to contribute to my formation as a scientist. Etienne, even if you are 120% of your time IGMM director (and I know you don't like that), you always had time for me when I needed it and you trust me as a scientist. This is something I truly appreciate and I hope I met your expectations. Nico, you were the most important pillar during my thesis and the major reason I managed to get to this point. Your daily guidance, your patience with me (even when I say BS) and your expertise shaped me in what I am, even if you drove me fuming angry sometimes. I consider you as my scientific mentor, either you like it or not, and I am happy, honored and thankful you took that role.

This work could not have been possible without the support of the Schwob Lab members, present and past. Thank you Baraah for bringing shine to the tough days, for driving me crazy when I needed to and for being someone I could talk freely. Thank you, Vincent, for listening all the times I drop dead in your office complaining about science, society or movies, but specially for all the "BS time" we had together. To Isabelle, Maxime, Sébastien, Marjorie and Vjeko thank you for all the good moments we had together, for all the comments, discussions and for being always nice to me (this is something lacking recently).

To all the friends that I met during this time: Jacinthe, Jona, Monica, Fatimat, Fabie, Mathias, thank you. My special thanks to the Spanish gang: Dr. Gero, Nuria, Yolanda, Clara, Pedro, apart from being friends, you forced me to do sport (which I need). To my special "bois": David, Igor and Adham, you are the closest people I had in Montpellier and you help me discover a lot of new things and to enjoy life. I hope I will manage to keep our friendship and our expectations for a truly long time. And for my friends that were always there: Jesus, Jose, Gaby y Sergio, thanks for supporting me.

To Lorene, the most influential person during these years. Thank you for being there, for trusting me and for supporting me. To guide me when I need it to, to make me happy and to help me when I was down. This thesis is as mine as it is yours, and no matter what happens, you are and you will be one of the most important people in my life.

Finally, to my family. I have been away for 4 years, and distance is tough. I miss you with all my heart, but I hope this journey serves to make you proud of what I have become. Para papa, mama, Rodri y Ale; este trabajo va dedicado a vosotros.

## Résumé

L'instabilité du génome est une épée à double tranchant pour les cellules, car c'est la principale force de l'évolution mais aussi une caractéristique des maladies humaines comme le cancer. Pour cette raison, les cellules ont des mécanismes finement régulés qui favorisent de faibles doses d'instabilité du génome. Beaucoup d'entre eux reposent sur la recombinaison homologue (RH), mais leur raison d'être et leur machinerie moléculaire sont encore à découvrir.

Des travaux pionniers du laboratoire ont démontré que les cellules peuvent entrer en mitose malgré une réplication incomplète de leur ADN, ce qui conduit à la survie des cellules mais aussi à l'augmentation de l'instabilité du génome. Dans ce travail, nous avons étudié les conséquences de la phase S prolongée dans les cellules et démontré que, dans ces conditions, les cellules s'arrêtent en début de mitose et effectuent une synthèse d'ADN mitotique (MiDAS) par un mécanisme lié à la RH pour survivre. Fait important, nous avons découvert un acteur important de ce processus, la phosphorylation de l'ADN polymérase  $\alpha$ . Cette phosphorylation est essentielle à la survie des cellules à phase S allongée, en provoquant l'éviction de Pol $\alpha$  de la chromatine et de la dissociation du réplisome. Ainsi, nous identifions la phosphorylation de Pol $\alpha$  comme élément clé du remodelage du réplisome permettant d'initier efficacement MiDAS. Fait important, nous avons également démontré que la phosphorylation de Pol $\alpha$  est nécessaire pour une méiose efficace, un autre mécanisme dépendant des RH, suggérant ainsi un rôle général de la phosphorylation de Pol $\alpha$  dans la recombinaison homologue.

Nous pensons qu'une meilleure compréhension des mécanismes qui favorisent l'instabilité du génome aidera non seulement à mieux comprendre l'évolution du génome, mais aussi pour lutter contre les situations qui exploitent ces mécanismes, comme les cellules cancéreuses.

**Mots clés** : réplication de l'ADN, recombinaison homologue, phosphorylation, ADN polymérase  $\alpha$ , méiose, instabilité du génome.

## **Abstract**

Genome instability is a double edge sword for cells, as it is the main force of evolution but also a hallmark for human diseases like cancer. For this reason, cells have finely regulated mechanisms that promote low doses of genome instability. Many of them rely on homologous recombination (HR), but their specific purposes and molecular machinery are still under investigation.

Seminal work from the lab demonstrated that cells can enter mitosis with incomplete DNA replication, and this leads to cell survival but also to increased genome instability. In this work, we studied the consequences of an extended S phase in cells and demonstrated that, in these conditions, cells arrest early in mitosis to perform mitotic DNA synthesis (MiDAS) via HR-related mechanism to survive. Importantly, we discovered an important player for this process, DNA polymerase  $\alpha$  phosphorylation. This phosphorylation is essential for survival of cells with extended S phase by promoting the removal of Pol $\alpha$  from chromatin and disruption of its binding to the replisome. Thus, we point Pol $\alpha$  phosphorylation as part of a mechanism of replisome remodeling needed for efficient initiation of MiDAS. Importantly, we also demonstrated that Pol $\alpha$  phosphorylation is required for productive meiosis, another HR-dependent mechanism, thus pointing at a general role of Pol $\alpha$  phosphorylation in homologous recombination.

We believe that a better understanding of the underlying mechanisms that promote genome instability will help not only to better understand genome evolution, but also for situations that exploit these mechanisms like cancer cells.

**Keywords:** DNA replication, Homologous Recombination, Phosphorylation, DNA Polymerase  $\alpha$ , Meiosis, Genome Instability.

<b>Abbreviations</b> .....	12
<b>Preface</b> .....	13
<b>Chapter i. Introduction</b> .....	16
<b>1. Cell cycle: regulation and link with genome instability</b> .....	17
1.1. What is the cell cycle? .....	17
1.2. Cyclin-dependent kinases (CDKs), the master regulators of cell cycle progression .....	19
1.3. Monitoring cell cycle: phases and checkpoints .....	21
1.3.1. G1 phase and START .....	21
1.3.2. S phase and intra-S checkpoint .....	23
1.3.3. Mitosis and Spindle Assembly Checkpoint (SAC) .....	27
1.4. Cell cycle deregulation and genome instability .....	28
<b>2. Mechanisms of DNA replication in Eukaryotes</b> .....	30
2.1. Preparing for synthesis: Origin licensing .....	30
2.2. Firing of origins: DNA replication initiation .....	33
2.3. Anatomy of a replication fork .....	35
2.3.1. Helicase activity .....	35
2.3.2. DNA synthesis activity .....	35
2.3.3. Scaffolding activity .....	36
2.3.4. DNA Polymerase $\alpha$ .....	37
2.4. Packing up replication: Termination and fork disassembly .....	40
<b>3. Controlling the damage: Mechanisms of DNA Damage Repair</b> .....	42
3.1. Sources and types of DNA damages and replication stress .....	42
3.2. How cells protect replication forks .....	43
3.3. Homologous Recombination as a fork restart mechanism .....	46
3.3.1. Generalities of homologous recombination .....	46
3.3.2. Break-induced replication as a fork restart mechanism .....	48
3.4. MiDAS, a new DNA synthesis mechanism during Mitosis .....	50
<b>4. Meiosis, the basis of sexual reproduction</b> .....	52
4.1. Meiotic commitment, main controllers and meiotic cyclins .....	52
4.2. Prophase I: Programmed damage and repair .....	54
4.2.1. Connection between meiotic replication and DSBs formation .....	54
4.2.2. Molecular machinery of DSB formation and recombination .....	56
4.2.3. Regulation of Prophase I and recombination .....	57

<b>Chapter ii. Consequences of extended S phase in <i>Saccharomyces cerevisiae</i> cells and role of DNA Polymerase <math>\alpha</math> phosphorylation</b> .....	60
1.1. Origin under-licensing extends S phase and promotes metaphase arrest and MiDAS .....	62
1.2. Extended S phase activates the DDR checkpoint and promotes homologous recombination upon mitotic entry.....	66
1.3. Candidate substrates of M-CDK in extended S phase: DNA Polymerase $\alpha$ .....	69
1.4. DNA Polymerase $\alpha$ mitotic phosphorylation is required for DDR activation.....	74
1.5. MiDAS in <i>cdc6-1</i> cells requires DNA Polymerase $\alpha$ phosphorylation and canonical BIR components.....	76
1.6. Pol $\alpha$ CDK phosphorylation is required to maintain a metaphase arrest in conditions of extended S phase .....	78
1.7. Slowing down mitotic exit ectopically rescues <i>cdc6-1 pola-cdk</i> lethality.....	80
1.8. Pol $\alpha$ phosphorylation controls its association to chromatin and interaction with the replisome .....	82
1.9. Summary of results Project II.....	85
1.10. Discussion Project I.....	86
<b>Chapter iii: Characterization and role of DNA polymerase <math>\alpha</math> phosphorylation in <i>Saccharomyces cerevisiae</i> meiosis</b> .....	96
1.1. DNA Pol $\alpha$ phosphomutants are deficient in meiosis in the W303 background .....	98
1.2. Pol $\alpha$ Cdk phosphorylation is not required for sporulation in SK1 background.....	99
1.3. Pol $\alpha$ is phosphorylated at CDK and non-CDK sites in meiosis .....	102
1.4. Mutating 45 Pol $\alpha$ phosphorylation sites leads to a delay in meiotic progression.....	106
1.5. Pol $\alpha$ -45A is proficient for meiotic crossover formation.....	108
1.6. Summary of results Project II.....	112
1.7. Discussion Project II.....	113
<b>Chapter iv: Conclusions</b> .....	119
<b>Chapter v: Methods</b> .....	122
1. List of strains .....	123
2. Yeast cell culture and related methods .....	127
3. Molecular Biology techniques.....	133
4. Microscopy based techniques.....	143
<b>Chapter vi: Bibliography</b> .....	145
<b>Chapter vii: Determination of S-Phase Duration Using 5-Ethynyl-2'-deoxyuridine Incorporation in <i>Saccharomyces cerevisiae</i> (Publication)</b> .....	178



## **List of figures and tables**

<b>Figure i.1.</b> Eukaryotic cell cycle.....	17
<b>Figure i.2.</b> Levels of CDK activity and corresponding expression of cyclins in <i>S. cerevisiae</i> ...	20
<b>Figure i.3.</b> START checkpoint and S phase entry in <i>S. cerevisiae</i> .....	22
<b>Figure i.4.</b> Activation of DDR checkpoint during S phase via Mec1 .....	26
<b>Figure i.5.</b> Origin licensing involves the loading of two MCM components facing each other. ....	32
<b>Figure i.6.</b> Replication profile of chromosome VI in <i>S. cerevisiae</i> . .....	34
<b>Figure i.7.</b> Composition of the replication fork in <i>S. cerevisiae</i> . .....	37
<b>Figure i.9.</b> Schematic representation of Pol $\alpha$ complex priming DNA.....	39
<b>Figure i.10.</b> Ubiquitination and unloading of CMG complex from terminated replication forks or forks that entered mitosis. ....	41
<b>Figure i.11.</b> Types of Replication Fork Barriers (RFB).....	43
<b>Figure i.12.</b> Examples of stalled fork processing in eukaryotes .....	45
<b>Figure i.13.</b> Schematic of homologous recombination pathway.....	47
<b>Figure i.14.</b> Schematic of Rad51-dependent and independent Break-Induced Replication upon a single-ended DSB. ....	49
<b>Figure i.15.</b> Levels of CDK activity and corresponding expression of cyclins/regulators in <i>S.</i> <i>cerevisiae</i> during meiosis .....	53
<b>Figure i.16.</b> Connection between pre-meiotic replication and meiotic recombination.....	55
<b>Figure i.17.</b> Molecular components of the Meiotic DSB formation machinery and chromosomal recombination axes .....	56
<b>Figure i.18.</b> Crossover and Non-crossover formation upon meiotic recombination.....	57
<b>Figure i.19.</b> Schematic of Prophase I regulation and progression .....	59
<b>Figure ii.1.</b> Decrease in origin licensing extends S phase, promoting metaphase arrest and MiDAS .....	65
<b>Figure ii.Supp1.</b> MiDAS decays during metaphase arrest .....	65
<b>Figure ii.2.</b> Extended S phase activates DDR checkpoint and promotes homologous recombination upon mitotic entry.....	68
<b>Figure ii.3.</b> DNA Polymerase $\alpha$ M-CDK phosphorylation is essential for the survival of cells with extended S phase .....	72
<b>Figure ii.Supp2.</b> The pol $\alpha$ -cdk mutant has no phenotype in normal cell cycle conditions .....	73
<b>Figure ii.4.</b> DNA Pol $\alpha$ CDK mitotic phosphorylation activates the DDR checkpoint in cells with extended S phase. ....	75
<b>Figure ii.5.</b> Pol $\alpha$ CDK phosphorylation is required for efficient MiDAS .....	77
<b>Figure ii.6.</b> Pol $\alpha$ CDK phosphorylation is required for a prolonged metaphase arrest.....	79
<b>Figure ii.7.</b> Artificial mitotic extension rescues pol $\alpha$ -cdk lethality upon extended S phase.....	81
<b>Figure ii.8.</b> Pol $\alpha$ eviction from chromatin and interactors depend on its phosphorylation status	84
<b>Figure ii.9.</b> The SAC is not required for survival of <i>cdc6-1</i> mutant.....	87
<b>Figure ii.10.</b> MiDAS triggers chromosome translocations .....	91
<b>Figure ii.11.</b> Replication forks are remodeled upon mitotic entry, allowing DDR activation and MiDAS .....	94

<b>Figure iii.1.</b> Pol $\alpha$ CDK phosphorylation is required for meiosis in the W303 background.....	<b>99</b>
<b>Figure iii.2.</b> Pol $\alpha$ CDK phosphorylation requirement for meiosis in the SK1 background is meiosis induction-dependent. ....	<b>101</b>
<b>Figure iii.3.</b> Pol $\alpha$ is phosphorylated during meiosis at CDK and non-CDK sites. ....	<b>105</b>
<b>Figure iii.4.</b> Extensive mutation of phosphorylation sites in Pol $\alpha$ delays meiotic completion in SK1 .....	<b>107</b>
<b>Figure iii.5.</b> Pol $\alpha$ phosphorylation is not required for meiotic CO formation .....	<b>111</b>
<b>Figure iii.6.</b> Pol12-23A displays a mobility shift in western blot. ....	<b>115</b>
<b>Figure iii.7.</b> S680 and S949 phosphorylated residues in Pol1 are located in the contact point with DNA. ....	<b>116</b>
<b>Figure iv.1.</b> Genetic variability is a normal process in cells.....	<b>120</b>
<b>Figure v.1.</b> Representative images of CFU assay in <i>cdc6-1</i> mutants.....	<b>129</b>
<b>Figure v.2.</b> Pol1-3PK immunoprecipitation and elution with V5 peptide .....	<b>139</b>
<b>Figure v.3.</b> Hawaii Plots of Pol1 and Pol1-cdk13A interactomes in S phase and Mitosis .....	<b>142</b>
<b>Figure v.4.</b> Workflow of Imagestream analysis to identify MiDAS cells. ....	<b>144</b>
<b>Table ii.1.</b> Identified mitotic phosphorylated sites in both Pol1 and Pol12 proteins .....	<b>71</b>
<b>Table iii.1.</b> Identified meiotic phosphorylated sites in both Pol1 and Pol12 proteins.....	<b>105</b>
<b>Table iii.2.</b> Genetic divergence between W303 and SK1, compared to S288C.....	<b>114</b>
<b>Table iv.1.</b> List of strains used in this thesis .....	<b>126</b>

## Abbreviations

<p>ACS – <u>A</u>RS <u>C</u>onsensus <u>S</u>equence  ADP - <u>A</u>denosine <u>D</u>iphosphate  APC – <u>A</u>naphase <u>P</u>romoting <u>C</u>omplex  APC/C - <u>A</u>naphase <u>P</u>romoting  <u>C</u>omplex/<u>C</u>yclosome  ARS – <u>A</u>utonomous <u>R</u>eplicating <u>S</u>equence  ATM - <u>A</u>taxia <u>T</u>elangiectasia <u>M</u>utated  ATP - <u>A</u>denosine <u>T</u>riphosphate  ATR - <u>A</u>taxia <u>T</u>elangiectasia <u>R</u>ad3-related  BIR – <u>B</u>reak-<u>I</u>nduced <u>R</u>eplication  BrdU - <u>B</u>romodeoxyuridine  CDK – <u>C</u>yclin <u>D</u>ependent <u>K</u>inase  CFS – <u>C</u>ommon <u>F</u>ragile <u>S</u>ite  CMG – <u>C</u>dc45-<u>M</u>CM-<u>G</u>INS complex  CO – <u>C</u>rossover  CryoEM - <u>C</u>ryogenic <u>E</u>lectron <u>M</u>icroscopy  CST – <u>C</u>dc13-<u>S</u>tn1-<u>T</u>en1  DDC – <u>D</u>NA <u>D</u>amage <u>C</u>heckpoint  DDK – <u>D</u>bf4-<u>D</u>ependent <u>K</u>inase  DDR – <u>D</u>NA <u>D</u>amage <u>R</u>esponse  DNA - <u>D</u>eoxyribonucleic <u>A</u>cid  DRC – <u>D</u>NA <u>R</u>eplication <u>C</u>heckpoint  DSB – <u>D</u>ouble <u>S</u>trand <u>B</u>reak  DSBR – <u>D</u>ouble <u>S</u>trand <u>B</u>reak <u>R</u>epair  dHJ – <u>D</u>ouble <u>H</u>olliday <u>J</u>unction  dNTP – <u>D</u>eoxynucleoside <u>T</u>riphosphate  dsDNA - <u>D</u>ouble <u>S</u>tranded <u>D</u>NA  EdU - 5-ethynyl-2'-deoxyuridine  FPC – <u>F</u>ork <u>P</u>rotection <u>C</u>omplex  GCR – <u>G</u>ross <u>C</u>hromosome <u>R</u>earrangements  GINS – (<u>G</u>o-<u>I</u>chi-<u>N</u>i-<u>S</u>an) Psf1,2,3 Sld5  HJ – <u>H</u>olliday <u>J</u>unction  HR – <u>H</u>omologous <u>R</u>ecombination  HU – <u>H</u>ydroxyurea</p>	<p>LOH – <u>L</u>oss <u>O</u>f <u>H</u>eterozygosity  MBF – <u>M</u>CB-<u>B</u>inding <u>F</u>actor  MCM – <u>M</u>inichromosome <u>M</u>aintenance  MCN – <u>M</u>eiotic <u>C</u>heckpoint <u>N</u>etwork  MEN – <u>M</u>itotic <u>E</u>xit <u>N</u>etwork  MiDAS – <u>M</u>itotic <u>D</u>NA <u>S</u>ynthesis  MMBIR – <u>M</u>icrohomology <u>B</u>reak-<u>I</u>nduced  <u>R</u>eplication  MMS – <u>M</u>ethyl-<u>m</u>ethanosulphonate  MRX – <u>M</u>re11 – <u>R</u>ad50 - <u>X</u>rs2  mESC – <u>M</u>ouse <u>E</u>mbryonic <u>S</u>tem <u>C</u>ell  NCO – <u>N</u>on-<u>C</u>rossover  NTD – <u>N</u>-<u>t</u>erminal <u>d</u>omain  OB – <u>O</u>ligonucleotide <u>B</u>inding  ORC – <u>O</u>rigin <u>R</u>ecognition <u>C</u>omplex  PCNA – <u>P</u>roliferating <u>C</u>ell <u>N</u>uclear <u>A</u>ntigen  PDE – <u>P</u>hosphodiesterase  Pol – <u>P</u>olymerase  RC – <u>R</u>eplication <u>C</u>omplex  RFB – <u>R</u>eplication <u>F</u>ork <u>B</u>arrier  RNA - <u>R</u>ibonucleic <u>a</u>cid  RPA – Rfa1-Rfa2-Rfa3 complex  rDNA – <u>R</u>ibosomal <u>D</u>NA  SAC – <u>S</u>pindle <u>A</u>ssembly <u>C</u>heckpoint  SBF – <u>S</u>CB-<u>B</u>inding <u>F</u>actor  SC – <u>S</u>ynthetic <u>C</u>omplete  SCF – <u>S</u>kp-<u>C</u>ullin- <u>F</u> Box complex  SDSA – <u>S</u>ynthesis-<u>d</u>ependent <u>S</u>trand  <u>A</u>nnealing  ssDNA – <u>S</u>ingle <u>S</u>tranded <u>D</u>NA  WT – <u>W</u>ild <u>T</u>ype  YPD – <u>Y</u>east <u>P</u>eptone <u>D</u>extrose  9-1-1 complex – Ddc1-Mec1-Rad17</p>
---	---

## **Preface**

The objective of every cell is to become two. In order to do so, cells undergo cell cycle, a process that ensures that the genome is precisely copied and transmitted to the two daughter cells. Because DNA is the element that confers identity to every cell, the cell cycle is a tightly-regulated process equipped with several DNA surveillance mechanisms. However, cell cycle regulation has also embedded mechanisms that tolerate and even promote low doses of genome instability, allowing genomic plasticity as a mechanism of evolution/adaptation. De-regulation of cell cycle control mechanisms or hyper-activity of DNA instability promoting mechanisms may lead to catastrophic events, like cell malignancy.

During this thesis, directed by Dr. Etienne Schwob and supervised by Dr. Nicolas Talarek, I investigated two different biological situations that involve genome instability in cells: Mitotic DNA Synthesis due to extended S phase, and Meiosis. Also, we focused the majority of our work in DNA Pol $\alpha$  phosphorylation, which we found to be an important player in the regulation of both aforementioned mechanisms. My thesis manuscript is organized in 7 chapters:

**Chapter i. Introduction**

**Chapter ii. Project 1. Results and Discussion**

**Chapter ii. Project 2. Results and Discussion**

**Chapter iv. Conclusions**

**Chapter v. Methods**

**Chapter vi. Bibliography**

**Chapter vii. Determination of S-Phase Duration Using 5-Ethynyl-2'-deoxyuridine Incorporation in *Saccharomyces cerevisiae* (Publication)**

**Project 1: Consequences of an extended S phase in *Saccharomyces cerevisiae* cells and role of mitotic DNA polymerase  $\alpha$  phosphorylation.**

It has been recently shown that slow-replicating cells can finish genome duplication during mitosis using a recombination-dependent replication system (MiDAS). Recombination-dependent DNA synthesis has been extensively described in bacteria and viruses, but it is still poorly understood in eukaryotes. However, MiDAS has been discovered in mammals and proposed as a potential source of genome instability in cancer cells. Using an inducible genetic system to reduce origin licensing to slow down DNA synthesis without interfering with fork progression rates, we describe the physiological response to incomplete DNA replication. Interestingly, we found out that M-CDK activation is a trigger for MiDAS, and that DNA polymerase  $\alpha$  is a substrate of M-CDK critical for the proper execution of this mechanism. This project summarizes the data from several members of my laboratory and myself about how cells perform MiDAS and how DNA Pol  $\alpha$  phosphorylation is required during this process.

**Project 2: Characterization and importance of DNA polymerase  $\alpha$  phosphorylation in meiosis using *Saccharomyces cerevisiae*.**

Concurrently, we observed that DNA Pol $\alpha$  phosphorylation has an impact on meiosis. Mitosis and meiosis are profoundly different cell divisions in terms of cell cycle regulation but they share similar recombination machineries. Our DNA Pol  $\alpha$  phosphorylation mutants have defective meiosis in a DSB-dependent manner, thus pointing at a general role of DNA Pol  $\alpha$  in recombination. During this project, I characterized the phosphorylation of DNA polymerase  $\alpha$  during the meiotic program and its requirement for meiosis. Because meiosis is a well-characterized process with established assays to monitor every step of the recombination pathway, I used meiosis as a model to pinpoint the function of Pol  $\alpha$  phosphorylation.

**Publication: Determination of S-Phase Duration Using 5-Ethynyl-2'-deoxyuridine Incorporation in *Saccharomyces cerevisiae* (October 21, 2022 doi: 10.3791/64490)**

Eukaryotic DNA replication is a highly regulated process that ensures that the genetic blueprint of a cell is correctly duplicated prior to chromosome segregation. As DNA synthesis defects underlie chromosome rearrangements, monitoring DNA replication has become essential to understand the basis of genome instability. *Saccharomyces cerevisiae* is a classical model to study cell cycle regulation, but key DNA replication parameters, such as the fraction of cells in the S phase or the S-phase duration, are still difficult to determine. This protocol uses short and non-toxic pulses of 5-ethynyl-2'-deoxyuridine (EdU), a thymidine analog, in engineered TK-hENT1 yeast cells, followed by its detection by Click reaction to allow the visualization and quantification of DNA replication with high spatial and temporal resolution at both the single-cell and population levels by microscopy and flow cytometry. This method may identify previously overlooked defects in the S phase and cell cycle progression of yeast mutants, thereby allowing the characterization of new players essential for ensuring genome stability.

# **Chapter i. Introduction**

# 1. Cell cycle: regulation and link with genome instability

## 1.1. What is the cell cycle?

The cell cycle is a concatenated series of molecular events that culminates with the generation of two daughter cells, genetically identical between themselves and to the mother cell. It consists in two major parts; Interphase, where genetic material is duplicated, and Mitosis, where the genetic and cytoplasmic material are equally segregated into two cells (Mitchinson J.M. 1971, **Figure i.1**). Interphase is the longest phase and formerly called the “resting phase”; cells synthesize most of their metabolites, prepare for cell division and perform other cell specific functions. It comprises 3 phases: G<sub>1</sub>, S phase and G<sub>2</sub>. In counterpart, Mitosis is a much shorter phase and comprises 4 phases: Prophase, Metaphase, Anaphase and Telophase. During this phase, metabolic and synthesis activity are low, but cells undergo drastic changes like chromosome condensation or the formation of supramolecular structures such as the mitotic spindle or the cytokinetic contractile ring.

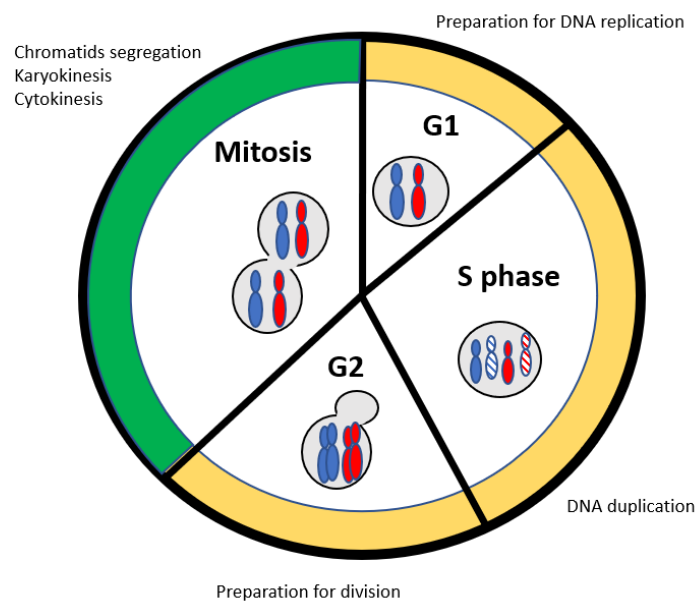


*Figure i.1. Eukaryotic cell cycle. The cell cycle is divided in two parts: Interphase (Yellow) that ensures proper genome duplication and Mitosis (Green) that equally segregates genetic material into two daughter cells.*

The cell cycle program has been proven to be not as rigid as originally described, displaying plasticity that allows for environmental adaptation. One classical example is asymmetric cell division, which promotes the unequal segregation of cytoplasmic and epigenetic components between daughter and mother cells, essential for cell differentiation (Conklin E.G. 1905, reviewed in Knoblich J.A. 2008). Another important level of fluctuation is the control of cell cycle duration and its phases, being readily different between species, and modulable depending on the inner and outer cellular context. One well known example is response to nutrients or temperature, WT haploid budding yeast has an estimated doubling time of 90 minutes in rich complete medium (YPD) and 140 minutes in Synthetic Complete medium (Sherman F., 2002).

In certain conditions, cells can even exit the cycling program and remain in no-growth conditions. G<sub>0</sub> phase is a non-replicative state that cells can enter permanently (senescence and differentiated cells) or temporally (quiescent cells or yeast spores) to accomplish different functions, like programmed cell death, advanced specialization or cell protection (Cheung T.H and Rando T.A. 2013; Storer M. *et al.*, 2013).

Every cell cycle phase requires the adequate and ordered execution of important molecular events; thus, cells have developed mechanisms of control (cell cycle dependent kinases – CDKs) and surveillance (Checkpoints). These mechanisms are specific of every phase and monitor different events of the cell, preventing cell cycle progression if certain requirements are not accomplished. Deregulation of these mechanisms of control and surveillance can derive into cellular catastrophes, like cell death via apoptosis or cell transformation, and they are usually linked to genome instability.

## **1.2. Cyclin-dependent kinases (CDKs), the master regulators of cell cycle progression**

Cyclin dependent kinases (CDKs) are the main regulator kinases of cell cycle. They consist of two subunits, a cyclin and a protein kinase, that will phosphorylate target proteins in a cell cycle-dependent manner.

Discovered in the 1970's (Hartwell L. *et al.*, 1974; Nurse P. *et al.*, 1976), CDKs belong to CMGC group of kinases based on the sequence of their kinase domain, alongside MAPK and DYRK kinases (Manning G. *et al.*, 2002). In *S. cerevisiae*, there is only one CDK (Cdc28 or Cdk1) that governs the entirety of cell cycle while in other eukaryotes more than one CDK is present, with 4 that control the cell cycle in mammals (Cdk1, Cdk2, Cdk4 and Cdk6; Lim S. and Kaldis P., 2013). Other CDKs exist in yeast (4 more) and mammals (12 more), but they are involved in other processes. CDKs are proline-directed serine/threonine-protein kinases, containing a hydrophobic pocket that accommodates a proline in +1 position (defining a minimal consensus site as S/T-P). However, there has been reports of non-consensus CDK phosphorylation that do not require a proline in +1 position (Satterwhite L.L. *et al.*, 1992; Kusubata M. *et al.*, 1993; Suzuki K. *et al.*, 2015). Therefore, it is proposed that S/T-P are the preferred substrate sequences for this kinase, but possibly not the only ones (Örd M. *et al.*, 2020).

CDK activity and target specificity change through cell division due to its association with cyclins (**Figure i.2**). Cyclins are proteins whose concentration varies in a cyclical fashion during cell cycle (Evans T. *et al.*, 1983). As for CDKs, different organisms have a different number of cyclins: *S. cerevisiae* has 20 cyclins, with 9 involved in cell cycle regulation, while in humans over 30 proteins are considered cyclins, only 10 involved in cell cycle regulation (Satyanarayana A. and Kaldis P. 2009; Lim S. and Kaldis P. 2013). For simplicity, cyclins are usually named depending on which phase of the cell cycle they are expressed and control (**Figure i.2**).

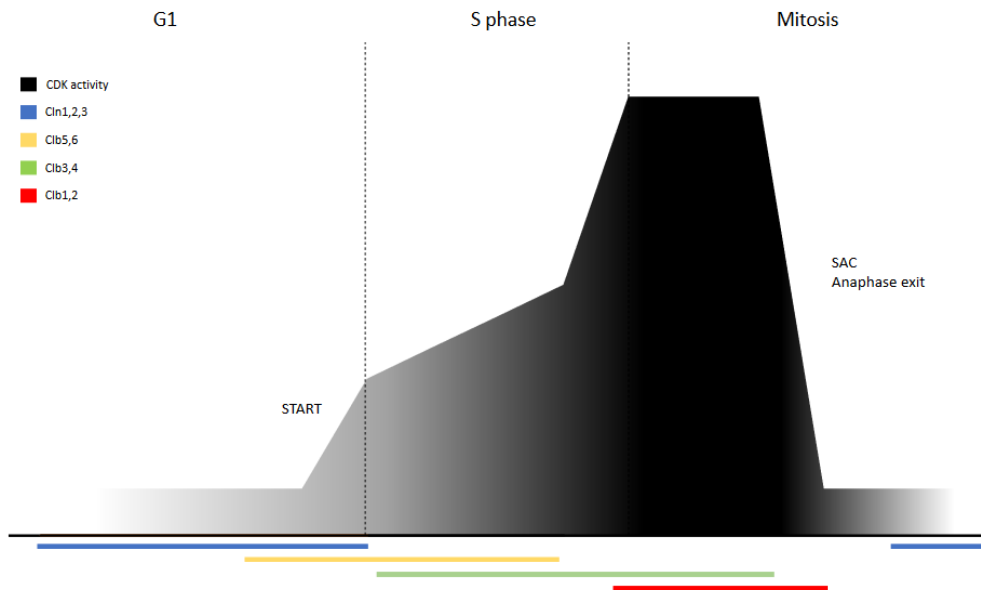


**Figure i.2. Levels of CDK activity and corresponding expression of cyclins in *S. cerevisiae*.** CDK activity (Black) increases prior to every phase transition, and decays at anaphase onset. G1 cyclins: *Cln1,2,3* (Blue). S cyclins: *Clb5,6* (Yellow). G2/M cyclins: *Clb3,4* (Green). M cyclins: *Clb1,2* (Red).

CDKs are not the only kinases that exert control over cell cycle. They work in collaboration with other kinases like DDK (Dbf4-dependent kinase – Cdc7, important for origin firing), Plk (Polo-like kinase – Cdc5, important in mitosis regulation) or Bub1 (budding inhibited by benzimidazole, important in Spindle Assembly Checkpoint). The coordinate action of CDK and other kinases allows an accurate regulation of cell cycle, mainly in the transition between phases and in checkpoint activation and amplification.

### **1.3. Monitoring cell cycle: phases and checkpoints**

Checkpoints are surveillance and control mechanisms that monitor the order, integrity and fidelity of major events of the cell cycle (Hartwell L.H. and Weinert T.A., 1989; Barnum K. and O’Connell M., 2014). Every cell cycle phase has a checkpoint associated to it, supervising different molecular events and differing in their molecular pathways. However, the majority of these mechanisms control cell cycle progression by direct modulation of Cyclin-CDK activity. Here, I present the main cell cycle checkpoints and how they modulate cell cycle progression.

#### **1.3.1. G<sub>1</sub> phase and START**

G<sub>1</sub> phase (Gap 1) is considered the first cell cycle phase after mitosis and the point of commitment to cell division. During G<sub>1</sub>, budding yeast cells prepare for DNA synthesis by licensing origins (explained in Chapter 2.1.), synthesizing metabolites and increasing in cell size. START, also known as “restriction point” in mammals, is the first checkpoint prior to DNA replication and monitors that cells have reached a critical cell size before S phase entry (Hartwell L.H. *et al.*, 1970). The main regulators of START in *S. cerevisiae* are *CLN3*, the earliest cell cycle cyclin gene, and *WHI5*, a transcriptional regulator gene (Richardson H.E. *et al.*, 1989; Jorgensen P. *et al.*, 2002).

Whi5 is a transcriptional repressor that associates with SBF (SCB-Binding Factor) and MBF (MCB-Binding Factor) transcription factors, preventing expression of many G<sub>1</sub> genes, including *CLN1* and *CLN2* cyclins (de Bruin R. *et al.*, 2004). Both *CLN3* and *WHI5* expression occur in telophase, but Cln3 concentration has been proposed to be inversely proportional to G<sub>1</sub> length and the signal for cell cycle entry (Liu X. *et al.*, 2015). When sufficient Cln3 accumulates, it phosphorylates Whi5 and consequently promotes its nuclear export, liberating SBF/MBF and allowing G<sub>1</sub> genes to be transcribed (Iyer V.R. *et al.*, 2001). Expression of *CLN1* and *CLN2* further contributes to Whi5 nuclear export, generating a positive feedback loop for irreversible cell cycle commitment (**Figure i.3**).

Another important regulator is the S-phase CDK inhibitor Sic1, present in the nucleus from telophase to late G<sub>1</sub> (Toyn J.H. *et al.*, 1997). It controls the transition between START and S phase due to its ability to inhibit Clb5,6-Cdc28 activity needed for the firing of replication origins and S-phase entry (Schwob E. and Nasmyth K., 1993; Mendenhall M.D. 1993; Schwob *et al.*, 1994; Barberis M. *et al.*, 2005). After START, Cln-CDK dependent phosphorylation of Sic1 promotes its ubiquitination by SCF<sup>Cdc4</sup> ubiquitin ligase and degradation, releasing Clb5,6-CDK inhibition and promoting S phase entry (Schwob E. *et al.*, 1994, **Figure i.3**). Interestingly, Sic1 degradation directed by SCF<sup>Cdc4</sup> is driven by extensive phosphorylation in multiple CDK sites, and not by residue-specific phosphorylation (Nash P. *et al.*, 2001). *SIC1* is not an essential gene but the presence of Sic1 is crucial for genome stability by providing cells sufficient time with low-CDK activity to license a large number of origins in G<sub>1</sub>. Cells lacking Sic1 enter S phase prematurely and replicate DNA from fewer origins (Lengronne A. and Schwob E., 2002).

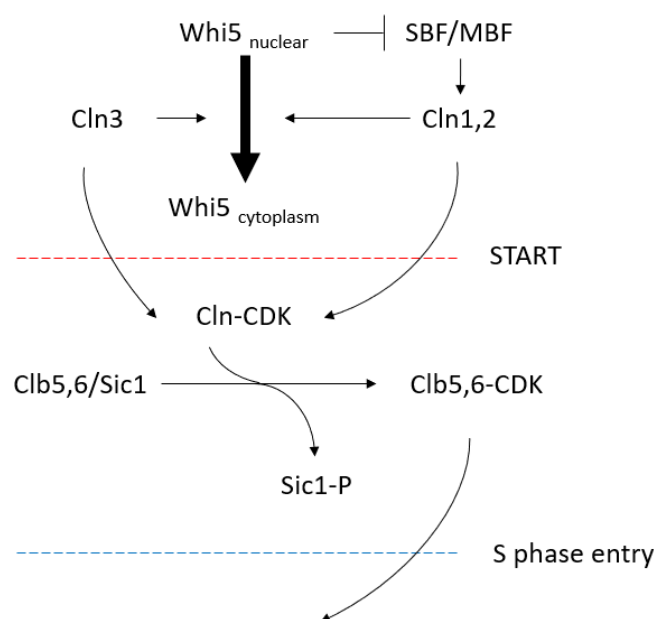


**Figure i.3. START checkpoint and S phase entry in *S. cerevisiae*** (Adapted from Liu X. *et al.*, 2015). *Whi5* inhibits both *SBF* and *MBF* transcription factors, preventing the expression of *G<sub>1</sub>* cyclins. Enough *Cln3* induces nuclear exclusion of *Whi5*, allowing cells to pass *START* and commit to cell cycle. *Cln1,2,3-CDK* promote the degradation of *Sic1* inhibitor, promoting *S* phase entry via increase of *Clb5,6-CDK* activity.

### **1.3.2. S phase and intra-S checkpoint**

DNA replication takes place during S phase in a well-orchestrated manner to faithfully duplicate the genome before cells enter mitosis. The molecular mechanisms leading to the establishment of a replication fork, its progression and termination are now well characterized (see Chapter 2).

Cells have surveillance mechanisms to monitor the progression of DNA replication, DNA damage and fork progression impediments that create replication stress. The mechanism sensing and repairing DNA damage across the cell cycle is named DNA Damage Response pathway (DDR). Extensive work in budding yeast and other organisms, particularly in S phase, has demonstrated the existence of two DDR branches that work in parallel: the DNA Replication Checkpoint (DRC) and the DNA Damage Checkpoint (DDC) (Branzei D. and Foiani M., 2007; Tourriere H. and Pasero P., 2007; Pardo B. *et al.*, 2017). DDC functions over the entire cell cycle while DRC is restricted to S phase due to its relationship with replication forks.

The molecular structures that activate DDR are Double Strand Breaks (DSBs) and RPA-coated single stranded DNA (RPA complex = Rfa1, Rfa2 and Rfa3 in budding yeast, ssDNA). The activating/sensor kinases of DDR are Tel1, yeast homologue of ATM recruited and activated at DSBs via the MRX complex (Mre11-Rad50-Xrs2), and Mec1, yeast homologue of ATR recruited at RPA-ssDNA accumulation sites (Sanchez Y. *et al.*, 1996).

Upon replication fork stalling, the main DDR sensor kinase, Mec1, is activated. However, it is proposed that checkpoint activation could also occur via Tel1 as the MRX complex is recruited at stalled replication forks (Tittel-Elmer M. *et al.*, 2009 and 2012). Moreover, Tel1 has been shown to overtake Mec1 function when its activity is compromised (Sanchez Y *et al.*, 1996; Kumar S. and Burgers P., 2013). For a question of simplicity and despite the known relevance of Tel1, I will describe DDR activation in S phase via Mec1 sensing (reviewed in Pardo B. *et al.*, 2017).

RPA-ssDNA promotes recruitment of Mec1 sensor kinase to chromatin via Ddc2, but its activation in S phase requires additional proteins (Rouse J. and Jackson S.P., 2002). The 9-1-1 complex (Ddc1-Mec3-Rad17 in *S. cerevisiae*) is loaded on chromatin upon ssDNA signaling and activates Mec1 in coordination with Dpb11 and Dna2 (Kumar S. and Burgers P., 2013). From here, DDR signal amplification can be achieved by two mechanisms (**Figure i.4**):

- Rad9-dependent mechanism (DDC), requiring phosphorylated Rad9 to scaffold Mec1 and Rad53 effector kinases (Weinert T.A. and Hartwell L.H., 1988; Sweeney F.D. *et al.*, 2005).
- Rad9-independent mechanism (DRC), relying on interaction of Mec1 with replication fork components such as Mrc1 or RFC<sup>Ctf18</sup> (Alcasabas A.A. *et al.*, 2001; Garcia-Rodriguez L.J. *et al.*, 2015).

Interestingly, both transduction mechanisms operate differently depending on the type of DNA damage, studied by using different genotoxic components like Hydroxyurea (HU) or Methyl-methanosulphonate (MMS). In budding yeast, DRC is considered as a fast and transient response to DNA damage, as it relies on replisome components to activate Rad53 (Katou Y. *et al.*, 2003; Bacal J. *et al.*, 2018). Importantly, *mrc1Δ* cells are highly sensitive to HU, but not to MMS (Osborn A.J and Elledge S.J, 2003; Hodgson B. *et al.*, 2007; Alabert C. *et al.*, 2009). As HU decreases the dNTP pool by direct inhibition of ribonucleotide reductase, replication fork speed is impaired, cells accumulate ssDNA and RPA can be exhausted, deriving into fork collapse (Slater M.L. 1973; Saintigny Y. *et al.*, 2001). DRC protects cells in HU treatment via Mrc1-dependent inhibition of late origin firing, preventing an increase in the number of active forks (Crabbe L. *et al.*, 2010).

On the other hand, DDC is active in “mid-late” S phase, as it requires high CDK activity to phosphorylate Rad9 for signal transduction, and is able to prolong checkpoint activation (Crabbe L. *et al.*, 2010; Wang G. *et al.*, 2012; Bacal J. *et al.*, 2018). Interestingly, *rad9Δ* cells are sensitive to MMS but not to HU, contrary to *mrc1Δ* (He W. *et al.*, 2008). MMS is a DNA alkylating agent that prevents normal replication fork progression by impairing replisome advancement, thus, survival is achieved by promoting DNA lesion bypass (Lundin C. *et al.*, 2005; He W. *et al.*, 2008). The specific function of Rad9 in DDC is still elusive, but it is proposed that, apart from promoting strong DDR activation, slows DNA replication and fork progression (Bacal J. *et al.*, 2018).

DDC and DRC pathways converge in the hyperphosphorylation and activation of the Rad53, DDR effector kinase. The Rad53 phosphorylation network, alongside other DDR-related kinases like Mec1, Tel1 or Dun1, controls different cell processes (Chen S. *et al.*, 2010). For instance: repression of late-origin firing (Santocanale C. and Diffley J.F.X., 1998; Lopez Mosqueda J. *et al.*, 2010; Greiwe J. *et al.*, 2022), induction of DNA damage response genes expression (Allen J.B. *et al.*, 1994), replication fork protection (Cobb J.A. *et al.*, 2003; Rossi S.A. *et al.*, 2015) and cell cycle arrest (Tercero J.A. *et al.*, 2003). The main function of the DDR checkpoint is to provide cells time, prevent further DNA damage and facilitate DNA repair.

Importantly, cell cycle modulation by DDR during S phase is different between species. In *Schizosaccharomyces pombe* and human cells, Rad53 activity prevents mitotic entry by directly interfering with CDK1 activity via Cdc25/CDC25A-B and Swe1/WEE1 (Raleigh J.M. and O'Connell M.J., 2000). In *S. cerevisiae*, the DDR does not strongly inhibit Cdc28 activity and cells arrest in early mitosis instead of at the G<sub>2</sub>/M transition (Sorger P.K. and Murray A.W., 1992). This arrest is maintained by the inhibition of the Mitotic Exit Network (MEN) and the stabilization of Pds1 to prevent anaphase entry (Hu F. *et al.*, 2001; Clarke D.J. *et al.*, 2001).

Another important function of the intra-S checkpoint is to finely regulate recombination. Paradoxically, DDR has been proved to both inhibit and promote recombination. During S phase, Mec1 prevents the formation of Rad52 repair foci and both Mec1 and Rad53 prevent DNA resection by inhibition of Exo1 and Dna2 nucleases (Lisby M. *et al.*, 2004; Morin I. *et al.*, 2008; Hu J. *et al.*, 2012). However, recombination foci and resection are favored in G<sub>2</sub>/M cells, for example, by the phosphorylation of Sae2 via Mec1/Tel1 (Baroni E. *et al.*, 2004; Gonzalez-Prieto R. *et al.*, 2013). Therefore, DDR function is to restrict and promote recombination events to G<sub>2</sub>/M (**Figure i.4.**).

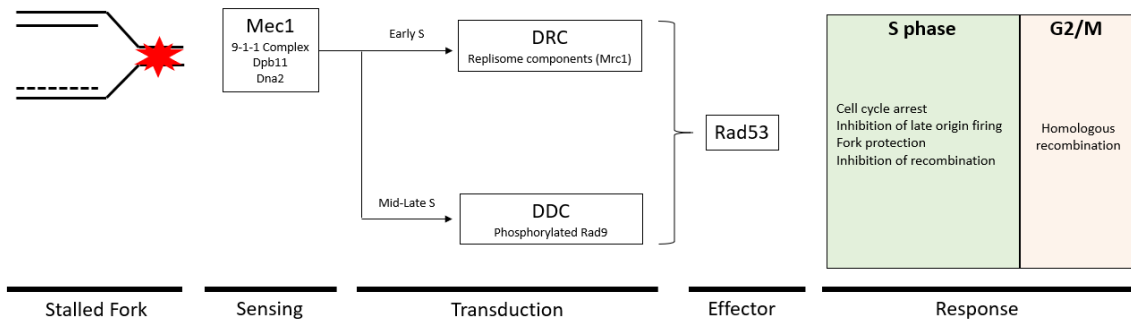


**Figure i.4. Activation of DDR checkpoint during S phase via Mec1.** RPA-ssDNA activates Mec1 during S phase thanks to the 9-1-1 complex, Dpb11 and Dna2. Amplification can be performed through Rad9 (DDC pathway) or replisome components (DRC pathway), converging in Rad53 phosphorylation and activation. DDR function in S phase is to promote cell cycle arrest, prevent extensive DNA damage and restrict DNA recombination to G<sub>2</sub>/M phase.

Finally, while DDR activation and cell cycle arrest are well understood, DDR deactivation and cell cycle re-entry (named recovery) is still unclear. DDR recovery requires the repair of the DNA damaged region and the dephosphorylation and deactivation of Rad53 by several phosphatases, like Ptc2 and Ptc3, (Leroy C. *et al.*, 2003; O'Neill B. *et al.*, 2007; Tsabar M. *et al.*, 2016). However, there is evidence that after prolonged DDR activation cells become “insensitive” to checkpoint activity. In prolonged HU arrest, Mrc1 is detached from chromatin and Rad53 is dephosphorylated and inactivated, allowing cells to resume growth even if DNA is not repaired (Uzunova S. *et al.*, 2014). The dynamics of DDR activation and deactivation and its consequences to cell cycle are still under deep investigation.

### **1.3.3. Mitosis and Spindle Assembly Checkpoint (SAC)**

Mitosis is the culmination of the cell cycle, believed to occur only after successful genome duplication. Cells enter mitosis in a state of high CDK activity where chromosomes are condensed for segregation but requires a decrease of CDK activity to promote anaphase onset and telophase.

During prophase, chromosomes condense as cohesin is removed from the majority of the genome, to the exception of centromeres, and the nuclear membrane starts to degrade (observation done in mammals - Waizenegger I.C. *et al.*, 2000). Simultaneously, the mitotic spindle elongates and aligns the chromosomes on the metaphase plate. At this stage, chromosomes reach their maximum compaction state, are connected to the mitotic spindle at their centromere and sister chromatids are bi-oriented. In anaphase, the decrease of CDK activity and increase in phosphatase activity drives further elongation of the mitotic spindle, sister chromatids separation and segregation to the opposite poles of the cell, resulting in telophase when separation is finished (Marston A., 2014).

The Spindle Assembly Checkpoint (SAC) is the checkpoint that prevents anaphase until all chromosomes are properly bi-oriented. SAC senses the attachment between kinetochores and mitotic spindle and can arrest cells in metaphase in case of improper attachment (Hoyt M. *et al.*, 1991; Hardwick K.G. *et al.*, 1999). Several kinases act at the kinetochores, like Mps1, Aurora B and Bub1, blocking the activity of the Anaphase Promoting Complex/Cyclosome (APC/C) via inhibition of Cdc20 (Hwang L.H. *et al.*, 1998; Qiao R. *et al.*, 2016). APC is a ubiquitin ligase complex essential for the degradation of several proteins, including mitotic cyclins and the Pds1 anaphase inhibitor, which is only active in association with Cdc20 or Cdh1 (Shirayama M. *et al.*, 1999). Activation of APC<sup>Cdc20</sup> will shift the kinase/phosphatase balance towards dephosphorylation activity, promoting chromosome segregation, anaphase exit and, among other events, Sic1 accumulation (Visintin R. *et al.*, 1998).

In *S. cerevisiae*, the SAC overlaps with the DDR-dependent function of Rad53 arresting cells in metaphase, but they are two independent mechanisms. Until now, Rad53 has not been reported to be phosphorylated as an outcome of SAC activation, but SAC-arrested cells display a low level of Rad53 phosphorylation due to the high mitotic CDK activity (Diani L. *et al.*, 2009). However, this modification does not cause Rad53 autophosphorylation nor promote a strong DDR activation. The possibility of a link between DDR and SAC is still under investigation (Magiera M. *et al.*, 2014; Lawrence K. *et al.*, 2015; Liakopoulos D., 2022).

#### **1.4. Cell cycle deregulation and genome instability**

A well-controlled cell cycle progression is imperative for the maintenance of genome stability. Indeed, there are many examples where cell cycle deregulation triggers genome instability:

- **Deregulation of G<sub>1</sub> length promotes genome instability.** Previous work in *S. cerevisiae* demonstrated that overexpression of G<sub>1</sub> cyclins (Tanaka S. and Diffley J.F.X., 2002) or the lack of Sic1 (Lengronne A. and Schwob E., 2002) affects origin licensing by causing premature S-phase entry, slowing down DNA replication and promoting gross chromosome rearrangements (GCRs). Indeed, G<sub>1</sub> deregulation has severe clinical implication in humans, as many tumor suppressors are acting in G<sub>1</sub> (reviewed in Malumbres M. and Barbacid M., 2001; i.e., inactivation of pRb protein, functional homologue of Whi5 – Gouyer V. *et al.*, 1998).
- **Chromosome mis-segregation is a known cause of instability and highly linked to replication stress.** Recent reports demonstrated that mitotic slippage (cell division without chromosome segregation) promotes apparition of replication stress and extensive genetic instability even during the first cell cycle after polyploidization (Gemble S. *et al.*, 2022). Interestingly, this phenotype is rescued by extending G<sub>1</sub>, pointing that aneuploidy-dependent DNA instability may be connected to inefficient origin licensing. Importantly, aneuploidy is one of the known hallmarks in human cancers, being considered both cause and consequence

of tumor evolution (Sansregret L. and Swanton C. 2016; reviewed in Ben-David U. and Amon A. 2019).

- **Unscheduled or non-canonical DNA synthesis is a source of instability.** There are known cases where DNA replication is not restricted to S phase, leading to severe genetic consequences. For example, forcing one round of DNA replication in G<sub>1</sub> or delaying replication to mitosis has been shown to promote genome instability (Reuswig K.U. *et al.*, BioRxiv; Minocherhomji S. *et al.*, 2015). Moreover, mild replication stress and improper DDR activity has been shown to impact chromosome segregation, inducing aneuploidy (Böhly N. *et al.*, 2019).

It is important to emphasize that not only cell cycle progression and its regulation operates in a cyclic fashion, but also its defects. This implies that small defects in specific phases can be carried, or even amplified, to later phases or even to the next cycles, leading to larger unanticipated consequences. One clear example is the synergistic effect between DNA replication stress and chromosome mis-segregation that amplifies genetic instability over successive cell cycles.

## **2. Mechanisms of DNA replication in Eukaryotes**

The mechanisms of origin licensing, firing and DNA synthesis are highly similar among eukaryotes, demonstrating that replication is an evolutionary conserved trait (Chia N. *et al.*, 2010, Makarova K.S. and Koonin E.V 2013). Interestingly, there are big differences between DNA replication in prokaryotes and eukaryotes. First, the main mechanisms of DNA replication in prokaryotes and certain viruses (phage T4) rely heavily on recombination-dependent replication, while eukaryotes rely on replication forks (Viret J.F. *et al.*; 1991, Kreuzer K.N., 2000). Second, viruses and bacteria have increased mutation rates compared to eukaryotes (reviewed in Drake J.W, 2006). Eukaryotic replication mechanisms have evolved to ensure the fidelity of DNA synthesis, thus allowing the maintenance of genome stability.

### **2.1. Preparing for synthesis: Origin licensing**

Replication origins are regions of the genome that serve as initiation points for DNA replication in S phase. They are defined as binding sites for hetero-hexameric ORC (Origin Recognition Complex: Orc1-6) and, in *S. cerevisiae*, they are represented by sequences called ARS (Autonomously Replicating Sequence) containing consensus motifs (Stinchcomb D. *et al.*, 1979). Budding yeast ARS are composed of two components, a strong T-rich ORC binding sites named ACS and B1 sequences, and weak ORC binding sites A-rich regions called B2 and B3 in reverse orientation (Marahrens Y. and Stillman B., 1992; Rao H. and Stillman B., 1995; Rowley A. *et al.*, 1995). The presence of sequence specific ARS is a trait of *S. cerevisiae* among eukaryotes, while mammalian replication origins follow no consensus sequence. However, there are some genetic features proposed for mammalian origins, like the presence of G-quadruplexes, CpG islands or transcription initiation sites (Martin M. *et al.*, 2011; Cayrou C. *et al.*, 2012; Dellino G. *et al.*, 2013). Over 600 origins have been described in budding yeast with different ORC binding affinities that compose all the possible initiation sites for DNA synthesis (Hoggard T. *et al.*, 2013; Liachko I. *et al.*, 2013; Bell S.P. and Labib K. 2016).

Origin licensing consists in the sequential loading of two inactive MCM helicase complexes (Mini-Chromosome Maintenance, Mcm2-7 hetero-hexamers) into chromatin in a convergent orientation (Diffley J.F.X. *et al.*, 1994). ORC is bound to chromatin throughout all the cell cycle in *S. cerevisiae*, but it is only in telophase and G<sub>1</sub>, when the licensing machinery is present and CDK levels are low, that the Cdc6 and Cdt1 licensing factors can recruit MCM to the ORC complex (Cocker J.H. *et al.*, 1996; Dimitrova D. *et al.*, 2002; Speck C. *et al.*, 2005). Cdc6 orthologues are found in all eukaryotes, from *S. pombe* (Kelly T. *et al.*, 1993) to humans (Williams R.S. *et al.*, 1997) and has been demonstrated to be essential for DNA replication and loading of MCM (Donovan S. *et al.*, 1997; Tanaka T. *et al.*, 1997). Interestingly, defective licensing does not prevent S phase entry nor checkpoint activation, leading to situations of reductional divisions (Piatti S. *et al.*, 1995) or increased genome instability (Bueno A. *et al.*, 1992; Bruschi C.V. *et al.*, 1995). There are evidences of a licensing checkpoint preventing S-phase entry in case of underlicensing, but its existence has been questioned only in cells exiting G<sub>0</sub> and starting S phase with under-licensed origins (Shreeram S. *et al.*, 2002; Matson J.P. *et al.*, 2019). However, it has been shown that origin licensing can be modulated in physiological situations of a short G<sub>1</sub>, as in pluripotent stem cells, where its efficiency is highly increased (Matson J.P. *et al.*, 2017).

The ORC-Cdc6 complex is the loading system for Cdt1-MCM binding to chromatin (**Figure i.5**, Noguchi Y. *et al.*, 2017). This process is dependent on energy as the MCM hetero-hexamers ring conformation varies upon ATP-ADP binding. MCM is loaded through an opening between Mcm2-Mcm5 in the presence of ATP and stabilized by Cdt1 (Frigola J. *et al.*, 2017). Finally, MCM ring closing is achieved by ATP hydrolysis and successive eviction of Cdt1 and Cdc6, forming the pre-RC (pre-Replication Complex, Ticaú S. *et al.*, 2015).

The loading mechanism of the second MCM hexamer is still unclear. Single molecule experiments showed that only one ORC complex is required for the loading of a second MCM (Ticaú S. *et al.*, 2015 and 2017; Gupta S. *et al.*, 2021), and supported by CryoEM experiments (Miller T.C.R. *et al.*, 2019). However, as *S. cerevisiae* origins contain low affinity ORC binding sites distanced from the ACS, it has been proposed that it could serve as an anchor point for a second ORC complex facing the first one and facilitating the second loading event (Coster G. and Diffley J.F.X., 2017). Both models are not

mutually exclusive, possibly alternating between mono/bi-ORC MCM loading depending on cellular conditions.

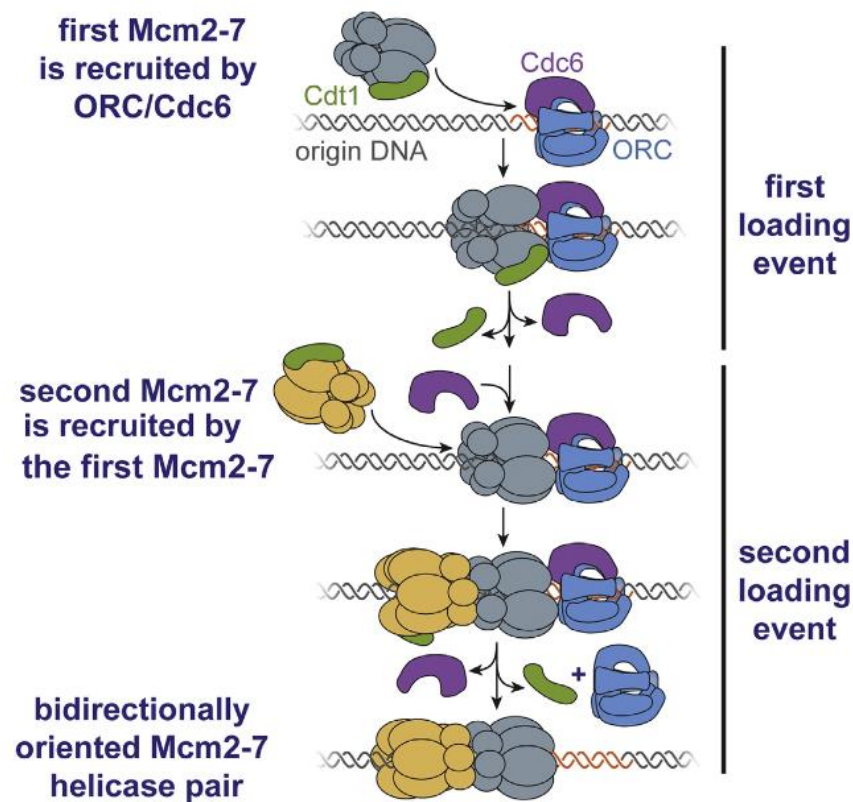


*Figure i.5. Origin licensing involves the loading of two MCM components facing each other (Ticau S. et al., 2015). ORC, Cdc6 and Cdt1 coordination are required for the loading of MCM complexes on origins.*

One of the particularities of licensing is the excess of MCM expressed compared to MCM loaded on chromatin and to the number of active replication forks in S phase. Partial depletion of MCM proteins (>90% in *D. melanogaster* S2 cells, 50% in *S. cerevisiae*) does not impact S-phase progression, but can reduce the number of active replication forks when the more limiting MCM proteins are depleted (Lei M. et al., 1996; Crevel G. et al., 2007; Crevel I. et al., 2011). This excess of MCM is a proposed mechanism to ensure the licensing of dormant origins, important for the rescue of stalled forks (Ge X.Q. et al., 2007; Ibarra A. et al., 2007; Yekezare M. et al., 2013). Indeed, an excess of MCM ensures maximum origin licensing, which is important due to the inability of re-licensing during S phase (in case of fork stalling) and due to the lack of a checkpoint monitoring origin licensing, at least in some cells (Mailand N. and Diffley J.F.X., 2005). Unused chromatin-bound MCM complexes are removed passively by incoming replication forks emanating

from nearby fired origins, thus preventing situations of re-replication and imposing new origin licensing in every cycle (Lebofsky R. *et al.*, 2006a).

## **2.2. Firing of origins: DNA replication initiation**

Origin firing initiates DNA synthesis and has to occur only once per cell cycle for each origin, to avoid re-replication of certain chromosomal regions. It is triggered by an increase of S-CDK and DDK activities, which convert pre-RCs into active bi-directional replisomes by activating the MCM helicase. Mcm2-7 are DDK substrates and recent cryo-EM structures showed that their phosphorylation requires the docking *in cis* of Dbf4 to one MCM for phosphorylation *in trans* of the opposite MCM (Sheu Y.J. and Stillman B., 2006; Greiwe J. *et al.*, 2022). This promotes the recruitment of Cdc45 and Sld3,7, the latter being substrates for S-CDK alongside Sld2 (Kamimura Y. *et al.*, 2001). Phosphorylated Sld3 and Sld7, Sld2 and Dpb11 are required for the recruitment of Pol  $\epsilon$  and GINS (Psf1,2,3 and Sld5), essential factors for DNA synthesis (Ilves I. *et al.*, 2010; Douglas M.E. *et al.*, 2018). Finally, several proteins are evicted from the complex, while Cdc45, GINS, and Mcm2-7 remain, forming the CMG active helicase, and Pol  $\epsilon$ . The mechanism of how CMG transitions from encircling dsDNA to ssDNA is being unraveled in eukaryotes, and requires melting of dsDNA and stabilization of ssDNA by proteins like RPA, Mcm10 and Sld2,3 (Warren E. *et al.*, 2008; Kanter D. *et al.*, 2011; Bruck I. *et al.*, 2011; Douglas ME. *et al.*, 2018).

The pattern of origin firing during S phase has been thought to occur in a stochastic manner when analyzing single molecules (Patel P.K. *et al.*, 2006), but has been proven to have preferential firing sites in population studies (Raghuraman M. *et al.*, 2001). Indeed, there are different factors that modulate the replication program, i.e., chromatin structure, subnuclear compartmentalization, limiting initiation factors or specific timing regulators such as Rif1 (Fragkos M. *et al.*, 2015a). Origins are distributed quite evenly across chromosomes so to complete DNA replication in due time (Agier N, *et al.*, 2018). Spatially they organize and fire in discrete sub-nuclear foci or replication factories, observed using microscopy-based techniques (Pasero P. *et al.*, 1997; Leonhardt H. *et al.*, 2000; Kitamura E. *et al.*, 2006; Cseresnyes Z. *et al.*, 2009; Saner N. *et al.*, 2013). Moreover, origins are classified based on their firing timing (early or late origins) and their probability to fire (efficient origins and dormant origins) (Raghuraman M.K. *et al.*, 2001; **Figure i.6**). Interestingly, origin usage is flexible and can be adapted to overcome

situations of replication stress, like inhibition of late origins by Rad53 or the activation of dormant origins (see Chapter 1.3.2; Santocanale C. and Diffley J.F.X. 1998).

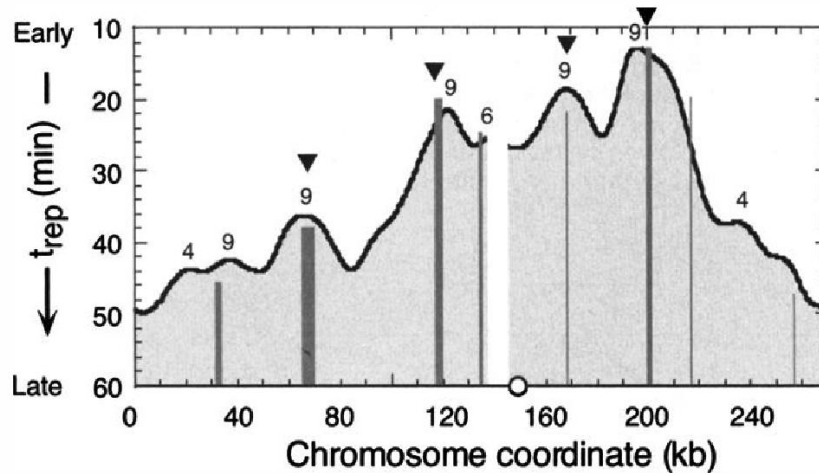


**Figure i.6. Replication profile of chromosome VI in *S. cerevisiae*.** (Raghuraman M.K. *et al.*, 2001). The mean replication time after  $G_1$  release ( $T_{rep}$ ) is indicated for each chromosome segment. Inverted black triangles mark four origins known to fire in >50% of cells. Grey bars represent restriction fragments known to contain an origin, their height is indicative of timing of firing. Numbers above the peaks indicate the robustness of the peaks on a scale of 1 to 9, larger numbers are indicative of more robust peaks.

The replication program not only determines the regions that replicate early and late but also impacts cell identity. For example, developmental studies demonstrated that undifferentiated cells have a different replication program compared to differentiated cells (Gilbert D.M. *et al.*, 2010). Moreover, modulation of replication speed can promote differentiation and reprogramming of mESC *in vitro* (Nakatani T. *et al.*, 2022). Interestingly, studies in yeast demonstrated that late replicating regions are a reservoir for mutagenesis (Lang G. *et al.*, 2011; Agier N. and Fischer G. 2011). Why late replicating regions are more unstable is still under debate. Unreplicated DNA can break or fail to condense during mitosis, as observed for human Common Fragile Sites (CFS) and Replication Slow Zones (RSZ) in budding yeast, generating a DSB that can lead to GCRs (Glover T.W. *et al.*, 1984; Hashash N. *et al.*, 2011). Therefore, origin usage is critical for the timely replication of different genomic regions and to ensure genetic stability and cell identity (as proposed by Egli D. and Chia Le Bin G., 2013; Georgiev D. and Egli D., 2017).

### **2.3. Anatomy of a replication fork**

Replication forks are intricate protein complexes that unwind and synthesize DNA. The composition of the core of the replication fork is stable during S phase, with several proteins that can be recruited transiently for different purposes, like fork speed modulation or fork protection. Here, I split the complex in 3 functional parts: helicase activity, synthesis activity and scaffolding/protection activity (**Figure i.7**).

#### **2.3.1. Helicase activity**

In eukaryotes, the DNA unwinding activity is held by the CMG (Cdc45-MCM-GINS) helicase. The MCM heterohexamer harbors the helicase activity and travels, after unwinding, by encircling ssDNA on the leading strand. The precise mechanism of how CMG unwinds DNA in eukaryotes is still not fully understood. The current model points at a strand-separating element as a steric exclusion that unwinds both DNA strands (Pike A. *et al.*, 2015). However, this model requires a structural element conserved in all eukaryotic helicases, which have not been identified yet. Recent Cryo-EM experiments propose a different model using a “separation pin model” (Yuan Z. *et al.*, 2020). Here, both strands pass through different tunnels of MCM, allowing separation. Importantly, the generated ssDNA is stabilized by proteins such as RPA, but this transient association does not activate the DDR checkpoint (Byun T.S. *et al.*, 2005).

#### **2.3.2. DNA synthesis activity**

DNA polymerases can only synthesize DNA in a 5` → 3` direction using an hydroxyl group available from a dNTP/NTP. Eukaryotic DNA synthesis activity relies in 3 B-family DNA polymerase complexes: DNA Pol  $\alpha$ , DNA Pol  $\epsilon$  and DNA Pol  $\delta$  (Bell S. and Labib K. 2016; Burgers P. and Kunkel T., 2017). These polymerases travel on DNA at a speed of 2 kb/min, completing DNA synthesis in approximately 20 minutes in *S. cerevisiae* (Techer H. *et al.*, 2013; Theulot B. *et al.*, 2022; Barba Tena J.D. *et al.*, 2022). Importantly, synthesis of the leading strand is carried out in a continuous fashion while lagging strand synthesis is discontinuous.

DNA polymerase Pol  $\epsilon$  (Pol  $\epsilon$ : *POL2*, *DPB2*, *DPB3*, *DPB4*) is the leading strand polymerase and is in direct contact with the CMG, while DNA polymerase Pol  $\delta$  (Pol  $\delta$ : *POL3*, *POL31*, *POL32*) is the polymerase responsible for lagging strand synthesis. Both polymerases are characterized by their high fidelity and processivity, due to their interaction with PCNA (Proliferating cell nuclear antigen) and proofreading activity (Chilkova O.*et al.*, 2007; Flood C.L. *et al.*, 2015). Interestingly, Pol  $\epsilon$  activity is not essential for yeast DNA replication (proven by removing the n-terminal catalytic domain of *POL2*), suggesting that Pol  $\delta$  can also perform DNA synthesis in the leading strand, as well as taking over other Pol  $\epsilon$  functions (Kesti T. *et al.*, 1999; Pavlov Y. and Shcherbakova P., 2010; Kunkel T. 2011). However, neither polymerases can initiate DNA synthesis by themselves, requiring the priming activity harbored by DNA Polymerase  $\alpha$  (Pol $\alpha$ : *POL1*, *POL12*, *PR11*, *PR12*).

All 3 polymerases connect differently to the replisome; thus, they have different resident times on chromatin and can be maintained or removed from the replication fork depending on their abundancy (Lewis JS. *et al.*, 2020). Pol  $\alpha$  is the most labile with shorter residence time while Pol  $\epsilon$  is the most stable, possibly due to its direct interaction with CMG (Kapadia N. *et al.*, 2020). How Pol  $\delta$  is tethered to the replisome, or even if it requires to be coupled with CMG, is still unknown (reviewed in Guillian T.A., 2021).

### **2.3.3. Scaffolding activity**

Both helicase and polymerase activities, in leading and lagging strand, must be coupled in the replisome to prevent the formation of ssDNA:

- Lagging-strand synthesis is coupled by the homotrimer Ctf4, that connects Pol $\alpha$  with CMG helicase by interacting with Sld5 (Gambus A. *et al.*, 2009; Simon A.C. *et al.*, 2014; Villa F. *et al.*, 2016; **Figure i.7**). This complex is also involved in other functions like rDNA copy number control, via interaction with other proteins like Tof1 or Dna2 (Villa F. *et al.*, 2016).
- Leading-strand synthesis is coupled by the interaction between Pol  $\epsilon$  and the CMG. Precisely, Pol2 and Dpb2 subunits of Pol  $\epsilon$  interact with Psf1 subunit of GINS. Surprisingly Pol  $\epsilon$  is seemingly placed ahead of the CMG helicase (Langston L.D. *et al.*, 2014; Sun J. *et al.*, 2015).

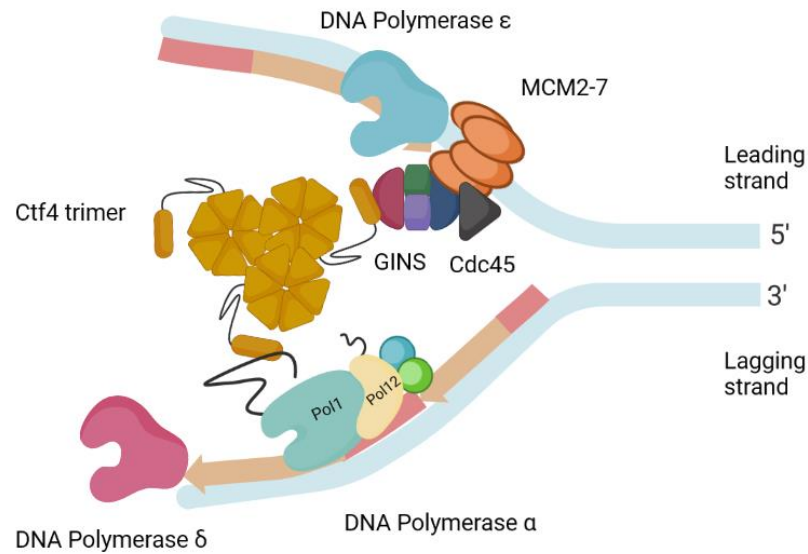


**Figure i.7. Composition of the replication fork in *S. cerevisiae*.** The CMG complex is located on the leading strand and unwinds DNA. DNA Pol $\epsilon$  and Pol $\delta$  synthesize leading and lagging strands, respectively, from DNA-RNA primers synthesized by DNA Pol $\alpha$ . Both activities are coordinated via scaffolding complexes like Ctf4 homotrimer or the Fork Protection Complex.

### **2.3.4. DNA Polymerase $\alpha$ .**

DNA Polymerase  $\alpha$  harbors the primase activity required for DNA replication initiation in eukaryotes. In *S. cerevisiae*, it consists of 4 subunits: Pol1, the main catalytic subunit, Pol12, the regulatory B-subunit, and the primases Pri1 and Pri2.

Pol  $\alpha$  synthesizes 30-nucleotide long RNA-DNA primers on both strands; the leading that will be extended by Pol  $\epsilon$ , and the lagging, extended by Pol  $\delta$  to produce Okazaki fragments of ~150 bp. Pol  $\alpha$  remains attached to the replisome and stabilized on chromatin via the interaction between Pol1 and Ctf4 (Simon A.C. *et al.*, 2014; Villa F. *et al.*, 2016), but this interaction is not essential. Indeed, the *ctf4 $\Delta$*  mutant is viable despite its slow DNA replication speed and checkpoint activation, indicating that Pol $\alpha$  is still present and active in the replisome on its own (Tanaka H. *et al.*, 2009). To date, Pol $\alpha$  is known to be loaded on chromatin in G<sub>1</sub> phase (Johnston L.H. *et al.*, 1987; Foiani M. *et al.*, 1989; Johnston L.H and Lowndes N.F. 1992; Koch C. and Nasmyth K., 1994), present at replication forks during S phase (Hiraga S. *et al.*, 2005) and released from chromatin during mitosis, presumably via phosphorylation by M-CDK (Desdouets C. *et al.*, 1998).

Besides Pri1 and Pri2 that carry priming RNA synthesis, Pol1 harbors the DNA polymerase activity and consists of a DNA polymerase domain, a Zn finger domain that recognizes and encircles ssDNA, and a non-functional exonuclease domain. Pol12 is a scaffold protein essential for the function of the polymerase. It contains two PDE domains and an OB domain. Importantly, both subunits present a disordered N-Terminal Domain (NTD) (**Figure i.8**).

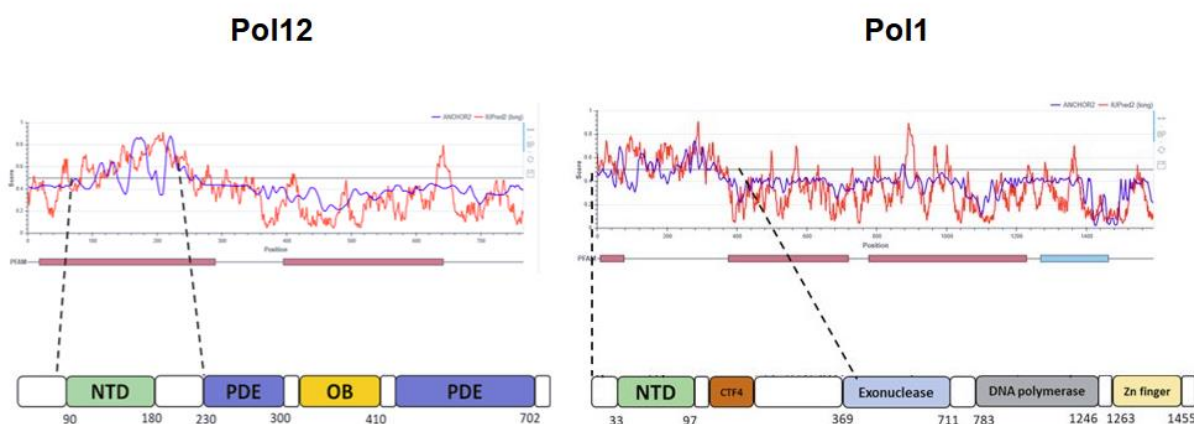


**Figure i.8. Pol1 and Pol12 protein domains and disorder analysis.** The graphs indicate the level of disorder of Pol1 and Pol12 proteins (red lane) revealing the presence of disordered domains in both subunits (Analysis done using UIPRED software). NTD = N-terminal Domain. PDE=Phosphodiesterase Domain. OB= Oligonucleotide Binding Domain. CTF4= Ctf4 binding domain. Exonuclease= Exonuclease Domain. Zn Finger= Zinc Finger Domain

Disordered regions are recurrent in proteins involved in DNA replication (Dpb3, Dpb4, Pol32, Sld2, Orc2; “The mechanisms of DNA replication” Bedina Zavev A., 2013) and they are also target for posttranslational modifications (PTM), making them potential candidates for cell cycle-dependent regulation of DNA replication (Bah A. and Forman-Kay J.D., 2016). Indeed, many of the reported Pol1 and Pol12 phosphorylated sites are located in disordered NTD of the proteins, in both mammals and budding yeast (Nasheuer H-P. *et al.*, 1991; Foiani M. *et al.*, 1995; Desdouets C. *et al.*, 1998; Voitenleitner C. *et al.*, 1999). Moreover, these NTDs serve as interactor domains with many other proteins, i.e. Ctf4, Cdc13 or H2A/B (Qi H. *et al.*, 2000; Sun *et al.*, 2011; Simon *et al.*, 2014; Villa F. *et al.*, 2016, Evrin C. *et al.*, 2018).

Structurally, Pol $\alpha$  is organized as described in the following scheme:

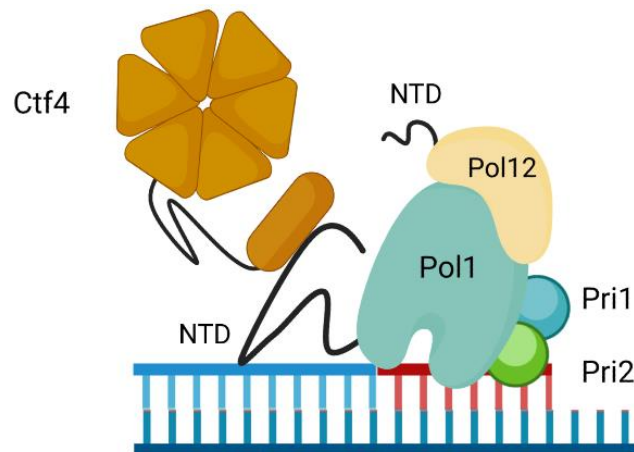


**Figure i.9. Schematic representation of Pol $\alpha$  complex priming DNA.** Pol1 encircles DNA (blue) and has contacts with Pol12, Pri1 and Pri2. It links the complex with the replisome via Ctf4 interaction in its NTD and synthesizes RNA:DNA primers (red fragment).

Interestingly, Pol $\alpha$  has been also proposed to act in other DNA synthesis mechanisms that do not involve a replication fork. As an example, Pol $\alpha$  has been observed to associate with CST complex (Cdc13, Stn1 and Ten1 in *S. cerevisiae*) and become essential for telomere maintenance (reviewed in Rice C. and Skordalakes, 2016; He Y. *et al.*, 2022). Also, certain HR mechanisms have been proposed to require Pol $\alpha$ -primase activity for efficient DNA synthesis, in particular Break-induced Replication (Lydeard J.R. *et al.*, 2010; Donnianni R.A. *et al.*, 2019; see Chapter 3). The function of Pol $\alpha$  involving DNA synthesis is extended beyond the replication fork, as it is implicated in several HR-dependent mechanisms. However, little is known about its regulation in these particular biological situations.

## **2.4. Packing up replication: Termination and fork disassembly**

DNA replication initiation and elongation in eukaryotes have been extensively studied, while termination is still obscure. Termination is defined as the convergence and unloading of two replisomes in usually random positions in the genome, depending on the replication program. However, there are regions more prone to replication termination: late replicating regions, those containing replication fork barriers (i.e. proteins bound to DNA at specific locations) and telomeres (one sided DNA ends) (reviewed in Dewar J.M. and Walter J.C. 2017). Data obtained from *Escherichia coli*, SV40 virus and recently in eukaryotes, mainly *S. cerevisiae* and *Xenopus laevis*, define several steps of DNA replication termination.

First, converging replication forks will generate topological stress due to the unwinding of DNA by helicase. For this reason, topoisomerases type I and II and fork rotation are crucial to remove supercoiled DNA and allow physical proximity of the two CMGs, known as ‘encounter’ (Sundin O. and Varshavsky A., 1980; Zechiedrich E.L. and Osheroff N., 1990). The current understanding is that CMGs ‘pass’ on each other without pausing, possibly because converging CMGs are on opposite DNA strands. This phenomenon was unexpected as forks stall upon certain steric impediments like DNA Protein Crosslinks (DPCs, Duxin J.P. *et al.*, 2014).

Fork disassembly and removal from chromatin is achieved via ubiquitination of the CMG complex by E3 ubiquitin ligases. In *S. cerevisiae* and metazoan, Mcm7 ubiquitination is performed by SCF<sup>Dia2</sup> and CUL2<sup>LRR1</sup>, respectively, during S phase (Mimura S. *et al.*, 2009; Moreno S.P. *et al.*, 2014; Maric M. *et al.*, 2014; Sonnevile R. *et al.*, 2017). This promotes the recruitment of the CDC48-p97 segregase that unfolds Mcm7 and forms a subcomplex that is no longer loaded into chromatin (**Figure i.10**). How Dia2/LRR1 E3 ubiquitin ligases act only on crossed CMGs and not on inactive or elongating MCMs is still unclear, but it is proposed that Dia2 and LRR1 interaction with MCM (via the Zn finger domains of Mcm3 and Mcm5) is occluded by active replication (Jenkyn-Bedford M. *et al.*, 2021).

Interestingly in metazoan, a second mechanism has been described involving ubiquitination of Mcm7 by TRAIPI E3 ubiquitin ligase during mitosis (Moreno S.P. *et al.*, 2019; Deng L. *et al.*, 2019; Sonnevile R. *et al.*, 2019; **Figure i.10**). In this context, TRAIPI acts only with high M-CDK activity and ubiquitinates any fork including those that have

not crossed each other, but possibly on stalled or collapsed forks. The presence of TRAIP to force replisome disassembly may explain the incompatibility of active replication and mitosis (Johnson R.T. and Rao P.N., 1970). Interestingly, there is no clear TRAIP orthologue in budding yeast. However, since cells lacking Dia2 are viable, although sick, it is proposed that other mechanisms could remove chromatin-bound CMG (Lengronne A. and Pasero P., 2014).

Finally, after the CMG complex has been evicted from chromatin, the remaining gap is filled to complete DNA replication. In metazoan, Pol  $\epsilon$  and  $\delta$  are proposed to finish synthesis of terminated forks concomitantly to replisome ‘encounters’ and disassembly (Dewar JM. *et al.*, 2015). However, the outcome of non-terminated forks evicted from chromatin is unknown, but it is proposed that, when it occurs via TRAIP in mitosis, it could serve as an initiation point for HR during mitosis (Sonneville R. *et al.*, 2019).

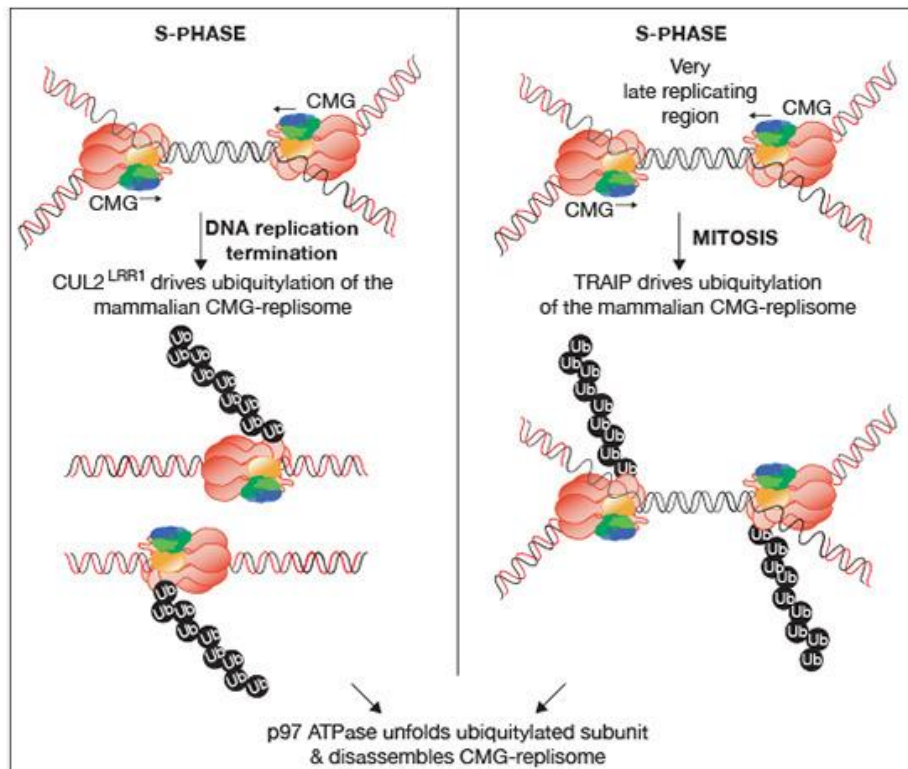


**Figure i.10. Ubiquitination and unloading of CMG complex from terminated replication forks or forks that entered mitosis (Villa F. *et al.*, 2021).** Mcm7 ubiquitination is required for unloading of CMG from chromatin and occurs by two different E3 ligases. LRR1 and Dia2 act in S phase and G<sub>2</sub> in crossed/terminated forks (left side of the figure), while TRAIP acts in mitosis in any chromatin bound CMG (right side of the figure). Both pathways converge in the unfolding and disassembly of CMG via p97 ATPase.

### **3. Controlling the damage: Mechanisms of DNA Damage Repair**

As described in Chapter 1.3.2, DDR allows sufficient time for DNA repair pathways to remove and repair DNA-related lesions. There are five major DNA repair pathways that act at different cell cycles phases: Base Excision Repair (BER), Nucleotide Excision Repair (NER), Mismatch Repair (MMR), Non-Homologous End Joining (NEHJ) and Homologous Recombination (HR). In this chapter, I describe how cells deal with arrested replication forks and how they can restart and finish DNA synthesis using HR. Importantly, DNA repair using HR due to incomplete or failed DNA replication is hypothesized as a potential mechanism contributing to genome instability.

#### **3.1. Sources and types of DNA damages and replication stress**

There are two types of DNA structures recognized by the DDR; RPA coated ssDNA and DSBs (Durocher D. and Jackson S.P., 2001). During S phase, they originate from collapsed or arrested replication forks that occur naturally due to replication fork barriers (RFBs), intrinsic properties of the replication program or damage created by genotoxic compounds (reviewed in Zeman M.K. and Cimprich K.A., 2014). As replication forks expose short stretches of ssDNA, there is a basal level of replication stress during S phase that, in normal conditions, is not sufficient to activate the DDR (Byun T.S. *et al.*, 2005). However, when fork progression is severely impaired, it results in stalled forks, where the replication machinery is stabilized and can resume synthesis, or collapsed forks, when the replisome machinery is absent or unable to restart, and synthesis is accomplished by other means.

RFBs are physical impediments that impact the replication molecular machinery in different ways (Branzei D. and Foiani M., 2010). Examples of RFBs are dsDNA damage (nicks, gaps or ssDNA), chromatin organization, secondary DNA structures (G-quadruplexes or R-loops) and proteins/complexes strongly bound to DNA, like DPCs or head-on collisions with transcription machinery (**Figure i.11**, Deshpande A.M. and Newlon C.S., 1996; Mirkin E.V. and Mirkin S.M. 2007; Zeman M.K. and Cimprich K.A., 2014). Also, deregulation of the replication program can trigger fork arrest. As an example, excessive origin firing can provoke depletion of the nucleotide pool, translating

into a decrease of replication speed, increase of ssDNA (associated with exhaustion of RPA) and eventually fork collapse (Poli J., *et al.*, 2012; Beck H. *et al.*, 2012).

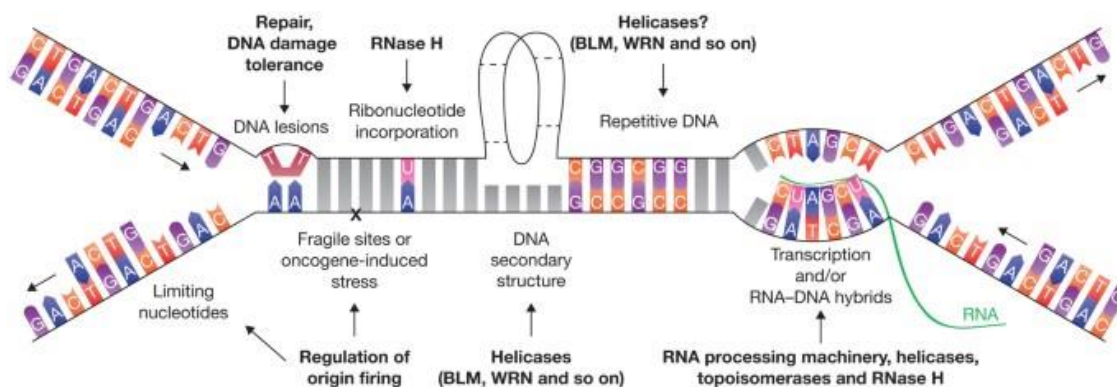


**Figure i.11. Types of Replication Fork Barriers (RFB)** (Zeman M.K. and Cimprich K.A. 2014). RFB are topological impediments to the replication fork progression that arise from external damaging agents, certain cellular processes, like transcription, or intrinsic structure of DNA, including G-quadruplexes or R-Loops.

A single stalled replication fork may not suppose a failure of the replication program. Adjacent origins or dormant origins can replicate DNA up to the site of fork arrest. However, improper protection of an arrested fork can promote its degradation, resulting in collapsed forks and DSBs, that are extremely toxic for cells. Interestingly, increased DNA damage linked to replication problems is one of the hallmarks of many human diseases, from anemia to different types of cancers, thus fork protection is essential to preserve genome stability (reviewed in Alhmod J.F. *et al.*, 2020).

### **3.2. How cells protect replication forks**

Studies with replication-impairing agents helped to understand the mechanisms of fork protection. First, uncoupling between helicase and DNA synthesis activities is prevented by the Ctf4 homotrimer (for lagging strand) and the Fork Protection Complex (FPC, for the leading strand) (Gambus A. *et al.*, 2009; Patel S.S. *et al.*, 2011; Roseaulin L.C. *et al.*, 2013; Baretic D. *et al.*, 2020). This complex not only stabilizes the replisome and restricts extensive ssDNA formation but also contributes to the signaling of the intra-S phase checkpoint, normal replication rates and proper chromosome segregation in mitosis (Alcasabas A.A. *et al.*, 2001; Yoshizawa-Sugata N. and Masai H., 2007). Even though Ctf4 and FPC are not required for DNA synthesis, they are found as components

of stable replisomes and they enhance replication fork speed (Gambus A. *et al.*, 2006; Yeeles J. *et al.*, 2015, 2017).

Certain DNA lesions can be bypassed without drastic impacts for the replication fork (Huang J. *et al.*, 2013; Sparks J.L. *et al.*, 2019). Small DNA-protein complexes, between 5-14 kDa, do not pose an impediment to the CMG helicase (Nakano T. *et al.*, 2013). Larger structures require the activity of the aforementioned FPC as well as the helicases Rrm3 and Pif1 or Rad30 protein to ensure proper fork progression at conflictive locus (Ivessa A.S. *et al.*, 2002 and 2003). Importantly, this occurs mainly in DNA lesions in the leading strand, as those located in the lagging strand do not impair helicase progression. (McInerney P. and O'Donnell M., 2004).

When DNA lesions block CMG progression, the DNA Damage Tolerance pathway ensures bypassing without replisome degradation (**Figure i.12 top pathway**). DNA-polymerase switching and DNA repriming allow the replisome to continue synthesis, leaving an unresolved DNA gap in the region of conflict (Kobayashi K. *et al.*, 2016; Lehmann C.P *et al.*, 2020). These regions can be replicated later using post-replicative DNA synthesis (**Figure i.12 top pathway**; Branzei D., 2011; Sale J.E. *et al.*, 2012). These methods reduce the time of fork arrest, preventing fork degradation and minimizing mutagenesis.

In severe situations of stalling, replication forks need to change conformation to acquire protective structures that maintain the integrity of the replisome. Fork regression promotes the formation of chicken feet / reversed forks, which protects replication forks (**Figure i.12 middle pathway**; Thangavel S. *et al.*, 2015; Lemaçon D. *et al.*, 2017). Reversed forks are 4-way DNA joined molecules, similar to Holliday Junctions, containing a 3' free end. These structures confer advantages to the fork: it limits extensive ssDNA formation, locates the DNA damage away from the replication machinery and allows for template switching (Cortez D. 2015). However, reversed forks require certain proteins to properly occur and to be protected. As an example, in *S. cerevisiae*, as regression and resection of stalled forks generates ssDNA, this is protected first by RPA and later replaced by Rad51 nucleofilament due to Rad52 recombinase activity (Krejci L. *et al.*, 2002). Interestingly, this has been also observed in human cells, where RAD51 not only protects ssDNA but also prevents extensive resection and fork degradation by endonucleases like MUS81 (Bugreev D. *et al.*, 2011; Zellweger R. *et al.*, 2015). From here, reversed forks can be reset

and DNA synthesis restarts using the intact replisome machinery or synthesis resumes from the 3' free end using recombination-dependent replication (reviewed in Petermann E. and Helleday T., 2010).

However, when forks are not properly protected, they can be degraded by nucleases and become collapsed forks (Lemaçon D. *et al.*, 2017). This situation generates a DSB, which can be an initiation point for chromosome rearrangements (**Figure i.12 bottom pathway**, Carr A.M *et al.*, 2011; Zeman M.K. and Cimprich K.A. 2014). DSBs can compromise DNA replication completion and genetic stability, so cells have mechanisms to rescue replication at the expense of genome instability, mainly using HR-related processes (Malkova A. and Ira G., 2013).

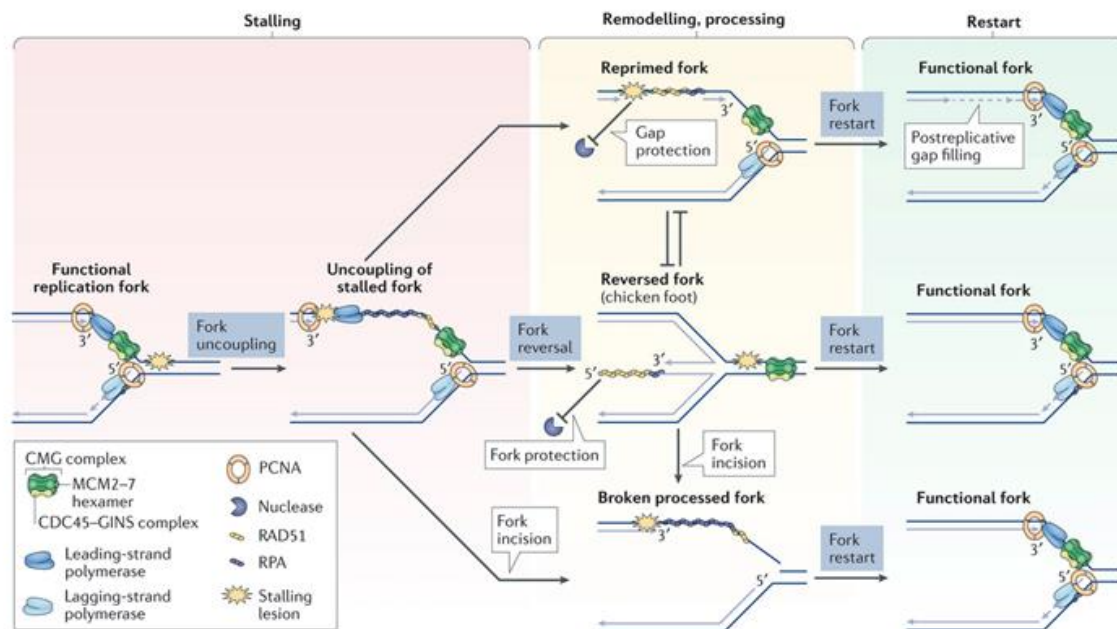


**Figure i.12. Examples of stalled fork processing in eukaryotes.** (Modified from Berti M. *et al.*, 2020). Replication forks react differently to different RFBs. Impediments can be bypassed, generating a gap that will be synthesized using post-replicative mechanisms (top pathway). When forks are severely stalled, they can be processed in protective structures called reversed forks that can resume synthesis using the same replication fork or HR mechanisms (middle pathway). The most dangerous situation is when fork stalling is irreversible, deriving into fork collapse generating a DSBs and DNA synthesis is resumed by HR mechanisms (bottom pathway).

### **3.3. Homologous Recombination as a fork restart mechanism**

Homologous recombination (HR) is a DNA repair mechanism that initiates from a DSB, a single ended DSB or a gap of ssDNA. It has been long considered as an “error free” DNA repair mechanism, but now it has been proven as a source of genetic instability (reviewed in Guirouilh-Barbat J. *et al.*, 2014). HR is implicated in many biological processes that increase genome variability, like hypermutability of immunoglobulins (Schatz D. and Swanson P.C., 2011), meiotic chromosome pairing (described in chapter 4) and, recently, in DNA synthesis completion in G<sub>2</sub>/M (Minocherhomji S. *et al.*, 2015).

#### **3.3.1. Generalities of homologous recombination**

The HR pathway divides into different branches depending on the outcome of different intermediate molecules. However, there are 3 phases common to all HR pathways: “Presynapsis” (**Figure i.13.1-2**), “Synapsis” (**Figure i.13.3**) and “Postsynapsis” (**Figure i.13.4-7**) (Li X. and Heyer W., 2008).

During presynapsis (**Figure i.13.1-2**), DSBs or one-ended DSBs are substrates of exonucleases, like Mre11 (via MRX complex), Exo1 or Sgs1/Dna2, promoting the formation of 3' protruding ends (Fiorentini P. *et al.*, 1997; Trujillo K.M. and Sung P. 2001; Gravel S. *et al.*, 2008). RPA-coated ssDNA will derive into Rad51 nucleofilaments thanks to the activity of Rad52, stabilizing the 3' end, preventing further DNA resection and promoting the search and invasion of a homologous or homoeologous DNA sequence (Ogawa T. *et al.*, 1993; Sung P. and Robberson D.L. 1995; Ma E. *et al.*, 2021). Synapsis (**Figure i.13.3**) occurs when the resected 3' end displaces and aligns a dsDNA molecule, forming a D-loop. D-loops may develop into different states that will lead to different types of recombination, being one of the key points on the fate of a DSB. When the second end of a DSB is engaged in the repair mechanism, also named second end capture, D-loops form robust intermediate recombination structures with two Holliday Junctions (pathway named Double Strand Break Repair: DSBR, **Figure i.13.4b**). The outcome of a DSB during DSBR is a crossover (exchange of DNA information between molecules) or a non-crossover (preserved DNA molecules) depending on how resolvases (Gen1-Slx1-Sls4 and Mus81-Mms4 complexes in *S. cerevisiae*) solve both Holliday Junctions (Boddy M.N. *et al.*, 2001; **Figure i.13.5c**). On the other hand, if there is no second end capture, the invading DNA strand can be rapidly dissociated and undergo Synthesis-Dependent

Strand Annealing (SDSA, **Figure i.13.5a and 6b**) or can perform extensive DNA synthesis by Break-Induced Replication (BIR, **Figure i.13.5b and 6b**).

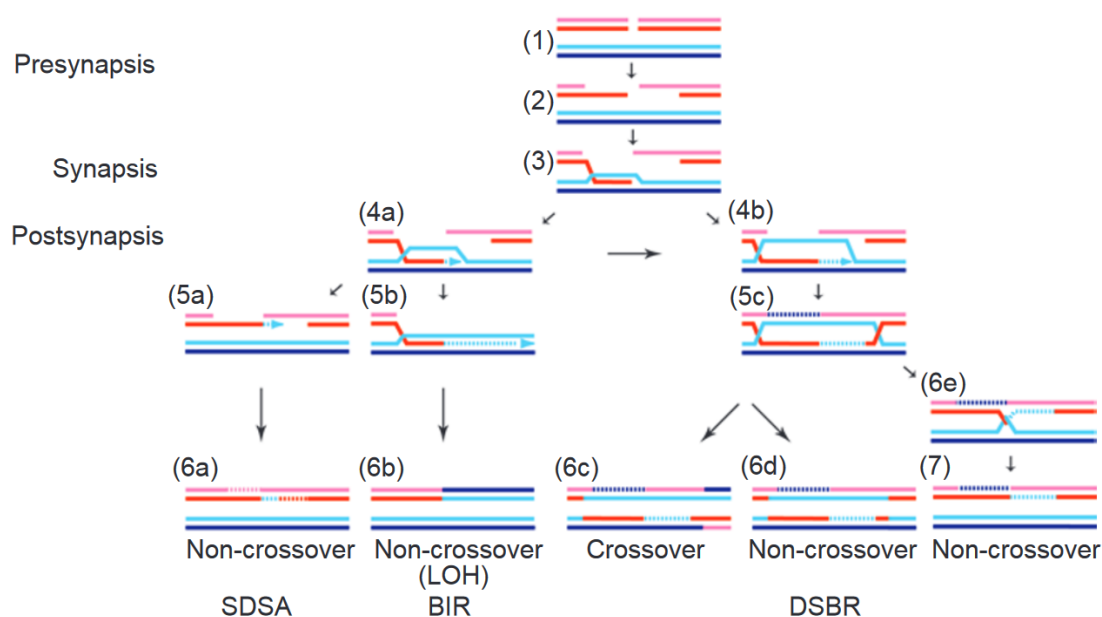


**Figure i.13. Schematic of homologous recombination pathway (Li X. and Heyer W., 2008).** DSBs are recognized (1), processed (2) and engaged with a homologous sequence to generate a D-loop (3). D-loops can be metabolized in 3 different ways that will define the outcome of a DSB: SDSA (Synthesis-Dependent Strand Annealing 5a/6a), BIR (Break-Induced Replication 5b/6b) and DSBR (Double Strand Break Repair 5c, 6c/d/e, 7).

Every branch of the HR pathway requires a DNA synthesis step for the proper repair of DSBs or ssDNA (**Figure i.13.5a-c**), but the precise synthesis mechanism, including the polymerases involved, is still a mystery. The current consensus is that both Pol $\alpha$  and Pol  $\delta$  complexes are required for efficient HR, while Pol  $\epsilon$  seems to have a minor implication, if any (reviewed in McVey M. *et al.*, 2016). In addition, there is increasing evidence that other families of polymerases are involved in HR, like the X-family, the A-family or the Y-Family of DNA polymerases, but in very specific HR functions like mitochondrial DNA replication (reviewed in McVey M. *et al.*, 2016).

### **3.3.2. Break-induced replication as a fork restart mechanism**

BIR is a branch of the HR pathway involving one-ended DSB and one of the proposed mechanisms for DNA synthesis restart after fork collapse (Malkova A. and Ira G., 2013; Mayle R. *et al.*, 2015). It has been extensively characterized in eukaryotes thanks to the use of endonucleases (SceI or HO-induced cuts) that force DSB repair in G<sub>2</sub>/M cells by this mechanism (McEachern M. and Haber J., 2006; Donniani R. and Symington L. 2013). From these systems, it has been shown that it has dramatic differences with canonical DNA replication; BIR is estimated to be 2800 times more mutagenic (due to reduced mismatch repair efficiency and Pol $\delta$  dissociation from DNA template), 2 times slower and performs extensive DNA synthesis for over 100 kb (Deem A. *et al.*, 2011; Liu L. *et al.*, 2021). While DSBR achieves the formation of a stable D-loop by a second end capture, BIR promotes D-loop formation and extension by a single end. This translates into the use of one unique template that will serve for the asynchronous and conservative synthesis of both Watson and Crick strands, promoting Loss of Heterozygosity (LOH) and accumulation of ssDNA in the lagging strand (Wilson M.A. *et al.*, 2013, **Figure i.14**).

BIR can operate using different molecular machineries, defining two BIR pathways: Rad51-dependent (canonical) and Rad51-independent (non canonical) (**Figure i.14**). In normal situations, canonical BIR is favored as it has been proposed that Rad51 inhibits the non-canonical pathway (VanHulle K. *et al.*, 2007). Canonical BIR requires an homology of minimum 70 bp between the 3' end and the donor molecule, promoted by Rad51 that prevents extensive DNA resection (Mehta A. *et al.*, 2017; So A. *et al.*, 2022). Non-canonical BIR takes over when Rad51 is not present; Rad52 is able to align the 3' end with less homologous and shorter regions, usually repetitive regions like Ty elements, and is prone to generate GCRs (Microhomology BIR =MMBIR; Malkova A. *et al.*, 1996; Ira G. and Haber J, 2002). Even though both canonical and non-canonical BIR have been well documented, with proteins involved exclusively in one branch, their precise molecular mechanism and genetic outcome is still under scrutiny (**Figure i.14**; Signon L. *et al.*, 2001; Malkova A. *et al.*, 2005; Kramara J. *et al.*, 2018).

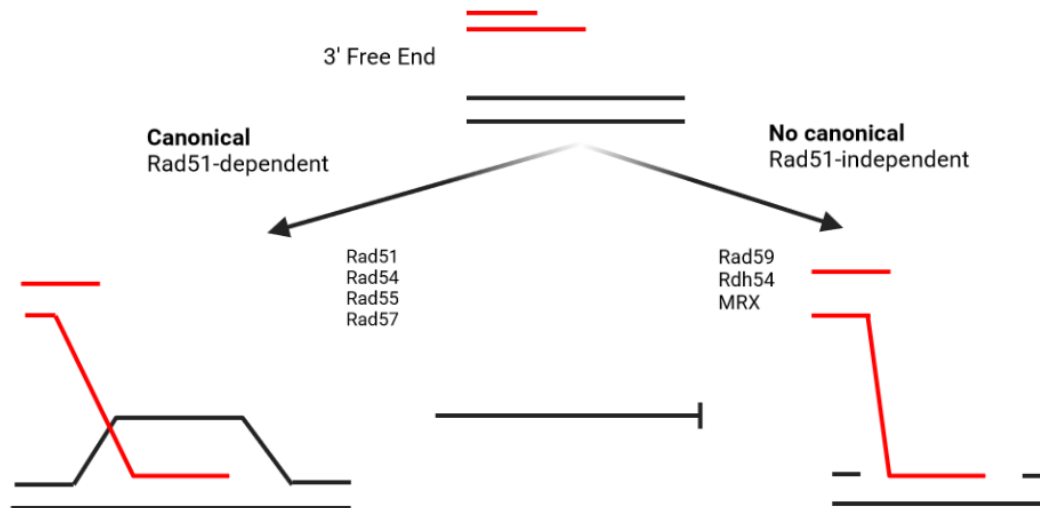


**Figure i.14. Schematic of Rad51-dependent and -independent Break-Induced Replication upon a single-ended DSB.** A free 3' end will engage D-loop formation from a single end and promote extensive DNA synthesis. Left and Right graphs represent canonical and non-anonical BIR, the proteins involved in the process and the potential joint molecules formed. (Adapted from Kramara J. et al., 2018)

Initially, BIR DNA synthesis was proposed to occur using a similar machinery as in the replisome; Mcm2-7 as helicase and the contribution of the 3 main DNA Polymerases (Lydeard J.R. et al., 2007 and 2010). However, the current model for BIR synthesis has evolved and many of the described proteins are not directly required in canonical DNA synthesis.

Pol $\delta$  seems to be the main polymerase, synthesizing both Watson and Crick strands (Lui L. et al., 2021). Interestingly, the Pol32 accessory subunit of Pol $\delta$ , dispensable for canonical DNA replication, is absolutely essential in this process (Malkova A. 1996; Davis A.P. et al., 2004). The other two main polymerases have been also tested in this context. Pol $\alpha$  primase activity and ligase I (Cdc9) seem to be required for BIR synthesis, suggesting that part of this synthesis has to be carried out discontinuously (Donnianni R.A. et al., 2019). Finally, Pol $\epsilon$ , that was originally suggested to be essential for BIR, does not seem to be required (Lydeard J.R. et al., 2007; Donnianni R.A. et al., 2019). Similarly, Mcm2-7, initially reported, was shown to be dispensable for BIR in some models and Pif1 is currently considered the BIR helicase (Lydeard J.R. et al., 2010; Wilson M.A. et al., 2013). In short, BIR synthesis seems to require mainly Pol $\delta$  (Pol32), Pol $\alpha$  priming activity and the helicase activity of Pif1.

BIR has been proposed as a mechanism to rescue DNA replication in S phase and G<sub>2</sub>/M cells. The models of initiation of BIR events in cells involved the formation of a DSB in a fork dependent or independent fashion (reviewed in Ait Saada A. *et al.*, 2018). DSBs can arise naturally in G<sub>2</sub>/M cells or become the outcome of a broken fork when it encounters a DNA nick. However, it has been proposed that BIR can arise in unresolved/unprotected forks that have been degraded by nucleases, like Mus81, promoting DNA synthesis in G<sub>2</sub> or mitosis (Lemaçon *et al.*, 2017).

### **3.4. MiDAS, a new DNA synthesis mechanism during Mitosis**

As mentioned in Chapter 2.4, replication forks are incompatible with mitotic environment of the cell, leading to the conclusion that DNA synthesis is restricted to S phase. Another argument is the presence of the intra-S checkpoint, that delays mitotic entry to ensure equal distribution of genetic material to daughter cells (Boddy M.N. and Russell P., 1999). However, recent studies showed that cells can complete genome duplication during mitosis, in a process named mitotic DNA synthesis (MiDAS) that is dependent on HR (Minocherhomji S *et al.*, 2015; Bhowmick R *et al.*, 2016).

MiDAS has been proposed to occur in different organisms, including *S. cerevisiae* (Ivanova S. *et al.*, 2020) and human cells (Minocherhomji S. *et al.*, 2015; Groelly F.J *et al.*, 2022). However, until now, studies about the mechanism and consequences of MiDAS have been addressed only in mammalian cells. Cytological and sequencing studies using BrdU/EdU labelled mitotic synthesized regions pointed out that MiDAS takes place in regions that are difficult to replicate: those devoid of replication origins, heterochromatic, highly transcribed or in conflict with DNA:RNA structures (Okamoto Y. *et al.*, 2018; Macheret M *et al.*, 2020; Ji F. *et al.*, 2020; Groelly F. *et al.*, 2022). A clear example concerns CFS, regions that are intrinsically late-replicating and highly unstable. MiDAS can be considered as a repair mechanism of under-replicated regions whose backside is an increase in genome instability, due to the use of a BIR mechanism (Minocherhomji S. *et al.*, 2015).

The initiation point of MiDAS has been thought to be a single-ended DSB from a degraded fork due to the activity of Mus81 (Minocherhomji S. *et al.*, 2015; Lemaçon *et al.*, 2017). However, recent reports showed that Mus81 is not always required for MiDAS, suggesting that either there are other nucleases replacing Mus81 or MiDAS does not necessarily need a DSB to occur from a collapsed fork, and could operate via other Recombination-dependent Replication pathways (Ait Saada A. *et al.*, 2018; Mocanu C. *et al.*, 2022).

Regarding the molecular requirements, several BIR components have been shown to be required for efficient MiDAS in mammalian cells:

- Pol32 (POLD3), non essential for DNA replication but strictly required for MiDAS, suggesting the implication of Pol $\delta$  polymerase (Minocherhomji S. *et al.*, 2015).
- Rad52, also required for MiDAS, a recombinase involved in RPA displacement but also in strand invasion (Bhowmick R *et al.*, 2016).
- Pif1 helicase that may replace CMG activity (Li S. *et al.*, 2021).
- Rad51, even though initial reports showed no requirement (Sotiriou S.K. *et al.*, 2016; Garribba L. *et al.*, 2020; Wassing I. *et al.*, 2021).
- Slx1-Slx4 and Mus81, nucleases that could degrade unprotected replication forks (Minocherhomji S. *et al.*; 2015; Lemaçon *et al.*, 2017; Garribba L. *et al.*, 2020).

MiDAS is still a new and poorly explored process, mainly due to the difficulty of delaying DNA replication to mitosis without activating the DDR checkpoint. One of the important questions is to address if it can naturally occur in cells, as all observations have been obtained by artificially impairing normal DNA replication (with drugs like Aphidicolin or FdU) or by promoting replication-transcription conflicts (using genetically engineered BRCA2<sup>-/-</sup> cells) (Minocherhomji S. *et al.*, 2015; Garribba L. *et al.*, 2020; Groelly F. *et al.*, 2022). The second question is to understand its molecular mechanism, even if it is proposed to operate via canonical BIR due to the requirement of Rad51, there are contradictory reports about how it is initiated or how the synthesis is performed (Mocanu C. *et al.*, 2022).

## **4. Meiosis, the basis of sexual reproduction**

Meiosis, gametogenesis or sporulation in budding yeast, is a specialized cell cycle that comprises two consecutive cellular divisions, producing 4 daughter cells. It is the required process for sexual reproduction and it is present in all eukaryotes. Interestingly, the products of meiosis, gametes, are cells with different genetic material between themselves and reduced compared to the mother. It is still unclear when and why meiosis arose in the evolution of eukaryotes, but it is clear that its function is to increase genetic variability within a population (reviewed in Cai K. and Xu S.S. 2007; Bergero R. *et al.*, 2021). The reason is a compulsory HR step in meiosis, essential for the correct segregation of paired chromosomes during the first meiotic division. In this chapter, I will describe the main mechanisms of meiosis regulation and its connection with HR.

### **4.1. Meiotic commitment, main controllers and meiotic cyclins**

Meiosis is a modified mitotic division; thus, its phases and regulation are similar. It is divided in 4 phases; pre-meiotic G<sub>1</sub>, pre-meiotic S phase, Meiosis I and Meiosis II and, in *S. cerevisiae*, is controlled by several waves of transcription that classify meiotic genes into very-early, early, middle and late (Chu S. *et al.*, 1998). Interestingly, the transition between meiotic phases is regulated by changes in Cyclin-CDK activity and target specificity, but the timing and types of cyclins used in meiosis differ from the mitotic program.

Meiotic commitment and the expression of most of meiotic genes depends on the Ime1 transcription factor (Smith H.E. *et al.*, 1990; Mandel S. and Kassir K.R., 1994). *IME1* expression is induced by nitrogen starvation, nonfermentable carbon sources and the product of both *MATa* and *MATα* loci, allowing pre-meiotic G<sub>1</sub> entry. Interestingly, meiosis and quiescence have similar nutritional requirements and as spores, the product of yeast meiosis, are in a growth-arrested state, it is theorized that meiosis is a specialization of quiescence for diploid cells (Sun S. and Gresham D., 2021).

Upon *IME1* expression and pre-meiotic G<sub>1</sub> entry, *IME2*, coding for a serine/threonine kinase related to CDK, is expressed (Deng C. and Saunders W.S., 2006). Ime2 phosphorylates and promotes the degradation of the Sic1 inhibitor, allowing pre-meiotic S phase entry (Dirick L. *et al.*, 1998). Surprisingly, Cln1,2,3 prevent meiosis via inhibition of *IME1* expression, thus, their absence is complemented by Ime1 and Ime2, controlling both G<sub>1</sub> and S phase entry in meiosis (Colomina N. *et al.*, 1999). Another difference is that cyclins Clb5,6 are essential for the initiation of pre-meiotic S phase, while in mitotic program their absence only delays DNA replication (Schwob E. *et al.*, 1994; Dirick L. *et al.*, 1998; **Figure i.15**).

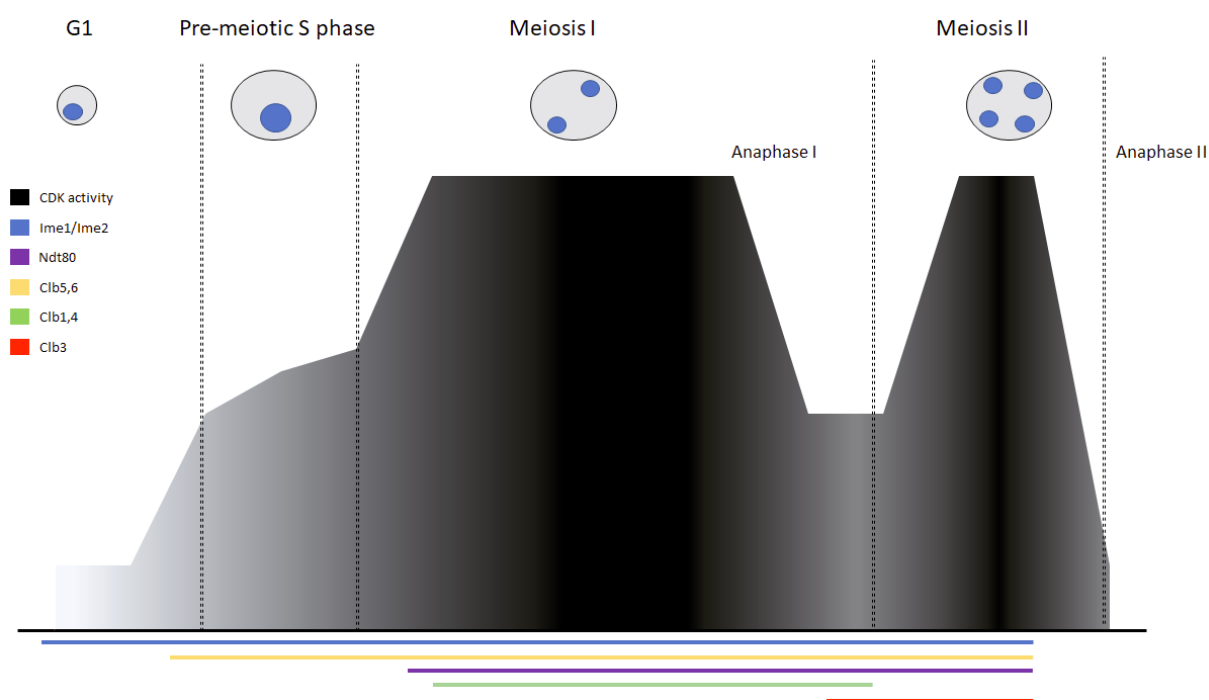


**Figure i.15.** Levels of CDK activity and corresponding expression of cyclins/regulators in *S. cerevisiae* during meiosis. CDK activity (Black) increases prior to every phase transition, and decays at the end of Meiosis I and II. Meiotic G<sub>1</sub> controllers: *Ime1/Ime2* (Blue). Pre-meiotic S phase cyclins: *Clb5,6* (Yellow). Meiosis I controllers: *Ndt80* (purple) and *Clb1,4* (Green). Meiosis II cyclins: *Clb3* (Red).

After a successful pre-meiotic S phase, Meiosis I entry is allowed by the increase of S-CDK activity and inhibition of M-CDK activity to ensure proper synapses and attachment of the meiotic spindle to kinetochores (Okaz E. *et al.*, 2012). It is important to note that Clb2 is not expressed during the meiotic program and M-CDK is mainly controlled first by Clb1 (end of Meiosis I) and then by Clb3 (Meiosis II), Clb4 having a minor role (Dahmann C. and Futcher B., 1995; **Figure i.15**). Of note, both anaphase I and anaphase

II require a decrease of CDK activity to allow homologous chromosomes and sister chromatids to segregate. This situation is dangerous because a decrease in CDK activity may allow origin re-licensing after Meiosis I and trigger chromosome re-replication due to the increase of CDK activity in Meiosis II. For this reason, CDK activity is only partially decreased at the MI-MII transition, and both Ime2 and Cdc5 collaborate to inhibit both origin licensing and origin firing (Phizicky D.V *et al.*, 2018).

#### **4.2. Prophase I: Programmed damage and repair**

As mentioned previously, during meiosis there is a compulsory homologous recombination step due to the programmed formation of DSBs in Prophase I. Meiotic DSBs mediated by Spo11 nuclease do not occur randomly across the genome, but are concentrated in specific regions named recombination hotspots (Gerton J. *et al.*, 2000). These regions are selected based on several criteria: the pre-meiotic replication program, chromatin accessibility and post-translational histone modifications.

##### **4.2.1. Connection between meiotic replication and DSBs formation**

The licensing and replication machinery between mitosis and meiosis is identical, relying on the same pre-RC components and same DNA polymerases, as explained in Chapter 2. However, it has been observed that pre-meiotic S phase is longer than mitotic S phase, even though replication speed is identical and origin usage is not dramatically different (Johnston L.H. *et al.*, 1982; Collins I. and Newlon C.S., 1994; Mori S. and Shirahige K., 2007; Blitzblau H.G. *et al.*, 2012). Examples are found across species: *S. cerevisiae* (Cha R.S. *et al.*, 2000), *Triturus vulgaris* (Callan H.G. and Taylor J.H, 1968) or *Caenorhabditis elegans* (Jaramillo-Lambert A. *et al.*, 2007).

Meiotic DSBs formation occurs approximately 90 min after cells have finished replication. Delaying meiotic replication also delays DSBs formation (Borde V. *et al.*, 2000) but replication is not essential per se for DSBs formation (Blitzblau H.G. *et al.*, 2012). Thus, DSBs can form in unreplicated dsDNA but the replication program marks the regions susceptible to undergo HR. Consistently, altering replication timing or replisome components change the recombination pattern of cells (Murakami H. and Keeny S. 2014; Wu P. and Nurse P., 2014; Pratto F. *et al.*, 2021).

The proposed mechanism is that replication forks contribute to the phosphorylation of Mer2 (meiosis recombination factor) by DDK. Mer2 requires phosphorylation by both S-CDK and DDK to promote DSBs formation and recombination (Wan L. *et al.*, 2008). The Dbf4 subunit of DDK interacts with replication forks via FPC and travels across the genome, promoting the local phosphorylation of Mer2 and the “licensing” of the recombination machinery in specific genomic regions (Murakami H. and Keeney S. 2014; **Figure i.16**).

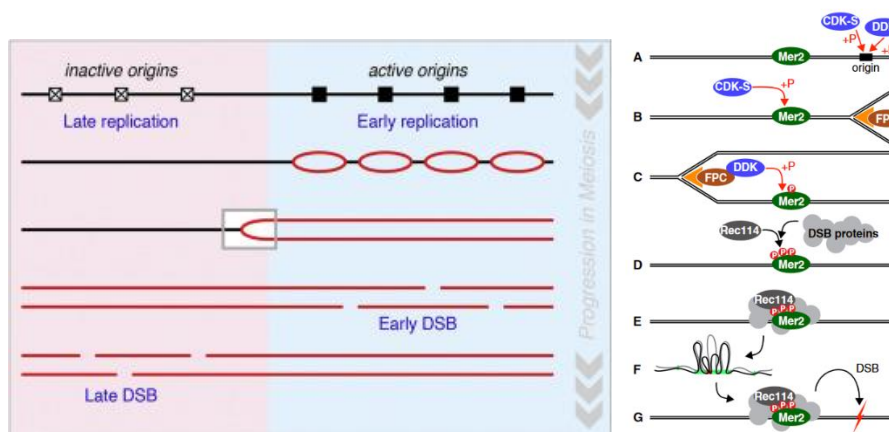


**Figure i.16.** Connection between pre-meiotic replication and meiotic recombination. DNA replication program marks the formation of early and late DSBs that may have a different recombination outcome. The proposed mechanism is that, during replication, DDK “primes” the recombination sites via phosphorylation of Mer2. (Adapted from Murakami H. and Keeney S. 2014)

It is important to note that the relation between recombination and replication is completely different in mitosis and meiosis. While mitotic recombination is a system to restart and complete genome replication, meiotic recombination serves to ensure proper chiasmata formation that allows homolog chromosomes to segregate in Prophase I (Padmore R. *et al.*, 1991).

## 4.2.2. Molecular machinery of DSB formation and recombination

The catalytic reaction for meiotic DSB formation is highly conserved in eukaryotes. Spo11, a meiosis-specific topoisomerase-like transesterase, is considered the most important protein in the formation of meiotic DSBs (Keeney S. 2001). It requires a set of accessory proteins, that varies from species, to effectively generate a DSB via a topoisomerase II-like mechanism (Diaz R.L. *et al.*, 2002; Shingu Y. *et al.*, 2010). In *S. cerevisiae*, Spo11 is accompanied by 10 different proteins, organized in 4 subcomplexes that orchestrate the formation of a DSB in different steps (reviewed in Lam I. and Keeney S. 2015; **Figure i.17**).

First, Spo11 nuclear localization and chromatin association is stabilized by Ski8, forming an initial subcomplex (Arora C. *et al.*, 2004). Simultaneously, chromatin-bound and phosphorylated Mer2 forms a complex with Rec14 and Mei4 that will help the formation of chromatin loops and chromosomal structural axes via Red1/Hop1 (Panizza S. *et al.*, 2011; **Figure i.17** right side). These loops will be the substrate for Spo11, inducing a DSB preferentially in nucleosome-free regions, thanks to the proteins Rec104 and Rec102 that bring Spo11/Ski8 to the chromosome axis (Wu T.C. and Lichten M. 1994; Ohta K. *et al.*, 1994). The final step is the recruitment of the MRX complex (Mre11-Rad50-Xrs2) for both the catalysis of DSB and the subsequent processing by resection (Borde V. *et al.*, 2004). The requirement of MRX complex to promote DSB formation is believed to ensure rapid and effective processing of DSBs (Lam I. and Keeney S. 2015).

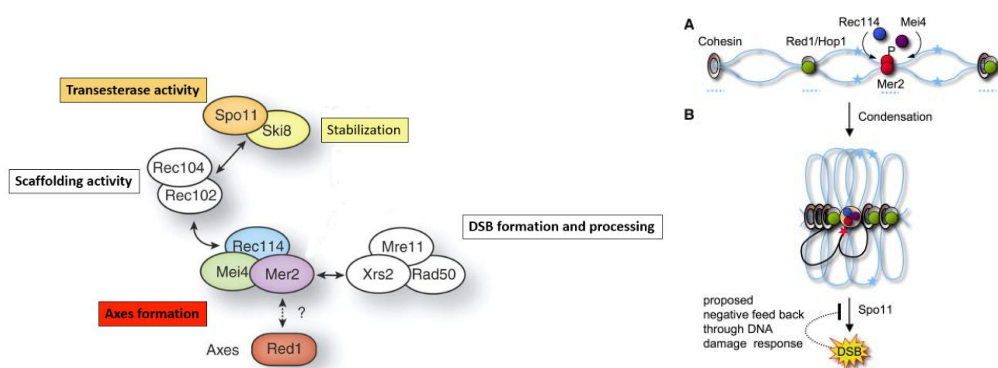


**Figure i.17. Molecular components of the Meiotic DSB formation machinery and chromosomal recombination axes.** Spo11 catalyzes a topo-isomerase II like reaction to form a DSB in the chromatin loops generated by the chromosomal axis. This process requires accessory subunits that form 4 molecular complexes. (Adapted from Panizza S. *et al.*, 2011 and Lam S. and Keeney S. 2015).

Meiotic DSBs follow a similar pathway as explained in Chapter 3.3, requiring the same molecular machinery. The meiotic recombination program resects 3' free ends, pairs homologous sequences, synthesizes DNA and resolves joint molecules. However, meiotic DSBs have a bias in processing, the most abundant HR pathways being SDSA or DSBR and leading to crossovers (CO) and non-crossovers (NCO) depending on how D-loops and dHJ are resolved (reviewed in Sanchez A. *et al.*, 2021, **Figure i.18**).

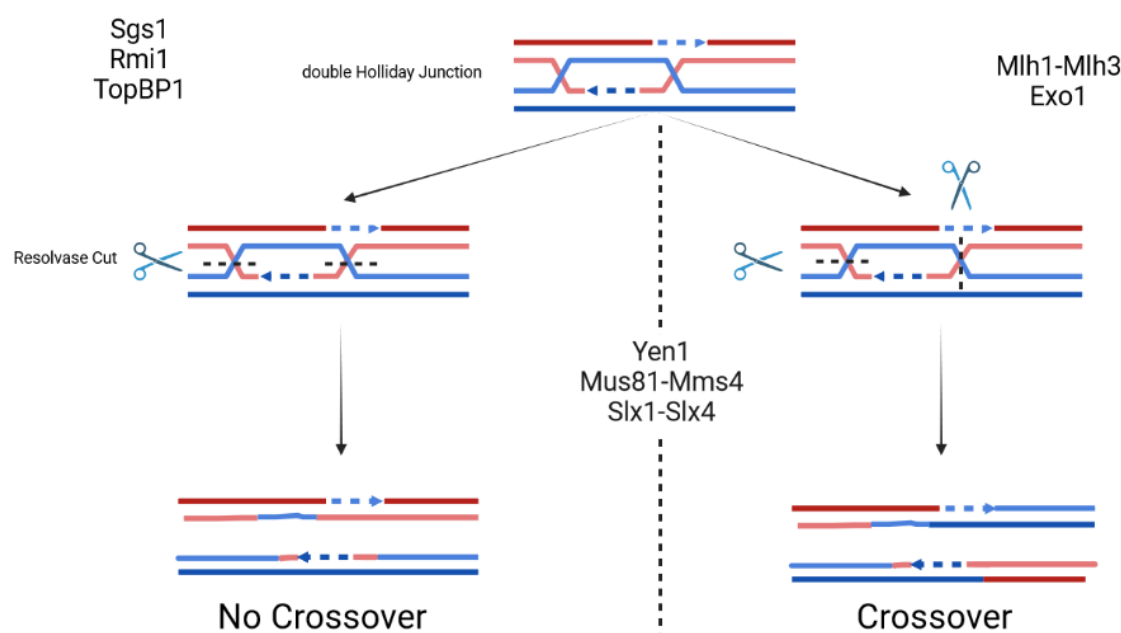


*Figure i.18. Crossover and Non-crossover formation upon meiotic recombination. Different factors can alter the outcome of a DSB into Crossover or No crossover products by processing D-loops and dHJ. Some proteins process dHJ into CO (Right pathway) while others from exclusively NCO (Left pathway). However, the outcome of a DSBs can be also decided arbitrarily (Middle proteins).*

#### **4.2.3. Regulation of Prophase I and recombination**

Meiotic recombination takes place during Prophase I, the first and longest phase of Meiosis I. It was historically named meiotic G<sub>2</sub> (reviewed in Marston A. and Amon A., 2004) but the current consensus is that cells undergo chromosome division as soon as they finish DNA replication. It is divided in 5 subphases: leptotene, zygotene, pachytene, diplotene and diakinesis (described by Oscar Hertwig in 1870; August Weismann in 1890 and Thomas Hunt Morgan in 1911).

Similar to what occurs during Mitosis, Prophase I is a state of high CDK activity, promoting chromosome condensation. However, the meiotic chromosome segregation machinery is modified to ensure the segregation of homologous chromosomes and not sister chromatids. Homologous chromosomes have contact points called chiasmata that are generated by the recombination process and observed during diplotene (Maguire M.P., 1962). Every pair of connected chromosomes, called bivalents, is interconnected by at least one chiasma and preventing its formation results chromosome mis-segregation and, ultimately, aneuploid gametes. This mechanism explains why bypassing meiotic recombination, like in *spo11Δ* mutant, generates unviable spores (Klapholz S. *et al.*, 1985). Apart from recombination, kinetochore structure is also modified in Meiosis I. Sister chromatids have to co-segregate to the same pole of the cell, thus kinetochores are fused and co-oriented due to the activity of the monopolin complex (Corbett K. *et al.*, 2011). The coordinate activity of both mechanisms allows Meiosis I to be a reductional division.

Prophase I is monitored by its own checkpoint, the Meiotic Checkpoint Network (MCN). The MCN integrates different mechanisms to ensure adequate Prophase I progression, including DDR. The latter is active due to DSBs formation and processing, both Mec1 and Tel1 being implicated (MacQueen A. and Hochwagen A. 2011; Subramanian V. and Hochwagen A. 2014). Both kinases will promote and regulate CO formation, prevent further DSBs formation, complete chromosome synapsis and provide cells enough time to complete the aforementioned events (Carballo J.A. and Cha R.S. 2007; Carballo J.A. *et al.*, 2008; Shinohara M. *et al.*, 2019). The role of the Rad53 kinase is still under debate because it is unclear if it is hyperphosphorylated and activated during Prophase I (Cartagena-Lirola H. *et al.*, 2008; Kar F.M. *et al.*, 2022). Thus, it is also proposed that meiotic DDR is adapted to DSBs formation, promoting a partial activation and rapidly processing of DSBs (Cartagena-Lirola H. *et al.*, 2008).

Finally, Prophase I progression and exit are dependent on Ndt80 and Cdc5 (Polo-kinase, **Figure i.19**). *NDT80*, a meiosis-specific transcription factor, controls the expression of *CDC5* and is the third main gene involved in meiotic commitment alongside *IME1* and *IME2* (Xu L. *et al.*, 1995; reviewed in Winter E. 2012). *NDT80* expression depends on several factors: expression of *IME1* (Gurevich V. and Kassir Y. 2010), decrease of Mec1 activity (Lydall D. *et al.*, 1996) and both S-CDK and DDK activity (Lo HC. *et al.*, 2008 and 2012). Mutant *ndt80* $\Delta$  cells arrest in pachytene, where chromosomes have started recombination but not finished it. Pachytene exit requires Cdc5, essential for the resolution of dHJ, control of the monopolin complex and loss of cohesin (Clyne RK. *et al.*, 2003).

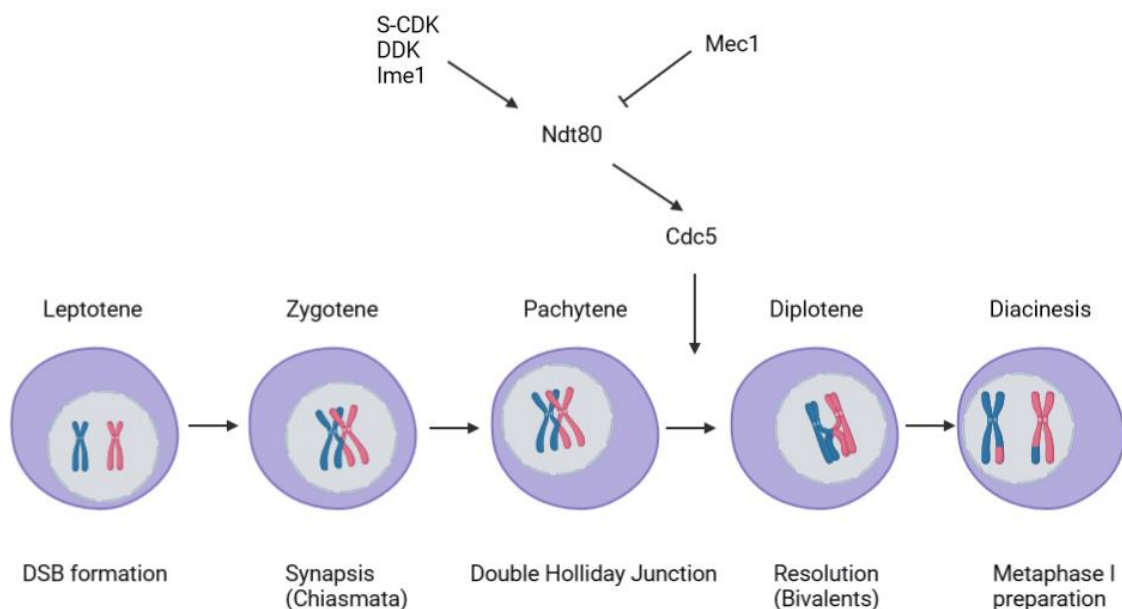


**Figure i.19. Schematic of Prophase I regulation and progression.** DSBs are formed during leptotene alongside chromosome condensation. This will promote the formation of chiasmata, helping the proper alignment of chromosomes and co-segregation of sister chromatids. Prophase I is under the control of the MCN checkpoint using Ndt80, which allows the expression of middle and late meiotic genes, promoting Pachytene exit and Prophase I completion after dHJ formation.

**Chapter ii. Consequences of extended S phase  
in *Saccharomyces cerevisiae* cells and role of  
DNA Polymerase  $\alpha$  phosphorylation**

Cell cycle regulation is essential for the correct maintenance and transmission of genetic material. However, low levels of genetic instability are tolerated and even promoted in cells as a mechanism to increase genome variability and, ultimately, to allow for genome evolution. Our interest is to understand these mechanisms not only from an evolutionary perspective, but as well as they can be exploited in pathological situations like cancer.

We focused on how HR arises as a mechanism to complete DNA replication during Mitosis (MiDAS). MiDAS has been observed in mammalian cells only upon artificial situations: treatment with low doses of DNA replication impairing agents (like aphidicolin and FdU) and in non-patient derived genetically engineered BRCA2<sup>-/-</sup> cells (Minocherhomji S. *et al.*, 2015; Garribba L. *et al.*, 2020; Bhowmick R. *et al.*, 2022; Groelly F. *et al.*, 2022). These approaches impact the normal progression of replication forks by slowing down fork velocity or favoring transcription-replication conflicts, thus delaying to mitosis the replication of certain genomic regions. However, they diverge from what can occur naturally in cells, as BRCA2<sup>-/-</sup> cells are usually genetically unstable and aphidicolin or FdU are not found in the natural cellular environment (Minocherhomji S. *et al.*, 2015; Garribba L. *et al.*, 2020). Our goal was to decipher the mechanism of MiDAS within a single cell cycle in which S phase was extended. To this end we used a conditional system that extends S phase, situation we believe could naturally occur in cells, yet at a much lower level.

We devised a system to genetically decrease origin licensing using a temperature-sensitive *CDC6* allele (*cdc6-1*). This mutant has been long known to have increased genome instability at semi-permissive temperatures of 28°C or 30 °C (Bruschi C.V. *et al.*, 1995). Here, I present several lines of evidence that the *cdc6-1* mutant can enter mitosis before having completed genome duplication, but then finishes DNA synthesis in mitosis (MiDAS) using a BIR-like mechanism, which could be the reason for the high genome instability of these cells. The use of this system allowed us to monitor the consequences of extended and incomplete DNA replication, which involves the activation of the DDR checkpoint during mitosis, leading to metaphase arrest and the formation of HR-related foci. Crucially, these phenotypes are dependent on mitotic entry, in particular on M-CDK activity. We searched for CDK substrates that are important for cells with extended S phase and identified DNA Polymerase  $\alpha$  as an essential player in this situation.

## **1.1. Origin under-licensing extends S phase and promotes metaphase arrest and MiDAS**

To understand the impact of extended S phase in cell cycle, we used a system to decrease origin licensing instead of slowing down or impairing fork progression. Cdc6 is a key licensing factor involved in the loading of MCM in telophase and G<sub>1</sub> (Zwerschke W. *et al.*, 1994). The *cdc6-1* allele is a temperature-sensitive allele that decreases its functionality with increasing temperature, presumably by decreasing its interaction with Mcm5 (Feng L. *et al.*, 2000). We defined 3 situations based on *cdc6-1* cells survival on plate; 25 °C as a permissive temperature, 30 °C as a semi-permissive temperature and 32 °C as a restrictive temperature because it was incompatible with cell growth (**Figure ii.1A**). Importantly, *cdc6-1* mutant is known to acquire GCR when grown at semi-permissive conditions (Bruschi C.V. *et al.*, 1995; unpublished data from E. Schwob).

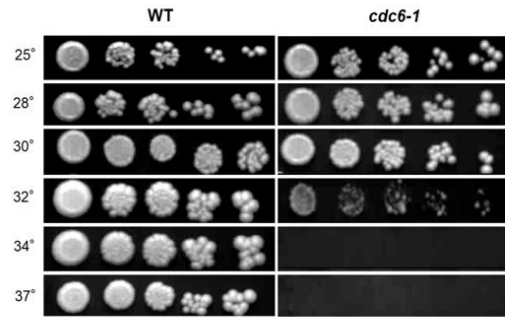
DNA combing analysis showed that origin density was barely if at all affected at 25°C (permissive temperature) in *cdc6-1* cells, while it was decreased more than 3-fold at 32°C, preventing full DNA replication and causing lethality of *cdc6-1* at restrictive temperatures (**Figure ii.1B**). We chose the semi-permissive temperature of 30 °C for our experiments because cell viability was preserved despite a 2-fold decrease in the number of active origins. At this temperature, *cdc6-1* cells replicated their DNA more slowly than *WT* cells, as measured by flow cytometry (**Figure ii.1C**). Whereas *WT* cells finished genome duplication approximately 45 min after the release from G<sub>1</sub>, *cdc6-1* cells did not complete genome replication even 60 min after the release, the estimated time of mitotic entry in these conditions. At this timepoint, we calculated that 30% of the genome was yet to be replicated.

One consequence of this extended S phase is a strong mitotic delay. Previous videomicroscopy experiments from the lab and microscopy analysis I performed showed that *cdc6-1* cells entered mitosis approximately 60 min after the release from G<sub>1</sub>, but remained in metaphase for up to 120 min, whereas *WT* control entered the next cell cycle 90 min after the release (**Figure ii.1D, Figure ii.Supp1B**). The criterion I used for the classification of mitotic phases was based on the position and morphology of the nucleus. During this long metaphase delay, cells displayed strong oscillations of their mitotic spindle, which drove the nucleus between mother and daughter cells. This phenomenon created situations where the nucleus and DNA masses were stretched between daughter and mother cells, even sometimes entirely within the daughter

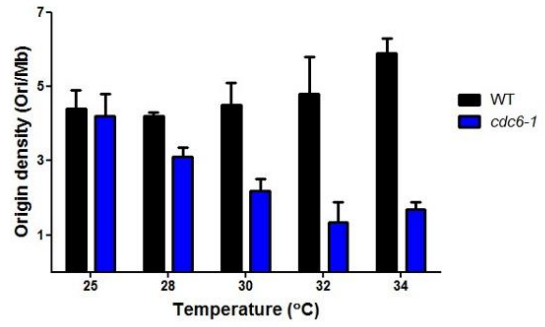
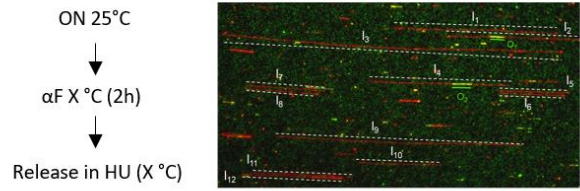
cell (Scheme in **Figure ii.1D**). However, despite the apparently stretched DNA, we believe that these cells did not transition beyond metaphase, as demonstrated in following sections.

Finally, we hypothesized that *cdc6-1* cells have to complete genome duplication during mitosis. To test this hypothesis, I performed short pulses of EdU (3 min) in *cdc6-1* cells delayed in metaphase. Microscopy analysis of EdU-pulsed cells showed a fraction of metaphase cells displayed clear nuclear EdU foci that colocalized with DAPI (**Figure ii.1E**). This indicates that *cdc6-1* cells synthesize DNA in mitosis (MiDAS) to complete genome duplication before anaphase and progression to the next cell cycle. To rule out the possibility that EdU-positive cells could be late S-phase cells and to understand the dynamics of MiDAS, I performed EdU-pulses at different times during the mitotic delay (**Figure ii.Supp1A**). I observed that both, the fraction of EdU-positive cells was higher in prophase and metaphase cells and decreased over time up to 120 min after the release. The intensity of EdU foci was strong in the early timepoints and became progressively lower when approaching anaphase. Importantly, no EdU MiDAS foci were detected in anaphase cells, suggesting that completion of MiDAS is a necessary condition for mitotic progression (**Figure ii.Supp1A**).

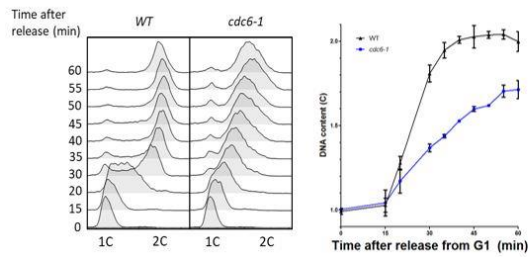
**A**



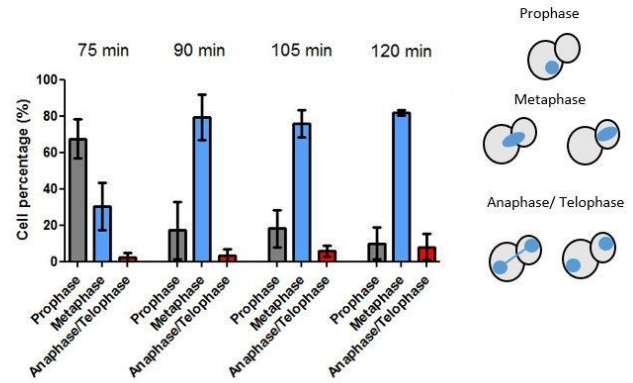
**B**



**C**



**D**



**E**

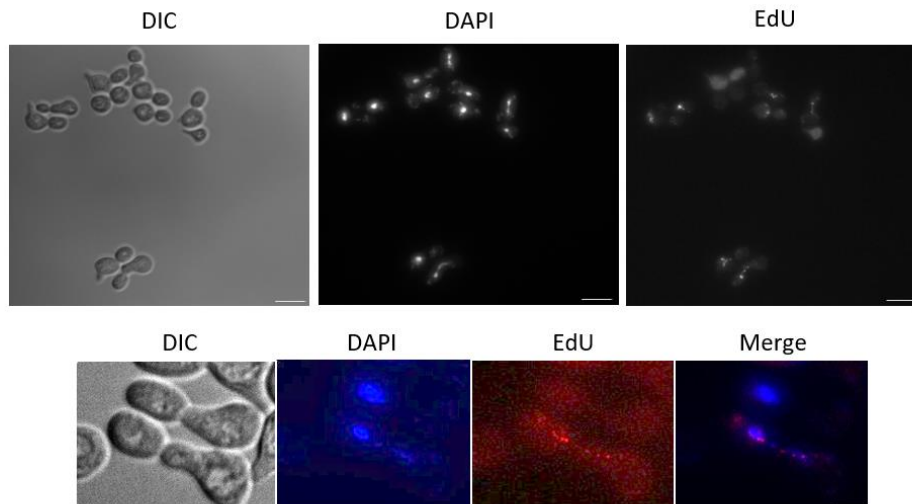


**Figure ii.1. Decrease in origin licensing extends S phase, promoting metaphase delay and MiDAS.**

(A) Top: Scheme of the licensing function of Cdc6. Bottom: Strains of the indicated genotypes were spotted at a serial five-fold dilutions on YPD plates and incubated at different temperatures to test for cell viability. (B) Top: Experimental workflow and representative images of DNA combing. Bottom: Origin density determined by DNA combing analysis of WT and *cdc6-1* cells grown at the indicated temperatures ( $n=3$ ). (C) Left: DNA content of WT and *cdc6-1* cells synchronized by  $\alpha$ -factor at 30°C and released at 30 °C. Right: quantification of the DNA content at each timepoint ( $n=3$ ). (D) Left: Percentage of *cdc6-1* cells in the different mitotic phases at the indicated time from the release of a  $G_1$  arrest at 30°C ( $n=3$ ). Right: Cartoons representing how cells were classified in the different mitotic phases (E) Representative images of MiDAS in *cdc6-1* cells (grown at 30 °C pulsed 90 minutes after release from  $G_1$  with 100 $\mu$ M of EdU for 3 min). Top: Scale bar = 10  $\mu$ m, Bottom: Scale bar = 3  $\mu$ m.

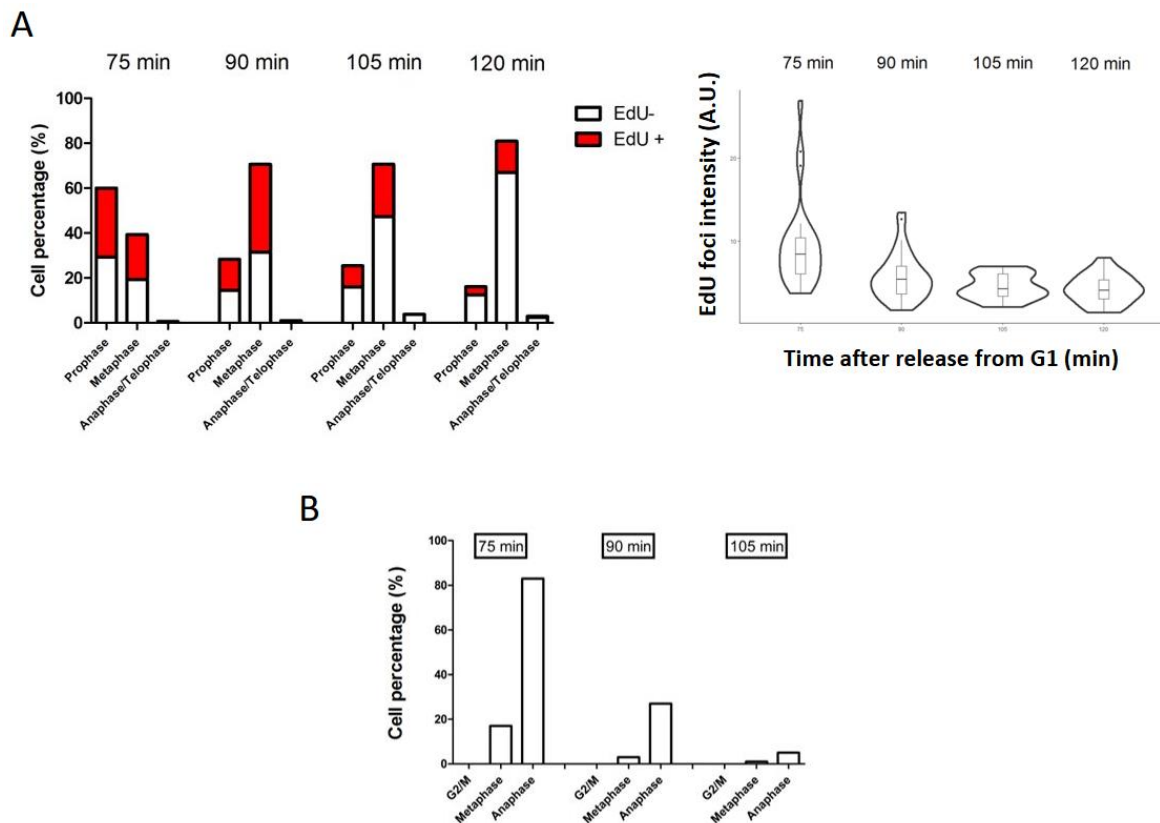


**Figure ii.Supp1. MiDAS declines during metaphase arrest.** (A) Left: Percentage of EdU-positive and EdU-negative *cdc6-1* cells in the different mitotic phases imaged at the indicated timepoints (3 min of 100  $\mu$ M EdU pulse,  $n=2$ ). Right: Quantification of the EdU signal intensity in *cdc6-1* cells at the indicated time after  $G_1$  release. (B) Percentage of WT cells in the different mitotic phases at the indicated time after  $G_1$  release.

## **1.2. Extended S phase activates the DDR checkpoint and promotes homologous recombination upon mitotic entry**

In the previous section I showed that the genetic system we used to extend S phase lead to a slower DNA replication, to MiDAS and to genetic instability in a high number of cells (as seen in Bruschi C.V. *et al.*, 1995), while having little impact on cell viability. Thus, we investigated why and how an incomplete DNA replication triggers a long metaphase delay and what occurs in these cells.

To test if DDR activation might be responsible for the long metaphase delay of *cdc6-1* cells, we checked the impact of DDR mutants (*rad53-11* and *chk1Δ*) in the context of extended S phase. This showed that a functional DDR is required for the survival of *cdc6-1* mutant at semi-permissive temperature, but dispensable at permissive conditions (**Figure ii.2A**).

This result led us to investigate further the role of the DDR checkpoint in the context of extended S phase. A simple readout to follow the DDR activation is the hyperphosphorylation level of Rad53 (Sanchez Y. *et al.*, 1996). After synchronization at 30 °C, where *cdc6-1* cells display an extended S phase, cells hyperphosphorylated Rad53 60 min after release, which is the estimated time of mitosis entry in these conditions (**Figure ii.2B, Top**). To test if mitotic entry is required for Rad53 hyperphosphorylation and DDR activation, we repeated the same experiment in conditions where mitotic entry is prevented by Swe1 overexpression. *SWE1* is the yeast ortholog of the Wee1 inhibitor of mitosis, which phosphorylates Cdk1 at Y15 (Y19 in *S. cerevisiae*) and prevents its activation by mitotic cyclins. Importantly, Rad53 was not hyper-phosphorylated in *cdc6-1* cells grown at 30°C when they were arrested in G<sub>2</sub> by Swe1 overexpression (**Figure ii.2B, Bottom**). This demonstrates that slow DNA replication caused by origin under-licensing does not activate the DDR during S phase, thus permitting mitotic entry, and that M-Cdk activity is required to convert replication forks in a structure that strongly activates the DDR in prophase and metaphase. Interestingly, blocking mitotic progression before anaphase (*MET-CDC20* arrest) or before cytokinesis (*cdc15* arrest) did not prevent Rad53 hyperphosphorylation, indicating that neither chromosome segregation, nor cell separation are responsible for DDR activation in *cdc6-1* cells (data not shown).

DDR activation may provide time for homologous recombination, which can be readily visualized by the formation of nuclear Rad52 foci (Baroni E. *et al.*, 2004; Gonzalez-Prieto R. *et al.*, 2013). We thus monitored Rad52-GFP foci formation in *WT* and *cdc6-1* cells synchronized and released from  $\alpha$ -factor arrest at 30 °C, as before (**Figure ii.2C and Figure ii.2D**). Dim Rad52 foci were observed in less than 15% of *WT* cells, which are considered as an outcome of low replication stress due to ssDNA generated at replication forks, yet insufficient to activate the DDR (Lisby M. *et al.*, 2001). In contrast, *cdc6-1* cells with an extended S phase displayed a stark accumulation of strong Rad52 foci around 40-60 min after release, which is the estimated time of mitotic entry in these conditions. Moreover, their appearance was concomitantly with Rad53 phosphorylation (**Figure ii.2C and Figure ii.2D**). In this situation, Rad52 foci were present in more than 80% of the cells, and much brighter compared to those observed in S phase; they also remained during the entire duration of the metaphase arrest. As one of the functions of Rad52 is to exchange RPA for Rad51, we also monitored the formation of RPA foci, as an indication for the presence of ssDNA. Interestingly, *RFA1-CFP* foci followed the same dynamics as Rad52 foci in *cdc6-1* cells. Prophase and metaphase cells showed intense RPA foci, concomitantly with DDR activation, which also remained during the entire duration of the metaphase arrest (**Figure ii.2D**). We conclude that *cdc6-1* cells contain vast amounts of ssDNA during the time they are arrested in metaphase, but we do not know yet if this ssDNA is only the cause for DDR activation or also a consequence of HR.

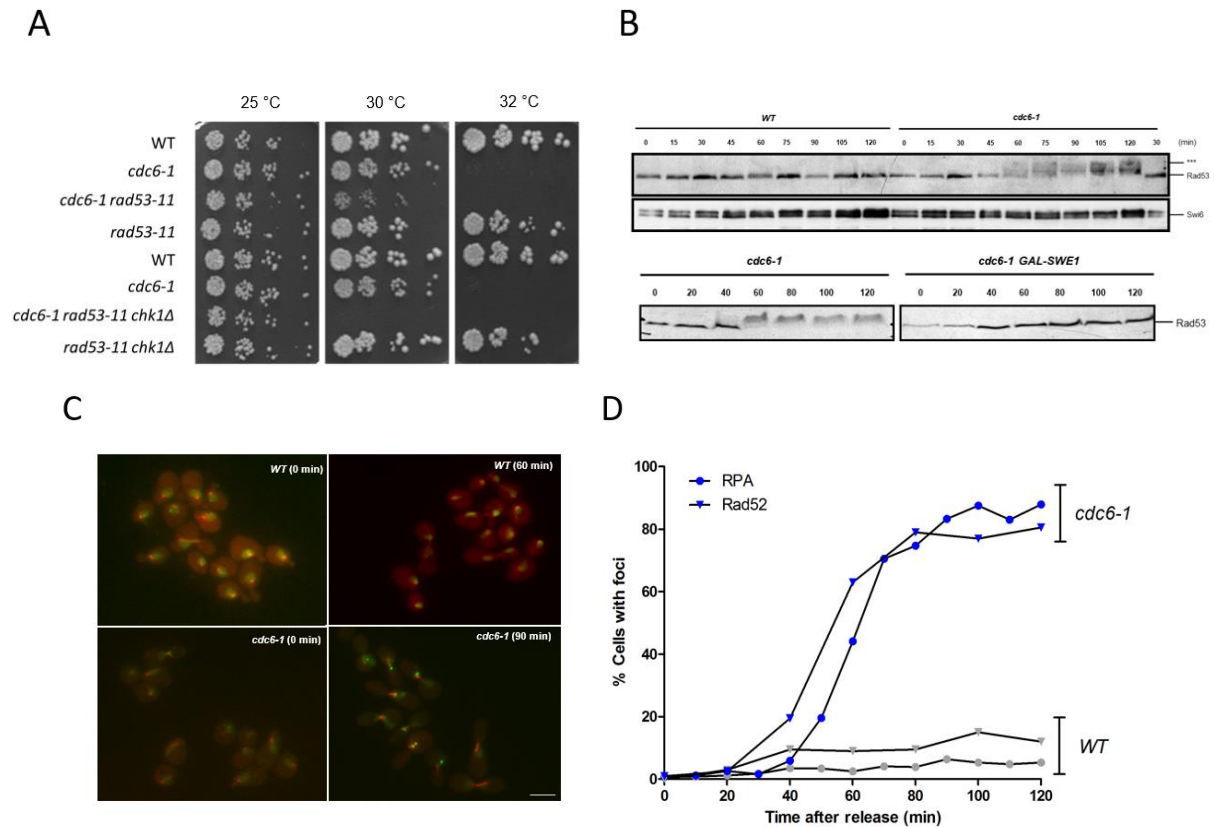


**Figure ii.2. Extended S phase activates the DDR and promotes homologous recombination upon mitotic entry.** (A) Viability of *cdc6-1* at 30 °C depends on the DDR: Strains of the indicated genotypes were spotted at a serial five-fold dilutions on YPD plates and incubated at different temperatures (B). Western blot analysis of Rad53 phosphorylation during a cell cycle. Top: WT and *cdc6-1* cells released from a G<sub>1</sub> arrest were incubated at 30 °C for the indicated time in minutes (\*\*\*) marks hyperphosphorylated form). Swi6 is used as loading control. Bottom: Rad53 phosphorylation depends on mitosis entry: *cdc6-1* and *cdc6-1* pGAL-SWE1 released from a G<sub>1</sub> arrest were incubated at 30 °C for the indicated time in minutes. (C) Representative images of Rad52-GFP foci in WT and *cdc6-1* cells grown at 30 °C in G<sub>1</sub> (0 min) or mitosis (60 min for WT and 90 min for *cdc6-1*). Scale bar = 10 μm (D) Percentage of WT and *cdc6-1* cells displaying Rad52-GFP or RFA-CFP foci, released from a G<sub>1</sub> arrest were incubated at 30 °C for the indicated time in minutes (n=3).

### **1.3. Candidate substrates of M-CDK in extended S phase: DNA Polymerase $\alpha$**

Biochemically, mitotic entry is defined by two parameters, the association of mitotic cyclins with CDK and the increase in total CDK activity. We demonstrated that cells experiencing an extended S phase activate the DDR in a M-CDK dependent manner. Therefore, we searched for mitotic CDK substrates that would be important in this context. We focused our search on replisome components known to be phosphorylated in mitosis.

DNA Polymerase  $\alpha$  had been shown to be phosphorylated during mitosis in both *S. cerevisiae* and human cells but its role has remained elusive (Foiani M *et al.*, 1995; Voitenleitner C. *et al.*, 1999). We thus tested if DNA Polymerase  $\alpha$  phosphorylation plays a role in cells with an extended S phase. First, we aimed to confirm that both Pol1 and Pol12 subunits were phosphorylated in mitosis. I immuno-precipitated PK-tagged Pol1 and Pol12 from *cdc6-1* cells 90 min after release from G<sub>1</sub> arrest at 30°C, during their extended metaphase, and mass spectrometry was performed to map phosphorylation sites on Pol1 and Pol12. We identified 29 and 26 potential phospho-sites for Pol1 and Pol12, respectively (including 14 and 16, respectively, with a high probability, **Table ii.1**). Interestingly, the identified phosphorylation sites were clustered in the IDR of both proteins and many of them matched the minimal CDK consensus S/T-P motif (6 out of 13 in Pol1; 6 out of 12 in Pol12 ; **Figure ii.3A**). This confirmed our hypothesis that Pol $\alpha$  was a M-CDK substrate in the context of an extended S phase. Thus, we decided to use preexisting phosphomutants of Pol1 and Pol12 in which all putative CDK sites were mutated to alanine (originally from Joachim Li). We named them *pol1-cdk13A*, *pol12-cdk12A*, and *pol $\alpha$ -cdk* (or *pol $\alpha$ -cdk25A*) when both alleles were combined.

It was known for long that Pol12 presented a mobility shift in mitosis (Foiani M. *et al.*, 1995). Using a Pol12 immunoprecipitation phosphatase assay, I confirmed that the shift was due to phosphorylation. Thereafter, I used the Pol12 mobility shift as a proxy for the phosphorylation status of Pol $\alpha$  (**Figure ii.3B**). Using this readout, we found that the Pol12 mobility shift appeared at 45 min after G<sub>1</sub> release, when M-CDK activity rises, and disappeared when wild-type cells entered the next cell cycle (75 min after G<sub>1</sub> release in these conditions) (**Figure ii.3B**). Interestingly, the *pol12-cdk12A* mutant showed no mobility shift throughout the cell cycle (**Figure ii.3B**). Thus, mutation to Ala of all putative CDK sites prevents the mobility shift, and potential conformational change, of Pol12 during mitosis. A similar analysis was done with Pol1, but since it is a much larger protein the phospho-shift was more difficult to monitor. We have evidence that mutating the 13 S/T-P sites of Pol1 also suppresses its shift (not shown).

We then tested the role of Pol $\alpha$  CDK phosphorylation in the context of an extended S phase. Cell viability assays presented in the following sections showed that *cdc6-1 pola-cdk* cells did not survive an extended S phase, indicating that phosphorylation of Pol $\alpha$  might be required for the completion of DNA synthesis in mitosis (**Figure ii.3C**). Importantly, we do not think that the synthetic lethality of *cdc6-1 pola-cdk* cells at 30°C is due to a lower DNA polymerase activity, as we were unable to detect any phenotype for the *pola-cdk* mutant at any temperature. We performed several tests to address the functionality of the Pol11-cdk13A and Pol12-cdk12A proteins in a normal S phase. We did not detect any defects in growth rate, cell size or S-phase duration in *pola-cdk* cells (**Figure ii.Supp2A-B**). Moreover, I did not detect any increased sensitivity to DNA damaging agents like Hydroxyurea (HU) or Methyl-Methanesulphonate (MMS) in the *pola-cdk* mutant (**Figure ii.Supp2C**). These data strongly suggest that Pol11-cdk13A and Pol12-cdk12A perform their canonical function in S phase as their wild-type Pol11 and Pol12 counterpart. Therefore, we hypothesized that the lethality observed in the context of an extended S phase was due to a different function of Pol $\alpha$  involving its phosphorylation in mitosis. A specific role for Pol $\alpha$  phosphorylation when S phase is slow would be consistent with my unexpected observation that *pola-cdk* is hyper-sensitive to MMS only when combined with the *rad5<sup>G353R</sup>* hypomorph allele present in the original W303 background. This could suggest a function of Pol $\alpha$  phosphorylation in the DNA damage tolerance pathways, as Rad5 is required for normal fork progression during MMS treatment (Ortiz-Bazan M.A. *et al.*, 2014, **Figure ii.Supp2C**).

Pol12				Pol1			
Position	Probability	Predicted CDK-site	Previously found	Position	Probability	Predicted CDK-site	Previously found
80	0.49	-	YES	3	0,59	-	YES
81	0.83	-	YES	5	0,99	-	YES
82	0.84	-	YES	31	0,99	-	YES
83	0.49	-	NO	149	0,99	-	NO
87	0.87	-	YES	169	0,97	-	YES
88	0.98	-	YES	170	0,99	Cdk	YES
97	0.48	-	YES	172	0,53	-	YES
100	0.99	-	YES	188	0,75	-	YES
101	0.99	Cdk	YES	189	0,49	-	YES
111	0.89	Cdk	YES	204	0,66	-	YES
124	0.99	-	YES	205	0,66	-	YES
126	0.99	-	YES	206	0,66	-	YES
128	0.25	-	NO	215	0,72	Cdk	YES
131	0.25	-	NO	240	0,99	Cdk	YES
136	0.95	-	YES	274	0,99	-	YES
146	0.53	-	NO	300	0,99	-	YES
147	0.44	-	NO	303	0,57	-	YES
153	0.99	Cdk	YES	304	0,57	-	YES
168	0.99	-	YES	305	0,88	Cdk	YES
180	0.9	-	YES	313	0,99	Cdk	YES
181	0.53	-	YES	321	0,80	Cdk	YES
182	0.36	-	YES	323	0,19	-	NO
185	0.99	Cdk	YES	325	0,19	-	NO
188	0.56	-	YES	328	0,99	-	YES
190	0.82	Cdk	YES	330	0,19	-	NO
304	0.99	Cdk	YES	560	0,56	-	NO
				562	0,53	-	NO
				568	0,54	-	NO
				1231	1	-	YES

*Table ii.1. Identified mitotic phosphorylated sites in Pol1 and Pol12. Phosphoproteomic analyses of Pol1 and Pol12 immuno-precipitated from mitotic cdc6-1 cells grown at 30 °C. Every potential phosphosite has an associated probability that determines the confidence of identification. A score above 0.75 indicates certainty of phosphorylation, thus a confirmed phosphosite, while below 0.75 indicates a possibility. Residues found in the same phosphopeptide are represented within the same rectangle. Residues that follow S/T-P motifs are labelled as “CDK”. If residues are found to be phosphorylated in pre-existing datasets, it is indicated in the last column.*

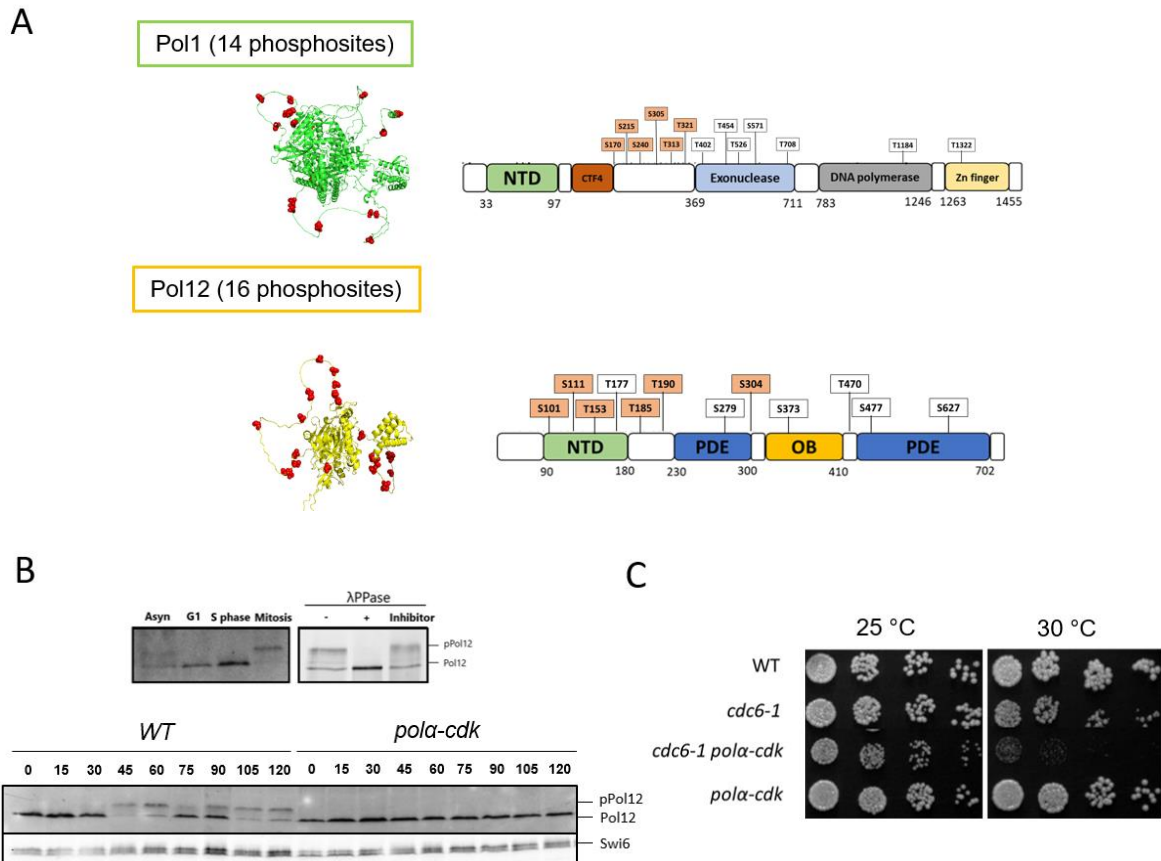


**Figure ii.3. DNA Polymerase  $\alpha$  M-CDK phosphorylation is essential for the survival of cells with extended S phase.** (A) Representation of identified phosphosites in Pol1 and Pol12. Left side: predicted structures of Pol1 (top) and Pol12 (Bottom) using AlphaFold. The confirmed phosphosites (probability >0.75) are indicated with red balls. Right: predicted CDK-sites in Pol1 and Pol12, in orange those confirmed in our phospho-mass spectrometry analysis. (B) Western blot analysis of Pol12 mobility shift. Top left: Pol12 shift occurs in mitotic cells. (Asyn = asynchronous, G<sub>1</sub> =  $\alpha$ -factor synchronized cells, S phase = HU treated cells, Mitosis = nocodazole-arrested cells). Top right: Immunoprecipitation phosphatase assay of Pol12 in mitosis. Bottom: Pol12 mobility shift depends on M-CDK phosphorylation: Western blot analysis of Pol12 and Pol12-cdk12A mobility shift: WT and pola-cdk cells released from a G<sub>1</sub> arrest were incubated at 30 °C for the indicated time in minutes. Swi6 is used as loading control. (C) Pola. CDK phosphorylation is essential for the survival of cdc6-1 cells at semi-permissive temperature: Strains of the indicated genotypes were spotted at a serial five-fold dilutions on YPD plates and incubated at different temperatures

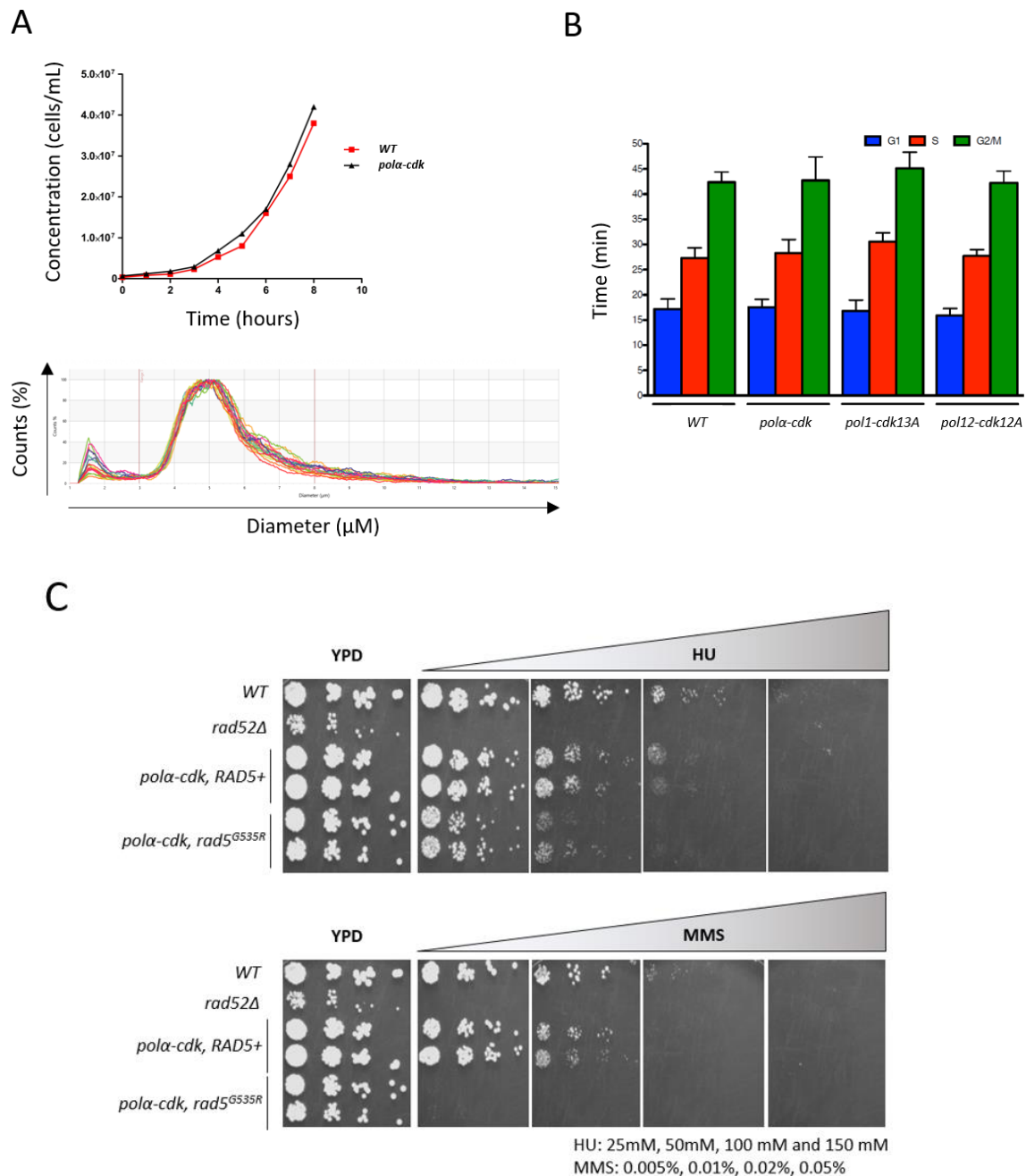


**Figure ii.Supp2. The *polα-cdk* mutants have no phenotype in normal cell cycle conditions. (A) Top: Representative growth curves of WT and *polα-cdk* mutant. Cell concentrations of exponentially growing culture were monitored at the indicated times in hours. Bottom: Overlay of WT and *polα-cdk* cell size measurements at the times indicated in the top panel (B) Cell cycle phases duration of WT and different *polα-cdk* mutants. ( $n=3$ ) (C) The *polα-cdk* mutant is not sensitive to HU or MMS, unless it is combined with *rad5<sup>G535R</sup>*: Strains of the indicated genotypes were spotted at a serial five-fold dilutions on YPD plates containing the indicated concentration of HU and MMS.**

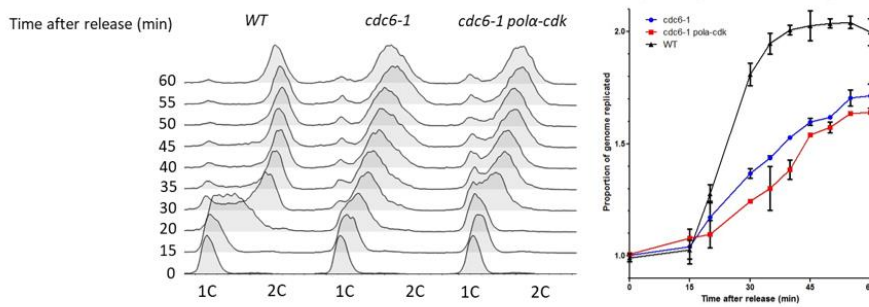
#### **1.4. DNA Polymerase $\alpha$ mitotic phosphorylation is required for DDR activation**

As Pol $\alpha$  mitotic phosphorylation is essential for the survival of cells with an extended S phase, we studied the impact of this PTM in the *cdc6-1* phenotypes at 30°C described previously.

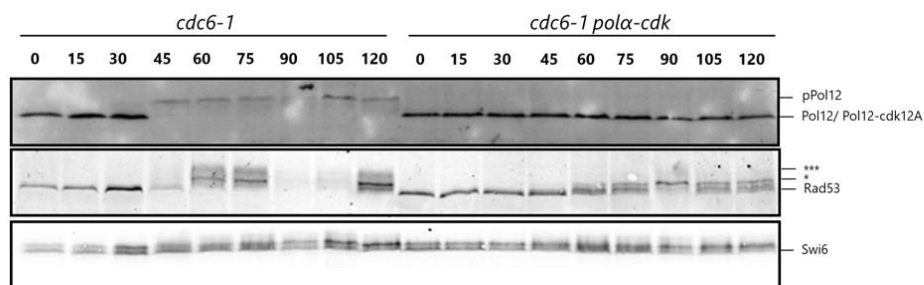
I found that *cdc6-1* and *cdc6-1 pol $\alpha$ -cdk* cells grown at 30°C had similarly slow rates of DNA replication, and reached mitotic entry (60 min) with approximately 70% of their genome duplicated (**Figure ii.4A**). However, Rad53 was not hyperphosphorylated as in *cdc6-1* cells, when Pol $\alpha$  cannot be phosphorylated by M-CDK (**Figure ii.4B**). Instead, a hypophosphorylated form of Rad53 was present in the *cdc6-1 pol $\alpha$ -cdk* mutant. This Rad53 hypophosphorylated form was seen previously in mitotic-arrested cells as a consequence of high M-CDK activity, without being related to DDR activation (Diani L. *et al.*, 2009). Our data suggests that the DDR is not active, or not fully active, during mitosis in *cdc6-1 pol $\alpha$ -cdk* cells.

As a defective DDR might impact on other *cdc6-1* phenotypes, including HR, we analyzed the formation of mitotic Rad52 foci in *cdc6-1 pol $\alpha$ -cdk* cells. We observed a more than 2-fold decrease in the number of cells with Rad52 foci, and their intensity was twice less (**Figure ii.4C**). This result indicates that *cdc6-1 pol $\alpha$ -cdk* cells have a defect in HR. Cells with Rad52 foci were also less numerous in S phase in the *cdc6-1 pol $\alpha$ -cdk* mutant as compared to the *cdc6-1* mutant (**Figure ii.4C**), indicating that the double mutant does not suffer from more replication stress during S phase. A similar trend was observed for RPA foci, with a 2-fold decrease in intensity and number of cells with RPA foci in the *cdc6-1 pol $\alpha$ -cdk* mutant (**Figure ii.4D**). Overall, these results show that the *cdc6-1 pol $\alpha$ -cdk* mutant has defects in establishing mitotic HR after an extended S phase, which could be due to the defect in DDR activation.

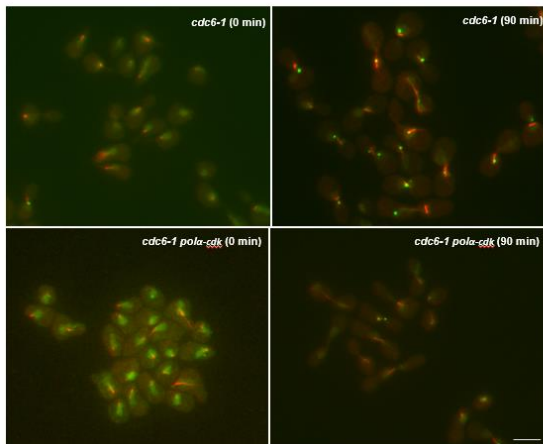
A



B



C



D

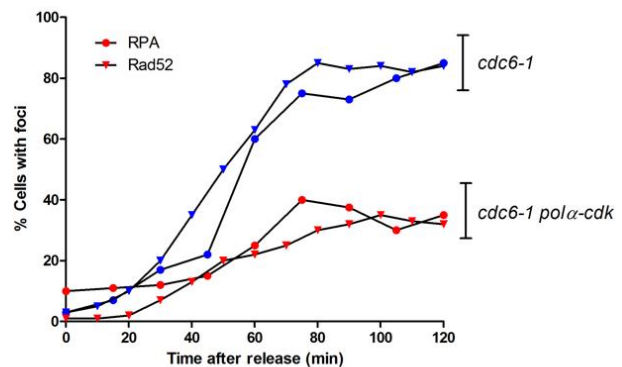


**Figure ii.4. DNA Pol $\alpha$  M-CDK phosphorylation activates the DDR in cells with extended S phase.** (A) Left: DNA content of WT, *cdc6-1* and *cdc6-1 pol $\alpha$ -cdk* cells synchronized in  $G_1$  and released at 30 °C. Right: quantification of the DNA content at each time point ( $n=3$ ) (B) Western blot analysis of Pol12, Pol12-cdk12A and Rad53 phosphorylation in *cdc6-1* and *cdc6-1 pol $\alpha$ -cdk* cells grown at 30°C (\*= hypophosphoform, \*\*\*= hyperphosphoform). Swi6 is used as loading control. Cells released from a  $G_1$  arrest were incubated at 30 °C for the indicated time in minutes. (C) Representative images of Rad52-GFP foci in *cdc6-1* and *cdc6-1 pol $\alpha$ -cdk* cells grown at 30 °C in  $G_1$  (0 min) or mitosis (90 min). Scale bar = 10  $\mu$ m. (D) Percentage of *cdc6-1* and *cdc6-1 pol $\alpha$ -cdk25A* cells displaying Rad52-GFP or RFA-CFP foci, released from a  $G_1$  arrest and incubated at 30 °C for the indicated time in minutes ( $n=3$ ).

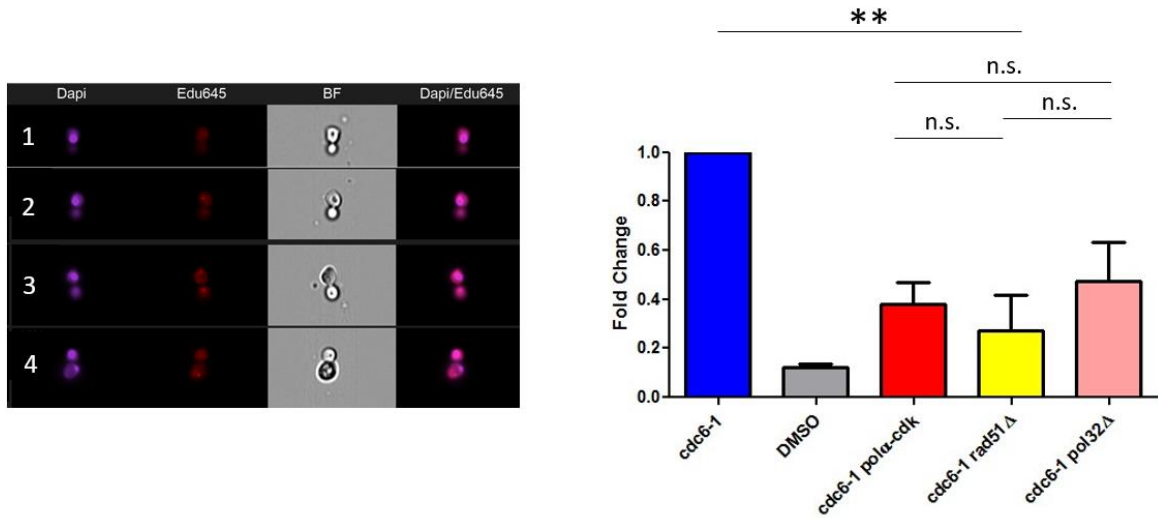
### **1.5. MiDAS in *cdc6-1* cells requires DNA Polymerase $\alpha$ phosphorylation and canonical BIR components**

After determining that Pol $\alpha$  phosphorylation promotes DDR and HR in mitosis of cells with an extended S phase, the next logical step was to test if the lack of Pol $\alpha$  phosphorylation also perturbs MiDAS. To address this question, I used Quantitative Image-Based Cytometry (QIBC) to monitor MiDAS in EdU-pulsed metaphase *cdc6-1* cells. Cells were synchronized in G<sub>1</sub> with  $\alpha$ -factor and released at 30 °C, then EdU was added for 10 min 90 min after the release. This timepoint was chosen because MiDAS is clearly detected in metaphase-delayed cells, but also to lower the probability of analyzing late S-phase cells (**Figure ii.Supp1A**). Mitotic cells were processed and analyzed based on specific criteria explained in Material and Methods, discriminating between MiDAS-positive cells (**Figure ii.5A**, categories 2 and 3) and MiDAS-negative cells (**Figure ii.5A**, categories 1 and 4).

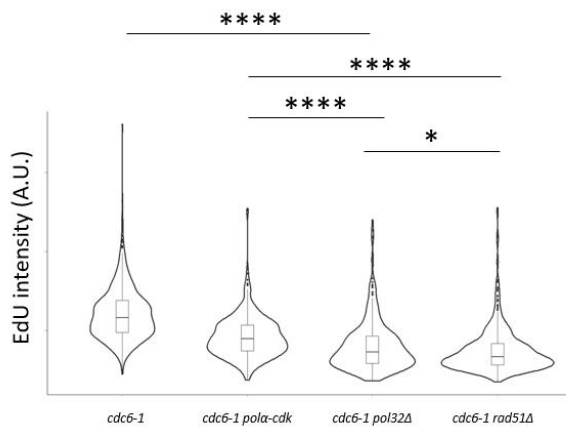
QIBC analysis showed that *cdc6-1 pola-cdk* had twice less MiDAS-positive cells compared to *cdc6-1* cells, yet was not completely abolished (**Figure ii.5A**). Like for Rad52 and RPA foci, EdU foci were also significantly less intense in *cdc6-1 pola-cdk* than in *cdc6-1* cells (**Figure ii.5B**). To test whether this EdU incorporation corresponds to recombination-dependent DNA synthesis, I repeated the experiment in *cdc6-1* cells lacking the HR factors Rad51 and Pol32, also shown important for MiDAS in mammalian cells (Minocherhomji S. *et al.*, 2015; Garribba L. *et al.*, 2020; Wassing I. *et al.*, 2021). Crucially, both *cdc6-1 pol32 $\Delta$*  and *cdc6-1 rad51 $\Delta$*  had fewer MiDAS-positive cells compared to control and dimmer nuclear EdU signal (**Figure ii.5A-B**). Interestingly, Pol32 is also essential for the survival of *cdc6-1* at semi-permissive temperature, and so was Pif1 helicase (**Figure ii.5C**), which are both components of BIR (Davis A.P. *et al.*, 2004; Malkova A. 1996; Lydeard J.R. *et al.*, 2010). These results indicate that:

- MiDAS in budding yeast with extended S phase relies on HR components, similar to mammalian cells, possibly using a BIR-like mechanism, and it is essential for their survival.
- DNA polymerase  $\alpha$  phosphorylation is required for efficient MiDAS in budding yeast.

A



B



C

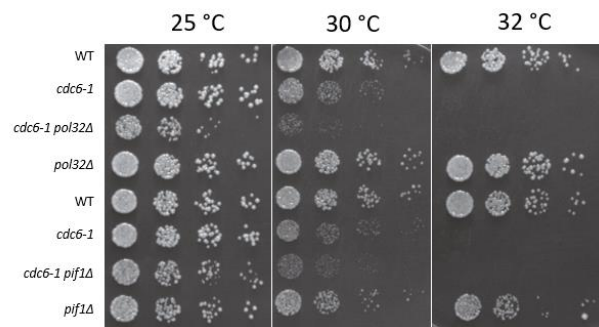


**Figure ii.5. *Pola* CDK phosphorylation is required for efficient MiDAS.** (A) Left: Representative images of budding yeast MiDAS observed with QIBC (1=MiDAS-negative cells. 2= MiDAS-positive cells. 3= MiDAS-positive cells with multiple foci. 4=Mitotic cells displaying extranuclear EdU focus). Right: Quantification of MiDAS-positive cells (normalized to *cdc6-1* as positive control,  $n=2$ ). Statistical test: An unpaired two-tailed *t*-test between the indicated strains is shown by \*\* ( $p < 0.001$ ). (B) Nuclear EdU intensity quantification in MiDAS-positive cells. Statistical test: An unpaired two-tailed *t*-test between the indicated strains is shown by \* ( $p < 0.01$ ) and \*\*\*\* ( $p < 0.001$ ). (C) Components of BIR are essential for *cdc6-1* survival at semi-permissive temperature: Strains of the indicated genotypes were spotted at a serial five-fold dilutions on YPD plates and incubated at different temperatures

## **1.6. Pol $\alpha$ CDK phosphorylation is required to maintain a metaphase arrest in conditions of extended S phase**

We identified Pol $\alpha$  M-CDK phosphorylation as a critical player in cells with extended S phase. This posttranslational modification is essential for the survival of cells with slow DNA replication and promotes several processes deriving from this situation: DDR activation, HR and MiDAS. All these processes might conceivably depend directly and individually on the phosphorylation of Pol $\alpha$ . Alternatively, the defect in DDR activation may not give cells sufficient time in metaphase to mount a solid HR and MiDAS. I therefore decided to compare mitotic progression in *cdc6-1* and *cdc6-1 pol $\alpha$ -cdk* mutants.

First I monitored DNA content by flow cytometry and found that, in contrast to *cdc6-1* cells, *cdc6-1 pol $\alpha$ -cdk* cells reentered G<sub>1</sub> starting at 105 min after the release, showing a 1C peak that increased with time (**Figure ii.6A**). This peak corresponds to cells that proceeded to the next cell cycle, indicating that at least a fraction of *cdc6-1 pol $\alpha$ -cdk* cells did not arrest in metaphase as long as *cdc6-1* cells. This was consistent with a faster appearance of telophase cells, compared to *cdc6-1* (**Figure ii.6B**).

To further investigate this, I monitored the levels of the mitotic cyclin Clb2 and the CDK inhibitor Sic1 as biochemical markers of mitotic entry and exit, respectively, in synchronous cultures of *cdc6-1* and *cdc6-1 pol $\alpha$ -cdk* cells at 30°C (**Figure ii.6C**) (Nasmyth K., 1993; Schwob *et al.*, 1994; Toyn J.H. *et al.*, 1997). Sic1 was abundant in G<sub>1</sub> and rapidly degraded before S-phase entry in both cultures, as expected. However, Sic1 reaccumulated much more slowly in later timepoints in *cdc6-1* than in *cdc6-1 pol $\alpha$ -cdk* cells, indicating that the latter progress more efficiently towards telophase and G<sub>1</sub> (**Figure ii.6C**). Clb2 behaved as a mirror image to Sic1, remaining present for a longer time in *cdc6-1* compared to *cdc6-1 pol $\alpha$ -cdk* cells that degraded Clb2 starting at 105 min (**Figure ii.6C**). These results demonstrate that *cdc6-1 pol $\alpha$ -cdk* cells exit mitosis faster than *cdc6-1* cells after an extended S phase, and that Pol $\alpha$  phosphorylation is therefore required for a prolonged metaphase arrest.

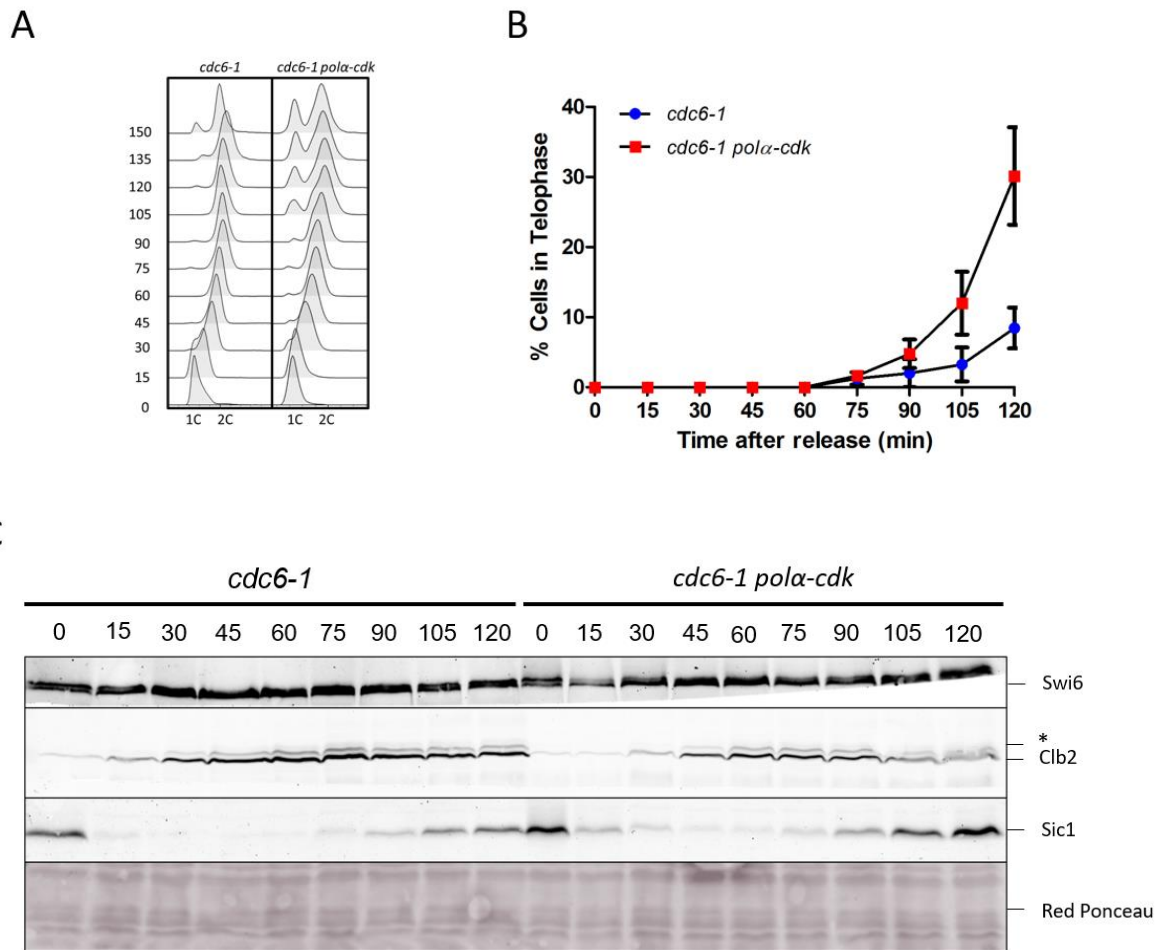


**Figure ii.6. *Pola* CDK phosphorylation is required for a prolonged metaphase arrest.** (A) DNA content by flow cytometry analysis of *cdc6-1* and *cdc6-1 polα-cdk* cells synchronized in  $G_1$  and released at 30 °C. (B) Percentage of *cdc6-1* and *cdc6-1 polα-cdk* cells in telophase: cells released from a  $G_1$  arrest were incubated at 30 °C for the indicated time in minutes ( $n=3$ ). (C) Western blot analysis of Sic1 and Clb2 in *cdc6-1* and *cdc6-1 polα-cdk* cells grown at 30 °C. \* marks phosphorylated Clb2. Swi6 and Ponceau Red are loading controls.

### **1.7. Slowing down mitotic exit ectopically rescues *cdc6-1 pola-cdk* lethality**

A key question is to understand why the *cdc6-1 pola-cdk* mutant is not able to survive an extended S phase. Is it because of premature mitotic exit or because MiDAS is defective? We reasoned that if an artificially extended mitosis were to rescue the lethality of *cdc6-1 pola-cdk* cells, it would mean that it stems mainly from the precocious mitotic exit and lack of time to perform MiDAS, rather than Pol $\alpha$  phosphorylation being directly required for MiDAS.

To this end, I first analyzed cell viability of *WT*, *cdc6-1* and *cdc6-1 pola-cdk* cells after one extended S phase, using a colony forming unit (CFU) assay. I incubated at 30 °C for different times asynchronously growing cultures of the various strains, then plated and incubated them at permissive temperature to determine the number of survivals (**Figure ii.7A**). *WT* and *cdc6-1* cells kept a good viability independently of the time spent at 30 °C. In contrast, *cdc6-1 pola-cdk* cells lost 50% of their viability after 2-3 hours at 30 °C, i.e. already after the first extended S phase (**Figure ii.7B**).

To test if extending mitosis independently of DDR would rescue this lethality, I incubated cells with non-cytostatic doses of the microtubule-depolymerizing agent nocodazole (Wang Y. and Burke D.J., 1995). I determined 1 $\mu$ M nocodazole as our working concentration because it did not impact *WT* CFU, but strongly decreased the viability of the *bub1 $\Delta$*  mutant (SAC-deficient mutant; **Figure ii.7C**). The treatment with nocodazole was performed during the incubation at 30 °C. Crucially, slowing down mitotic progression with this low dose of nocodazole was sufficient to restore the viability of *cdc6-1 pola-cdk* cells to the level of *WT* and *cdc6-1* cells, while *WT* and *cdc6-1* viability were unaltered by the treatment (**Figure ii.7B**). Therefore, extending mitosis by activating the SAC fully suppresses the lethality of *cdc6-1 pola-cdk* cells, indicating that the main reason for this lethality is precocious anaphase and mitotic exit. Interestingly, while *WT* and *cdc6-1* had similar colony size after plating, *cdc6-1 pola-cdk* cells treated with nocodazole displayed a variety of colony sizes, and this growth defect persisted after replating these cells at permissive temperature (**Figure ii.7D**). This suggests that although nocodazole has restored viability to *cdc6-1 pola-cdk* cells, the latter may have generated genomic variants of compromised fitness.

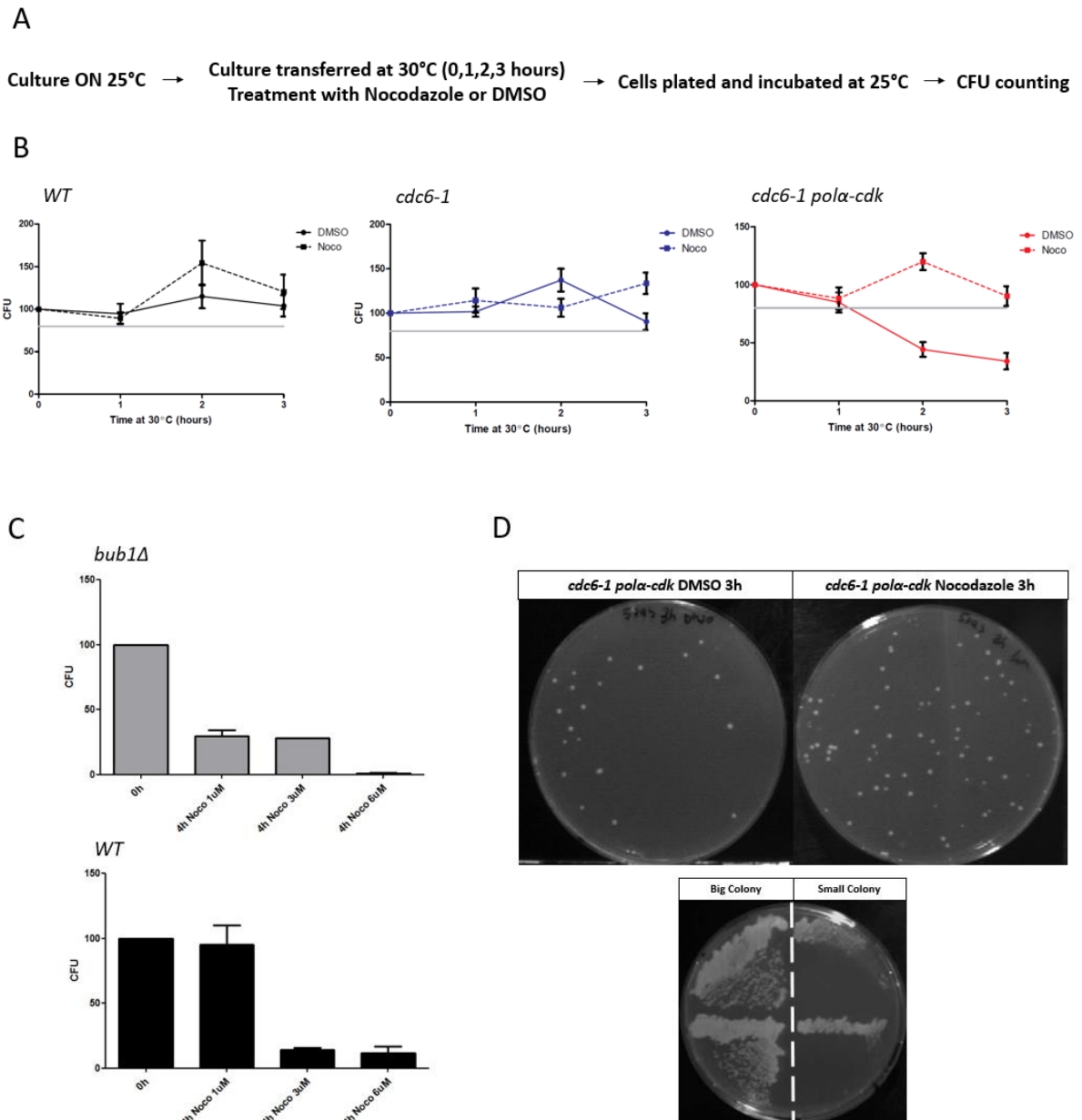


**Figure ii.7. Artificial mitotic extension rescues *cdc6-1 polα-cdk25A* lethality.** (A) Experimental workflow. (B) CFU of WT, *cdc6-1* and *cdc6-1 polα-cdk* strains after incubation at 30 °C for 0, 1, 2 or 3 hours with DMSO (line) or nocodazole (dashed line). Gray bar indicates CFU=80 (n=3). (C) Nocodazole toxicity in *bub1Δ* and WT cells: CFU of WT and *bub1Δ* cells prior to or after a 4h treatment with increasing concentration of nocodazole (n=3). (D) Representative plates of *cdc6-1 polα-cdk* CFU obtained following a treatment with DMSO (top left) or nocodazole (top right). Bottom: A representative plate of small and large CFU streaked for single colonies.

## **1.8. Pol $\alpha$ phosphorylation controls its association to chromatin and interaction with the replisome**

We showed that DNA Polymerase  $\alpha$  phosphorylation is an essential player for the survival of cells with an extended S phase, being required for an efficient DDR, prolonged metaphase arrest and efficient MiDAS, but we do not have information on the consequences, at the molecular level, of this phosphorylation.

It is known that Pol $\alpha$  is evicted from chromatin in mitosis (Desdouets C. *et al.*, 1998), so we tested if Pol $\alpha$  M-CDK phosphorylation is required for this process. We performed cellular fractionation assay in *WT* and *cdc6-1* to monitor Pol1 and Pol12 binding to chromatin, using Orc6 as a chromatin-bound marker and Pkg1 as a non-chromatin bound marker. We saw that phosphorylation of Pol12 was concomitant with its eviction from chromatin, both in *WT* and *cdc6-1* cells, and that only the phosphoform of Pol12 was released from chromatin (**Figure ii.8A**). The same experiment performed with the *pola-cdk* mutant showed that Pol12 was never evicted from chromatin, neither in *WT* nor *cdc6-1* cells at any cell cycle stage (**Figure ii.8A**). We also monitored Pol1 and Pol1-cdk13A chromatin binding; Pol1 was evicted from chromatin in mitosis but not in its non-phosphorylatable form (data not shown). We concluded that mitotic phosphorylation of both Pol1 and Pol12 by M-CDK causes its release from chromatin (**Figure ii.8B**). Interestingly, this removal of Pol $\alpha$  from chromatin is not essential in normal cell cycle conditions, but is crucial in cells with an extended S phase. We speculate that the persistence of Pol $\alpha$  on chromatin in mitosis is the reason for the lethality of cells with an extended S phase.

As the CMG is known to be disassembled at mitotic entry (Deng L. *et al.*, 2019), concomitantly with Pol $\alpha$  eviction, we wondered if both events are linked. To test this hypothesis, I analyzed the interactome of Pol1 in S phase, as well as that of Pol1 and Pol1-cdk13A in mitosis, in synchronous *cdc6-1* cultures at semi-permissive temperature.

Our mass spectrometry analysis detected 27 proteins highly enriched in Pol1 coimmunoprecipitations compared to negative control (untagged Pol1). These proteins comprised 7 groups: “Pol $\alpha$  complex”, “CTF4/CMG complex”, “FACT complex”, “HR-related”, “Fork Protection Complex”, “Heat Shock proteins and chaperones” and “Unknown” (**Figure ii.8C**). The fact that the majority of proteins bound to Pol1 in S phase are replisome components was already an indication that our immunoprecipitation was highly specific. Pol1 pulled down the 3 other subunits of the Pol $\alpha$  complex, as expected, but also proteins from Ctf4, CMG, FACT and FPC complexes (**Figure ii.8C-D**). This data indicate that we can detect known Pol1 interactors, like Pol12 or Ctf4 (Villa F. *et al.*, 2016), but also undocumented and possibly indirect Pol1 interactors, like Mrc1 or Pob3.

Strikingly, *cdc6-1* cells harvested in mitosis, at a time they still synthesize DNA, showed a different Pol1 interactome. Indeed, only Pol12, Pri1 and Pri2 were bound to Pol1, but no other replisome component (**Figure ii.8D**). This suggests that Pol $\alpha$  phosphorylation in mitosis causes its dissociation, as an intact tetramer, from the replisome. It does not answer, however, to what happens to the rest of the replisome when cells enter mitosis. Importantly, repeating the same mitotic Pol1 interactome analysis, but this time with the non-phosphorylatable Pol $\alpha$ -cdk form, restored its association with Ctf4, CMG, FACT and 2 members of the FPC (**Figure ii.8D**). This indicates that Pol $\alpha$  phosphorylation by M-CDK represents the main mechanism of fork remodeling upon mitotic entry, and that either CMG remains bound or that its removal from chromatin depends on Pol $\alpha$  phosphorylation.

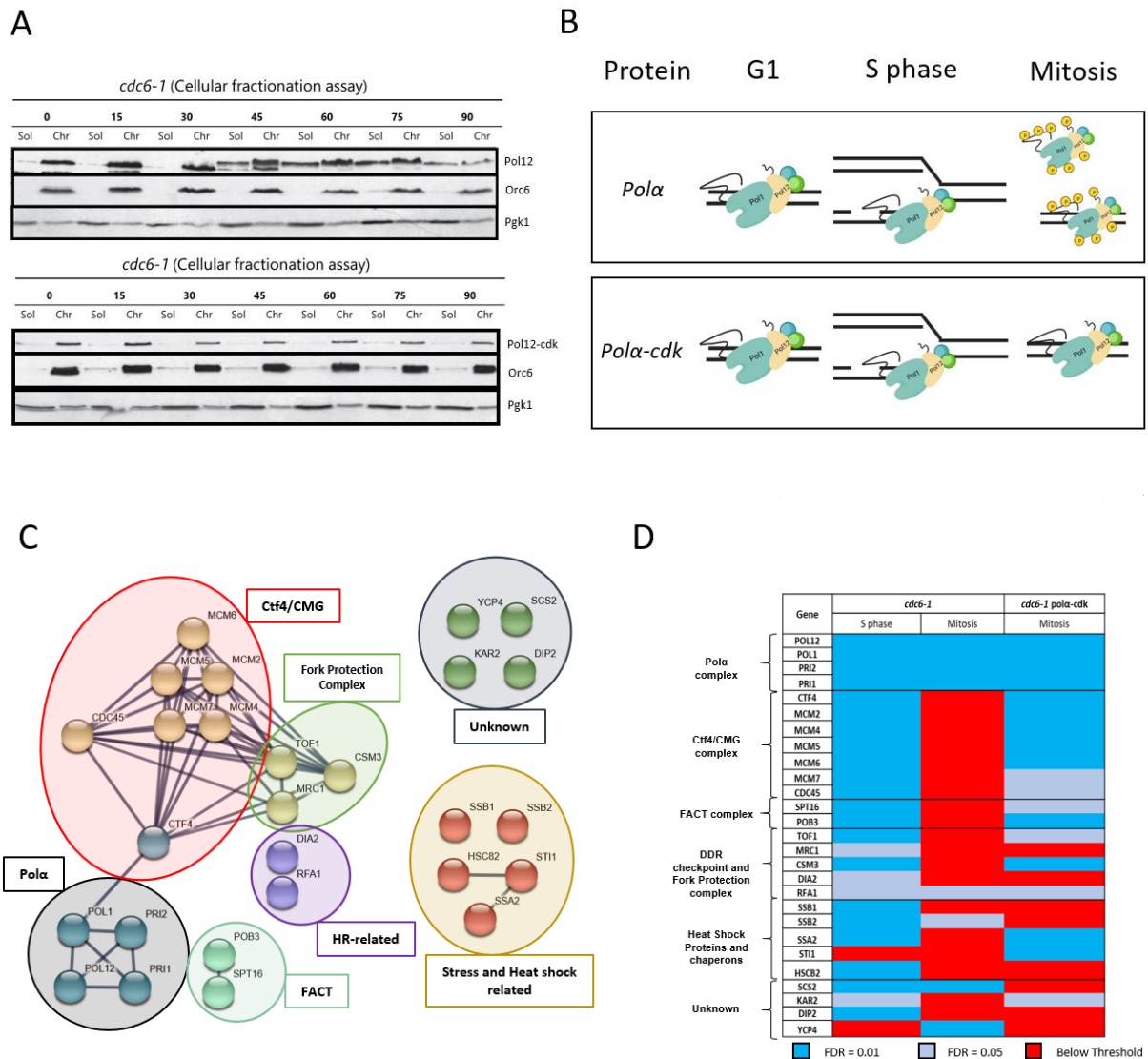


**Figure ii.8. *Pol $\alpha$*  eviction from chromatin and interactors depend on its phosphorylation status. (A) Cellular fractionation assay. Western blot monitoring the distribution between chromatin (Chr) and soluble (Sol) fractions of *Pol12*, *Pol12-ckd*, *Orc6* and *Pgk1*. *cdc6-1* cells synchronized in *G*<sub>1</sub> were release at 30 °C for the indicated time in minutes. (B) Schematic of *Pol $\alpha$*  and *Pol $\alpha$ -ckd* chromatin binding dynamics through the cell cycle. (C) Representation of proteins found in the interactome of *Pol12*, organized in 7 groups. Lanes between nodes represent functional and physical interaction between proteins (based on Biogrid STRING analysis with 0.900 confidence score). (D) Summary of the interactomes of *Pol12* and *Pol12-ckd13A* in S phase and mitosis (FDR = False Discovery Ratio, *n*=3).**

## **1.9. Summary of results in Project I**

- Cells can survive an extended S phase at the expense of genome stability.
- Incomplete and ongoing DNA replication activates DDR upon mitotic entry.
- DDR activation promotes metaphase arrest, homologous recombination and MiDAS, essential for the survival of cells with extended S phase.
- Budding yeast MiDAS after extended S phase depends on canonical BIR factors.
- DNA Polymerase  $\alpha$  is a M-CDK substrate essential for the activation of DDR, efficient MiDAS and, ultimately, survival of cells with an extended S phase.
- The function of Pol $\alpha$  phosphorylation is to allow its eviction from chromatin and to allow recombination-dependent DNA synthesis.

*Active replication forks are subjected to remodeling in mitosis due to M-CDK activity. This allows DDR activation, facilitating both HR and MiDAS. DNA Pol $\alpha$  CDK phosphorylation is essential in this process, releasing the complex from chromatin and disrupting its interactions with the replisome.*

## **1.10. Discussion Project I**

In this project, we studied the consequences of S-phase extension by lowering the number of active origins on cell cycle progression and genome instability. We show that in these conditions budding yeast cells perform DNA synthesis in prophase-metaphase and share similarities to the proposed mechanism of human MiDAS. These cells acquire genome instability in exchange for their survival, which is dangerous but also a means to create new genome variants. Importantly, we demonstrated that M-CDK activity is essential for this process and we proposed a model where replication forks are subjected to a remodeling upon mitotic entry to allow efficient DDR activation and HR. We also demonstrate that Pol $\alpha$  phosphorylation and eviction from chromatin is a critical event for fork remodeling, compromising cell survival if it does not occur.

### **The DDR is activated after, not during the extended S phase**

First, our results with the *cdc6-1* model confirm that DDR during S phase does not detect a decrease of the DNA synthesis rate. A 2-fold reduction of active origins was sufficient to slow down DNA replication without triggering DDR during S phase, allowing for mitotic entry with incomplete genome duplication. In this situation, cells only detect replication forks during mitosis by remodeling them, which activates the DDR and promotes HR repair pathways. Our explanation for the lack of DDR activation during S phase of *cdc6-1* cells at semi-permissive temperature is that forks progress fully unperturbed and moreover with a reduced number of them, thus without generating enough ssDNA that could activate Mec1. This also strengthens the idea that budding yeast checks neither origin licensing, nor DNA synthesis rate, nor replication completion, consistent with previous work showing that cells enter mitosis on time and perform cell division even when licensing and DNA replication are fully prevented (Piatti S. *et al.*, 1995; Torres-Rosell J. *et al.*, 2007; Dulev S. *et al.*, 2009). It would be interesting to check whether the scenario described here for *cdc6-1* cells holds for other mutants known to have a slower replication and high GCR rates, like *sic1 $\Delta$*  or *clb5 $\Delta$*  (Epstein C. B. and Cross F. R., 1992; Schwob E. and Nasmyth K., 1993; Schwob E. *et al.*, 1994; Lengronne A. and Schwob E., 2002).

A functional DDR checkpoint is essential for the survival of cells with an extended S phase, as we detected loss of viability in *cdc6-1 chk1Δ* and *cdc6-1 rad53-11* at semi-permissive temperature. For this reason, we study the physiological response to an extended S phase by focusing our studies on the DDR checkpoint. Of note, we did not investigate the role of SAC as we detected no viability loss of *cdc6-1* in combination with SAC mutants (e.g. *cdc6-1 mad2Δ*, **Figure ii.9**). However, we cannot exclude the possibility that the SAC could cooperate with the DDR in arresting cells in mitosis (as proposed in Magiera M. *et al.*, 2014). It could be interesting to study if *cdc6-1 mad2Δ* or *cdc6-1 bub1Δ* have defects in metaphase arrest upon extended S phase, by monitoring cell cycle markers like Clb2 or Sic1, or even defects in MiDAS.

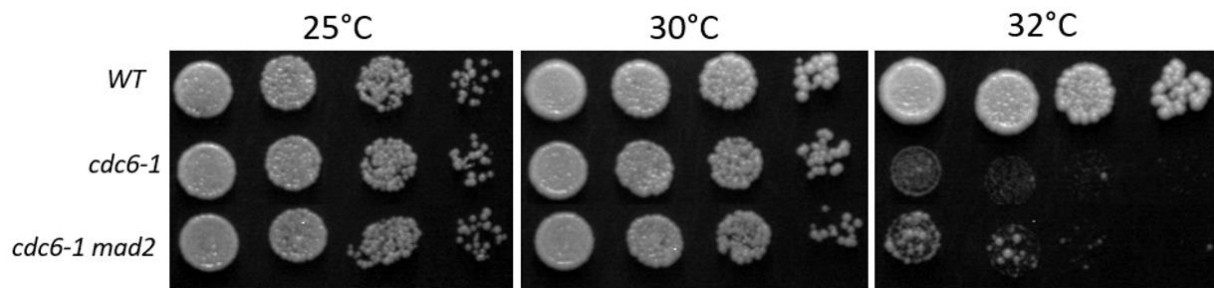


**Figure ii.9.** SAC is not required for survival of *cdc6-1* mutant. Strains of the indicated genotypes were spotted at a serial five-fold dilutions on YPD plates and incubated at different temperatures.

Our findings suggest that replication forks are the element that activates DDR in mitosis after an extended S phase. Indeed, it has been long known that replication forks are incompatible with a mitotic environment, as seen in cell fusion experiments where replicating chromosomes got “pulverized” upon exposure to a mitotic cytoplasm (Rao P.N. and Johnson R.T., 1970). The proposed mechanism is that high M-CDK activity promotes disassembly of the replisome and generate breaks and complex chromosome rearrangements (Deng L. *et al.*, 2019). However, there is no report about mitotic unloading of the CMG in budding yeast and no known yeast orthologue of TRAIIP ubiquitin ligase, required for this process in metazoan (Sonneville R. *et al.*, 2019). For the moment, we confirm that Pol $\alpha$  is evicted from chromatin during mitosis when it is phosphorylated (Desdouets C. *et al.* 1998). We also prove that it disrupts all interactions between Pol $\alpha$  and the replisome. Importantly, our interactome data of the Pol1-cdk mutant show that Pol $\alpha$  maintains its interactions with the replisome in mitosis when it cannot be phosphorylated, and this persistent interaction is the reason why the DDR is

not activated. This suggests that the presence of active replication forks during mitosis is not sufficient to activate the DDR, and that forks need to be remodeled, at least by evicting Pol $\alpha$ .

How remodeled replication forks activate DDR is still unclear. DDR activation operates via Mec1/Tell1, recognizing either ssDNA or DSBs (Sanchez Y. *et al.*, 1996). As we detect the formation of Rad52 repair foci and RPA foci in mitotic cells after an extended S phase, one could possibly argue that fork remodeling and eviction of replisome components (including Pol $\alpha$ ) exposes ssDNA and triggers DDR. We draw two possibilities:

- Pol $\alpha$  phosphorylation triggers DDR activation by itself, possibly by uncoupling lagging strand synthesis and helicase activity, leading to long tracks of ssDNA.
- Pol $\alpha$  phosphorylation promotes the eviction of other replisome components, exposing ssDNA in both leading and lagging strands.

To test this hypothesis, we need to investigate more in detail the mechanism of replisome disassembly, and monitor which replisome components are maintained on chromatin during MiDAS.

Importantly, it is also known that BIR can accumulate ssDNA due to the asynchronous synthesis of Watson and Crick strands (Wilson M.A. *et al.*, 2013). As we demonstrate that budding yeast MiDAS uses components of the BIR machinery, we cannot exclude that RPA foci are an outcome of this synthesis. We are currently running experiments in *cdc6-1 pol32 $\Delta$*  and *cdc6-1 rad51 $\Delta$*  yeast strains to determine if mitotic RPA foci are formed and if DDR is active when MiDAS is reduced. Moreover, we consider to perform live microscopy of *cdc6-1* with tagged RPA and Rad52 proteins. This will determine whether RPA and Rad52 foci formation are concomitant or sequential and if they colocalize, giving a complementary insight on how the mechanism works.

Finally, we consider only ssDNA and not DSBs as trigger of the DDR in our model because we have so far failed to detect DSBs by PFGE in *cdc6-1* cells grown at various temperatures. This contrasts with other systems, where collapsed replication forks are substrates of nucleases like Mus81 (Regairaz M. *et al.*, 2011). Moreover, *cdc6-1 mus81 $\Delta$*  cells display neither a defect in cell survival nor a reduction of mitotic Rad52 foci formation. This will be discussed in the next section, but we consider that MiDAS might occur in yeast *cdc6-1* cells using a different form of Recombination-dependent replication (RdR) not involving a DSB.

We believe that the conditional *cdc6-1* system is an extremely useful tool to detect the first events that occur in cells after one extended S phase. However, one bias of our system is that it is replication fork-centered, in other words, both DDR activation and initiation of MiDAS are explained from the context of a remodeled fork. Thus, we are not able to examine the impact of unreplicated DNA in mitosis located away from a replisome. Recent non-published data from David MacAlpine's lab (personal communication) suggest that unreplicated DNA can trigger the DDR response and a metaphase arrest in budding yeast cells. This was observed by preventing priming activity at replication origins without interfering with the helicase activity, leaving an unreplicated dsDNA region at the origin that is presumably synthesized during mitosis (system described in Hoffman R.A. *et al.*, 2021). Therefore, it is also important to explore if, apart from replication forks, unreplicated dsDNA gaps can trigger mitotic DDR activation and MiDAS by itself.

### **Proposed mechanism of MiDAS and consequences for the cell**

In this work, we show that MiDAS occurs in subnuclear foci, uses a HR-dependent mechanism and arises as a consequence of an extended S phase, thus its purpose is to complete DNA replication. Importantly, there is one report of DNA synthesis during mitosis in budding yeast (Ivanova T. *et al.*, 2020). This study suggested that DNA synthesis can occur in normal cycling yeast cells during mitosis, except in metaphase. However, there are two critical differences with our work; their nuclear EdU signal is diffused across the nucleus and they proposed this synthesis occurs after chromosome segregation has started. I would like to draw the difference between both works, that are surely two different mechanisms with different biological origins and purposes. However, we consider that our work is the first proper characterization of MiDAS in budding yeast cells. Moreover, we designed our experiments based on the information of MiDAS in metazoan organisms.

We examine the impact of different mutants in budding yeast MiDAS using QIBC. We chose *pola-cdk*, to test if replisome remodeling is required, *pol32Δ*, to test if BIR is involved in this synthesis, and *rad51Δ*, as a canonical BIR factor but with conflictive data on its relevance in MiDAS (Minocherhomji S. *et al.*, 2015; Garribba L. *et al.*, 2020; Wassing I. *et al.*, 2021). Interestingly, all mutants display a decrease in both the number of MiDAS-positive cells and the intensity of EdU signal. So, we conclude that MiDAS requires both replisome remodeling and BIR machinery to occur. Our understanding is that mitotic forks will be remodeled, activating DDR and promoting cell cycle arrest, but also facilitating BIR to initiate DNA

synthesis. It could be interesting to exploit our system to monitor the proteins required for budding yeast MiDAS (like Rad52, Mus81 or Pif1) to start defining the molecular requirements for this synthesis.

There is a clear contradiction in our proposed MiDAS model requiring BIR to take place. Indeed, BIR has been defined to occur from a DSB but we do not detect broken chromosomes in our system. For this reason, we think that MiDAS can occur using a BIR-like mechanism that does not involve a break. This type of RdR has been observed already in *S. pombe*, where HR has been demonstrated to restart collapsed replication forks without a break (RTS1 termination locus; Mizuno K. *et al.*, 2009; Lambert S. *et al.*, 2010). This model requires Rad51 to facilitate the invasion of a 3' end that could originate from a back-tracked fork instead of a DSB. Thus, we hypothesize that fork remodeling could generate a 3' end, possibly by the fork going backwards, and generate an initiation point for Rad51 and Pol32 to perform DNA synthesis.

One of the characteristics of BIR and MiDAS is its high mutagenicity, which could be the reason of the accumulation of GCRs in *cdc6-1* cells. We have initiated experiments to better characterize MiDAS and to understand the types of rearrangements that arise from this synthesis. We are using long-read nanopore sequencing to determine the number and type of translocations after one extended S phase and BrdU sequencing to determine the regions that undergo MiDAS. With **Figure ii.10A and ii.10B**, I show examples of mitotic BrdU incorporation profiles in Chromosome XIV in *cdc6-1* and WT grown at 30 °C, indicating that we can monitor where MiDAS occurs, and a circus plot with all the detected translocations in *cdc6-1* after one cycle with extended S phase. A representative example of a translocated read is shown in **Figure ii.10C**, the read contains DNA from Chromosome V and Chromosome XV, but only half of the read contains BrdU. These reads will help us to determine not only regions that undergo translocations, but as well the donor and acceptor DNA molecules. Our ultimate goal is to reconstitute the mutagenesis map that arises from MiDAS in budding yeast cells.

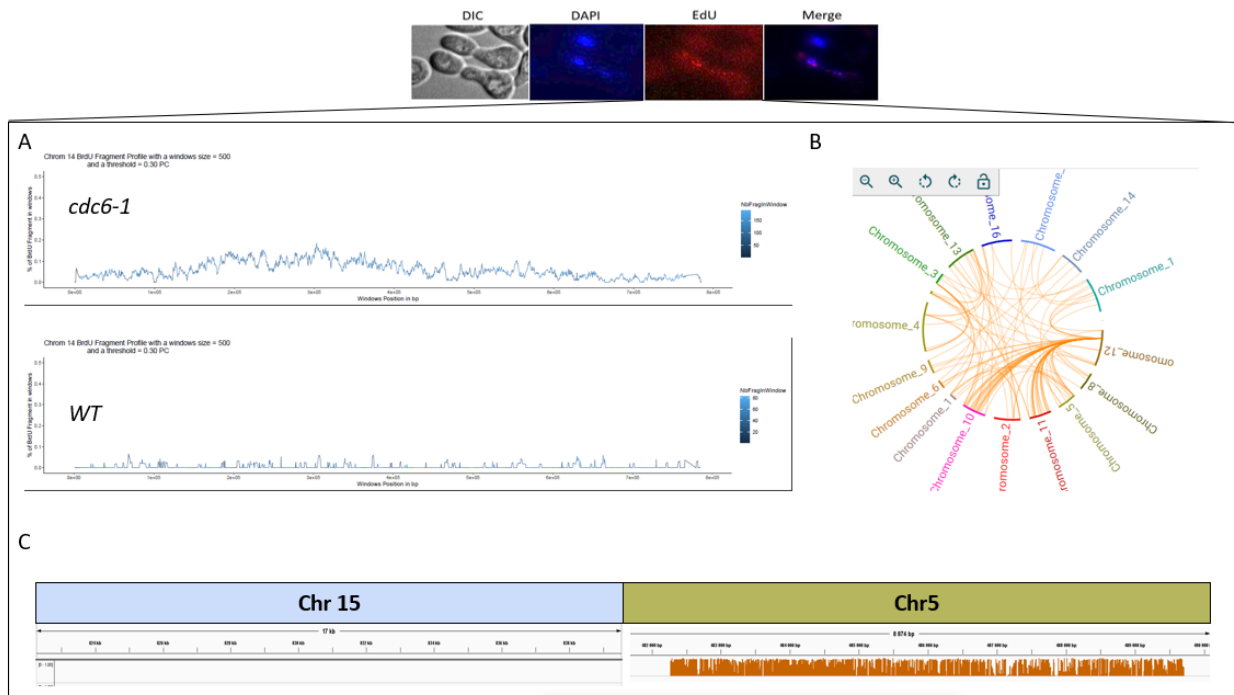


**Figure ii.10. MiDAS triggers chromosome translocations.** WT and *cdc6-1* cells were synchronized in  $G_1$ , released and pulsed with BrdU during mitosis at 30 °C. (A) Examples of BrdU incorporation profiles of chromosome XIV in *cdc6-1* and WT strains. (B) Circos plot of *cdc6-1* after one cycle with extended S phase. Every lane represents a translocation between the indicated chromosomes. 143 translocations event were identified. (C) Example of translocated read in *cdc6-1* mutant after extended S phase. The read contains fragments of Chr XV and Chr V, but only the latter displays BrdU signal. BrdU indicates the donor molecule in the translocation.

Importantly, the role of Pol $\alpha$  phosphorylation in MiDAS is more complex than what we initially thought. The *cdc6-1 pola-cdk* mutant displays three important phenotypes after its extended S phase: premature mitotic exit, reduced MiDAS and increased lethality. Our CFU assay demonstrate that the *pola-cdk* mutant dies after the first cycle with extended S phase, which emphasizes how important is to efficiently deal with unreplicated DNA in mitosis. However, the reason of death is not only the reduction of MiDAS but mainly premature mitotic exit, as mitotic extension with nocodazole rescues the lethality. This piece of data is critical for us because it demonstrates that SAC activation can substitute for the function of DDR in this context, and that the remnant synthesis in the *pola-cdk* mutant is sufficiently proficient to restore viability. Therefore, the lethality of *cdc6-1 pola-cdk* is rather linked to a defect in DDR activation and cell cycle arrest than to a defect in MiDAS.

Finally, we are intrigued by two things: how this remnant synthesis in the *polα-cdk* mutant is achieved and why MiDAS failure leads to cell death in budding yeast. We do not know if the remnant synthesis in *polα-cdk* cells is just a less efficient RdR or depending on a different backup mechanism. One hypothesis is that, as the replisome seems to be loaded and intact in *cdc6-1 polα-cdk* mutant, it could just continue DNA synthesis during mitosis but not complete it because cells divide prematurely due to the lack of the DDR activation. On the other hand, it has been shown that cells have backup mechanisms to deal with incomplete DNA replication in mitosis (Spies J. *et al.*, 2019). When MiDAS fails, cells protect unreplicated DNA regions via Shieldin complex (53BP1 protein), carrying it to the next S phase and allowing a second chance to finish genome duplication using a canonical replication fork. Thus, we believe it is important to further understand how budding yeast cells deal with unreplicated DNA and if they have other less efficient mechanisms that could compensate for inefficient MiDAS.

### **Role of Polα phosphorylation in replisome remodeling**

The main aim of this project is to understand the role of Polα phosphorylation in the context of an extended S phase. We focused on Polα as its phosphorylation has been long reported to occur in mitosis during a normal cell cycle in both human cells and in budding yeast, but whose function has remained unknown (Voitenleitner C. *et al.*, 1999; Foiani M. *et al.*, 1995; Desdouets C. *et al.*, 1998).

Our mass spectrometry analysis demonstrates that Pol1 and Pol12 phosphorylation occurs mainly in the disordered NTD of both proteins, including CDK sites. However, we focused so far only on CDK sites as we show they are necessary and sufficient for the regulation of Polα chromatin binding. We do not know if the other phosphorylation sites are required for this process, but we speculate that they are either dispensable or non-functional, as proposed for about 65% of total phosphorylation sites in the proteome (Lienhard G.E., 2008; Landry C.R. *et al.*, 2009). Alternatively, M-CDK phosphorylation may serve as priming sites for other kinases (e.g. regulation of Mer2; Wan L. *et al.*, 2008). Importantly, to study how Polα phosphorylation is regulated in the *cdc6-1* context, we use *POL1* and *POL12* mutants with all putative CDK sites abrogated, as partial CDK mutants do not display strong phenotypes. This could be an indication that CDK phosphorylation in Polα could be promiscuous, some CDK sites being able to compensate for others, and suggesting that is not the location of a phosphosite but rather the number of CDK phosphorylation sites that regulates its function.

Our cellular fractionation assay confirms the proposed function of Pol $\alpha$  phosphorylation; its binding to chromatin is dependent on its phosphorylation status, being evicted in mitosis due to M-CDK activity (Desdouets C. *et al.*, 1998). Interestingly, the presence of Pol $\alpha$  on chromatin is toxic only when cells enter mitosis with under-replicated DNA. We demonstrate that the *pola-cdk* mutant, which is never evicted from chromatin, has no phenotype in an unperturbed cell cycle, suggesting that CDK phosphorylation is neither required nor detrimental for the canonical DNA polymerase activity in S phase. Importantly, we recently generated the phosphomimic mutants of *POL1* and *POL12* for all CDK sites, and showed that these mutations are lethal for cells in the absence of *WT* Pol $\alpha$ . This suggests that Pol $\alpha$  CDK phosphorylation is incompatible with DNA synthesis in S phase, being the reason why it is restricted to mitosis, when replication is supposed to be finished.

We wonder why Pol $\alpha$  unloading from chromatin is essential in mitosis following an extended S phase and not in mitosis following a normal S phase condition. We argue that it is not only its presence on chromatin, but its maintained interactions with the replisome that makes its presence toxic. One of our most important line of evidence of replisome remodeling is the interactome of Pol1 during S phase, mitosis and its dependency on phosphorylation status. We find that the Pol $\alpha$  complex maintains its integrity through all the cell cycle and, as expected, it interacts with the replisome only in S phase. In mitosis, when it is phosphorylated and evicted from chromatin, we are not able to find any replisome member interacting with it. Interestingly, we do not find any new interactor of Pol1, suggesting that phosphorylation and eviction from chromatin isolates Pol $\alpha$ . Importantly, preventing Pol $\alpha$  CDK phosphorylation and detachment from chromatin maintains the interactions with the majority of replisome components in mitosis. Thus, we hypothesize that the replisome in the *cdc6-1 pola-cdk* is still loaded on chromatin during mitosis. The consequence is a failure to activate the DDR. As the mutant displays less mitotic RPA foci, which are less intense, it is possible that this replisome is physically limiting the exposure of ssDNA or the recruitment of RPA. Interestingly, even though it needs further confirmation, we do not find Mrc1 in the interactome of the *pola-cdk* mutant in mitosis, which could also explain the lack of the DDR activation.

We propose that Pol $\alpha$  phosphorylation and eviction from chromatin are required to remodel, and possibly to disassemble, the replisome in a mitotic environment. This involves the unloading of replisome components and/or the recruitment of new proteins to enable the DDR activation and efficient MiDAS (**Figure ii.11**). We wonder why this is completely dispensable in normal S phase conditions and restricted to mitosis. One possibility is that Pol $\alpha$  CDK phosphorylation and eviction from chromatin is not required in replisome termination/disassembly in S phase. As Pol $\alpha$  is found on the lagging strand, replisomes could pass each other after “an encounter” by disrupting Ctf4-Pol1 interaction, promoting CMG ubiquitination and unloading normally. Therefore, chromatin-bound Pol $\alpha$  becomes a problem when replisomes need to be unloaded without encountering another CMG.

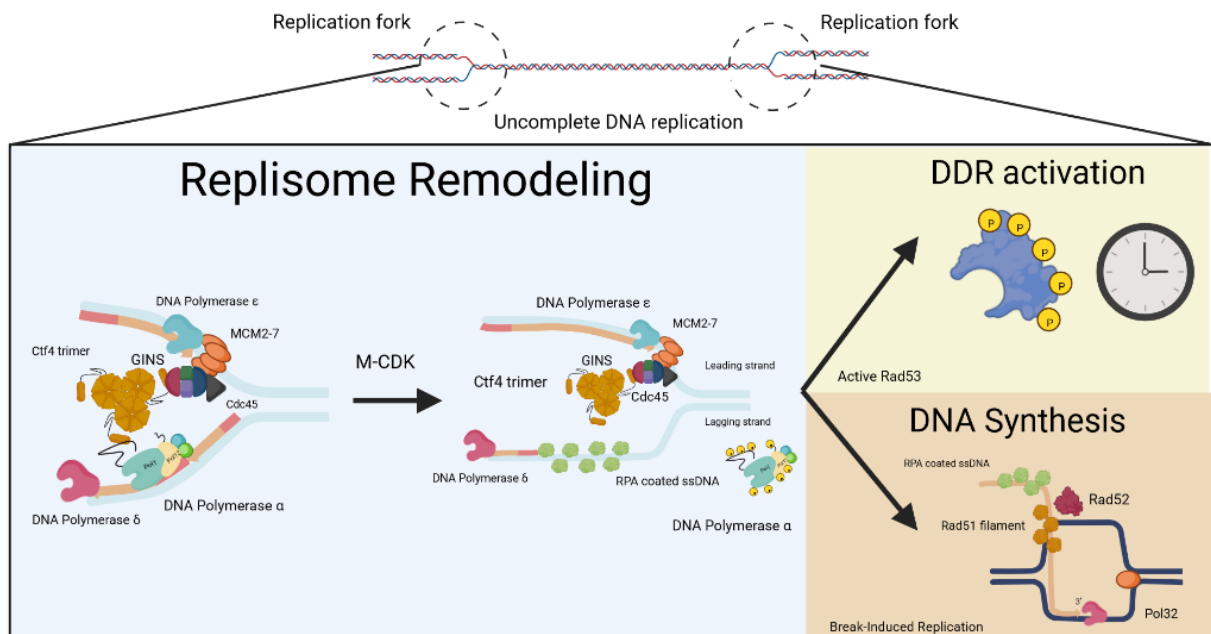


**Figure ii.11.** Replication forks are remodeled upon mitotic entry, allowing DDR activation and MiDAS. M-CDK activity will phosphorylate and promote the eviction of Pol $\alpha$  from chromatin and from the replisome. This will allow for DDR activation, that arrest cells in metaphase, and facilitating MiDAS via RdR

Interestingly, we found another situation where the *polα-cdk* mutant displays a phenotype. It is only when the mutant harboring the hypomorph allele *rad5<sup>G535R</sup>* is treated with MMS. Rad5 is a E3 ubiquitin ligase involved in DNA damage in S phase, particularly in DNA damage bypass (Minca E.C. and Kowalski D., 2010). What is interesting it that Rad5 has been reported to allow normal S phase progression in the presence of MMS (Ortiz-Bazan M.A. *et al.*, 2014). One possibility is that in the *rad5<sup>G535R</sup>* background, replication forks progress slowly in the presence of MMS, mimicking the situation we have in *cdc6-1* grown at semi-permissive temperature, and promoting mitotic entry with incomplete DNA replication. If it is the case, we hypothesize that MMS-treated *rad5<sup>G535R</sup>* may require the same mechanisms for survival as *cdc6-1*, including the phosphorylation of Polα, replisome remodeling and MiDAS, making it an interesting model to study.

Finally, we believe that the next step of this project is to molecularly characterize the mechanism of replisome remodeling and MiDAS. We plan to monitor the fate of replisome components in mitosis after a normal or extended S phase and to identify the protein complex that performs MiDAS. Our goal is to determine which replisome factors are recycled for the MiDAS mechanism and which ones are removed. To do so, we plan to repeat our cellular fractionation assays with different proteins (like Mcm2-7 or Ctf4) and to identify by mass spectrometry the partners of Pol32 in MiDAS conditions. All this data will allow us to determine how a canonical replication fork is remodeled into a recombination-dependent fork to finish DNA in mitosis.

**Chapter iii: Characterization and role of  
DNA polymerase  $\alpha$  phosphorylation in  
*Saccharomyces cerevisiae* meiosis.**

Meiosis is a modified cell cycle that generates genetically different haploid cells due to a compulsory HR step. As explained in the introduction, recombination and meiosis have an intricate relation, as HR is essential for the proper segregation of homolog chromosomes in meiosis I. Defects in meiotic recombination lead to cell arrest in pachytene, but bypassing recombination (*spo11Δ*) restores meiotic progression with the production of unviable gametes.

While testing the phenotypes of homozygous diploid *pola-cdk* mutants, we discovered that their sporulation efficiency was much reduced compared to WT. Since the same mutants did not show any defect in the vegetative cell cycle, we considered that this sporulation defect was probably linked to a meiosis-specific process, such as HR. Indeed, we found that the sporulation defect of *pola-cdk* mutants in the W303 background was fully dependent on DSB formation (i.e. rescued by *spo11Δ*), suggesting that Pol $\alpha$  phosphorylation has a role not only in mitotic but also in meiotic recombination.

Pol $\alpha$  phosphorylation has never been addressed in the meiotic context, thus we decided to characterize and determine the impact of this PTM on meiosis completion. SK1 is the favorite genetic background used for meiotic studies in *S. cerevisiae* because of its high sporulation efficiency and the vast number of assays available to monitor every step of the recombination pathway. We transferred our *pol1-cdk13A* and *pol12-cdk12A* mutations into this background, aiming to pinpoint the precise step of recombination requiring Pol $\alpha$  phosphorylation, outside the context of an extended S phase. We confirmed that Pol $\alpha$  is phosphorylated before the first meiotic division, yet its profile seemed different compared to what we observed in mitosis. Unfortunately, the initial meiotic phenotype detected in the W303 *pola-cdk* mutants was gradually lost in SK1 strains engineered for a robust and highly-synchronized meiosis.

## **1.1. DNA Pol $\alpha$ phosphomutants are deficient in meiosis in the W303 background**

We first determined the sporulation efficiency of homozygous *pol1-cdk13A*, *pol12-cdk12A* and *pol $\alpha$ -cdk* mutants on plate (SpoRR). By quantifying the number of tetrads formed after 48 hours of incubation, we observed that both *pol1-cdk13A* and *pol12-cdk12A* reached only 20% and 40% of sporulation efficiency, respectively, while *WT* diploids reached 85%. Interestingly, *pol $\alpha$ -cdk* diploids had a greater, additive defect with a sporulation efficiency of 12% (**Figure iii.1A**). Of note, the remaining tetrads produced viable spores. When I repeated this experiment and performed a kinetic of tetrad formation by counting the percentage of tetrads every 6 hours during 72 hours, I found that while *WT* diploids produced 50% tetrads by 40h and >80% at 72 hours, *pol1-cdk13A* and *pol $\alpha$ -cdk* mutants started to sporulate only after 40h and reached a maximum of 20 and 15 %, respectively, at 72h (**Figure iii.1B**). I conclude that all W303 *pol $\alpha$ -cdk* diploids are strongly delayed in meiotic progression, and that 80% of them simply fail to complete meiosis. The phenotype of *pol $\alpha$ -cdk* mutants is not fully penetrant since 20% of diploids produce viable haploid progeny.

As we already determined that Pol $\alpha$  phosphorylation plays a role in mitotic recombination, we hypothesized that it could be involved in meiotic recombination. In meiosis, Spo11 initiates meiotic recombination by introducing hundreds of DSBs in prophase I chromosomes (Keeney S., 2001). *SPO11*-deleted cells make no DSBs, bypass meiotic recombination and undergo MI and MII divisions, but produce unviable spores (Klapholz S. *et al.*, 1985). To test if the sporulation defects of *pol $\alpha$ -cdk* mutants stem from a problem in meiotic recombination, we scored the sporulation efficiency of *spo11 $\Delta$*  and *spo11 $\Delta$  pol $\alpha$ -cdk* mutants (**Figure iii.1A**). Both *spo11 $\Delta$*  and *spo11 $\Delta$  pol $\alpha$ -cdk* diploids sporulated efficiently, similar to *WT* diploids, indicating that Pol $\alpha$  CDK phosphorylation is required for efficient meiosis and sporulation only if DSBs are made. This strengthens our hypothesis that Pol $\alpha$  phosphorylation plays a role not only in mitotic but also meiotic recombination.

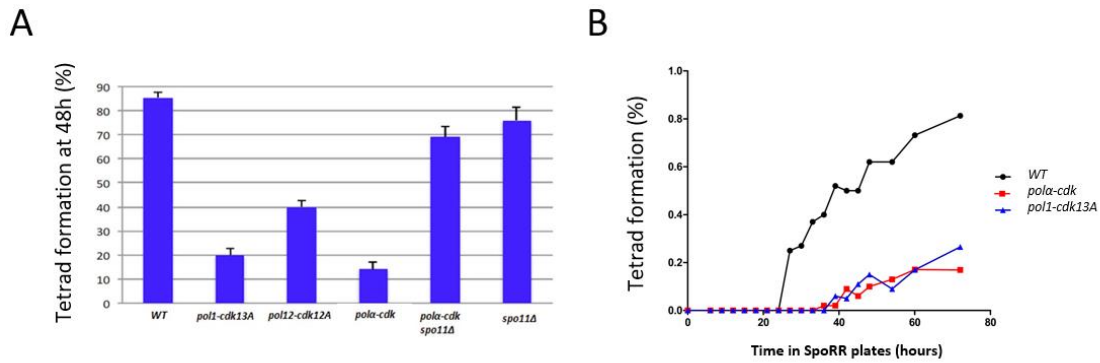


**Figure iii.1. *Polα* CDK phosphorylation is required for meiosis in the W303 background. (A)** Percentage of tetrad formation on SpoRR plates after 48 hours of incubation ( $n=3$ ). **(B)** Kinetics of tetrad formation on SpoRR plates. The number of tetrads was counted every 6 hours for 60 hours and at 72 hours after plating on SpoRR. ( $n=2$ ).

## **1.2. *Polα* CDK phosphorylation is not required for sporulation in SK1 background**

To more precisely characterize the role of *Polα* CDK phosphorylation in meiotic recombination, we transferred our mutants into the SK1 background, the reference strain for *S. cerevisiae* meiotic studies (Kane S.M. and Roth R., 1974). When I performed the same time course analysis of tetrad formation as before, I found that the *polα-cdk* mutants reached the same level of tetrads as in the *WT* control, but at later timepoints. Surprisingly, the complete failure to produce tetrads in most W303 *polα-cdk* mutant diploids changed to a simple sporulation delay in the SK1 background (**Figure iii.2A**). Of note, SK1 *polα-cdk* spore viability was also unaffected. To determine if the sporulation delay was HR-dependent, *SPO11* was deleted again in the SK1 *polα-cdk* mutants. As seen for the W303 background, this delay was bypassed when no DSBs are made (**Figure iii.2B**). We conclude that *polα-cdk* mutants have meiotic recombination defects, but that they are much weaker in the SK1 background, probably because of its more robust meiotic progression. One reason for the hypomorph behavior of *polα-cdk* mutants could be that additional phosphorylation events are necessary to control *Polα* in meiosis.

Despite the incomplete penetrance of *pola-cdk* phenotypes in SK1, they still showed a delay in sporulation. We decided to take advantage of the high meiotic synchrony of the SK1 background to study *pola-cdk* meiotic progression in detail. First, I used the classical liquid YPA-SPM protocol to monitor pre-meiotic S phase and meiotic divisions in both *WT* and *pola-cdk* diploids (see Materials and Methods). DNA content analysis by FACS showed no difference in pre-meiotic S phase progression between *WT* and *pola-cdk* diploids. Moreover and unexpectedly, microscopy showed that both *WT* and *pola-cdk* strains progressed in the first and second meiotic divisions with almost identical kinetics, except perhaps for a slight (1h) delay (**Figure iii.2C and 2D**). This disappointing result suggests that the meiotic phenotypes of *pola-cdk* mutants depend heavily on the strain and methods used to induce meiosis.

I also used the highly synchronous SK1 meiotic induction system based on over-expression of the *IME1* transcription factor (modified from Chia M. *et al.*, 2016). Using this protocol, we can precisely monitor pre-meiotic G<sub>1</sub> (0-2h), pre-meiotic S phase (2-4h), Meiosis I (4-7h) and Meiosis II (7-9h) (**Figure iii.2E**). Consistently with our previous data, the *pola-cdk* mutant showed no delay in pre-meiotic S phase. Unfortunately, the slight meiotic division delay of *pola-cdk* diploids was completely lost in this system (**Figure iii.2F and 2G**). These set of data led us to conclude that the *pola-cdk* mutants behave as hypomorphs in the SK1 background, losing their phenotype when meiotic synchrony and efficiency is increased.

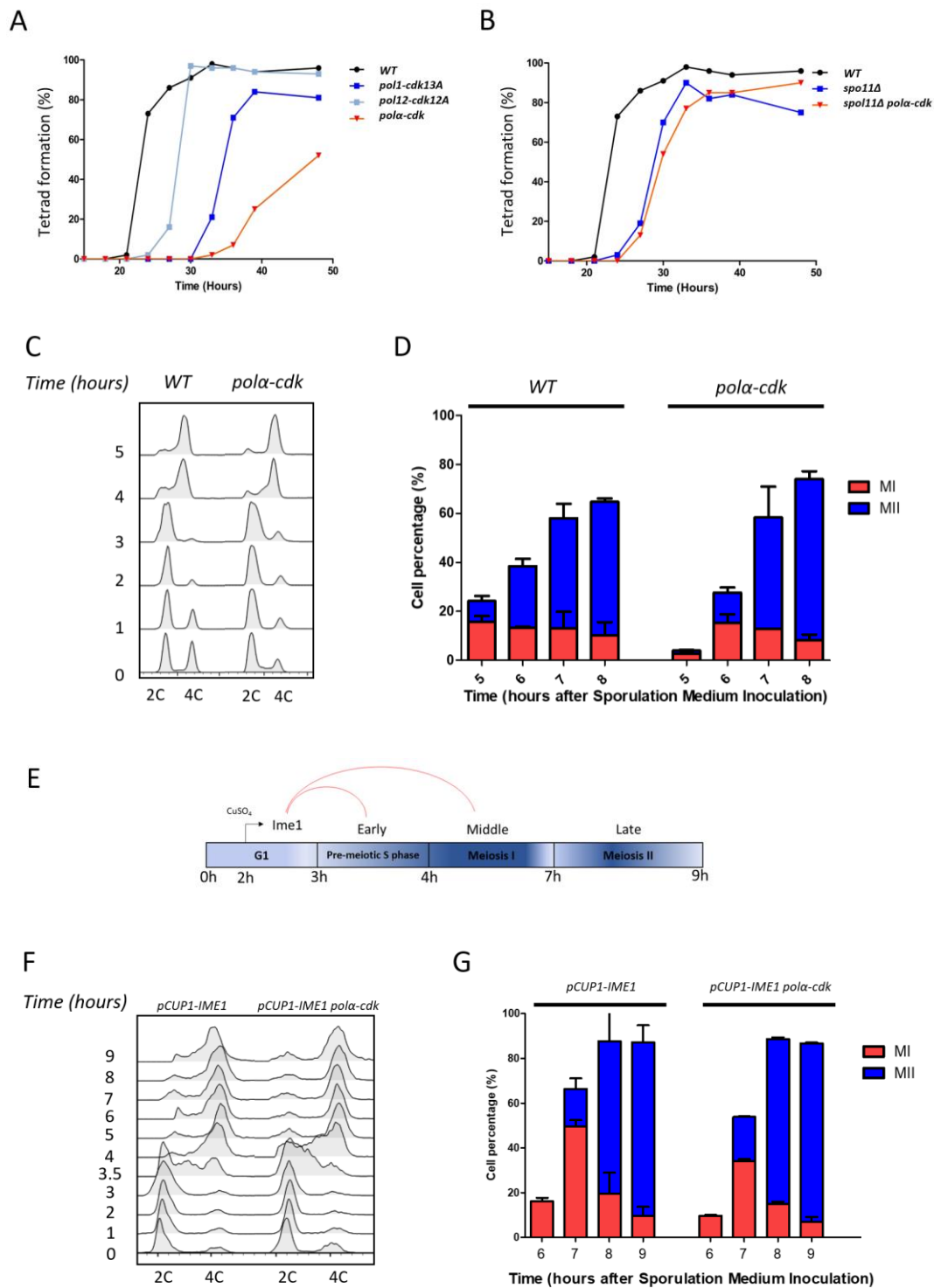


**Figure iii.2. Polα-cdk meiotic phenotypes are condition-dependent.** (A-B) Percent tetrads on SpoRR plates after 48 hours. Tetrads were counted every 6 hours for 48 hours after plating cells on SpoRR (n=3). (C and F) DNA content of WT and polα-cdk mutants after transfer in sporulation medium. (D and G) Percentage of MI and MII cells determined by microscopy (MI = meiosis I; cells with 2 distinct nuclear masses. MII = meiosis II; cells with 4 distinct nuclear masses) (n=3). (E) Scheme of the pCUP1-IME1 synchronization protocol.

### **1.3. Pol $\alpha$ is phosphorylated at CDK and non-CDK sites in meiosis**

To explain the loss of the meiotic phenotypes of the *pola-cdk* mutants in the SK1 background using highly efficient and synchronous protocols, we envisioned that Pol $\alpha$  might be phosphorylated on additional sites, besides CDK sites, in meiosis, and that these other sites become predominant in strains or conditions of robust meiosis. Hence, I decided to map Pol $\alpha$  phosphorylation sites in meiosis using the *pCUP1-IME1* synchronization protocol.

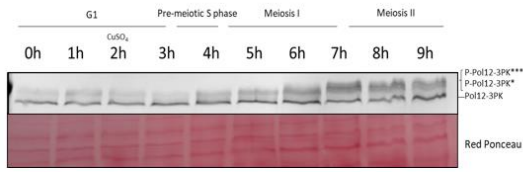
I first monitored Pol12 mobility shift as a proxy for the phosphorylation status of Pol $\alpha$ . Western blot analysis showed that Pol12 presents a mobility shift right after pre-meiotic S phase (4h), which was maintained throughout both meiotic divisions. Interestingly, an even slower migrating Pol12 form appeared at 7h after induction of meiosis, which was never detected in mitosis, consistent with the idea that Pol $\alpha$  is phosphorylated to a higher level or by more kinases in meiosis (**Figure iii.3A**). The first phosphorylation took place before recombination was completed, since slow-migrating forms of Pol12 were present in pachytene-arrested cells (*pCUP1-IME1 ndt80 $\Delta$* , **Figure iii.3B**). Of note, *ndt80 $\Delta$* -arrested cells finish DNA replication, form DSBs but do not complete recombination and remain mononuclear, arresting before the first meiotic division. Slow migrating forms of Pol12 kept accumulating with time in *ndt80 $\Delta$* , in contrast to WT meiosis where Pol12 phospho-forms peaked at 8 hours and then decreased upon meiosis completion (**Figure iii.3C**). Pachytene-arrested cells do not show the second, hyperphosphorylated form of Pol12.

To check if these mobility shifts were due to CDK phosphorylation as seen in mitosis, I performed the same analysis with the Pol12-*cdk12A* mutant. Interestingly, mutating all S/T-P of Pol12 did not cause a complete conversion to fast-migrating forms in meiosis, in contrast to the situation in mitosis; Pol12-*cdk12A* cells maintained a dim but clearly shifted Pol12 band (**Figure iii.3D**). These shifts were confirmed to be phosphorylation-dependent using an immunoprecipitation phosphatase assay (**Figure iii.3D**). These data indicate that Pol12 is phosphorylated before completion of the first meiotic division. Our results with Pol12-*cdk12A* strongly suggest that CDK may not be the only kinase phosphorylating Pol $\alpha$  during meiosis. This could be a reason for the incomplete penetrance of Pol $\alpha$ -*cdk* mutant phenotypes in meiosis.

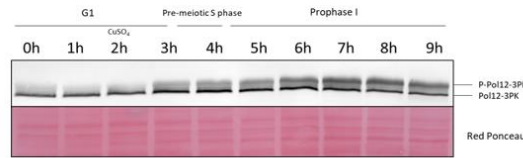
We therefore decided to map the Pol $\alpha$  phosphorylation sites in both *pCUP1-IME1* and *pCUP1-IME1 pol $\alpha$ -cdk* strains during meiosis. I immuno-precipitated Pol1 and Pol12 at 5 and 7 hours after inoculation in the sporulation medium, corresponding to Meiosis I and Meiosis II respectively using the *pCUP1-IME1* synchronization, followed by phospho-mass spectrometry analysis. We identified 20 and 17 meiotic phosphosites in Pol1 and Pol12, respectively, 11 (Pol1) and 10 (Pol12) of them with a high probability score. Among the latter, only 3 (Pol1) and 5 (Pol12) were S/T-P CDK sites despite the good MS coverage of other putative CDK sites (12 out of 13 for Pol1, 10 out of 12 for Pol12; **Table iii.1**). Interestingly, the majority of identified phospho-peptides resided in the NTD of both proteins, similarly to what was observed in mitosis, but with a weaker preference for canonical S/T-P motifs (**Figure iii.3E**). The same experiment was repeated using the *pol $\alpha$ -cdk* strain, which showed that CDK sites were not phosphorylated anymore as expected, but also that other residues remained phosphorylated in both proteins (**Table iii.1** and **Figure iii.3E**).

Our experiments demonstrate that Pol1 and Pol12 are phosphorylated at CDK and non-CDK sites during meiosis. Moreover, mutating putative CDK phosphosites does not fully abolish Pol $\alpha$  phosphorylation in meiosis, which led us to postulate that this residual phosphorylation events are sufficient to regulate Pol $\alpha$  functions in this biological context.

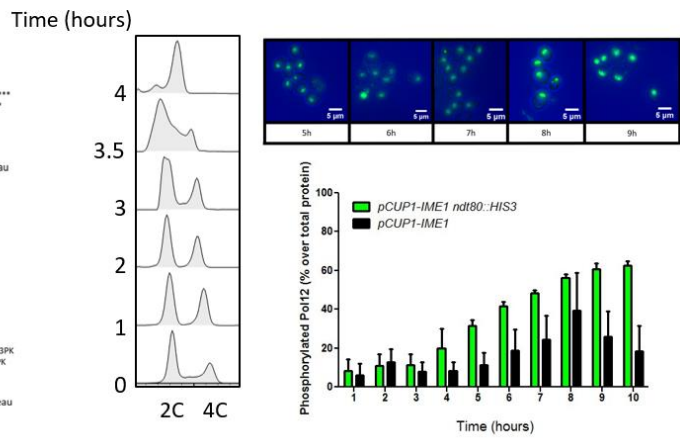
A



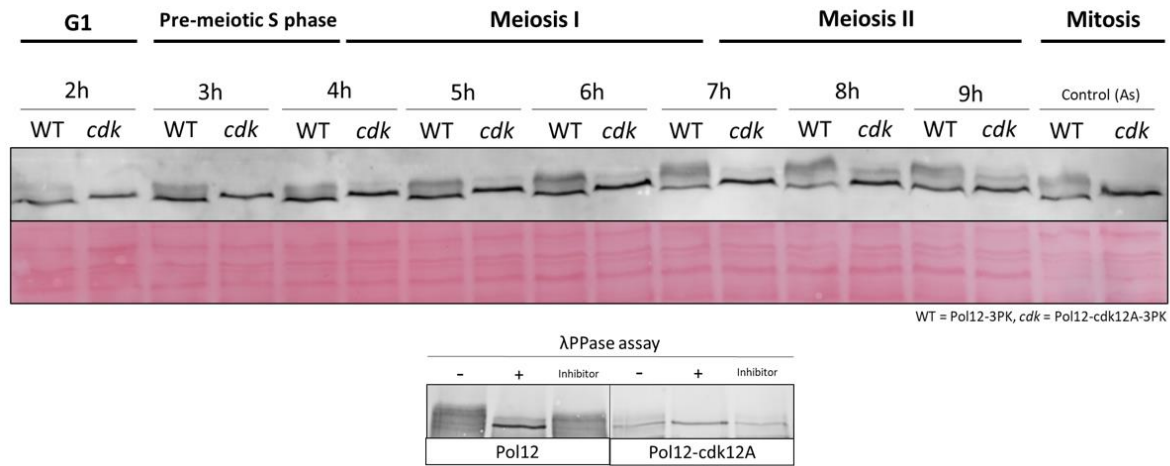
B



C



D



E

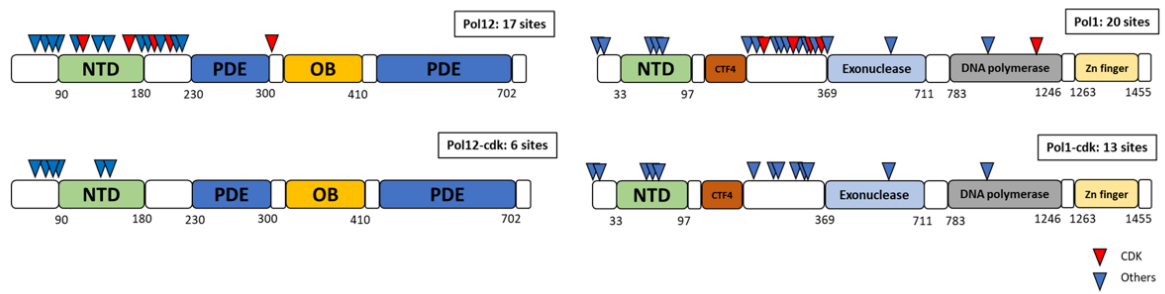


**Figure iii.3. Pola is phosphorylated during meiosis at CDK and non-CDK sites. (A and B)** Western blot of Pol12 during meiotic progression in WT and *ndt80Δ* backgrounds (\* and \*\*\* mark two phospho-forms of Pol12). Ponceau Red is used as loading control. **(C)** Flow cytometry and microscopy analysis of meiotic progression of the *pCUP1-IME1 ndt80Δ* strain. Quantification of phosphorylated Pol12 during meiosis in WT and *ndt80Δ* (*n*=3). **(D)** Western blot of Pol12 and Pol12-*cdk12A* during meiotic progression. Controls are asynchronously growing POL12 and *pol12-cdk12A* cells. Phosphatase assay of Pol12 and Pol12-*cdk12A* in Meiosis I. **(E)** Schematic of meiotic phosphorylation sites identified in Pol1, Pol12 and their *cdk*-mutated versions during meiosis. Red arrowheads mark identified CDK sites. Blue arrowheads mark non CDK-sites.

Pol12					Pol1				
Position	Probability	Predicted CDK-site	Found Pol12- <i>cdk12A</i>	Previously found	Position	Probability	Predicted CDK-site	Found Pol1- <i>cdk13A</i>	Previously found
80	0.76	-	+	YES	3	0.59	-	+	YES
81	0.93	-	+	YES	5	0.99	-	+	YES
83	0.5	-	+	NO	82	0.33	-	+	YES
88	0.87	-	+	YES	83	0.33	-	+	YES
100	0.48	-	-	YES	84	0.33	-	+	YES
101	0.48	Cdk	-	YES	188	0.86	-	+	YES
126	0.99	-	+	YES	189	0.5	-	+	YES
136	0.98	-	+	YES	204	0.76	-	+	YES
177	0.79	Cdk	-	YES	205	0.62	-	-	YES
180	0.79	-	-	YES	206	0.62	-	-	YES
181	0.58	-	-	YES	214	1	-	+	YES
182	0.58	-	-	YES	215	1	Cdk	-	YES
185	0.97	Cdk	-	YES	240	0.99	Cdk	-	YES
187	0.36	-	-	YES	298	1	-	+	NO
188	0.51	-	-	YES	303	0.32	-	-	YES
190	0.94	Cdk	-	YES	304	0.48	-	-	YES
304	0.98	Cdk	-	YES	305	0.48	-	-	YES
					680	0.99	-	+	NO
					949	0.79	-	+	NO
					1184	0.99	Cdk	-	NO
					169	0.99	-	Only in Pol1- <i>cdk13A</i>	YES

**Table iii.1. Pol1 and Pol12 meiotic phosphorylated sites identified by mass spectrometry.** Every potential phospho-site has an associated probability score that determines the confidence of identification. A score above 0.75 indicates certainty of phosphorylation, thus a confirmed phospho-site, while a score below 0.75 indicates just a possibility. Residues found in the same identified phospho-peptide are represented within the same rectangle. Residues that follow S/T-P motifs are labelled as “Cdk”. If residues are found to be phosphorylated in the *polα-cdk* mutant, it is indicated with a “+”. If residues are found to be phosphorylated in previous datasets, it is indicated in the last column.

#### **1.4. Mutating 45 Pol $\alpha$ phosphorylation sites leads to a delay in meiotic progression**

Based on our mass spectrometry data, we decided to construct new Pol $\alpha$  mutants with more phosphorylation sites mutated, hoping to more drastically affect the phosphorylation of Pol $\alpha$ . We designed DNA fragments of *POL1* and *POL12* that contained mutations for 22 and 23 phosphorylation sites, respectively, in the intrinsically-disordered NTD of both proteins (**Figure iii.4A**). These fragments were synthesized, cloned in *POL1* and *POL12* genes using Gap repair and introduced into SK1 yeast cells using a CRISPR-Cas9 approach. We named the new set of meiotic phospho-mutants *pol1-22A*, *pol12-23A* and *pol $\alpha$ -45A* when both Pol1 and Pol12 phospho-mutants were combined. To check if so many mutations might alter the canonical function of Pol $\alpha$ , I first compared the doubling time and cell size of these new mutants with *WT*, in mitotically dividing cells (**Figure iii.4B**). From this analysis, I concluded that the new phosphorylation mutants had no phenotype in cell cycle progression or S-phase duration, suggesting that they remained proficient for the function of Pol $\alpha$  during S phase. Therefore, we assumed that any phenotype observed during meiosis would be related to meiosis-specific functions such as recombination, rather than a consequence of replication problems. To detect such putative phenotypes, I monitored meiotic progression in the new phospho-mutants using liquid synchronization protocols.

When the new Pol $\alpha$  meiotic phospho-mutants were released into meiosis using the classical YPA-SPM protocol, I saw no defect in pre-meiotic S phase, but a 1-2 hours delay in the completion of meiotic divisions (**Figure iii.4C and 4D**). This phenotype is still far from the sporulation defect observed in W303, but was more pronounced than in the SK1 *pol $\alpha$ -cdk* mutants (compare **Figure iii.4D and Figure iii.1D**).

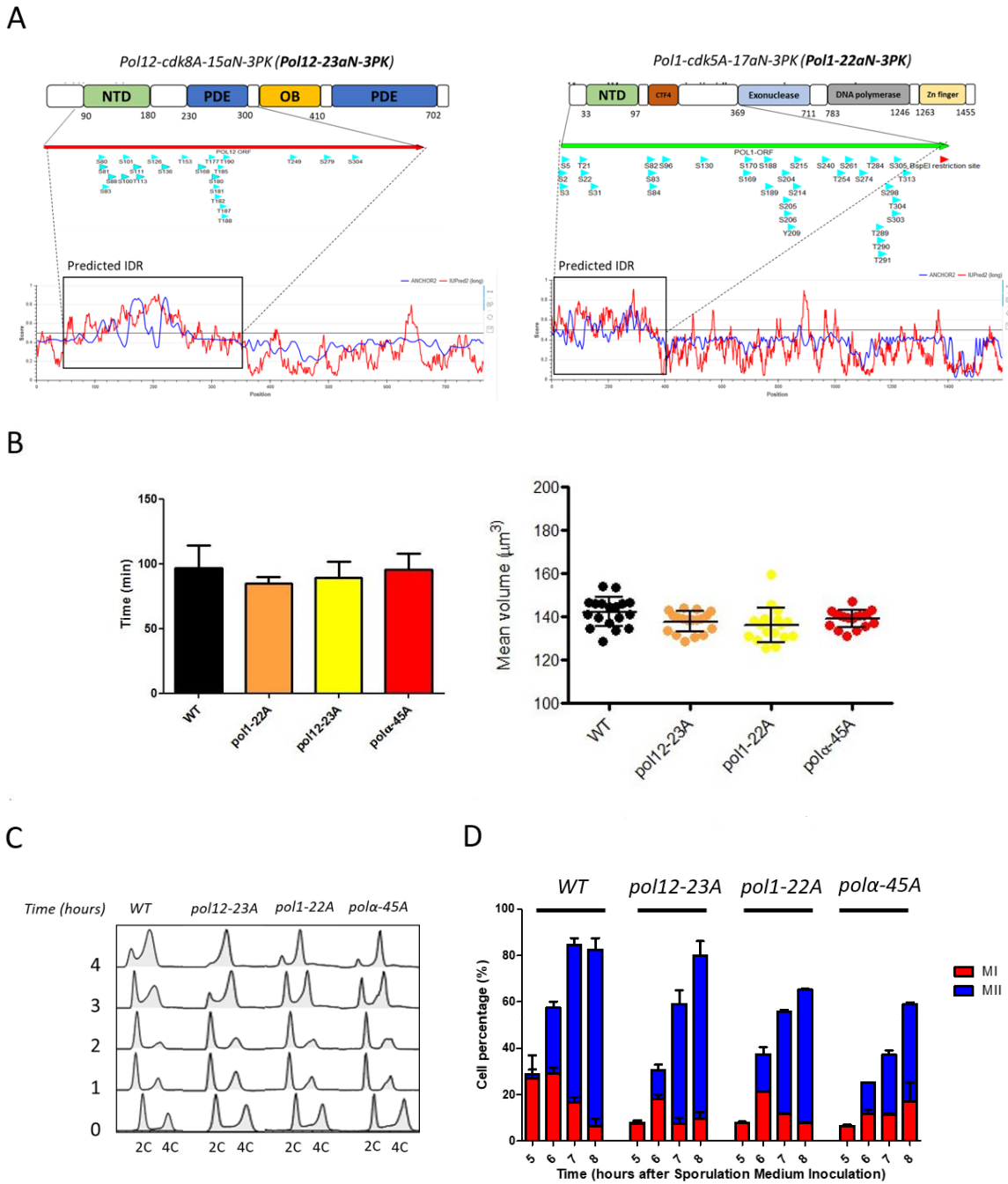


**Figure iii.4. Extensive mutation of phosphorylation sites in *Pola* slightly delays meiotic completion in *SK1*.** (A) **Top:** Scheme of phosphorylated sites mutated in *Pol1* and *Pol12*. **Bottom:** Representation of predicted IDRs in *Pol1* and *Pol12* using the IUPRED Software. (B) DNA content of WT, *pol1-22A*, *pol12-23A* and *polα-45A* after meiosis induction. (C) Percentage of MI and MII cells determined by microscopy analysis (MI = meiosis I, cells with 2 distinct nuclear masses. MII = meiosis II, cells with 4 distinct nuclear masses) ( $n=3$ ). (D) Calculated doubling time and cell size measurements of WT and the new *Pola* phospho-mutants ( $n=3$ )

### **1.5. Pol $\alpha$ -45A is proficient for meiotic crossover formation**

As we observed a phenotype, although mild, in meiotic progression in the new set of meiotic Pol $\alpha$  phospho-mutants, we decided to further characterize this phenotype and analyze putative HR defects using the highly-synchronous *pCUP1-IME1* system.

Pre-meiotic S phase was similar in *WT* and *pol1-22A* cells, and perhaps slightly delayed in the *pol $\alpha$ -45A* mutant (to a maximum of 30 min) (**Figure iii.5.A**). However, *pol12-23A* meiotic DNA replication was extended up to 1 hour compared to control, so we decided to exclude it from the analysis and focused on *pol1-22A* and *pol $\alpha$ -45A*. For both mutants, we observed a delay of 1 to 2 hours in meiosis I completion, similar to the one observed using the YPA-SPM protocol (**Figure iii.5B**). We hypothesized that these delays could be possibly due to problems in recombination, as *pol1-23A* displayed no S phase defects and *pol $\alpha$ -45A* only mild ones.

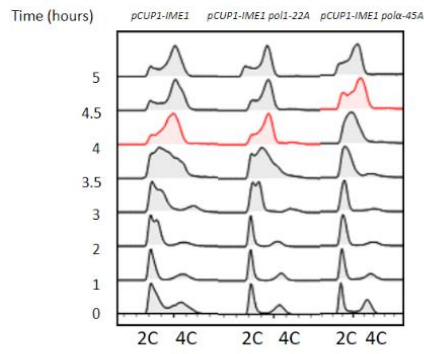
We then tested if these MI delays were dependent on DSBs formation. Importantly, combination of *pol $\alpha$*  mutants and *spo11-Y135F* (a catalytic dead allele of *SPO11*) did not affect pre-meiotic S phase progression, even suppressing the small delay observed with *pol $\alpha$ -45A* (**Figure iii.5C**). The 1 to 2 hour-delay in meiosis I completion was completely suppressed when combined to *spo11-Y135F*, suggesting to be dependent on DSB formation (**Figure iii.4F**). This is our first indication that Pol $\alpha$  phosphorylation might be required for efficient meiosis in the SK1 background, in a recombination-dependent manner and using a highly efficient synchronization protocol.

The outcome of a DSB that undergoes meiotic recombination is the formation of crossover and non-crossover molecules. There is a bias towards NCO versus CO formation during meiosis, controlled at different levels through different mechanisms and proteins (reviewed in Youds J.L. and Boulton S.J., 2011). Even though we were not able to detect a strong meiotic defect, we wondered if the final balance of CO/NCO was affected in the *pol $\alpha$*  phospho-mutants.

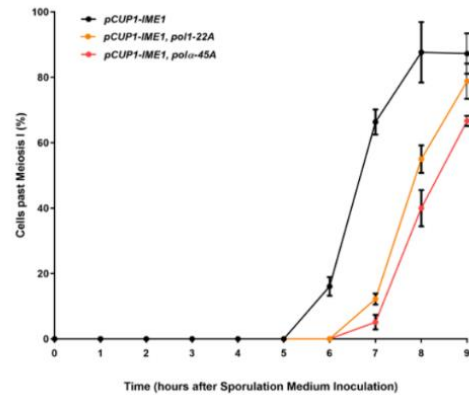
To address this question, we performed Southern Blot analyses to monitor and quantify the formation of CO at the *HIS4::LEU2* meiotic recombination hotspot (Hunter N. and Kleckner N., 2001; Scheme in **Figure iii.5E**). The two hetero-alleles used were introduced in our *pol $\alpha$*  phospho-mutants containing the *pCUP1-IME1* construct. After meiosis induction, we followed the formation of DSBs and CO species through meiotic progression (**Figure iii.5E - top blot**). We detected no striking difference in the

percentage of COs at the end point of meiosis in any *polα* phosphorylation mutants (**Figure iii.5E**). This result suggests that HR does take place in our *polα* phospho-mutants, and that COs formed efficiently. Whether other meiotic HR-related species, such as NCOs or DSBs, are affected in our meiotic Polα phospho-mutants remains to be determined. Our results with Polα meiotic phospho-mutants are globally disappointing, as we failed to identify a set of mutations that gives a clear phenotype in the *pCUP1-IME1 SK1* strain.

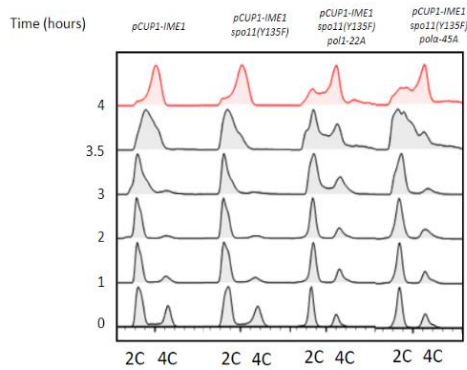
A



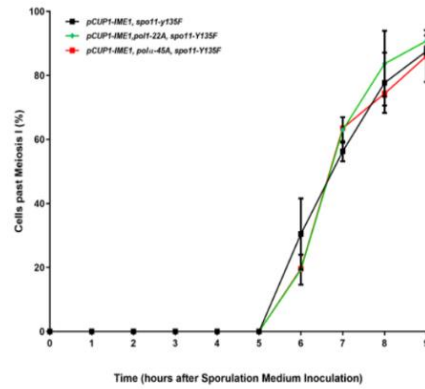
B



C



D



E

HIS4-LEU2 Hotspot for meiotic recombination  
(Hunter N. & Kleckner N., Cell 2001)

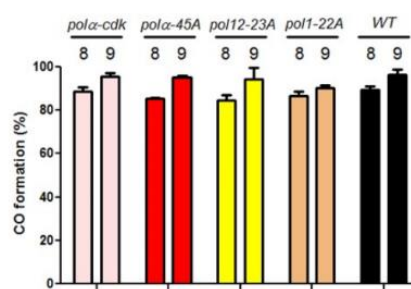
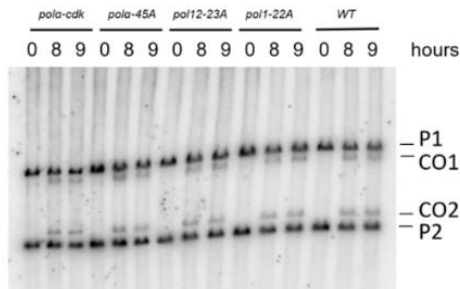
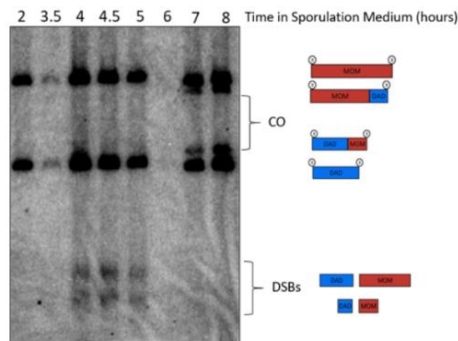
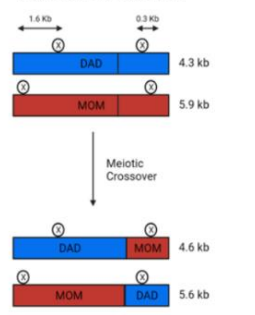


**Figure iii.5. *Polα* IDR phosphorylation is not required for meiotic CO formation.** (A and C) DNA content of WT, *pol12-23A* and *pola-45A*, *spo11-Y135F*, *pol12-23A spo11-Y135F* and *pola-45A spo11-Y135F* after meiosis induction. The estimated timepoint where most cells have finished DNA synthesis is labelled in red. (B-D) Percentage of MI and MII cells determined by microscopy (cells presenting either 2 or 4 distinct nuclear masses) ( $n=3$ ). (E) Southern blot analysis of the *HIS4:LEU2* recombination hotspot. Top: Schematic of observed CO and DSB species upon meiosis induction. Bottom: Southern blot and quantification of CO1 and CO2 species at 8 and 9 hours after meiosis induction in WT and *Polα* phosphomutants ( $n=2$ ; Valerie Borde).

## **1.6. Summary of results Project II**

- DNA Polymerase  $\alpha$  is phosphorylated in meiosis, and has a recombination-related role in the W303 background.
- Pol $\alpha$  CDK phosphorylation is important for meiosis in W303, but not in SK1.
- Pol $\alpha$  CDK and non-CDK phosphorylation occurs in meiosis at the time of homologous recombination in SK1.
- Extensive mutations of Pol $\alpha$  phosphorylation sites delays meiosis I completion in SK1.
- Pol $\alpha$  phosphorylation is not involved in CO formation in SK1.
- The function and role of Pol $\alpha$  phosphorylation in meiotic recombination is unclear.

*DNA Polymerase  $\alpha$  phosphorylation seems involved in meiotic homologous recombination. However, the phosphorylation pattern and requirement are different to the one involved in mitotic recombination and MiDAS.*

## **1.7. Discussion Project II**

In this project we studied the impact of DNA Polymerase  $\alpha$  phosphorylation in meiosis. When I initiated this project, our hypothesis was that Pol $\alpha$  phosphorylation was required for mitotic HR, at a molecular step that we wished to identify. Meiosis is characterized by a compulsory HR step (Keeney S. 2001) and our preliminary data indicated that the *pol $\alpha$ -cdk* mutant was deficient in meiotic HR. As molecular assays to monitor meiotic recombination are well characterized, we thought to identify precisely which HR step required Pol $\alpha$  phosphorylation before extrapolating our findings to the mitotic HR.

We confirmed that Pol $\alpha$  was phosphorylated during meiosis at the time of homologous recombination. However, we made two striking observations concerning this phosphorylation. First, the *pol $\alpha$ -cdk* mutant phenotype was dependent on the yeast background and methods used to induce meiosis. Second, Pol $\alpha$  was also phosphorylated at non-CDK sites, which seemed relevant for meiosis completion. This led us to conclude that preventing CDK phosphorylation was not sufficient to cause a meiotic defect. Increasing the number of mutated phospho-sites generated a small delay in meiosis completion, dependent on DSBs formation, that suggested a function in meiotic HR.

### **Meiosis have different requirements in W303 and SK1 backgrounds**

One of the challenges we encountered while working on meiosis was the change of yeast background. SK1 is the accepted background for meiotic studies in *S. cerevisiae* and all the meiotic-specific assays were set up in SK1. We aimed to exploit SK1 meiotic synchrony and efficiency to pinpoint the function of Pol $\alpha$  phosphorylation during meiotic HR. However, our main problem was that when I used a highly synchronization procedure in SK1, the *pol $\alpha$ -cdk* mutant lost completely the sporulation defects we initially detected in W303.

Interestingly, even if W303 and SK1 are both *S. cerevisiae* species, they are highly divergent (Winzeler E.A. *et al.*, 2003). Studies comparing different yeast backgrounds shown that W303 is closer to S288C (reference yeast background), while SK1 is one of the most divergent ones, precisely 5 times more divergent to S288C (Schacherer J. *et al.*, 2007; **Table ii.2**).

Strain	Number of SNPs	Number of Deletions
W303	7955	7
SK1	37424	36

Table iii.2. Genetic divergence between W303 and SK1 compared to S288C (Schacherer J. et al., 2007).

This divergence is responsible for the biological differences between backgrounds: tendency to flocculate, colony morphology, meiotic efficiency or even lethality of some genes (e.g. *POL32* is essential in SK1, but not in W303). This differences also affect how we work with strains in the laboratory, for example they have different efficiency in transformation or in gene editing with CRISPR-Cas9 technology.

We speculate that, as W303 and SK1 are genetically divergent, their meiosis are regulated differently, hence potentially explaining why Pol $\alpha$  CDK phosphorylation is essential in one and not the other. One possibility is that W303 meiosis is inefficient, then small deregulations have severe consequences, while SK1, that has been genetically engineered for meiotic studies, has a robust regulation to ensure meiosis completion (Kane S.M. and Roth R., 1974). This will imply that Pol $\alpha$  CDK phosphorylation has a low impact on meiosis progression, only observed in inefficient meiosis conditions. It could be interesting to test if the Pol $\alpha$  mutants with extensive mutations in phosphorylation sites have a stronger meiotic phenotype in the W303 background, as they showed stronger phenotypes in the SK1 background.

### **Pol $\alpha$ phosphorylation takes place differently in meiosis and mitosis**

One important result from Project 1 is that mutating CDK sites in Pol $\alpha$  caused important phenotype and we assumed that was enough to alter the normal phosphorylation status of the complex. We never observed a phospho-shift for Pol12-cdk12A in mitotic cells, whereas we did so in meiotic cells. We identified many meiosis CDK and non-CDK phosphorylation sites in Pol $\alpha$  or Pol $\alpha$ -cdk. This was critical, as we suspected that non CDK phosphorylation was sufficient to allow timely meiosis.

To address if Pol $\alpha$  non-CDK phospho-sites were relevant, we decided to increase the number of mutations of both mutants. Importantly, we decided to restrict the mutated regions to the N-terminal IDR domain of both proteins for two reasons: the majority of identified phospho-sites were found clustered in this region and we feared to impact the normal function of Pol $\alpha$  by mutating other regions, like the DNA Polymerase activity site. The outcome of this approach were mutants that did not impact cell cycle progression during vegetative growth, but presented a small delay in meiosis I completion. One possible explanation of why we do not have a strong phenotype is that Pol $\alpha$  phosphorylation still occurs at other sites in the new mutants. Indeed, western blot analysis of Pol12-23A showed a shift that is presumably phosphorylation-driven (**Figure iii.6**)

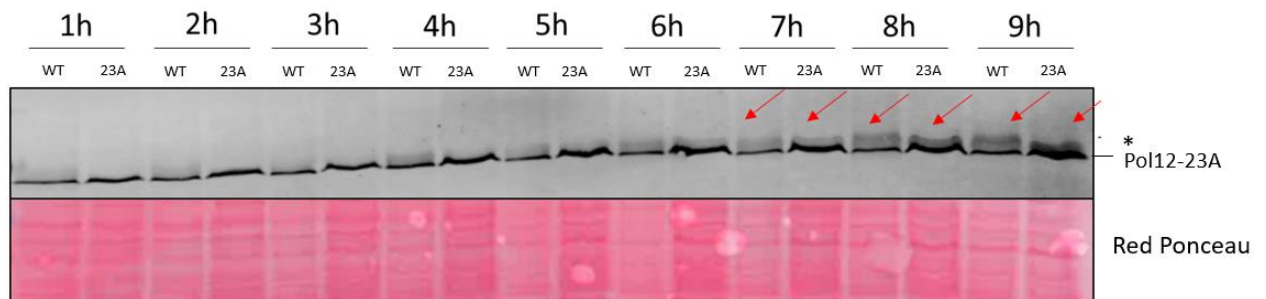


**Figure iii.6.** *Pol12-23A displays a mobility shift in western blot. pCUP1-IME1 and pCUP1-IME1 pol $\alpha$ -45A cells were synchronized and released into meiosis using the pCUP1-IME1 protocol. Western blot was performed, showing slow migrating species of Pol12 and Pol12-23A (indicated with red arrows).*

One caveat of the design of our new phospho-mutants is that we did not mutate phospho-sites outside the NTD. This includes several putative CDK sites but also identified phosphorylation sites in the catalytic site of Pol1. In particular, there are 2 phosphorylation sites in Pol1 (680 and 949) that are located in the contact between Pol1 and DNA (**Figure iii.7**). As we suspect that the function of Pol $\alpha$  phosphorylation is to evict the complex from chromatin, as it does in mitosis, these two sites are interesting candidates to mutate.

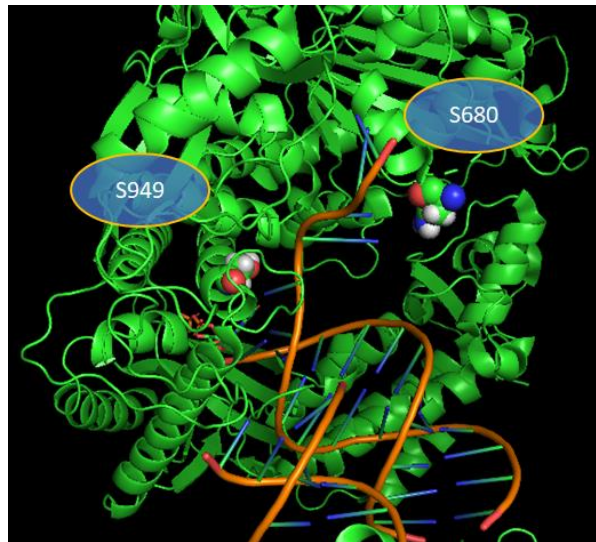


*Figure iii.7. S680 and S949 phosphorylated residues in Pol1 are located in the contact point with DNA. Crystal structure of Pol1 interacting with DNA, highlighting phosphorylated residues 680 and 949 (PDB: 4fyd)*

We have little evidence to propose that Pol $\alpha$  phosphorylation is involved in meiosis at the HR level. However, we believe that our mutants are not deficient enough to cause a strong phenotype in highly efficient and synchronous meiotic systems. For this reason, we are currently generating new mutants with more phosphorylation sites abrogated, including all putative CDK sites, all phospho-sites identified in our mass spectrometry analysis and phospho-sites identified in the literature (i.e. of phosphorylation datasets: Albuquerque C.P. *et al.*, 2008; Holt L.J. *et al.*, 2009; Swaney D.L. *et al.*, 2013; Lanz M.C. *et al.*, 2021). In parallel, we consider to study the role of Pol $\alpha$  phosphorylation in W303 by transferring described meiotic synchronization protocols to this background. For instance, the pCUP1-*IME1* system may be introduced to induce a more synchronous and efficient meiosis in W303 background. We expect that, by using a less efficient biological system, meiotic defects will manifest easier and will help us to pinpoint the specific function of Pol $\alpha$  phosphorylation.

## **Meiotic and Mitotic recombination are intrinsically different**

As MiDAS is still a poorly characterized system, meiosis was the perfect biological context to start pinpointing the molecular mechanism of Pol $\alpha$  phosphorylation in recombination. The rationale of this project was to characterize the function of Pol $\alpha$  phosphorylation in meiotic recombination and extrapolate it to our system with extended S phase. However, meiotic recombination and MiDAS are deeply different, both in origin, outcome and mechanisms.

First, the biological purpose of both recombination systems is different. MiDAS arises from accidental incomplete DNA replication (as proposed in Bhowmick R. and Hickson I.A., 2017) and, based on our system, uses a non-cleaved replication fork as a template to complete DNA synthesis during mitosis. Meiosis, is the other hand, has a programmed mechanism to induce DSBs that will help the proper segregation of chromosomes in prophase I (Klapholz S. *et al.*, 1985). Even though both mechanisms ultimately shape genome evolution, we consider meiosis as a programmed mechanism used by cells while MiDAS as a survival mechanism for cells that did not manage to finish chromosome duplication before mitosis.

Second, mitosis and meiosis are two different cellular contexts. Mitotic entry and prophase I entry both depend on an increase in CDK activity. However, during mitosis CDK is associated with M-cyclins (Clb1,2,3,4) whereas in prophase I, it is still associated with S-cyclins (Clb5,6). Moreover, during meiosis there are kinases not present in mitosis, like Ime2. The different kinases acting in meiosis could explain the different phosphorylation pattern of Pol $\alpha$  compared to what we described in mitosis.

Third, the molecular requirements for MiDAS and meiotic recombination are different. We propose that MiDAS takes places through a BIR-like mechanism, that is highly mutagenic for cells (Osia B. *et al.*, 2022). Conversely, meiosis uses other types of HR-pathways, like DSBR and SDSA, that are less dangerous than BIR to repair DSBs, as they restrict the DNA region to be repair. Importantly, not only the recombination machinery but also the checkpoint is different. While MiDAS occurs when the DDR and Rad53 are active and its function is essential for survival, meiosis apparently does not require Rad53 (Cartagena-Lirola H. *et al.*, 2008). It was hypothesized that Spo11-dependent DSBs are “overlooked” by the DDR, but not DSBs derived from genotoxic agents, like phleomycin, suggesting an adaptation of the checkpoint to meiosis (Cartagena-Lirola H. *et al* 2008).

Finally, Pol $\alpha$  complex is found in a different genetic context in both situations. Pol $\alpha$  travels with the replisome when MiDAS occurs, being in the point of initiation of recombination. During meiosis, DSBs occur after S phase is finished and, even though the recombination program is modulated by the replication program (Murakami H. and Keeney S., 2014), the replisome must have duplicated the region before DSBs occur, thus locating Pol $\alpha$  away from the DSB sites. Thereby, we consider that the role of Pol $\alpha$  phosphorylation in meiosis might be different to the one in mitosis. Importantly, there are characteristics of Pol $\alpha$  that we do not know in the meiotic context: its chromatin binding dynamics, its interactome, the stability of the polymerase complex during meiosis... Moreover, even though we detected no impact in CO formation, we cannot exclude that it can be involved in other processes, like DSB or NCO formation.

For these reasons, I believe that mitotic and meiotic recombination should be treated as two different cellular processes, suggesting that Pol $\alpha$  phosphorylation might have two different functions.

## **Chapter iv: Conclusions**

## v. General Discussion and Conclusions

One of the important ideas of this work is to understand how cells balance genome stability with genome variability. Genome variability is not inherently detrimental for cells, but requires careful regulation. Indeed, evolution cannot be explained solely by accidental spontaneous mutations. Cells have embedded mechanisms in their regulation, like HR or meiosis, that promote a slow and regulated genetic diversity. However, these mechanisms need to be tightly regulated or cells can rapidly mutate, leading to malignant situations like cancer development (Bishop A.J. and Schiestl R.H., 2002; Feichtinger J. and McFarlane R.J., 2019).

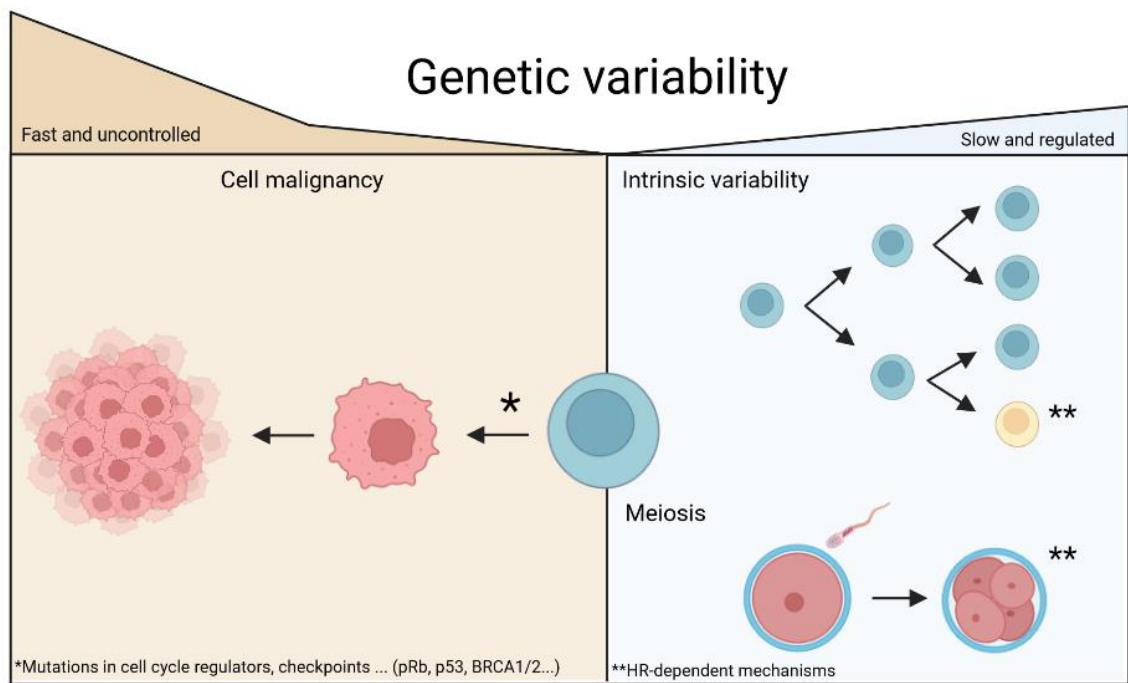


*Figure iv.1. Genetic variability is a normal process in cells. Cells use different mechanisms to promote slow and regulated genetic variability. However, deregulation of this mechanisms derives into catastrophic situations as cell malignancy.*

In eukaryotes, the replication machinery evolved to ensure genome stability, while in bacteria and viruses, replication is achieved using recombination mechanisms (Viret J.F. *et al.*, 1991; Kreuzer K., 2000). This translates into striking differences in mutagenesis rates between domains of life, being increased in viruses and bacteria (Drake J.W. 2006) probably because the latter have to adapt rapidly to changing biological situations.

Importantly, eukaryotes do not refrain genetic variability fully, as HR is a normal part of cell cycle regulation. Meiosis scrambles parental genomes to increase the variability of a population, but it is unable to generate new structural variants of chromosomes. On the other hand, MiDAS is a last resort mechanism that arises to complete genome duplication in difficult-to-replicate regions, mainly late-replicating regions. However, the drawback of this mechanism is the increase in genome instability. Interestingly, late-replicating regions have been shown to be a reservoir for mutations and replication timing influences mutagenesis of certain regions of the genome (Lang G.I. and Murray A.W., 2011; Agier N. and Fischer G., 2012, Agier *et al.*, 2018). Thus, it is an interesting idea that eukaryotic genomes evolved in a way to protect certain regions from mutations by promoting early replication (like centromeres in budding yeast; McCarroll R.M. and Fangman W.L., 1988; Feng W. *et al.*, 2009) and allow mutagenesis by HR-related mechanisms in late replicating regions (Ji F. *et al.*, 2020). In conclusion, we postulate that eukaryotic cells have mechanisms to promote controlled and slow genetic variability in specific genomic regions.

One of the reasons why eukaryotic cells tightly control genetic variability may be the complexity of their genomes. Small genetic alterations have substantial impacts on cell identity and on cellular functions, cancer development being a clear example. Genome instability is one of the hallmarks of cancer and a single mutated gene can drive into cell malignancy (Hanahan D. and Weinberg R.A., 2011; Martinez-Jimenez F. *et al.*, 2020). It is also important to note that many of cancer driver genes are implicated in either cell cycle regulation or DNA repair pathways (TP53, pRB, BRCA1/2 ...), which loss derives into a selfish growth and cumulative increase of genome instability. Indeed, cancer is a canonical example of Darwinian evolution, were the fittest, the better adapted, survives. In other words, cells that mutate more have more chances to become insensitive to growth restrictions and to acquire malignant capacities to overcome the normal cell population.

For these reasons, we believe that a better understanding of the mechanisms that promote genome instability; like meiosis, MiDAS and cell cycle regulation, are essential not only to understand evolution, but to develop therapeutic approaches for diseases like cancer.

## **Chapter v: Methods**

## 1. List of strains

All the *S. cerevisiae* strains used in this work are derivatives of W303 or SK1 backgrounds. They are listed in the following table:

### **Identifier (W303)    Genotype**

**E1027** MAT $\alpha$ , *ade2-1, trp1-1, can1-100, leu2-3,112, his3-11,15, ura3, GAL, chk1::LEU2*

**E1057** MAT $\alpha$ , *ade2-1, trp1-1, can1-100, leu2-3,112, his3-11,15, ura3-1, GAL, psi+, rad52::TRP1*

**E1265** MAT $\alpha$ , *ade2-1, trp1-1, can1-100, leu2-3,112, his3-11,15, ura3, GAL, rad53-11, chk1::LEU2*

**E2031** MAT $\alpha$ , *ade2-1, trp1-1, can1-100, leu2-3,112, his3-11,15, GAL, psi+, ura3::URA3/GPD-TK(7x), AUR1c::ADH-hENT1*

**E2437** MAT $\alpha$ , *ade2-1, trp1-1, can1-100, leu2-3,112, his3-11,15, ura3, bub1::SpHIS5, LEU2::tetR-GFP, CEN5::tetO2X112::HIS3 (1,4 Kb)*

**E2887** MAT $\alpha$ , *ade2-1, trp1-1, can1-100, leu2-3,112, his3-11,15, ura3, GAL, psi+, cdc6-1, chk1::LEU2, SPC29-CFP(Kan)*

**E2889** MAT $\alpha$ , *ade2-1, trp1-1, can1-100, leu2-3,112, his3-11,15, ura3, GAL, psi+, cdc6-1, rad53-11, chk1::LEU2*

**E3087** MAT $\alpha$ , *ade2-1, trp1-1, can1-100, leu2-3,112, his3-11,15, GAL, psi+, RAD5, ura3::URA3/GPD-TK(5x), AUR1c::ADH-hENT1*

**E3403** MAT $\alpha$ , *ade2-1, trp1-1, can1-100, leu2-3,112, his3-11,15, ura3-1, cdc6-1, RAD52-GFP, URA3::mCherry-TUB1*

**E3408** MAT $\alpha$ , *ade2-1, trp1-1, can1-100, leu2-3,112, his3-11,15, ura3-1, RAD52-GFP, URA3::mCherry-TUB1*

**E3689** MAT $\alpha$ , *ade2-1, trp1-1, can1-100, leu2-3,112, his3-11,15, ura3, GAL, psi+, cdc6-1, URA3::GAL-SWE1, RAD52-GFP*

**E3879** MAT $\alpha$ , *ade2-1, trp1-1, can1-100, leu2-3,112, his3-11,15, ura3, GAL, psi+, cdc6-1, rad51::LEU2, URA3::GPD-TK (5 copies), AUR1c::ADH-hENT1*

**E3888** MAT $\alpha$ , *ade2-1, trp1-1, can1-100, leu2-3,112, his3-11,15, ura3, GAL, psi+, cdc6-1, URA3::GPD-TK (5x), AUR1c::ADH-hENT1*

**E4523** MAT $\alpha$ , *RAD52-GFP, URA3::mCherryTUB1, pol1-cdk13A, pol12-cdk12A*

**E4572** MAT $\alpha$ , *cdc6-1, RAD52-GFP, URA3::mCherryTUB1, pol1-cdk13A, pol12-cdk12A*

**E4575** MAT $\alpha$ , *RAD52-GFP, URA3::mCherryTUB1, pol1-cdk13A, pol12-cdk12A*

**E4580** MAT $\alpha$ /alpha, *RAD52-GFP/RAD52-GFP, URA3::mCherry-TUB1 /URA3::mCherry-TUB1, pol1-cdk13A/pol1-cdk13A*

**E4581** MAT $\alpha$ /alpha, *RAD52-GFP/RAD52-GFP, URA3::mCherryTUB1/ura3, pol12-cdk12A/pol12-cdk12A*

**E4698** MATa, *ade2-1, trp1-1, can1-100, leu2-3,112, his3-11,15, pif1::KanMX4, RAD52-GFP, URA3::mCherry-TUB1*

**E4701** MATa, *ade2-1, trp1-1, can1-100, leu2-3,112, his3-11,15, ura3, GAL, psi+, RAD5*

**E4703** MATa/alpha diploid, *ade2-1, trp1-1, can1-100, leu2-3,112, his3-11,15, ura3, GAL, psi+, RAD5*

**E4865** MATalpha, *ade2-1, trp1-1, can1-100, leu2-3,112, his3-11,15, ura3, GAL, DDC2-YFP, pol32::KanMX*

**E4866** MATa, *ade2-1, trp1-1, can1-100, leu2-3,112, his3-11,15, ura3, GAL, cdc6-1, DDC2-YFP, pol32::KanMX, URA3::mCherry-TUB1*

**E4867** MATa, *ade2-1, trp1-1, can1-100, leu2-3,112, his3-11,15, ura3, GAL, cdc6-1, DDC2-YFP, pif1::KanMX*

**E5287** MATalpha, *ade2-1, trp1-1, can1-100, leu2-3,112, his3-11,15, ura3, GAL, psi+, pol1-cdk13A, pol12-cdk12A, RFA1-CFP, RAD52-GFP, URA3::mCherryTUB1*

**E5585** MATalpha, *ade2-1, trp1-1, can1-100, leu2-3,112, his3-11,15, GAL, psi+, RAD5, pol1-cdk13A, pol12-cdk12A*

**E5588** MATa/alpha, *RAD5, pol1-cdk13A/id, pol12-cdk12A/id, RFA1-CFP/RFA1, URA3::mCherryTUB1/ura3-1*

**E5614** MATa/alpha, *ade2-1, trp1-1, can1-100, leu2-3,112, his3-11,15, GAL, psi+, RAD5/RAD5, pol1-cdk13A/pol1-cdk13A, spo11::KanMX4/spo11::KanMX4, spo13::LEU2/spo13::LEU2, MTW1-4GFP::KanMX6/MTW1*

**E5620** MATa/alpha, *ade2-1, trp1-1, can1-100, leu2-3,112, his3-11,15, GAL, psi+, RAD5/RAD5, spo11::KanMX4/spo11::KanMX4, spo13::LEU2/spo13::LEU2, MTW1-4GFP::KanMX6/MTW1*

**E5793** MATa, *ade2-1, trp1-1, can1-100, leu2-3,112, his3-11,15, ura3, GAL, psi+, RAD5, cdc6-1, pol1-cdk13A, pol12-cdk12A, URA3::GPD-TK (5 copies), AUR1c::ADH-hENT1*

**E5956** MATa, *ade2-1, trp1-1, can1-100, leu2-3,112, his3-11,15, GAL, psi+, cdc6-1, RAD5, URA3::GPD-TK(5x), AUR1c::ADH-hENT1*

**E5964** MATa, *ade2-1, trp1-1, can1-100, his3-11,15, ura3-1, GAL, psi+, cdc6-1, LEU2::GPD1-OsTIR1, DNA2-AID\*-myc9::HYG, mcm4::MCM4-5FLAG (hphNT), POL1-3PK, CTF4-6HA::HIS3, RAD5+*

**E6004** MATa, *ade2-1, trp1-1, can1-100, his3-11,15, ura3-1, GAL, psi+, cdc6-1, LEU2::GPD1-OsTIR1, DNA2-AID\*-myc9::HYG, mcm4::MCM4-5FLAG (hphNT), CTF4-6HA::HIS3, RAD5, pol1-cdk13a-3PK, pol12-cdk12a*

**E6012** MATa, *ade2-1, trp1-1, can1-100, his3-11,15, ura3-1, RAD5, cdc6-1, leu2::GPD1-OsTIR::LEU2, DNA2-AID\*-myc9::HYG, mcm4::MCM4-5FLAG (hphNT), CTF4-6HA::HIS3*

**E6098** MATa, *ade2-1, trp1-1, can1-100, his3-11,15, ura3-1, GAL, psi+, cdc6-1, RAD5, DNA2-AID\*-myc9::HYG, CTF4-6HA::HIS3, POL12-3PK, POL1-3PK, mcm4::MCM4-5FLAG (hphNT)*

**E6354** MATa, *ade2-1, trp1-1, can1-100, leu2-3,112, his3-11,15, GAL, psi+, cdc6-1, RAD5, URA3::GPD-TK(5x), AUR1c::ADH-hENT1, pol32::KanMX4*

**Identifier (SK1)      Genotype**

**E5645** MATa/alpha, ho::LYS2, lys2, ura3, leu2::hisG, trp1::hisG, his3::hisG (SK1 background)

**E5681** MATa/alpha, ho::LYS2, lys2, ura3, spo11::hisG-URA3-hisG (SK1 background)

**E5790** MATa/alpha, ho::LYS2, lys2, ura3, leu2::hisG, trp1::hisG, his3::hisG, pol12-cdk12a (SK1 background)

**E5841** MATa/alpha, ho::LYS2, lys2, ura3, leu2::hisG, trp1::hisG, his3::hisG, pol1-cdk13a (SK1 background)

**E5852** MATa/alpha, ho::LYS2, leu2, his, ura3, pol1-cdk13a, pol12-cdk12a (SK1 background)

**E5900** MATa/alpha, ho::LYS2, leu2, his, ura3, pol1-cdk13a, pol12-cdk12a, spo11::hisG-URA3-hisG (SK1 background)

**E5905** MATa/alpha, ho::LYS2, leu2, his, ura3, lys2, pol1-cdk13a, spo11::hisG-URA3-hisG (SK1 background)

**E5931** MATa/alpha, ura3::BrdInc-URA3, HIS3/his3::hisG, leu2::HisG, TRP1, HIS4-LEU2-(BAMHI; +ori)/his4-x::LEU2-(NgoMIV;+ori)-URA3, POL12-3PK, irt::KanMX-pCUP1-3HA-IME1 (SK1 background)

**E5934** MATa/alpha, ura3::BrdInc-URA3, leu2::HisG, TRP1, HIS4-LEU2-(BAMHI; +ori)/his4-x::LEU2-(NgoMIV;+ori)-URA3, POL1-3PK, irt::KanMX-pCUP1-3HA-IME1 (SK1 background)

**E5937** MATa/alpha, ura3::BrdInc-URA3, leu2::HisG, TRP1, HIS4-LEU2-(BAMHI; +ori)/his4-x::LEU2-(NgoMIV;+ori)-URA3, pol12-cdk12a-3PK, pol1-cdk13a-3PK, irt::KanMX-pCUP1-3HA-IME1 (SK1 background)

**E6144** MATa/alpha, pol12-cdk12a-3PK, KanMX-pCUP1-3HA-IME1, GAL-NDT80::TRP1 (SK1 background)

**E6249** MATa/alpha ura3 ho::hisG leu2::hisG irt1::KanMX-pCUP1-3HA-IME1 Pif1-Myc::HphMx pol1-22A-3PK pol12-23A-3PK spo11(Y135F)-6His3Flag::NatMx (SK1 background)

**E6250** MATa/alpha ura3 ho::hisG leu2::hisG irt1::KanMX-pCUP1-3HA-IME1 Pif1-Myc::HphMx pol1-22A-3PK spo11(Y135F)-6His3Flag::NatMx (SK1 background)

**E6252** MATa/alpha, ho::LYS2, lys2, ura3, leu2::hisG, trp1::hisG, his3::hisG, pol12-23A-3PK (SK1 background)

**E6257** MATa/alpha, ho::LYS2, lys2, ura3, leu2::hisG, trp1::hisG, his3::hisG, pol1-22A-3PK (SK1 background)

**E6260** MATa/alpha, ho::LYS2, lys2, ura3, leu2::hisG, trp1::hisG, his3::hisG, pol1-22A-3PK pol12-23A-3PK (SK1 background)

**E6292** MATa/alpha, ura3 ho::hisG leu2::hisG, HIS4::LEU2-(BamHI; +ori)/his4-X::LEU2-(NgoMIV; +ori)--URA3, irt1::KanMX-pCUP1-3HA-IME1 pol12-23A-3PK pol1-22A-3PK (SK1 background)

**E6326** MATa/alpha, *ura3 ho::hisG leu2::hisG, his4-X::LEU2-(NgoMIV; +ori)--URA3/HIS4::LEU2-(BamHI; +ori) irt1::KanMX-pCUP1-3HA-IME1 pol1-22A-3PK* (SK1 background)

**E6334** MATa/alpha, *ura3::BrdUInc-URA3 HIS3 TRP1 ura3 ho::hisG leu2::hisG, HIS4::LEU2-(BamHI; +ori)/his4-X::LEU2-(NgoMIV; +ori)--URA3, POL12-3PK POL1-3PK irt1::KanMX-pCUP1-3HA-IME1* (SK1 background)

**Table v.1. List of strains used in this thesis. Strain background is indicated in different colors (Black: W303 background, Green: SK1 background)**

## **2. Yeast cell culture and related methods**

Yeast cells were cultured using the standards methods for *S. cerevisiae*:

- Solid agar plates: 9 cm Petri dishes were filled with solidified media and cells were plated using plastic disposable loops or glass beads. Cells did not exceed a maximum of 2 days growth on plate prior experimentation.
  - YEPD (YPD) plates: 1% Yeast Extract, 2% Peptone, 2% Glucose, 2% Bacto-agar.
  - YP-Glycerol Plates (3% Glycerol Plates): 1% Yeast Extract, 2% Peptone, 3% Glycerol, 2% Bacto-agar.
  - Selection plates: if drugs were used as selection marker, they were added to YEPD plates (Geneticin 200ug/mL, Aureobasidin A 0.5 ug/mL). If autotrophy was used for selection, minimum plates were used supplemented with the required amino-acids.
  - SpoRR plates: 2.5 g/L Yeast Extract, 1 g/L Glucose, 20 g/L Potassium Acetate, 1.5% wt/vol bacto-agar, 75 mg/L of adenine, histidine, leucine, lysine, methionine, tryptophan and uracil.
  
- Liquid culture: cells were grown in a glass flask with a ratio 1:3 (flask volume:media) at a speed of 150 rpm, except indicated otherwise.
  - YPD: 1% Yeast Extract, 2% Peptone, 2% Glucose
  - Semi-YPD: 1% Yeast Extract, 2% Peptone, 1% Glucose
  - SC: (for 1L) 2.2g Yeast Nitrogen Base, 5.5g Ammonium sulfate, 20 mL AAA (50x), 100 mL Glucose 20%
  - YPA: 1% Yeast Extract, 2% Peptone, 1% Potassium Acetate
  - SPM: 1% Potassium Acetate, 0.02% Raffinose, 0.001% Polypropylene glycol (PPG)

## **2.1. On-plate protocols**

### **2.1.1. Survival assay: CFU assay**

This assay was designed to analyze cell viability of *cdc6-1* mutants after different exposure to 30 °C. We estimate that 2 hours exposure is enough to induce one cycle of extended S phase in the majority of *cdc6-1* cells. The experiment is performed as follows:

1. Grow *cdc6-1* cells ON at 25 °C (permissive conditions).
2. The day after, dilute the culture to have exponentially growing cells. Let cells perform at least 2 divisions after dilution.
3. Dilute the culture to a concentration of  $2 \times 10^6$  cells/mL. Split in two cultures, one will be treated with 1 $\mu$ M Nocodazole and the other one with 1% DMSO.
4. Transfer the sub-cultures at 30 °C, add Nocodazole/DMSO and incubate for 3 hours. Every hour, take a 1 mL aliquot, centrifuge (2000 rpm, 2 min), wash with 1 mL of water, measure cell concentration with a cell counter and plate on YPD plates to have approximately 100 CFU.
5. Incubate YPD plates at 25 °C (permissive temperature) for 2-3 days.

CFU were counted on every plate, using three technical replicates per timepoint and a total of 3 biological replicates (Examples **Figure iv.1**). Plates were randomized and counting was done blindly. Per strain, total CFU at timepoint 0 was normalized to 100, and the other timepoints were normalized accordingly. Importantly, the nocodazole concentration used has been reported to extend but not block mitosis (Wang Y. and Burke D.J., 1995). Moreover, treatment with 1 $\mu$ M nocodazole was not toxic for WT strain but was for the SAC deficient *bub1 $\Delta$*  mutant.

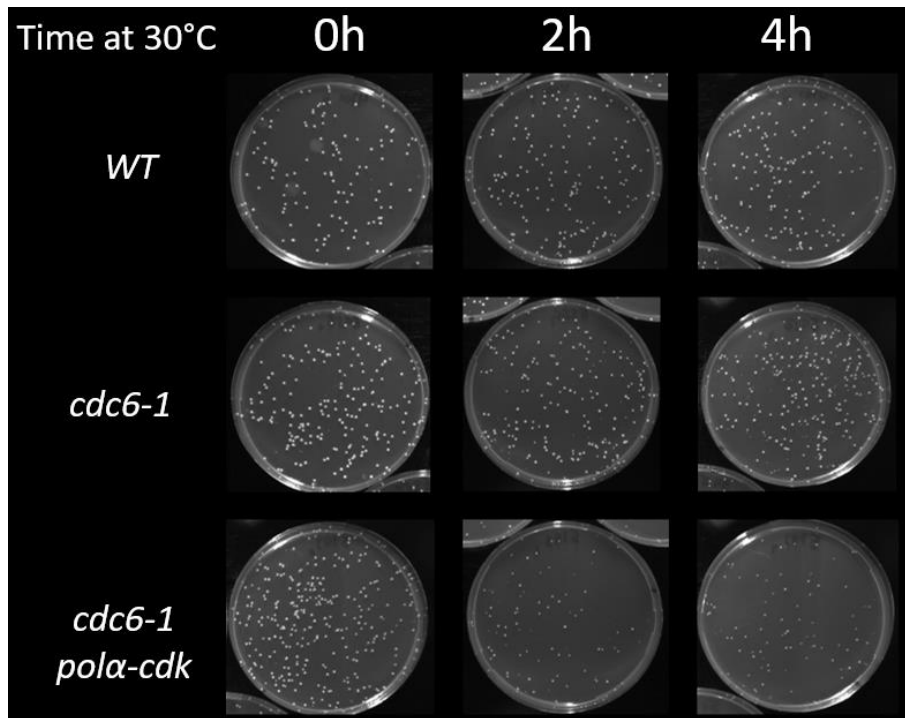


Figure v.1. Representative images of CFU assay in *cdc6-1* mutants.

## **2.2. In-liquid protocols**

### **2.2.1. $\alpha$ -factor synchronization**

For all the experiments involving cell cycle kinetics, cells were synchronized in G<sub>1</sub>. Asynchronous cells were grown at 25 °C in YPD or SC media to  $2-3 \times 10^6$  cells/ml and  $\alpha$ -factor (1  $\mu$ g/mL) was added for 1 hour and 5 min twice. Importantly, this step was done at 30 °C in the *cdc6-1* mutants to ensure partial inactivation of the Cdc6 protein during the licensing step in G<sub>1</sub>. Then cells were release into the cell cycle by removing  $\alpha$ F either by centrifugation (1500 rpm for 3 min) and resuspension in  $\alpha$ -factor free media (small cultures) or by adding pronase (50  $\mu$ g/mL, large cultures). In addition, for the experiments measuring mitotic defects,  $\alpha$ -factor (5  $\mu$ g/mL) was added to the cell culture 45 min after release to arrest cells in the next G<sub>1</sub>.

### **2.2.2. In vivo incorporation of EdU and click-it reaction**

The EdU incorporation protocol has been already described in Talarek N. *et al.*, 2015 and Barba Tena J.D. *et al.*, 2022 (Chapter vii). Genetically-engineered yeast cells containing hENT1 (human Equilibrative Nucleoside Transporter) and TK (Thymidine Kinase) were used in all experiments involving EdU incorporation. Here is the protocol for EdU labelling starting from an exponentially growing culture in SC media ( $2 \times 10^6$  cells/mL approximately):

1. Transfer 1 mL of cell culture to a 2.0 mL microfuge tube containing 1  $\mu$ L of 10 mM EdU. Mix well by inversion.
2. Incubate for 3–10 min at 30 °C under agitation in a shaking water bath.
3. Stop the reaction with the addition of 100  $\mu$ L 100% ethanol.
4. Pellet the cells for 2 min at 10,000  $\times$  g in a microfuge. Remove the supernatant using a vacuum pipette.
5. Resuspend the cell pellet in 500  $\mu$ L 70% ethanol. Mix well by vortexing.
6. Leave for  $\geq$ 1 h at RT at 20 tilts/min on a variable speed rocker to permeabilize the cells.
7. Pellet the cells for 2 min at 10,000  $\times$  g in a microcentrifuge. Discard the supernatant with a vacuum pipette.
8. Resuspend cells in 100  $\mu$ L PBS, depending on the size of the pellet, and store at 4°C or -20°C for longer periods of time.

#### For Click-it reaction

1. Pellet the cells for 2 min at 10,000  $\times$  g in a microfuge. Discard the supernatant with a vacuum pipette.
2. Resuspend the cell pellet in 200  $\mu$ L of PBS + 1% bovine serum albumin (BSA). Incubate for 30 min at RT. Pellet the cells for 2 min at 10,000  $\times$  g in a microcentrifuge. Discard the supernatant with a vacuum pipette.
3. Prepare fresh Azide Dye buffer by mixing the reagents in the following order (quantity for one tube): 36  $\mu$ L of PBS, 2  $\mu$ L of 0.2 M CuSO<sub>4</sub>, 0.2  $\mu$ L of 2 mM Cy5-Azide (FACS)/Dy-530 Azide (microscopy analysis), and 2  $\mu$ L of 1 M ascorbic acid.
4. Resuspend the cell pellet with 40  $\mu$ L of freshly made Azide Dye mix. Incubate at RT in the dark for 60 min.
5. Pellet the cells for 2 min at 10,000  $\times$  g in a microcentrifuge. Discard the supernatant with a vacuum pipette. Wash the cells 3 times with 300  $\mu$ L 10% ethanol in PBS.

### **2.2.3. Measurement of cell cycle phase duration**

The duration of different cell cycle phases was determined as described in Barba Tena J.D. *et al.*, 2022 (Appendix 1). Briefly, asynchronous and exponentially growing cells were pulse-labelled with 10 $\mu$ M EdU for 5 min. Using bivariate PI-EdU FACS, we determined the fraction of cells in G<sub>1</sub>, S phase and G<sub>2</sub>/M cells. Then, we calculated the doubling time of every strain by monitoring cell divisions for 7 hours. Knowing both, the proportion of cells in every phase and the doubling time, we calculated the duration of every cell cycle phase as:

### **2.2.4. Meiotic induction on SpoRR plates**

1. Patch diploid cells on YP-Glycerol\_plate and grow them for 2 days at 30°C. This step is performed to avoid petite yeast and boost mitochondrial activity.
2. Inoculate one colony in 5 ml YPD and let cells grow ON at 30°C.
3. From saturated culture, centrifuge 2 min 2,000 rpm to pellet cells. Wash cells twice with 2 ml water.
4. Resuspend in 1-5 ml water. Plate between 1 x 10<sup>7</sup> to 5 x 10<sup>7</sup> cells per plate using sterile glass beads on SpoRR plates. Incubate at 30°C

Score for dyads and tetrads after 24 h, and every 6-12 h afterwards. Sporulation efficiency should be 80-90% for WT.

### **2.2.5. Meiotic Synchronization: YPA-SPM protocol**

1. Patch diploid cells on YP-Glycerol\_plate and grow them for 2 days at 30°C. This step is performed to avoid petite yeast and boost mitochondrial activity.
2. Inoculate one colony in liquid YPD ON to reach a saturated culture.
3. Wash saturated culture in freshly-prepared YPA media. Inoculate 1.5 x 10<sup>6</sup> cells/mL and let grow at 30°C, 250 rpm, in a volume of 1:10 (liquid:air) during 16 hours.
4. Rinse the cells with freshly made SPM media and inoculate 2x10<sup>7</sup> cells/mL in SPM media. Keep same incubation parameters as mentioned above.

Cells perform pre-meiotic S phase between 3-4 hours after SPM inoculation and by 6 hours most of them have finished both meiotic divisions. At 7 hours, spores and tetrads can be seen.

### **2.2.6. Meiotic Synchronization: pCUP1-IME1 protocol**

This protocol is original from Chia M. and van Werven F. 2016, with modifications from Valerie Borde's lab and myself. All strains contained the *pCUP1-IME1* construct.

1. Inoculate 1 colony from fresh YPD or YP-Glycerol\_plate in 5 mL YPD. Let them grow at 30 °C, 150 rpm, for 19 hours.
2. From the saturated culture, dilute it 1/100 in YPD in a volume ratio 1:10 (culture: flask). Grow at 30 °C, 250 rpm for 5 hours.
3. The culture should be in exponential phase. Inoculate cells in semi-YPD medium to have the day after  $1 \times 10^8$  cells/ml (they should be entering stationary phase). Grow at 30 °C, 250 rpm with 1:10 ratio.
4. Wash cells once with Potassium Acetate 1%. Dilute 4.8 times the culture into freshly made SPM medium. Grow at 30 °C, 250 rpm with 1:10 ratio.
5. After 2 hours, add CuSO<sub>4</sub> to the medium to reach a concentration of 50 μM.

Pre-meiotic S phase should occur between 3 and 4 hours, DSBs formation from 4 to 6 hours and meiotic divisions between 6 to 9 hours

### **3. Molecular Biology techniques**

#### **3.1. Yeast transformation: LiOAC protocol**

1. Grow an ON preculture in YPD (5-10 ml per transformation) to reach  $\sim 1 \times 10^7$  cells/ml the next morning
2. Dilute to  $2.5 \times 10^6$  cells/mL and wait at least that cells perform two cell divisions.
3. Centrifuge 2 min at 3500 rpm and discard supernatant.
4. Resuspend the pellet in 1 mL LiAc 1M.
5. Centrifuge 1 min at 3,500 rpm and discard supernatant.
6. Estimate cell pellet and resuspend with an equal volume of LiAc 1M.
7. For transformation, mix:
  - 12  $\mu$ L cell suspension
  - 4  $\mu$ L ssDNA (Salmon Sperm DNA, 10 mg/ml)
  - 1-5  $\mu$ L transforming DNA (0.2-1  $\mu$ g for plasmids, or 5-10x more for integration)
  - 45  $\mu$ L PEG 4000 50%
8. Mix well by flicking tubes and incubate 60 min at RT (30 min for diploids)
9. Add 6  $\mu$ L sterile glycerol 60%, mix well by flicking and incubate 60 min at RT (30 min for diploids)
10. Heat shock 10 min at 42°C (5 min for diploids or temperature sensitive mutants)
11. Dilute with 200  $\mu$ L sterile H<sub>2</sub>O and spread on selective plates; incubate 2-3 days at 30°C

#### **For GAP repair cloning**

Cloning was performed by exploiting the ability of *S. cerevisiae* to repair DNA fragments (Kitazono A.A., 2009). W303 budding yeast cells were co-transformed with an amplified PCR fragment containing part of POL1 or POL12 harboring our mutations of interest and a linearized plasmid containing a cloned non-mutated version of our target gene. This plasmid was digested in the region to mutate using two restriction enzymes that generate non-cohesive ends to prevent ligation. After transformation, cells were selected based on plasmid resistance, plasmids were extracted, amplified in bacteria and sequenced to confirmed the insertion of desired mutations.

### For CRISPR-Cas9 editing

Gene editing was performed using CRISPR-Cas9 technology in SK1 yeast background. We used SK1 strains that contained POL1 and POL12 genes followed by a KanMX resistance cassette in the 3' UTR of the ORF. We co-transformed our SK1 strains with a plasmid encoding Cas9 and a gRNA against the KanMX cassette (provided by Valerie Borde, original from B. Futcher) and with PCR product of our mutated genes (*pol1-22A* or *pol12-23A*) with 100 bp upstream and downstream the ORF. Yeast transformants were selected based on auxotrophic markers (Leucine) or drug resistance (Nourseothricine), counter-selected for G418 resistance and analyzed by genome sequencing.

### 3.2. Colony PCR

PCR was performed directly from yeast colonies to monitor different genetic markers without the requirement to extract genomic DNA. Yeast biomass was collected from the colony, resuspended in 10 µL H<sub>2</sub>O and heated for 10 min at 95 °C. Afterwards, traditional PCR was performed. Here I attach the protocol and PCR conditions for two genetic markers I followed:

- For *RAD5*

**D1124 (L)** 5'-GCAGCAGGACCATGTAAACG-3'  
**D1125 (R)** 5'-AAACTCGTTACTCCACTGCG-3'

<b>PCR reaction</b> (Gibco) stock				<b>50</b>	<b>µl</b>	<b>Mix</b>	<b>375</b>	<b>µl</b>
1 x	PCR buffer (-MgCl <sub>2</sub> )	10x		5	µl	37,5		µl
0,2 mM	dNTP mix	10mM		1	µl	7,5		µl
3 mM	MgCl <sub>2</sub>	50mM		3	µl	22,5		µl
0,5 µM	primers (each)	10µM		2,5	µl x2	18,75		µl x2
0,25 ng/µl	DNA	? ng/µl		1	µl			
1 U	Taq DNA pol	50U/µl	(from Léon)	1	µl	7,5		µl
	H <sub>2</sub> O			34	µl	255		µl

**PCR:** 35 cycles

	94 °C	5 min
Denaturation	94 °C	30 s
Annealing	52 °C	20 s
Elongation	68 °C	30 s
	68 °C	5 min

**Enzyme digestion:** *Mnl*1 (1h at 37°C).  
To 25µl PCR, add 2µl buffer **NEB2**, 0.2µl BSA and 0.2µl *Mnl*1

**Gel:** Run a 2.5% gel to separate the restriction fragments (microwawe carefully !!)

<b>Fragments:</b>	<b>W303</b>	<b>W303R</b>	<b>PCR product</b>
	155bp	182bp	337bp
	120bp	155bp	
	62bp		

- **For HIS4::LEU2 Recombination locus**

Protocol from Valerie Borde's Lab.

Goal of genotyping = determine if the flanking heterozygous XhoI sites (X) and the central NgoIV (N) or BamHI (B) site have not been converted during meiosis.

- To check for the presence of the left flanking XhoI sites:
  - o PCR1=pr1917 (LEU2intR)+pr1918 (HIS4-918F)
- To check for the presence of NgoIV and BamHI polymorphisms:
  - o PCR2= pr1235 (NFS1rev)+pr1236 (RRP7rev)
- To check for the presence of the right flanking XhoI sites:
  - o PCR3=pr1233 (STE50rev)+pr1234 (YCL33Crev)

PCRs with Phusion polymerase :

For PCR1:

2' 98°C

30 times :

10" 98°C

15" 58°C

4' 72°C

1 time :

5' 72°C.

For PCR2 and 3:

2' 98°C

30 times :

10" 98°C

15" 61°C

1' 72°C

1 time :

5' 72°C.

Then digest PCR products :

- PCR1 with XhoI
- PCR1 with BamHI
- PCR2 with XhoI.

Run in parallel with PCR using the starting strains (derived from ANT1427 and ANT1428) as controls.

pr1917 GTAGGGCCATGAAAGCGGCC  
pr1918 TGGTCCTCGAAGAAGTGCAAC  
pr1235 TGACCTGACCATTTGATGGAGT  
pr1236 TGGATTGAATTTTCTCTTAGCTTTC  
pr1233 CGGGGGTGACATTGTCACCTT  
pr1234 GGTTTAAAGACGCACTGTTCA

### **3.3. DNA content flow cytometry analysis**

DNA replication profiles were generated by monitoring cell cycle progression by FACS. This protocol is described in details in Barba Tena J.D. *et al.*, 2022:

1. From a growing culture, pellet the cells for 2 min at 10,000 × g in a microfuge.
2. Remove the supernatant using a vacuum pipette.
3. Resuspend the cell pellet in 500 μL 70% ethanol. Mix well by vortexing.
4. Leave for ≥1 h at RT at 20 tilts/min on a variable speed rocker to permeabilize the cells.
5. Pellet the cells for 2 min at 10,000 × g in a microcentrifuge. Discard the supernatant with a vacuum pipette.
6. Resuspend the pellet in 200 μL PBS containing 0.1 mg/mL RNase A and 0.2 mg/mL proteinase K.
7. Incubate for 1-2 h at 50 °C with occasional shaking (or overnight at 37 °C).
8. Pellet the cells for 2 min at 10,000 × g in a microcentrifuge. Discard the supernatant with a vacuum pipette.
9. Resuspend the cell pellet in 100 μL PBS.
10. Transfer 10-30 μL (depending on the cell concentration) to a flow cytometer tube containing 300 μL of 50 mM Tris-HCl, pH 7.5, and 0.5 μM Sytox Green.
11. Sonicate 2x, for 2 s each time, at an amplitude of 40-50%.
12. Leave in the dark until processing the samples on a flow cytometer.
13. Read the Sytox Green samples using an excitation blue laser at 488 nm and a 530/30 BP filter (Flow cytometer Novocyte ACEA, operated by NovoExpress Software).

### **3.4. Protein extraction and Western blot**

8–20 ml of yeast culture was centrifuged and resuspended in 1 ml of 10% TCA. Cells were concentrated to 200 μL in 10% TCA, and 200 μL glass beads (Zirconia/Silica Beads; BioSpec Products, Inc.) was added. Cells were then lysed using a Bullet Blender (Next Advance), 2x 3 min at power 8. The supernatant was transferred to a new tube, the beads were washed twice with 200 μL 10% TCA, and extracts were pooled. Extracts were centrifuged at 3,000 rpm for 10 min, and the pellet was resuspended in 100–200 μL Laemmli buffer containing 5–10 μL Tris base (1 M). The extracts were boiled for 5 min, centrifuged for 5 min at 12,000 rpm, and transferred to new tube. Protein concentration was determined by Bradford assay.

10–15 µg whole-cell extracts were run on 8-15% acryl–bisacrylamide gels. Proteins were transferred to nitrocellulose membranes (Protran; Whatman) using wet blotting and revealed using standard immunoblotting and ECL procedures. Primary antibodies were rabbit polyclonal anti-DNA Pol $\alpha$  B subunit (Pol12; 1:1,000; clone 6D2; obtained from Marco Foiani), mouse monoclonal anti-Rad53 (clone EL7; 1:20; obtained from Marco Foiani), rabbit polyclonal anti-Swi6 (1:100,000 from clone R12), mouse monoclonal anti-PK (1:2,000, Biorad-serotec MCA1360G), rabbit polyclonal anti-Sic1 (1:5,000 gift from Lee Johnston clone R189), rabbit polyclonal anti-Clb2 (1:2,000 from Kim Nasmyth's lab, clone R98.12), mouse monoclonal anti- Orc6 (1:1,000, clone SB49 from Steve Bell and John Diffley labs), mouse monoclonal anti-Pgk1 (1:2,500, Invitrogen 459250). Secondary antibodies were anti-mouse IgG-HRP (1:25,000, Sigma) anti-rabbit IgG-HRP (1:30,000, Sigma), anti-rabbit IgG-IR800 (1:20,000, Thermo SA5-35571) and anti-mouse IgG-IR680 (1:20,000, Thermo 35518)

### **3.5. Cellular fractionation assay**

The procedure for chromatin purification is based on the method described by (Desdouets C. *et al.*, 1998). Briefly cells were arrested with  $\alpha$ -factor at  $2 \times 10^6$  cells/mL. The arrest and release of *cdc6-1* cells were performed at 30°C. Aliquots of cells were collected every 15 minutes, and aliquots were saved for FACS and budding index analysis. Cells were resuspended in 500 µL Solution I (100 mM Pipes-KOH pH 9.4, 10 mM DTT) and incubated for 10 minutes at 30°C. Cells were collected (2000 g, 2 minutes) and resuspended in 380 µL Solution II (50 mM KPO<sub>4</sub>, pH 7.5, 0.6 M sorbitol, 10 mM DTT), Zymolyase was added to a final concentration of 0.5 µg/µL and the samples were incubated for 30 minutes at 30°C with shaking, in order to digest the cell wall and obtain spheroplasts. Spheroplasts were washed 3 times with 500 µL Solution III (0.4M Sorbitol, 150 mM potassium acetate, 2 mM magnesium acetate, 20 mM Pipes-KOH, pH 6.8, Protease Inhibitor 1X), resuspended in 180 µL Solution III and lysed by addition of Triton X-100 to a final concentration of 1%. The chromatin-enriched fraction was isolated after centrifugation for 15 minutes at 15,000 g on a 30% sucrose cushion, and the supernatant was carefully removed (soluble fraction). Laemmli 6X and 1X were added to the soluble and chromatin fraction, respectively. Samples were boiled for 6 min, protein dosage was performed with Bradford assay and 15-20 µg proteins were loaded on a 12.5% polyacrylamide gel.

### **3.6. Protein immunoprecipitation**

To perform mass spectrometry analysis of Pol1 and Pol12, we used PK-tagged versions of our proteins of interest. Immunoprecipitations and co-immunoprecipitations were performed as follows:

1. Cultures were centrifuged (1500 rpm, 3 min, 4 °C) to obtain approximately  $1 \times 10^{10}$  cells.
2. After 2 washes with 50 mL 20 mM HEPES pH 7.9 and one wash with 20 mL Lysis Buffer, cells were resuspended in Lysis Buffer Supplemented (1g of pellet = 1 mL of Lysis Buffer Supplemented) and “popcorn” was made by freezing drops of cells in liquid nitrogen.
3. “Popcorn” was physically broken using Freezer Mill 6770 (15 CPS, 1.5 minutes, twice).
4. After thawing the powder, Glycerol Mix was added (1/4 of the volume) and chromosomal DNA was digested with benzonase (8 uL of Pierce Universal Nuclease, Fisher per 5 mL of sample) for 30 min on ice.
5. Clarification was made by centrifuging at 25,000 x g, 30 min at 4 °C, twice. Aliquots for total extracts (Input) were taken.
6. Incubation with Dynabeads coupled to anti-PK antibody was made during 2 hours, at 4°C with rotation. Dynabeads preparation and Ig coupling was done using the protocol provided by Invitrogen (Catalog No. MAN0015803).
7. Beads were washed 4 times with 2 mL Wash buffer and eluted depending on the analysis afterwards.
  - a. For phosphorylation mapping. Beads were eluted by adding 50 µL Laemmli 1X and boiling for 5 minutes to detach and solubilize proteins from the beads.
  - b. For interactome analyses. Beads were incubated for 30 min at RT with V5 peptide (0.74 mg/mL) on a rotating wheel. Then, supernatant was recovered and solubilized with Laemmli 1X by boiling for 5 min. By using this approach, we recover our protein of interest and the interactors without carrying anti-PK antibody (as seen in **Figure iv.2**).
  - c. For phosphatase assay. Beads were incubated 30 min with  $\lambda$  phosphatase (3 µL of PMP Buffer, 3 µL of  $\lambda$  PPase and 3 µL  $MnCl_2$ , NEB, PO753S) prior resuspension and solubilization with Laemmli 1X.

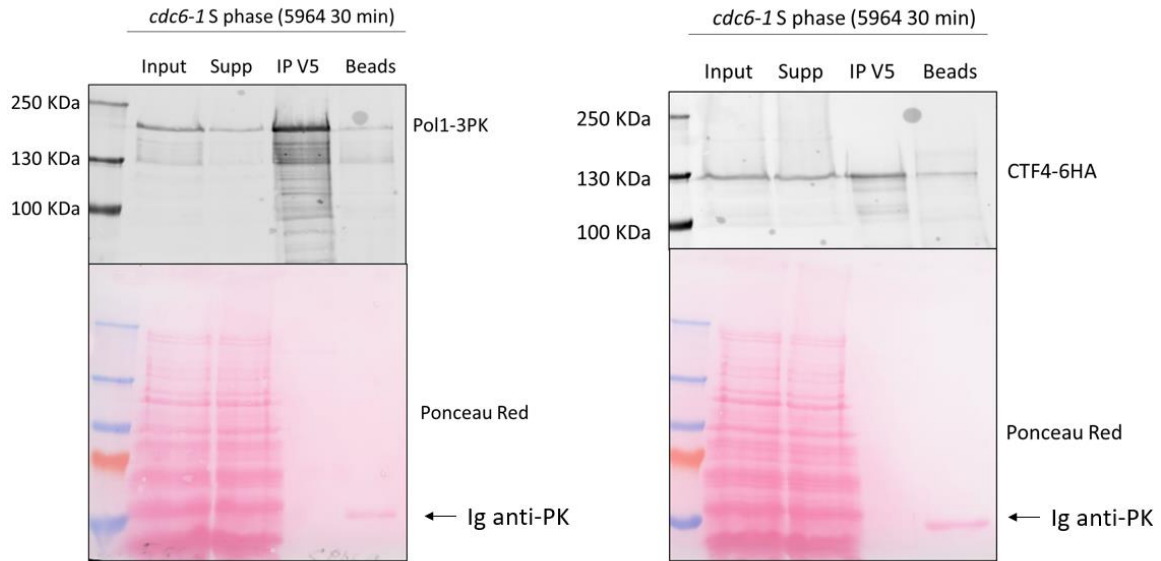


**Figure v.2. *Pol1-3PK immunoprecipitation and elution with V5 peptide.*** *Pol1-3PK immunoprecipitation from S-phase cells was performed by eluting with V5 peptide (Left blot). This method allows to efficiently pull down Pol1, its partners, like Ctf4 (right blot), but without contamination with anti-PK antibodies.*

- Lysis Buffer

HEPES 100 mM

Potassium Acetate 50 mM

Magnesium Acetate 10 mM

EDTA 2 mM

- Lysis Buffer Supplemented

HEPES 100 mM

Potassium Acetate 50 mM

Magnesium Acetate 10 mM

EDTA 2 mM

Sodium Fluoride 2 mM

**Beta-glycerol Phosphate 60 mM**

DTT 1 mM

PIC 1%

**Ortho-vanadate 1 mM**

Protein Inhibitor Cocktail Tablet, EDTA free (2 Tablets per 10 mL)

- Glycerol Mix

HEPES 100 mM

Potassium Acetate 300 mM

Magnesium Acetate 10 mM

EDTA 2 mM

Glycerol 50%

IGEPAL 0.5%

**Beta-glycerol Phosphate 81 mM**

DTT 1 mM

PIC 1%

**Ortho-vanadate 1 mM**

Protein Inhibitor Cocktail Tablet, EDTA free (2 Tablets per 10 mL)

- Wash Buffer

HEPES 100 mM

Potassium Acetate 100 mM

Magnesium Acetate 10 mM

IGEPAL 0.1%

Sodium Fluoride 2 mM

**Beta-glycerol Phosphate 81 mM**

PIC 1%

**Ortho-vanadate 1 mM**

Protein Inhibitor Cocktail Tablet, EDTA (2 Tablets per 10 mL)

### **3.7. Mass spectrometry analysis (in collaboration with Serge Urbach and Khadija el Koulali, FPP, Montpellier)**

Immunoprecipitation samples were loaded on gradient SDS-PAGE gels, stained with Silver and bands of interest were purified and resuspended in 10  $\mu$ L tampon A (0.1% formic acid). 2  $\mu$ L of purified bands were injected in a HPLC (RSLC U3000, Thermo Fisher Scientific) coupled to a mass spectrometer equipped with a nanoelectrospray (Q Exactive HF, Thermo Fisher Scientific).

Identified peptides were separated in a capillary column (0.075 mm x 500 mm, Acclaim Pepmap 100, Thermo Fisher Scientific) followed by a gradient separation in tampon B (range 2%-40%, 0.1% Formic Acid, 80% acetonitrile) at 300 nL/min. The mass spectrometry spectra were registered using Xcalibur 4.1 software with 128LowQtt.meth protocol and analyzed using MaxQuant software. Two databases were used to determine contaminants and yeast proteins (contaminants\_fpp\_180320.fasta, RefProteome\_YEASTcano\_2020\_02\_UP000002311.fasta).

- For phosphorylation mapping: all analysis, from phosphopeptide identification to phosphosite identification, were done with a fixed value of 1% FDR. For meiotic experiments, a total of 3 biological replicas were performed. For mitotic experiments, 1 biological replica was performed. For meiotic experiment, 3 biological replicas were performed.
- For interactome identification: peptide identification was done with a fixed value of 1% FDR and graphs and statistical test were done with Perseus Software. Immunoprecipitation from a Non-PK tagged strain was used as a negative control and analysis were performed on 3 biological replicas per sample (a total of 12 samples, **Figure iv.3**).

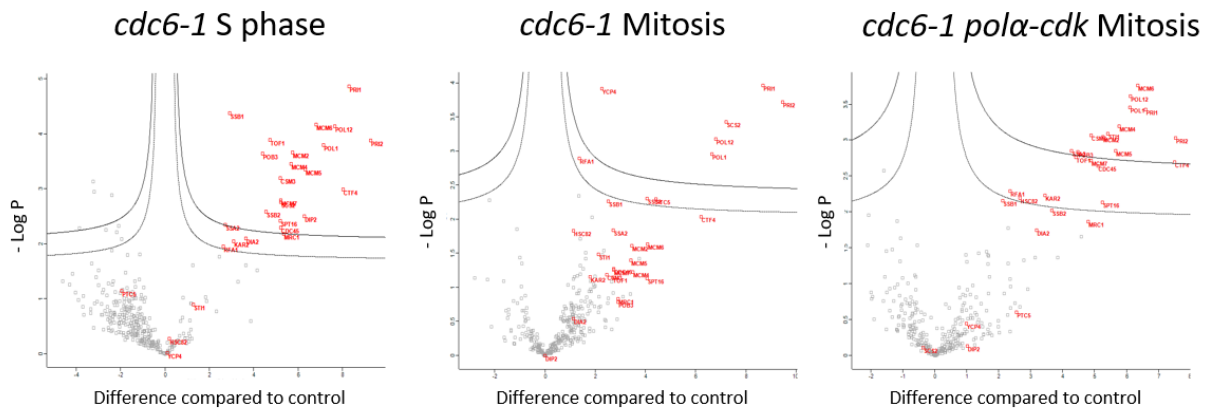


**Figure v.3. Hawaii Plots of Pol1 and Pol1-cdk13A interactomes in S phase and Mitosis.** Plots show enriched proteins in the sample compared to negative control. Relevant proteins are labelled in red. Curves lanes correspond to FDR of 1% and 5%.

### **3.8. DNA combing analysis in budding yeast cells**

For DNA combing, yeast strains expressing high levels of thymidine kinase (TK) as well as a human nucleoside transporter (hENT1) were grown in YPD at 25 °C and arrested for 2 h with  $\alpha$ -factor at different temperatures. BrdU was added to 50  $\mu$ M 30 minutes prior release. Cells were then filtered to eliminate  $\alpha$ -factor and resuspended in YPD 50  $\mu$ M BrdU at different temperatures. Cells were collected at the indicated times and treated for genomic DNA purification and DNA combing (as described in Schwob E. *et al.*, 2009). DNA was counterstained with a mouse anti-ssDNA antibody (MAB3034, Chemicon, 1 :300) and BrdU detected with a rat anti-BrdU antibody (OBT0030, AbCys, 1:20), revealed respectively with anti-mouse Alexa 546 and antirat Alexa 488 (Molecular Probes, 1:50). DNA fiber images were acquired on a Leica DMRA microscope equipped with a Photometrics CoolSnap CCD camera, and analyzed using MetaMorph and GraphPadPrism software. More than 200 fibers longer than 100 kb were analyzed on average for each time point, and the experiment was repeated three times by two different researchers.

### **3.9. Southern Blot analysis of HIS4::LEU2 recombination locus (performed by Valerie Borde, Institut Curie, Paris)**

Cells were synchronized and released into meiosis using the *pCUP1-IME1* synchronization protocol previously explained. Approximately  $1 \times 10^8$  cells were used per timepoint. Genomic DNA purification, digestion, processing and Southern blotting analysis was performed as described in Oh S.D. *et al.*, 2009.

## **4. Microscopy based techniques**

### **4.1. Fluorescent microscopy and analysis**

Microscopy analysis was performed as described in Magiera M. *et al.*, 2015. Briefly, cells were grown in SC medium, centrifuged, resuspended in 90  $\mu$ L SC medium, and fixed by the addition of 10  $\mu$ L 80% ethanol. If required, DAPI staining was performed by incubating cells with DAPI 0.5  $\mu$ g/mL for 30 min in the dark and washing once with PBS.

Then, cell suspension was briefly sonicated and concentrated to the desired density. 1.7  $\mu$ L cell suspension was put on a microscope slide and observed using the upright Leica Thunder microscope (operated with the LasX Software) using an 100X objective (Apochromat 0.7-1.4 NA oil) with the adequate lasers and filters (Brightfield, EdU – Cy3, DAPI – Hoechst, Rad52 – GFP, RPA - GFP, Tubulin – Texas Red). Image analysis was performed using the FIJI or ImageJ software. A minimum of 100 cells was analyzed per timepoint and all the analysis were done blindly or by different members of the lab.

### **4.2. Quantitative Image-Based Cytometry**

Mutant *cdc6-1* strains were grown in SC, synchronized in G<sub>1</sub> at 30 °C using  $\alpha$ -factor and released into the cell cycle. After 90 min, cells were pulse-labelled during 10 min with 25  $\mu$ M EdU (or DMSO as negative control). Cells were fixed, permeabilized and click reaction was performed as described previously using Azide-647. Finally, cells were stained with DAPI, sonicated and prepared for acquisition.

Acquisition was done with the ImageStream X MKII (operated by the ISX software) with a magnification of 60X taking images of Brightfield, DAPI and EdU using the lasers 405 nm (Violet - DAPI) and 640 nm (red – EdU/Azide). Every set of mutants was treated and acquired the same day to avoid technical variability and a total of 10,000 images per sample were obtained.

The analysis of the images was performed using the IDEAS software. After analysis, the percentage of MiDAS-positive cells and intensity of EdU signal per nucleus was extracted and analyzed with Prism and RStudio software. The following workflow was used to identify MiDAS-positive cells, and works similarly to gating in classic FACS (**Figure iv.4**):

1. Focused cells were selected based on the *Gradient\_MS\_BF* parameter.
2. Mitotic arrested cells (Dumbbell cells) were selected based on circularity of cells, selecting only “elongated cells” (cells with a big bud), using the parameters *Area\_BF* and *Aspect\_Ratio\_Intensity\_BF*. This is considered as total mitotic cells.
3. EdU positive cells were identified based on the signal to noise ratio with background. For this, I use the “peak mask” and “spot counting feature”, that calculates the difference between a pixel and those nearby. This is considered as MiDAS positive cells.
4. To discard false positives, only cells where EdU signal colocalizes completely with DAPI signal were selected, thus excluding cells with extranuclear EdU foci, using the *Bright\_Detail\_Similarity\_R3\_EdU\_DAPI* parameter. This is subtracted from MiDAS-positive cells.

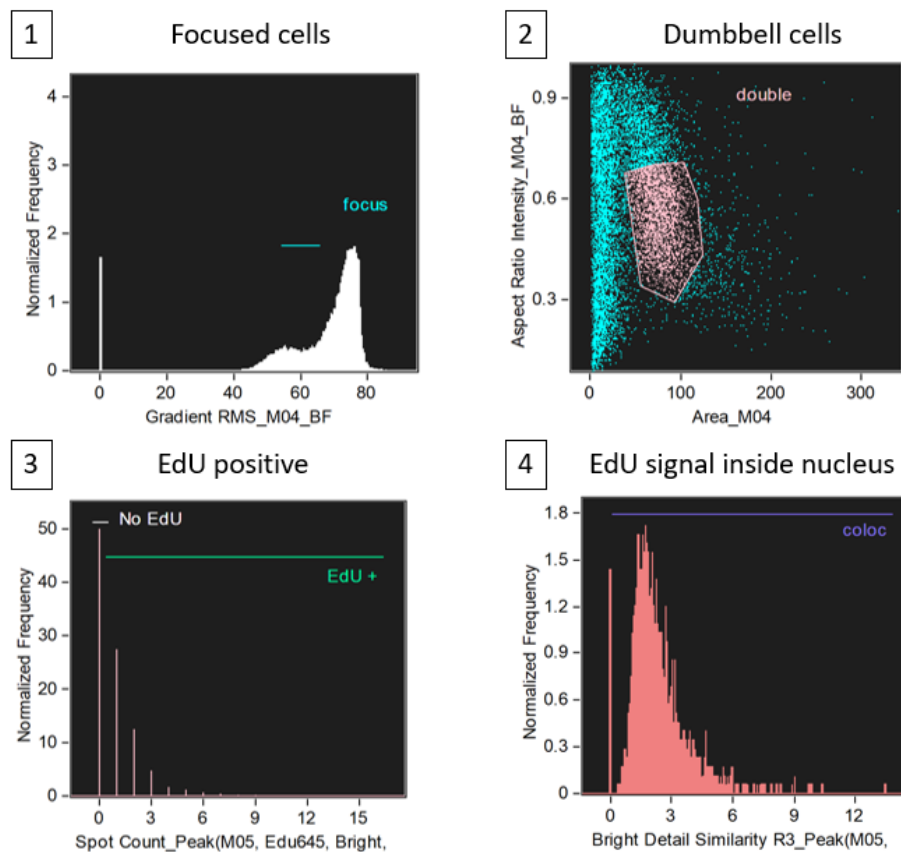


Figure v.4. Workflow of Imagestream analysis to identify MiDAS cells.

## **Chapter vi: Bibliography**

- Agier, N., Delmas, S., Zhang, Q., Fleiss, A., Jaszczyszyn, Y., van Dijk, E., Thermes, C., Weigt, M., Cosentino-Lagomarsino, M., & Fischer, G. (2018). The evolution of the temporal program of genome replication. *Nature Communications*, 9(1), Article 1. <https://doi.org/10.1038/s41467-018-04628-4>
- Agier, N., & Fischer, G. (2012). The Mutational Profile of the Yeast Genome Is Shaped by Replication. *Molecular Biology and Evolution*, 29(3), 905–913. <https://doi.org/10.1093/molbev/msr280>
- Ait Saada, A., Lambert, S. A. E., & Carr, A. M. (2018). Preserving replication fork integrity and competence via the homologous recombination pathway. *DNA Repair*, 71, 135–147. <https://doi.org/10.1016/j.dnarep.2018.08.017>
- Alabert, C., Bianco, J. N., & Pasero, P. (2009). Differential regulation of homologous recombination at DNA breaks and replication forks by the Mrc1 branch of the S-phase checkpoint. *The EMBO Journal*, 28(8), 1131–1141. <https://doi.org/10.1038/emboj.2009.75>
- Albuquerque, C. P., Smolka, M. B., Payne, S. H., Bafna, V., Eng, J., & Zhou, H. (2008). A multidimensional chromatography technology for in-depth phosphoproteome analysis. *Molecular & Cellular Proteomics: MCP*, 7(7), 1389–1396. <https://doi.org/10.1074/mcp.M700468-MCP200>
- Alcasabas, A. A., Osborn, A. J., Bachant, J., Hu, F., Werler, P. J., Bousset, K., Furuya, K., Diffley, J. F., Carr, A. M., & Elledge, S. J. (2001). Mrc1 transduces signals of DNA replication stress to activate Rad53. *Nature Cell Biology*, 3(11), 958–965. <https://doi.org/10.1038/ncb1101-958>
- Alhmoud, J. F., Woolley, J. F., Al Moustafa, A.-E., & Malki, M. I. (2020). DNA Damage/Repair Management in Cancers. *Cancers*, 12(4), Article 4. <https://doi.org/10.3390/cancers12041050>
- Allen, J. B., Zhou, Z., Siede, W., Friedberg, E. C., & Elledge, S. J. (1994). The SAD1/RAD53 protein kinase controls multiple checkpoints and DNA damage-induced transcription in yeast. *Genes & Development*, 8(20), 2401–2415. <https://doi.org/10.1101/gad.8.20.2401>
- Arora, C., Kee, K., Maleki, S., & Keeney, S. (2004). Antiviral protein Ski8 is a direct partner of Spo11 in meiotic DNA break formation, independent of its cytoplasmic role in RNA metabolism. *Molecular Cell*, 13(4), 549–559. [https://doi.org/10.1016/s1097-2765\(04\)00063-2](https://doi.org/10.1016/s1097-2765(04)00063-2)
- Bacal, J., Moriel-Carretero, M., Pardo, B., Barthe, A., Sharma, S., Chabes, A., Lengronne, A., & Pasero, P. (2018). Mrc1 and Rad9 cooperate to regulate initiation and elongation of DNA replication in response to DNA damage. *The EMBO Journal*, 37(21), e99319. <https://doi.org/10.15252/emboj.201899319>
- Bah, A., & Forman-Kay, J. D. (2016). Modulation of Intrinsically Disordered Protein Function by Post-translational Modifications. *Journal of Biological Chemistry*, 291(13), 6696–6705. <https://doi.org/10.1074/jbc.R115.695056>
- Barba Tena, J. de D., Schwob, E., & Talarek, N. (2022). Determination of S-Phase Duration Using 5-Ethynyl-2'-deoxyuridine Incorporation in *Saccharomyces cerevisiae*. *JoVE*, 188, e64490. <https://doi.org/10.3791/64490>

- Barberis, M., De Gioia, L., Ruzzene, M., Sarno, S., Coccetti, P., Fantucci, P., Vanoni, M., & Alberghina, L. (2005). The yeast cyclin-dependent kinase inhibitor Sic1 and mammalian p27Kip1 are functional homologues with a structurally conserved inhibitory domain. *Biochemical Journal*, 387(Pt 3), 639–647. <https://doi.org/10.1042/BJ20041299>
- Baretić, D., Jenkyn-Bedford, M., Aria, V., Cannone, G., Skehel, M., & Yeeles, J. T. P. (2020). Cryo-EM Structure of the Fork Protection Complex Bound to CMG at a Replication Fork. *Molecular Cell*, 78(5), 926–940.e13. <https://doi.org/10.1016/j.molcel.2020.04.012>
- Barnum, K. J., & O’Connell, M. J. (2014). Cell cycle regulation by checkpoints. *Methods in Molecular Biology (Clifton, N.J.)*, 1170, 29–40. [https://doi.org/10.1007/978-1-4939-0888-2\\_2](https://doi.org/10.1007/978-1-4939-0888-2_2)
- Baroni, E., Viscardi, V., Cartagena-Lirola, H., Lucchini, G., & Longhese, M. P. (2004). The Functions of Budding Yeast Sae2 in the DNA Damage Response Require Mec1- and Tel1-Dependent Phosphorylation. *Molecular and Cellular Biology*, 24(10), 4151–4165. <https://doi.org/10.1128/MCB.24.10.4151-4165.2004>
- Beck, H., Nähse-Kumpf, V., Larsen, M. S. Y., O’Hanlon, K. A., Patzke, S., Holmberg, C., Mejlvang, J., Groth, A., Nielsen, O., Syljuåsen, R. G., & Sørensen, C. S. (2012). Cyclin-Dependent Kinase Suppression by WEE1 Kinase Protects the Genome through Control of Replication Initiation and Nucleotide Consumption. *Molecular and Cellular Biology*, 32(20), 4226–4236. <https://doi.org/10.1128/MCB.00412-12>
- Bell, S. P., & Labib, K. (2016). Chromosome Duplication in *Saccharomyces cerevisiae*. *Genetics*, 203(3), 1027–1067. <https://doi.org/10.1534/genetics.115.186452>
- Ben-David, U., & Amon, A. (2020). Context is everything: Aneuploidy in cancer. *Nature Reviews. Genetics*, 21(1), 44–62. <https://doi.org/10.1038/s41576-019-0171-x>
- Bergero, R., Ellis, P., Haerty, W., Larcombe, L., Macaulay, I., Mehta, T., Mogensen, M., Murray, D., Nash, W., Neale, M. J., O’Connor, R., Ottolini, C., Peel, N., Ramsey, L., Skinner, B., Suh, A., Summers, M., Sun, Y., Tidy, A., ... Immler, S. (2021). Meiosis and beyond – understanding the mechanistic and evolutionary processes shaping the germline genome. *Biological Reviews*, 96(3), 822–841. <https://doi.org/10.1111/brv.12680>
- Berti, M., Cortez, D., & Lopes, M. (2020). The plasticity of DNA replication forks in response to clinically relevant genotoxic stress. *Nature Reviews. Molecular Cell Biology*, 21(10), 633–651. <https://doi.org/10.1038/s41580-020-0257-5>
- Bhowmick, R., & Hickson, I. D. (2017). The “enemies within”: Regions of the genome that are inherently difficult to replicate. *F1000Research*, 6, 666. <https://doi.org/10.12688/f1000research.11024.1>
- Bhowmick, R., Lerdrup, M., Gadi, S. A., Rossetti, G. G., Singh, M. I., Liu, Y., Halazonetis, T. D., & Hickson, I. D. (2022). RAD51 protects human cells from transcription-replication conflicts. *Molecular Cell*, 82(18), 3366–3381.e9. <https://doi.org/10.1016/j.molcel.2022.07.010>
- Bhowmick, R., Minocherhomji, S., & Hickson, I. D. (2016). RAD52 Facilitates Mitotic DNA Synthesis Following Replication Stress. *Molecular Cell*, 64(6), 1117–1126. <https://doi.org/10.1016/j.molcel.2016.10.037>

- Bishop, A. J. R., & Schiestl, R. H. (2002). Homologous Recombination and Its Role in Carcinogenesis. *Journal of Biomedicine and Biotechnology*, 2(2), 75–85. <https://doi.org/10.1155/S1110724302204052>
- Blake, D., Luke, B., Kanellis, P., Jorgensen, P., Goh, T., Penfold, S., Breikreutz, B.-J., Durocher, D., Peter, M., & Tyers, M. (2006). The F-box protein Dia2 overcomes replication impedance to promote genome stability in *Saccharomyces cerevisiae*. *Genetics*, 174(4), 1709–1727. <https://doi.org/10.1534/genetics.106.057836>
- Blitzblau, H. G., Chan, C. S., Hochwagen, A., & Bell, S. P. (2012). Separation of DNA replication from the assembly of break-competent meiotic chromosomes. *PLoS Genetics*, 8(5), e1002643. <https://doi.org/10.1371/journal.pgen.1002643>
- Boddy, M. N., Gaillard, P.-H. L., McDonald, W. H., Shanahan, P., Yates, J. R., & Russell, P. (2001). Mus81-Eme1 are essential components of a Holliday junction resolvase. *Cell*, 107(4), 537–548. [https://doi.org/10.1016/s0092-8674\(01\)00536-0](https://doi.org/10.1016/s0092-8674(01)00536-0)
- Boddy, M. N., & Russell, P. (1999). DNA replication checkpoint control. *Frontiers in Bioscience: A Journal and Virtual Library*, 4, D841-848. <https://doi.org/10.2741/boddy>
- Böhly, N., Kistner, M., & Bastians, H. (2019). Mild replication stress causes aneuploidy by deregulating microtubule dynamics in mitosis. *Cell Cycle*, 18(20), 2770–2783. <https://doi.org/10.1080/15384101.2019.1658477>
- Borde, V., Goldman, A. S., & Lichten, M. (2000). Direct coupling between meiotic DNA replication and recombination initiation. *Science (New York, N.Y.)*, 290(5492), 806–809. <https://doi.org/10.1126/science.290.5492.806>
- Borde, V., Lin, W., Novikov, E., Petrini, J. H., Lichten, M., & Nicolas, A. (2004). Association of Mre11p with double-strand break sites during yeast meiosis. *Molecular Cell*, 13(3), 389–401. [https://doi.org/10.1016/s1097-2765\(04\)00034-6](https://doi.org/10.1016/s1097-2765(04)00034-6)
- Branzei, D. (2011). Ubiquitin family modifications and template switching. *FEBS Letters*, 585(18), 2810–2817. <https://doi.org/10.1016/j.febslet.2011.04.053>
- Branzei, D., & Foiani, M. (2007). Interplay of replication checkpoints and repair proteins at stalled replication forks. *DNA Repair*, 6(7), 994–1003. <https://doi.org/10.1016/j.dnarep.2007.02.018>
- Bruck, I., Kanter, D. M., & Kaplan, D. L. (2011). Enabling association of the GINS protein tetramer with the mini chromosome maintenance (Mcm)2-7 protein complex by phosphorylated Sld2 protein and single-stranded origin DNA. *The Journal of Biological Chemistry*, 286(42), 36414–36426. <https://doi.org/10.1074/jbc.M111.282822>
- Bruschi, C. V., McMillan, J. N., Cogliavina, M., & Esposito, M. S. (1995). The genomic instability of yeast *cdc6-1/cdc6-1* mutants involves chromosome structure and recombination. *Molecular & General Genetics: MGG*, 249(1), 8–18. <https://doi.org/10.1007/BF00290230>
- Brush, G. S., Najor, N. A., Dombkowski, A. A., Cukovic, D., & Sawarynski, K. E. (2012). Yeast IME2 functions early in meiosis upstream of cell cycle-regulated SBF and MBF targets. *PLoS One*, 7(2), e31575. <https://doi.org/10.1371/journal.pone.0031575>

- Bueno, A., & Russell, P. (1992). Dual functions of CDC6: A yeast protein required for DNA replication also inhibits nuclear division. *The EMBO Journal*, *11*(6), 2167–2176. <https://doi.org/10.1002/j.1460-2075.1992.tb05276.x>
- Bugreev, D. V., Rossi, M. J., & Mazin, A. V. (2011). Cooperation of RAD51 and RAD54 in regression of a model replication fork. *Nucleic Acids Research*, *39*(6), 2153–2164. <https://doi.org/10.1093/nar/gkq1139>
- Burgers, P. M. J., & Kunkel, T. A. (2017). Eukaryotic DNA Replication Fork. *Annual Review of Biochemistry*, *86*, 417–438. <https://doi.org/10.1146/annurev-biochem-061516-044709>
- Byun, T. S., Pacek, M., Yee, M., Walter, J. C., & Cimprich, K. A. (2005). Functional uncoupling of MCM helicase and DNA polymerase activities activates the ATR-dependent checkpoint. *Genes & Development*, *19*(9), 1040–1052. <https://doi.org/10.1101/gad.1301205>
- Cai, X., & Xu, S. S. (2007). Meiosis-Driven Genome Variation in Plants. *Current Genomics*, *8*(3), 151–161.
- Callan, H. G., & Taylor, J. H. (1968). A radioautographic study of the time course of male meiosis in the newt *Triturus vulgaris*. *Journal of Cell Science*, *3*(4), 615–626. <https://doi.org/10.1242/jcs.3.4.615>
- Carballo, J. A., & Cha, R. S. (2007). Meiotic roles of Mec1, a budding yeast homolog of mammalian ATR/ATM. *Chromosome Research*, *15*(5), 539–550. <https://doi.org/10.1007/s10577-007-1145-y>
- Carballo, J. A., Johnson, A. L., Sedgwick, S. G., & Cha, R. S. (2008). Phosphorylation of the Axial Element Protein Hop1 by Mec1/Tel1 Ensures Meiotic Interhomolog Recombination. *Cell*, *132*(5), 758–770. <https://doi.org/10.1016/j.cell.2008.01.035>
- Carr, A. M., Paek, A. L., & Weinert, T. (2011). DNA replication: Failures and inverted fusions. *Seminars in Cell & Developmental Biology*, *22*(8), 866–874. <https://doi.org/10.1016/j.semcdb.2011.10.008>
- Cartagena-Lirola, H., Guerini, I., Manfrini, N., Lucchini, G., & Longhese, M. P. (2008). Role of the *Saccharomyces cerevisiae* Rad53 Checkpoint Kinase in Signaling Double-Strand Breaks during the Meiotic Cell Cycle. *Molecular and Cellular Biology*, *28*(14), 4480–4493. <https://doi.org/10.1128/MCB.00375-08>
- Cayrou, C., Grégoire, D., Coulombe, P., Danis, E., & Méchali, M. (2012). Genome-scale identification of active DNA replication origins. *Methods (San Diego, Calif.)*, *57*(2), 158–164. <https://doi.org/10.1016/j.ymeth.2012.06.015>
- Cha, R. S., Weiner, B. M., Keeney, S., Dekker, J., & Kleckner, N. (2000). Progression of meiotic DNA replication is modulated by interchromosomal interaction proteins, negatively by Spo11p and positively by Rec8p. *Genes & Development*, *14*(4), 493–503.
- Chen, S., Albuquerque, C. P., Liang, J., Suhandynata, R. T., & Zhou, H. (2010). A proteome-wide analysis of kinase-substrate network in the DNA damage response. *The Journal of Biological Chemistry*, *285*(17), 12803–12812. <https://doi.org/10.1074/jbc.M110.106989>
- Cheung, T. H., & Rando, T. A. (2013). Molecular regulation of stem cell quiescence. *Nature Reviews. Molecular Cell Biology*, *14*(6), 10.1038/nrm3591. <https://doi.org/10.1038/nrm3591>

- Chia, M., & van Werven, F. J. (2016). Temporal Expression of a Master Regulator Drives Synchronous Sporulation in Budding Yeast. *G3: Genes/Genomes/Genetics*, 6(11), 3553–3560. <https://doi.org/10.1534/g3.116.034983>
- Chia, N., Cann, I., & Olsen, G. J. (2010). Evolution of DNA Replication Protein Complexes in Eukaryotes and Archaea. *PLOS ONE*, 5(6), e10866. <https://doi.org/10.1371/journal.pone.0010866>
- Chilkova, O., Stenlund, P., Isoz, I., Stith, C. M., Grabowski, P., Lundström, E.-B., Burgers, P. M., & Johansson, E. (2007). The eukaryotic leading and lagging strand DNA polymerases are loaded onto primer-ends via separate mechanisms but have comparable processivity in the presence of PCNA. *Nucleic Acids Research*, 35(19), 6588–6597. <https://doi.org/10.1093/nar/gkm741>
- Chu, S., DeRisi, J., Eisen, M., Mulholland, J., Botstein, D., Brown, P. O., & Herskowitz, I. (1998). The transcriptional program of sporulation in budding yeast. *Science (New York, N.Y.)*, 282(5389), 699–705. <https://doi.org/10.1126/science.282.5389.699>
- Chu, S., & Herskowitz, I. (1998). Gametogenesis in yeast is regulated by a transcriptional cascade dependent on Ndt80. *Molecular Cell*, 1(5), 685–696. [https://doi.org/10.1016/s1097-2765\(00\)80068-4](https://doi.org/10.1016/s1097-2765(00)80068-4)
- Clarke, D. J., Mondesert, G., Segal, M., Bertolaet, B. L., Jensen, S., Wolff, M., Henze, M., & Reed, S. I. (2001). Dosage suppressors of pds1 implicate ubiquitin-associated domains in checkpoint control. *Molecular and Cellular Biology*, 21(6), 1997–2007. <https://doi.org/10.1128/MCB.21.6.1997-2007.2001>
- Clyne, R. K., Katis, V. L., Jessop, L., Benjamin, K. R., Herskowitz, I., Lichten, M., & Nasmyth, K. (2003). Polo-like kinase Cdc5 promotes chiasmata formation and cosegregation of sister centromeres at meiosis I. *Nature Cell Biology*, 5(5), 480–485. <https://doi.org/10.1038/ncb977>
- Cobb, J. A., Bjergbaek, L., Shimada, K., Frei, C., & Gasser, S. M. (2003). DNA polymerase stabilization at stalled replication forks requires Mec1 and the RecQ helicase Sgs1. *The EMBO Journal*, 22(16), 4325–4336. <https://doi.org/10.1093/emboj/cdg391>
- Cocker, J. H., Piatti, S., Santocanale, C., Nasmyth, K., & Diffley, J. F. (1996). An essential role for the Cdc6 protein in forming the pre-replicative complexes of budding yeast. *Nature*, 379(6561), 180–182. <https://doi.org/10.1038/379180a0>
- Collins, I., & Newlon, C. S. (1994). Chromosomal DNA replication initiates at the same origins in meiosis and mitosis. *Molecular and Cellular Biology*, 14(5), 3524–3534. <https://doi.org/10.1128/mcb.14.5.3524-3534.1994>
- Conklin, E. G. (1905). Mosaic development in ascidian eggs. *Journal of Experimental Zoology*, 2(2), 145–223. <https://doi.org/10.1002/jez.1400020202>
- Corbett, K. D., Yip, C. K., Ee, L.-S., Walz, T., Amon, A., & Harrison, S. C. (2010). The monopolin complex cross-links kinetochore components to regulate chromosome-microtubule attachments. *Cell*, 142(4), 556–567. <https://doi.org/10.1016/j.cell.2010.07.017>
- Cortez, D. (2015). Preventing Replication Fork Collapse to Maintain Genome Integrity. *DNA Repair*, 32, 149–157. <https://doi.org/10.1016/j.dnarep.2015.04.026>

- Coster, G., & Diffley, J. F. X. (2017). Bidirectional eukaryotic DNA replication is established by quasi-symmetrical helicase loading. *Science (New York, N.Y.)*, 357(6348), 314–318. <https://doi.org/10.1126/science.aan0063>
- Crabbé, L., Thomas, A., Pantesco, V., De Vos, J., Pasero, P., & Lengronne, A. (2010). Analysis of replication profiles reveals key role of RFC-Ctf18 in yeast replication stress response. *Nature Structural & Molecular Biology*, 17(11), 1391–1397. <https://doi.org/10.1038/nsmb.1932>
- Crevel, G., Hashimoto, R., Vass, S., Sherkow, J., Yamaguchi, M., Heck, M. M. S., & Cotterill, S. (2007). Differential requirements for MCM proteins in DNA replication in Drosophila S2 cells. *PLoS One*, 2(9), e833. <https://doi.org/10.1371/journal.pone.0000833>
- Cseresnyes, Z., Schwarz, U., & Green, C. M. (2009). Analysis of replication factories in human cells by super-resolution light microscopy. *BMC Cell Biology*, 10(1), 88. <https://doi.org/10.1186/1471-2121-10-88>
- Dahmann, C., & Futcher, B. (1995). Specialization of B-type cyclins for mitosis or meiosis in *S. cerevisiae*. *Genetics*, 140(3), 957–963. <https://doi.org/10.1093/genetics/140.3.957>
- Davis, A. P., & Symington, L. S. (2004). RAD51-Dependent Break-Induced Replication in Yeast. *Molecular and Cellular Biology*, 24(6), 2344–2351. <https://doi.org/10.1128/MCB.24.6.2344-2351.2004>
- de Bruin, R. A. M., McDonald, W. H., Kalashnikova, T. I., Yates, J., & Wittenberg, C. (2004). Cln3 activates G1-specific transcription via phosphorylation of the SBF bound repressor Whi5. *Cell*, 117(7), 887–898. <https://doi.org/10.1016/j.cell.2004.05.025>
- Deem, A., Keszthelyi, A., Blackgrove, T., Vayl, A., Coffey, B., Mathur, R., Chabes, A., & Malkova, A. (2011). Break-induced replication is highly inaccurate. *PLoS Biology*, 9(2), e1000594. <https://doi.org/10.1371/journal.pbio.1000594>
- Dellino, G. I., Cittaro, D., Piccioni, R., Luzi, L., Banfi, S., Segalla, S., Cesaroni, M., Mendoza-Maldonado, R., Giacca, M., & Pelicci, P. G. (2013). Genome-wide mapping of human DNA-replication origins: Levels of transcription at ORC1 sites regulate origin selection and replication timing. *Genome Research*, 23(1), 1–11. <https://doi.org/10.1101/gr.142331.112>
- Deng, C., & Saunders, W. S. (2001). RIM4 encodes a meiotic activator required for early events of meiosis in *Saccharomyces cerevisiae*. *Molecular Genetics and Genomics: MGG*, 266(3), 497–504. <https://doi.org/10.1007/s004380100571>
- Deng, L., Wu, R. A., Sonnevile, R., Kochenova, O. V., Labib, K., Pellman, D., & Walter, J. C. (2019). Mitotic CDK Promotes Replisome Disassembly, Fork Breakage, and Complex DNA Rearrangements. *Molecular Cell*, 73(5), 915–929.e6. <https://doi.org/10.1016/j.molcel.2018.12.021>
- Desdouets, C., Santocanale, C., Drury, L. S., Perkins, G., Foiani, M., Plevani, P., & Diffley, J. F. (1998). Evidence for a Cdc6p-independent mitotic resetting event involving DNA polymerase alpha. *The EMBO Journal*, 17(14), 4139–4146. <https://doi.org/10.1093/emboj/17.14.4139>
- Deshpande, A. M., & Newlon, C. S. (1996). DNA replication fork pause sites dependent on transcription. *Science (New York, N.Y.)*, 272(5264), 1030–1033. <https://doi.org/10.1126/science.272.5264.1030>

- Dewar, J. M., Budzowska, M., & Walter, J. C. (2015). The mechanism of DNA replication termination in vertebrates. *Nature*, 525(7569), 345–350. <https://doi.org/10.1038/nature14887>
- Dewar, J. M., & Walter, J. C. (2017). Mechanisms of DNA replication termination. *Nature Reviews Molecular Cell Biology*, 18(8), Article 8. <https://doi.org/10.1038/nrm.2017.42>
- Diani, L., Colombelli, C., Nachimuthu, B. T., Donnianni, R., Plevani, P., Muzi-Falconi, M., & Pellicoli, A. (2009). Saccharomyces CDK1 phosphorylates Rad53 kinase in metaphase, influencing cellular morphogenesis. *The Journal of Biological Chemistry*, 284(47), 32627–32634. <https://doi.org/10.1074/jbc.M109.048157>
- Diaz, R. L., Alcid, A. D., Berger, J. M., & Keeney, S. (2002). Identification of residues in yeast Spo11p critical for meiotic DNA double-strand break formation. *Molecular and Cellular Biology*, 22(4), 1106–1115. <https://doi.org/10.1128/MCB.22.4.1106-1115.2002>
- Diffley, J. F. X., Cocker, J. H., Dowell, S. J., & Rowley, A. (1994). Two steps in the assembly of complexes at yeast replication origins in vivo. *Cell*, 78(2), 303–316. [https://doi.org/10.1016/0092-8674\(94\)90299-2](https://doi.org/10.1016/0092-8674(94)90299-2)
- Dimitrova, D. S., Prokhorova, T. A., Blow, J. J., Todorov, I. T., & Gilbert, D. M. (2002). Mammalian nuclei become licensed for DNA replication during late telophase. *Journal of Cell Science*, 115(Pt 1), 51–59.
- Donnianni, R. A., & Symington, L. S. (2013). Break-induced replication occurs by conservative DNA synthesis. *Proceedings of the National Academy of Sciences of the United States of America*, 110(33), 13475–13480. <https://doi.org/10.1073/pnas.1309800110>
- Donnianni, R. A., Zhou, Z.-X., Lujan, S. A., Al-Zain, A., Garcia, V., Glancy, E., Burkholder, A. B., Kunkel, T. A., & Symington, L. S. (2019). DNA Polymerase Delta Synthesizes Both Strands during Break-Induced Replication. *Molecular Cell*, 76(3), 371-381.e4. <https://doi.org/10.1016/j.molcel.2019.07.033>
- Donovan, S., Harwood, J., Drury, L. S., & Diffley, J. F. X. (1997). Cdc6p-dependent loading of Mcm proteins onto pre-replicative chromatin in budding yeast. *Proceedings of the National Academy of Sciences of the United States of America*, 94(11), 5611–5616.
- Douglas, M. E., Ali, F. A., Costa, A., & Diffley, J. F. X. (2018). The mechanism of eukaryotic CMG helicase activation. *Nature*, 555(7695), 265–268. <https://doi.org/10.1038/nature25787>
- Drake, J. W. (1999). The Distribution of Rates of Spontaneous Mutation over Viruses, Prokaryotes, and Eukaryotes. *Annals of the New York Academy of Sciences*, 870(1), 100–107. <https://doi.org/10.1111/j.1749-6632.1999.tb08870.x>
- Dulev, S., de Renty, C., Mehta, R., Minkov, I., Schwob, E., & Strunnikov, A. (2009). Essential global role of CDC14 in DNA synthesis revealed by chromosome underreplication unrecognized by checkpoints in cdc14 mutants. *Proceedings of the National Academy of Sciences of the United States of America*, 106(34), 14466–14471. <https://doi.org/10.1073/pnas.0900190106>
- Durocher, D., & Jackson, S. P. (2001). DNA-PK, ATM and ATR as sensors of DNA damage: Variations on a theme? *Current Opinion in Cell Biology*, 13(2), 225–231. [https://doi.org/10.1016/s0955-0674\(00\)00201-5](https://doi.org/10.1016/s0955-0674(00)00201-5)

- Duxin, J. P., Dewar, J. M., Yardimci, H., & Walter, J. C. (2014). Repair of a DNA-protein crosslink by replication-coupled proteolysis. *Cell*, *159*(2), 346–357. <https://doi.org/10.1016/j.cell.2014.09.024>
- Egli, D., & Le Bin, G. C. (2013). Tying replication to cell identity. *Nature Reviews Molecular Cell Biology*, *14*(6), Article 6. <https://doi.org/10.1038/nrm3593>
- Epstein, C. B., & Cross, F. R. (1992). CLB5: A novel B cyclin from budding yeast with a role in S phase. *Genes & Development*, *6*(9), 1695–1706. <https://doi.org/10.1101/gad.6.9.1695>
- Evans, T., Rosenthal, E. T., Youngblom, J., Distel, D., & Hunt, T. (1983). Cyclin: A protein specified by maternal mRNA in sea urchin eggs that is destroyed at each cleavage division. *Cell*, *33*(2), 389–396. [https://doi.org/10.1016/0092-8674\(83\)90420-8](https://doi.org/10.1016/0092-8674(83)90420-8)
- Evrin, C., Maman, J. D., Diamante, A., Pellegrini, L., & Labib, K. (2018). Histone H2A-H2B binding by Pol  $\alpha$  in the eukaryotic replisome contributes to the maintenance of repressive chromatin. *The EMBO Journal*, *37*(19), e99021. <https://doi.org/10.15252/embj.201899021>
- Feichtinger, J., & McFarlane, R. J. (2019). Meiotic gene activation in somatic and germ cell tumours. *Andrology*, *7*(4), 415–427. <https://doi.org/10.1111/andr.12628>
- Feng, L., Hu, Y., Wang, B., Wu, L., & Jong, A. (2000). Loss control of Mcm5 interaction with chromatin in *cdc6-1* mutated in CDC-NTP motif. *DNA and Cell Biology*, *19*(7), 447–457. <https://doi.org/10.1089/10445490050085933>
- Feng, W., Bachant, J., Collingwood, D., Raghuraman, M. K., & Brewer, B. J. (2009). Centromere Replication Timing Determines Different Forms of Genomic Instability in *Saccharomyces cerevisiae* Checkpoint Mutants During Replication Stress. *Genetics*, *183*(4), 1249–1260. <https://doi.org/10.1534/genetics.109.107508>
- Fiorentini, P., Huang, K. N., Tishkoff, D. X., Kolodner, R. D., & Symington, L. S. (1997). Exonuclease I of *Saccharomyces cerevisiae* functions in mitotic recombination in vivo and in vitro. *Molecular and Cellular Biology*, *17*(5), 2764–2773. <https://doi.org/10.1128/MCB.17.5.2764>
- Flood, C. L., Rodriguez, G. P., Bao, G., Shockley, A. H., Kow, Y. W., & Crouse, G. F. (2015). Replicative DNA Polymerase  $\delta$  but Not  $\epsilon$  Proofreads Errors in Cis and in Trans. *PLOS Genetics*, *11*(3), e1005049. <https://doi.org/10.1371/journal.pgen.1005049>
- Foiani, M., Liberi, G., Lucchini, G., & Plevani, P. (1995). Cell cycle-dependent phosphorylation and dephosphorylation of the yeast DNA polymerase alpha-primase B subunit. *Molecular and Cellular Biology*, *15*(2), 883–891. <https://doi.org/10.1128/MCB.15.2.883>
- Foiani, M., Lindner, A. J., Hartmann, G. R., Lucchini, G., & Plevani, P. (1989). Affinity labeling of the active center and ribonucleoside triphosphate binding site of yeast DNA primase. *The Journal of Biological Chemistry*, *264*(4), 2189–2194.
- Fragkos, M., Ganier, O., Coulombe, P., & Méchali, M. (2015). DNA replication origin activation in space and time. *Nature Reviews Molecular Cell Biology*, *16*(6), Article 6. <https://doi.org/10.1038/nrm4002>
- Frigola, J., He, J., Kinkelin, K., Pye, V. E., Renault, L., Douglas, M. E., Remus, D., Cherepanov, P., Costa, A., & Diffley, J. F. X. (2017). Cdt1 stabilizes an open MCM ring for helicase loading. *Nature Communications*, *8*, 15720. <https://doi.org/10.1038/ncomms15720>

- Gambus, A., Jones, R. C., Sanchez-Diaz, A., Kanemaki, M., van Deursen, F., Edmondson, R. D., & Labib, K. (2006). GINS maintains association of Cdc45 with MCM in replisome progression complexes at eukaryotic DNA replication forks. *Nature Cell Biology*, 8(4), 358–366. <https://doi.org/10.1038/ncb1382>
- Gambus, A., van Deursen, F., Polychronopoulos, D., Foltman, M., Jones, R. C., Edmondson, R. D., Calzada, A., & Labib, K. (2009). A key role for Ctf4 in coupling the MCM2-7 helicase to DNA polymerase  $\alpha$  within the eukaryotic replisome. *The EMBO Journal*, 28(19), 2992–3004. <https://doi.org/10.1038/emboj.2009.226>
- Gapud, E. J., Dorsett, Y., Yin, B., Callen, E., Bredemeyer, A., Mahowald, G. K., Omi, K. Q., Walker, L. M., Bednarski, J. J., McKinnon, P. J., Bassing, C. H., Nussenzweig, A., & Sleckman, B. P. (2011). Ataxia telangiectasia mutated (Atm) and DNA-PKcs kinases have overlapping activities during chromosomal signal joint formation. *Proceedings of the National Academy of Sciences of the United States of America*, 108(5), 2022–2027. <https://doi.org/10.1073/pnas.1013295108>
- Gapud, E. J., & Sleckman, B. P. (2011). Unique and redundant functions of ATM and DNA-PKcs during V(D)J recombination. *Cell Cycle (Georgetown, Tex.)*, 10(12), 1928–1935. <https://doi.org/10.4161/cc.10.12.16011>
- García-Rodríguez, L. J., De Piccoli, G., Marchesi, V., Jones, R. C., Edmondson, R. D., & Labib, K. (2015). A conserved Pole binding module in Ctf18-RFC is required for S-phase checkpoint activation downstream of Mec1. *Nucleic Acids Research*, 43(18), 8830–8838. <https://doi.org/10.1093/nar/gkv799>
- Garrimba, L., Bjerregaard, V. A., Gonçalves Dinis, M. M., Özer, Ö., Wu, W., Sakellariou, D., Pena-Diaz, J., Hickson, I. D., & Liu, Y. (2020). Folate stress induces SLX1- and RAD51-dependent mitotic DNA synthesis at the fragile X locus in human cells. *Proceedings of the National Academy of Sciences*, 117(28), 16527–16536. <https://doi.org/10.1073/pnas.1921219117>
- Ge, X. Q., Jackson, D. A., & Blow, J. J. (2007). Dormant origins licensed by excess Mcm2–7 are required for human cells to survive replicative stress. *Genes & Development*, 21(24), 3331–3341. <https://doi.org/10.1101/gad.457807>
- Gemble, S., Wardenaar, R., Keuper, K., Srivastava, N., Nano, M., Macé, A.-S., Tjihuis, A. E., Bernhard, S. V., Spierings, D. C. J., Simon, A., Goundiam, O., Hochegger, H., Piel, M., Fojier, F., Storchová, Z., & Basto, R. (2022). Genetic instability from a single S phase after whole-genome duplication. *Nature*, 604(7904), Article 7904. <https://doi.org/10.1038/s41586-022-04578-4>
- Georgieva, D., & Egli, D. (2017). Tying genetic stability to cell identity. *Cell Cycle*, 16(12), 1139–1140. <https://doi.org/10.1080/15384101.2017.1324126>
- Gerton, J. L., DeRisi, J., Shroff, R., Lichten, M., Brown, P. O., & Petes, T. D. (2000). Global mapping of meiotic recombination hotspots and coldspots in the yeast *Saccharomyces cerevisiae*. *Proceedings of the National Academy of Sciences*, 97(21), 11383–11390. <https://doi.org/10.1073/pnas.97.21.11383>
- Gilbert, D. M. (2010a). Evaluating genome-scale approaches to eukaryotic DNA replication. *Nature Reviews. Genetics*, 11(10), 673–684. <https://doi.org/10.1038/nrg2830>

- Gilbert, D. M. (2010b). Cell fate transitions and the replication timing decision point. *Journal of Cell Biology*, 191(5), 899–903. <https://doi.org/10.1083/jcb.201007125>
- Glover, T. W., Berger, C., Coyle, J., & Echo, B. (1984). DNA polymerase alpha inhibition by aphidicolin induces gaps and breaks at common fragile sites in human chromosomes. *Human Genetics*, 67(2), 136–142. <https://doi.org/10.1007/BF00272988>
- González-Prieto, R., Muñoz-Cabello, A. M., Cabello-Lobato, M. J., & Prado, F. (2013). Rad51 replication fork recruitment is required for DNA damage tolerance. *The EMBO Journal*, 32(9), 1307–1321. <https://doi.org/10.1038/emboj.2013.73>
- Gouyer, V., Gazzéri, S., Bolon, I., Drevet, C., Brambilla, C., & Brambilla, E. (1998). Mechanism of retinoblastoma gene inactivation in the spectrum of neuroendocrine lung tumors. *American Journal of Respiratory Cell and Molecular Biology*, 18(2), 188–196. <https://doi.org/10.1165/ajrcmb.18.2.3008>
- Gravel, S., Chapman, J. R., Magill, C., & Jackson, S. P. (2008). DNA helicases Sgs1 and BLM promote DNA double-strand break resection. *Genes & Development*, 22(20), 2767–2772. <https://doi.org/10.1101/gad.503108>
- Greiwe, J. F., Miller, T. C. R., Locke, J., Martino, F., Howell, S., Schreiber, A., Nans, A., Diffley, J. F. X., & Costa, A. (2022). Structural mechanism for the selective phosphorylation of DNA-loaded MCM double hexamers by the Dbf4-dependent kinase. *Nature Structural & Molecular Biology*, 29(1), 10–20. <https://doi.org/10.1038/s41594-021-00698-z>
- Groelly, F. J., Dagg, R. A., Petropoulos, M., Rossetti, G. G., Prasad, B., Panagopoulos, A., Paulsen, T., Karamichali, A., Jones, S. E., Ochs, F., Dionellis, V. S., Puig Lombardi, E., Miossec, M. J., Lockstone, H., Legube, G., Blackford, A. N., Altmeyer, M., Halazonetis, T. D., & Tarsounas, M. (2022). Mitotic DNA synthesis is caused by transcription-replication conflicts in BRCA2-deficient cells. *Molecular Cell*, 82(18), 3382–3397.e7. <https://doi.org/10.1016/j.molcel.2022.07.011>
- Guilliam, T. A. (2021). Mechanisms for Maintaining Eukaryotic Replisome Progression in the Presence of DNA Damage. *Frontiers in Molecular Biosciences*, 8. <https://www.frontiersin.org/articles/10.3389/fmolb.2021.712971>
- Guirouilh-Barbat, J., Lambert, S., Bertrand, P., & Lopez, B. S. (2014). Is homologous recombination really an error-free process? *Frontiers in Genetics*, 5, 175. <https://doi.org/10.3389/fgene.2014.00175>
- Gupta, S., Friedman, L. J., Gelles, J., & Bell, S. P. (2021). A helicase-tethered ORC flip enables bidirectional helicase loading. *ELife*, 10, e74282. <https://doi.org/10.7554/eLife.74282>
- Gurevich, V., & Kassir, Y. (2010). A Switch from a Gradient to a Threshold Mode in the Regulation of a Transcriptional Cascade Promotes Robust Execution of Meiosis in Budding Yeast. *PLOS ONE*, 5(6), e11005. <https://doi.org/10.1371/journal.pone.0011005>
- Hanahan, D., & Weinberg, R. A. (2011). Hallmarks of Cancer: The Next Generation. *Cell*, 144(5), 646–674. <https://doi.org/10.1016/j.cell.2011.02.013>
- Hardwick, K. G., Li, R., Mistrot, C., Chen, R. H., Dann, P., Rudner, A., & Murray, A. W. (1999). Lesions in many different spindle components activate the spindle checkpoint in the

- budding yeast *Saccharomyces cerevisiae*. *Genetics*, 152(2), 509–518.  
<https://doi.org/10.1093/genetics/152.2.509>
- Hartwell, L. H., Culotti, J., & Reid, B. (1970). Genetic Control of the Cell-Division Cycle in Yeast, I. Detection of Mutants. *Proceedings of the National Academy of Sciences of the United States of America*, 66(2), 352–359.
- Hartwell, L. H., & Weinert, T. A. (1989). Checkpoints: Controls that ensure the order of cell cycle events. *Science (New York, N.Y.)*, 246(4930), 629–634.  
<https://doi.org/10.1126/science.2683079>
- Hashash, N., Johnson, A. L., & Cha, R. S. (2011). Regulation of fragile sites expression in budding yeast by MEC1, RRM3 and hydroxyurea. *Journal of Cell Science*, 124(2), 181–185.  
<https://doi.org/10.1242/jcs.077313>
- Hashash, N., Johnson, A. L., & Cha, R. S. (2012). Topoisomerase II- and condensin-dependent breakage of MEC1ATR-sensitive fragile sites occurs independently of spindle tension, anaphase, or cytokinesis. *PLoS Genetics*, 8(10), e1002978.  
<https://doi.org/10.1371/journal.pgen.1002978>
- He, W., Zhao, Y., Zhang, C., An, L., Hu, Z., Liu, Y., Han, L., Bi, L., Xie, Z., Xue, P., Yang, F., & Hang, H. (2008). Rad9 plays an important role in DNA mismatch repair through physical interaction with MLH1. *Nucleic Acids Research*, 36(20), 6406–6417. <https://doi.org/10.1093/nar/gkn686>
- He, Y., Song, H., Chan, H., Liu, B., Wang, Y., Sušac, L., Zhou, Z. H., & Feigon, J. (2022). Structure of Tetrahymena telomerase-bound CST with polymerase  $\alpha$ -primase. *Nature*, 608(7924), 813–818. <https://doi.org/10.1038/s41586-022-04931-7>
- Hiraga, S.-I., Hagihara-Hayashi, A., Ohya, T., & Sugino, A. (2005). DNA polymerases alpha, delta, and epsilon localize and function together at replication forks in *Saccharomyces cerevisiae*. *Genes to Cells: Devoted to Molecular & Cellular Mechanisms*, 10(4), 297–309.  
<https://doi.org/10.1111/j.1365-2443.2005.00843.x>
- Hodgson, B., Calzada, A., & Labib, K. (2007). Mrc1 and Tof1 Regulate DNA Replication Forks in Different Ways during Normal S Phase. *Molecular Biology of the Cell*, 18(10), 3894–3902.  
<https://doi.org/10.1091/mbc.E07-05-0500>
- Hoffman, R. A., MacAlpine, H. K., & MacAlpine, D. M. (2021). Disruption of origin chromatin structure by helicase activation in the absence of DNA replication. *Genes & Development*, 35(19–20), 1339–1355. <https://doi.org/10.1101/gad.348517.121>
- Hogard, T., Shor, E., Müller, C. A., Nieduszynski, C. A., & Fox, C. A. (2013). A Link between ORC-Origin Binding Mechanisms and Origin Activation Time Revealed in Budding Yeast. *PLOS Genetics*, 9(9), e1003798. <https://doi.org/10.1371/journal.pgen.1003798>
- Holt, L. J., Tuch, B. B., Villén, J., Johnson, A. D., Gygi, S. P., & Morgan, D. O. (2009). Global analysis of Cdk1 substrate phosphorylation sites provides insights into evolution. *Science (New York, N.Y.)*, 325(5948), 1682–1686. <https://doi.org/10.1126/science.1172867>
- Hoyt, M. A., Totis, L., & Roberts, B. T. (1991). *S. cerevisiae* genes required for cell cycle arrest in response to loss of microtubule function. *Cell*, 66(3), 507–517.  
[https://doi.org/10.1016/0092-8674\(81\)90014-3](https://doi.org/10.1016/0092-8674(81)90014-3)

- Hu, F., Wang, Y., Liu, D., Li, Y., Qin, J., & Elledge, S. J. (2001). Regulation of the Bub2/Bfa1 GAP complex by Cdc5 and cell cycle checkpoints. *Cell*, *107*(5), 655–665. [https://doi.org/10.1016/s0092-8674\(01\)00580-3](https://doi.org/10.1016/s0092-8674(01)00580-3)
- Hu, J., Sun, L., Shen, F., Chen, Y., Hua, Y., Liu, Y., Zhang, M., Hu, Y., Wang, Q., Xu, W., Sun, F., Ji, J., Murray, J. M., Carr, A. M., & Kong, D. (2012). The intra-S phase checkpoint targets Dna2 to prevent stalled replication forks from reversing. *Cell*, *149*(6), 1221–1232. <https://doi.org/10.1016/j.cell.2012.04.030>
- Huang, J., Liu, S., Bellani, M. A., Thazhathveetil, A. K., Ling, C., de Winter, J. P., Wang, Y., Wang, W., & Seidman, M. M. (2013). The DNA Translocase FANCM/MHF Promotes Replication Traverse of DNA Interstrand Crosslinks. *Molecular Cell*, *52*(3), 434–446. <https://doi.org/10.1016/j.molcel.2013.09.021>
- Hwang, L. H., Lau, L. F., Smith, D. L., Mistrot, C. A., Hardwick, K. G., Hwang, E. S., Amon, A., & Murray, A. W. (1998). Budding yeast Cdc20: A target of the spindle checkpoint. *Science (New York, N.Y.)*, *279*(5353), 1041–1044. <https://doi.org/10.1126/science.279.5353.1041>
- Ibarra, A., Schwob, E., & Méndez, J. (2008). Excess MCM proteins protect human cells from replicative stress by licensing backup origins of replication. *Proceedings of the National Academy of Sciences of the United States of America*, *105*(26), 8956–8961. <https://doi.org/10.1073/pnas.0803978105>
- Ilves, I., Petojevic, T., Pesavento, J. J., & Botchan, M. R. (2010). Activation of the MCM2-7 Helicase by Association with Cdc45 and GINS Proteins. *Molecular Cell*, *37*(2), 247–258. <https://doi.org/10.1016/j.molcel.2009.12.030>
- Ira, G., & Haber, J. E. (2002). Characterization of RAD51-independent break-induced replication that acts preferentially with short homologous sequences. *Molecular and Cellular Biology*, *22*(18), 6384–6392. <https://doi.org/10.1128/MCB.22.18.6384-6392.2002>
- Ivanova, T., Maier, M., Missarova, A., Ziegler-Birling, C., Dam, M., Gomar-Alba, M., Carey, L. B., & Mendoza, M. (2020). Budding yeast complete DNA synthesis after chromosome segregation begins. *Nature Communications*, *11*(1), Article 1. <https://doi.org/10.1038/s41467-020-16100-3>
- Ivessa, A. S., Lenzmeier, B. A., Bessler, J. B., Goudsouzian, L. K., Schnakenberg, S. L., & Zakian, V. A. (2003). The *Saccharomyces cerevisiae* helicase Rrm3p facilitates replication past nonhistone protein-DNA complexes. *Molecular Cell*, *12*(6), 1525–1536. [https://doi.org/10.1016/s1097-2765\(03\)00456-8](https://doi.org/10.1016/s1097-2765(03)00456-8)
- Ivessa, A. S., Zhou, J.-Q., Schulz, V. P., Monson, E. K., & Zakian, V. A. (2002). *Saccharomyces* Rrm3p, a 5' to 3' DNA helicase that promotes replication fork progression through telomeric and subtelomeric DNA. *Genes & Development*, *16*(11), 1383–1396. <https://doi.org/10.1101/gad.982902>
- Iyer, V. R., Horak, C. E., Scafe, C. S., Botstein, D., Snyder, M., & Brown, P. O. (2001). Genomic binding sites of the yeast cell-cycle transcription factors SBF and MBF. *Nature*, *409*(6819), 533–538. <https://doi.org/10.1038/35054095>

- Jaramillo-Lambert, A., Ellefson, M., Villeneuve, A. M., & Engebrecht, J. (2007). Differential timing of S phases, X chromosome replication, and meiotic prophase in the *C. elegans* germ line. *Developmental Biology*, 308(1), 206–221. <https://doi.org/10.1016/j.ydbio.2007.05.019>
- Jenkyn-Bedford, M., Jones, M. L., Baris, Y., Labib, K. P. M., Cannone, G., Yeeles, J. T. P., & Deegan, T. D. (2021). A conserved mechanism for regulating replisome disassembly in eukaryotes. *Nature*, 600(7890), Article 7890. <https://doi.org/10.1038/s41586-021-04145-3>
- Ji, F., Liao, H., Pan, S., Ouyang, L., Jia, F., Fu, Z., Zhang, F., Geng, X., Wang, X., Li, T., Liu, S., Syeda, M. Z., Chen, H., Li, W., Chen, Z., Shen, H., & Ying, S. (2020). Genome-wide high-resolution mapping of mitotic DNA synthesis sites and common fragile sites by direct sequencing. *Cell Research*, 30(11), 1009–1023. <https://doi.org/10.1038/s41422-020-0357-y>
- Johnston, L. H., & Lowndes, N. F. (1992). Cell cycle control of DNA synthesis in budding yeast. *Nucleic Acids Research*, 20(10), 2403–2410. <https://doi.org/10.1093/nar/20.10.2403>
- Johnston, L. H., White, J. H., Johnson, A. L., Lucchini, G., & Plevani, P. (1987). The yeast DNA polymerase I transcript is regulated in both the mitotic cell cycle and in meiosis and is also induced after DNA damage. *Nucleic Acids Research*, 15(13), 5017–5030. <https://doi.org/10.1093/nar/15.13.5017>
- Jorgensen, P., Nishikawa, J. L., Breikreutz, B.-J., & Tyers, M. (2002). Systematic Identification of Pathways That Couple Cell Growth and Division in Yeast. *Science*, 297(5580), 395–400. <https://doi.org/10.1126/science.1070850>
- Kamimura, Y., Tak, Y. S., Sugino, A., & Araki, H. (2001). Sld3, which interacts with Cdc45 (Sld4), functions for chromosomal DNA replication in *Saccharomyces cerevisiae*. *The EMBO Journal*, 20(8), 2097–2107. <https://doi.org/10.1093/emboj/20.8.2097>
- Kane, S. M., & Roth, R. (1974). Carbohydrate metabolism during ascospore development in yeast. *Journal of Bacteriology*, 118(1), 8–14. <https://doi.org/10.1128/jb.118.1.8-14.1974>
- Kanter, D. M., & Kaplan, D. L. (2011). Sld2 binds to origin single-stranded DNA and stimulates DNA annealing. *Nucleic Acids Research*, 39(7), 2580–2592. <https://doi.org/10.1093/nar/gkq1222>
- Kapadia, N., El-Hajj, Z. W., Zheng, H., Beattie, T. R., Yu, A., & Reyes-Lamothe, R. (2020). Processive Activity of Replicative DNA Polymerases in the Replisome of Live Eukaryotic Cells. *Molecular Cell*, 80(1), 114-126.e8. <https://doi.org/10.1016/j.molcel.2020.08.014>
- Kar, F. M., Vogel, C., & Hochwagen, A. (2022). Meiotic DNA breaks activate a streamlined phospho-signaling response that largely avoids protein-level changes. *Life Science Alliance*, 5(10). <https://doi.org/10.26508/lsa.202201454>
- Katou, Y., Kanoh, Y., Bando, M., Noguchi, H., Tanaka, H., Ashikari, T., Sugimoto, K., & Shirahige, K. (2003). S-phase checkpoint proteins Tof1 and Mrc1 form a stable replication-pausing complex. *Nature*, 424(6952), 1078–1083. <https://doi.org/10.1038/nature01900>
- Keeney, S. (2001). Mechanism and control of meiotic recombination initiation. *Current Topics in Developmental Biology*, 52, 1–53. [https://doi.org/10.1016/s0070-2153\(01\)52008-6](https://doi.org/10.1016/s0070-2153(01)52008-6)

- Kelly, T. J., Martin, G. S., Forsburg, S. L., Stephen, R. J., Russo, A., & Nurse, P. (1993). The fission yeast *cdc18+* gene product couples S phase to START and mitosis. *Cell*, *74*(2), 371–382. [https://doi.org/10.1016/0092-8674\(93\)90427-R](https://doi.org/10.1016/0092-8674(93)90427-R)
- Kesti, T., Flick, K., Keränen, S., Syväoja, J. E., & Wittenberg, C. (1999). DNA Polymerase  $\epsilon$  Catalytic Domains Are Dispensable for DNA Replication, DNA Repair, and Cell Viability. *Molecular Cell*, *3*(5), 679–685. [https://doi.org/10.1016/S1097-2765\(00\)80361-5](https://doi.org/10.1016/S1097-2765(00)80361-5)
- Kile, A. C., & Koepp, D. M. (2010). Activation of the S-Phase Checkpoint Inhibits Degradation of the F-Box Protein Dia2. *Molecular and Cellular Biology*, *30*(1), 160–171. <https://doi.org/10.1128/MCB.00612-09>
- Kitamura, E., Blow, J. J., & Tanaka, T. U. (2006). Live-Cell Imaging Reveals Replication of Individual Replicons in Eukaryotic Replication Factories. *Cell*, *125*(7), 1297–1308. <https://doi.org/10.1016/j.cell.2006.04.041>
- Kitazono, A. A. (2009). Improved gap-repair cloning method that uses oligonucleotides to target cognate sequences. *Yeast (Chichester, England)*, *26*(9), 497–505. <https://doi.org/10.1002/yea.1680>
- Klapholz, S., Waddell, C. S., & Esposito, R. E. (1985). The role of the SPO11 gene in meiotic recombination in yeast. *Genetics*, *110*(2), 187–216. <https://doi.org/10.1093/genetics/110.2.187>
- Knoblich, J. A. (2008). Mechanisms of Asymmetric Stem Cell Division. *Cell*, *132*(4), 583–597. <https://doi.org/10.1016/j.cell.2008.02.007>
- Kobayashi, K., Guillian, T. A., Tsuda, M., Yamamoto, J., Bailey, L. J., Iwai, S., Takeda, S., Doherty, A. J., & Hirota, K. (2016). Repriming by PrimPol is critical for DNA replication restart downstream of lesions and chain-terminating nucleosides. *Cell Cycle (Georgetown, Tex.)*, *15*(15), 1997–2008. <https://doi.org/10.1080/15384101.2016.1191711>
- Koch, C., & Nasmyth, K. (1994). Cell cycle regulated transcription in yeast. *Current Opinion in Cell Biology*, *6*(3), 451–459. [https://doi.org/10.1016/0955-0674\(94\)90039-6](https://doi.org/10.1016/0955-0674(94)90039-6)
- Kramara, J., Osia, B., & Malkova, A. (2018). Break-Induced Replication: The Where, The Why, and The How. *Trends in Genetics*, *34*(7), 518–531. <https://doi.org/10.1016/j.tig.2018.04.002>
- Krejci, L., Song, B., Bussen, W., Rothstein, R., Mortensen, U. H., & Sung, P. (2002). Interaction with Rad51 is indispensable for recombination mediator function of Rad52. *The Journal of Biological Chemistry*, *277*(42), 40132–40141. <https://doi.org/10.1074/jbc.M206511200>
- Kreuzer, K. N. (2000). Recombination-dependent DNA replication in phage T4. *Trends in Biochemical Sciences*, *25*(4), 165–173. [https://doi.org/10.1016/s0968-0004\(00\)01559-0](https://doi.org/10.1016/s0968-0004(00)01559-0)
- Kumar, S., & Burgers, P. M. (2013). Lagging strand maturation factor Dna2 is a component of the replication checkpoint initiation machinery. *Genes & Development*, *27*(3), 313–321. <https://doi.org/10.1101/gad.204750.112>
- Kunkel, T. A. (2011). Balancing eukaryotic replication asymmetry with replication fidelity. *Current Opinion in Chemical Biology*, *15*(5), 620–626. <https://doi.org/10.1016/j.cbpa.2011.07.025>

- Kusubata, M., Matsuoka, Y., Tsujimura, K., Ito, H., Ando, S., Kamijo, M., Yasuda, H., Ohba, Y., Okumura, E., & Kishimoto, T. (1993). Cdc2 kinase phosphorylation of desmin at three serine/threonine residues in the amino-terminal head domain. *Biochemical and Biophysical Research Communications*, 190(3), 927–934. <https://doi.org/10.1006/bbrc.1993.1138>
- Lam, I., & Keeney, S. (2014). Mechanism and regulation of meiotic recombination initiation. *Cold Spring Harbor Perspectives in Biology*, 7(1), a016634. <https://doi.org/10.1101/cshperspect.a016634>
- Lambert, S., Mizuno, K., Blaisonneau, J., Martineau, S., Chanet, R., Fréon, K., Murray, J. M., Carr, A. M., & Baldacci, G. (2010). Homologous Recombination Restarts Blocked Replication Forks at the Expense of Genome Rearrangements by Template Exchange. *Molecular Cell*, 39(3), 346–359. <https://doi.org/10.1016/j.molcel.2010.07.015>
- Landry, C. R., Freschi, L., Zarin, T., & Moses, A. M. (2014). Turnover of protein phosphorylation evolving under stabilizing selection. *Frontiers in Genetics*, 5. <https://www.frontiersin.org/articles/10.3389/fgene.2014.00245>
- Lang, G. I., & Murray, A. W. (2011). Mutation Rates across Budding Yeast Chromosome VI Are Correlated with Replication Timing. *Genome Biology and Evolution*, 3, 799–811. <https://doi.org/10.1093/gbe/evr054>
- Langston, L. D., Zhang, D., Yurieva, O., Georgescu, R. E., Finkelstein, J., Yao, N. Y., Indiani, C., & O'Donnell, M. E. (2014). CMG helicase and DNA polymerase  $\epsilon$  form a functional 15-subunit holoenzyme for eukaryotic leading-strand DNA replication. *Proceedings of the National Academy of Sciences*, 111(43), 15390–15395. <https://doi.org/10.1073/pnas.1418334111>
- Lanz, M. C., Yugandhar, K., Gupta, S., Sanford, E. J., Faça, V. M., Vega, S., Joiner, A. M. N., Fromme, J. C., Yu, H., & Smolka, M. B. (2021). In-depth and 3-dimensional exploration of the budding yeast phosphoproteome. *EMBO Reports*, 22(2), e51121. <https://doi.org/10.15252/embr.202051121>
- Lawrence, Katherine, Chau, T., & Engebrecht, J. (2015). DNA Damage Response and Spindle Assembly Checkpoint Function throughout the Cell Cycle to Ensure Genomic Integrity. *PLoS Genetics*, 11, e1005150. <https://doi.org/10.1371/journal.pgen.1005150>
- Lebofsky, R., Heilig, R., Sonnleitner, M., Weissenbach, J., & Bensimon, A. (2006). DNA Replication Origin Interference Increases the Spacing between Initiation Events in Human Cells. *Molecular Biology of the Cell*, 17(12), 5337–5345. <https://doi.org/10.1091/mbc.E06-04-0298>
- Lehmann, C. P., Jiménez-Martín, A., Branzei, D., & Tercero, J. A. (2020). Prevention of unwanted recombination at damaged replication forks. *Current Genetics*, 66(6), 1045–1051. <https://doi.org/10.1007/s00294-020-01095-7>
- Lei, M., Kawasaki, Y., & Tye, B. K. (1996). Physical interactions among Mcm proteins and effects of Mcm dosage on DNA replication in *Saccharomyces cerevisiae*. *Molecular and Cellular Biology*, 16(9), 5081–5090. <https://doi.org/10.1128/MCB.16.9.5081>
- Lemaçon, D., Jackson, J., Quinet, A., Brickner, J. R., Li, S., Yazinski, S., You, Z., Ira, G., Zou, L., Mosammamarast, N., & Vindigni, A. (2017). MRE11 and EXO1 nucleases degrade reversed forks and elicit MUS81-dependent fork rescue in BRCA2-deficient cells. *Nature Communications*, 8(1), Article 1. <https://doi.org/10.1038/s41467-017-01180-5>

- Lengronne, A., & Pasero, P. (2014). Closing the MCM cycle at replication termination sites. *EMBO Reports*, 15(12), 1226–1227. <https://doi.org/10.15252/embr.201439774>
- Lengronne, A., & Schwob, E. (2002). The yeast CDK inhibitor Sic1 prevents genomic instability by promoting replication origin licensing in late G(1). *Molecular Cell*, 9(5), 1067–1078. [https://doi.org/10.1016/s1097-2765\(02\)00513-0](https://doi.org/10.1016/s1097-2765(02)00513-0)
- Leonhardt, H., Rahn, H.-P., Weinzierl, P., Sporbart, A., Cremer, T., Zink, D., & Cardoso, M. C. (2000). Dynamics of DNA Replication Factories in Living Cells. *The Journal of Cell Biology*, 149(2), 271–280.
- Leroy, C., Lee, S. E., Vaze, M. B., Ochsenbein, F., Ochsenbier, F., Guerois, R., Haber, J. E., & Marsolier-Kergoat, M.-C. (2003). PP2C phosphatases Ptc2 and Ptc3 are required for DNA checkpoint inactivation after a double-strand break. *Molecular Cell*, 11(3), 827–835. [https://doi.org/10.1016/s1097-2765\(03\)00058-3](https://doi.org/10.1016/s1097-2765(03)00058-3)
- Lewis, J. S., Spenklink, L. M., Schauer, G. D., Yurieva, O., Mueller, S. H., Natarajan, V., Kaur, G., Maher, C., Kay, C., O'Donnell, M. E., & van Oijen, A. M. (2020). Tunability of DNA Polymerase Stability during Eukaryotic DNA Replication. *Molecular Cell*, 77(1), 17-25.e5. <https://doi.org/10.1016/j.molcel.2019.10.005>
- Li, S., Wang, H., Jehi, S., Li, J., Liu, S., Wang, Z., Truong, L., Chiba, T., Wang, Z., & Wu, X. (2021). PIF1 helicase promotes break-induced replication in mammalian cells. *The EMBO Journal*, 40(8), e104509. <https://doi.org/10.15252/emboj.2020104509>
- Li, X., & Heyer, W.-D. (2008). Homologous recombination in DNA repair and DNA damage tolerance. *Cell Research*, 18(1), Article 1. <https://doi.org/10.1038/cr.2008.1>
- Liachko, I., Youngblood, R. A., Keich, U., & Dunham, M. J. (2013). High-resolution mapping, characterization, and optimization of autonomously replicating sequences in yeast. *Genome Research*, 23(4), 698–704. <https://doi.org/10.1101/gr.144659.112>
- Liakopoulos, D. (2021). Coupling DNA Replication and Spindle Function in *Saccharomyces cerevisiae*. *Cells*, 10(12), Article 12. <https://doi.org/10.3390/cells10123359>
- Lienhard, G. E. (2008). Non-functional phosphorylations? *Trends in Biochemical Sciences*, 33(8), 351–352. <https://doi.org/10.1016/j.tibs.2008.05.004>
- Lim, S., & Kaldis, P. (2013). Cdks, cyclins and CKIs: Roles beyond cell cycle regulation. *Development (Cambridge, England)*, 140(15), 3079–3093. <https://doi.org/10.1242/dev.091744>
- Lisby, M., Barlow, J. H., Burgess, R. C., & Rothstein, R. (2004). Choreography of the DNA damage response: Spatiotemporal relationships among checkpoint and repair proteins. *Cell*, 118(6), 699–713. <https://doi.org/10.1016/j.cell.2004.08.015>
- Lisby, M., Rothstein, R., & Mortensen, U. H. (2001). Rad52 forms DNA repair and recombination centers during S phase. *Proceedings of the National Academy of Sciences of the United States of America*, 98(15), 8276–8282. <https://doi.org/10.1073/pnas.121006298>
- Liu, L., Yan, Z., Osia, B. A., Twarowski, J., Sun, L., Kramara, J., Lee, R. S., Kumar, S., Elango, R., Li, H., Dang, W., Ira, G., & Malkova, A. (2021). Tracking break-induced replication shows that it

- stalls at roadblocks. *Nature*, 590(7847), 655–659. <https://doi.org/10.1038/s41586-020-03172-w>
- Liu, X., Wang, X., Yang, X., Liu, S., Jiang, L., Qu, Y., Hu, L., Ouyang, Q., & Tang, C. (n.d.). Reliable cell cycle commitment in budding yeast is ensured by signal integration. *ELife*, 4, e03977. <https://doi.org/10.7554/eLife.03977>
- Lo, H.-C., Wan, L., Rosebrock, A., Fitcher, B., & Hollingsworth, N. M. (2008). Cdc7-Dbf4 regulates NDT80 transcription as well as reductional segregation during budding yeast meiosis. *Molecular Biology of the Cell*, 19(11), 4956–4967. <https://doi.org/10.1091/mbc.e08-07-0755>
- Lopez-Mosqueda, J., Maas, N. L., Jonsson, Z. O., DeFazio Eli, L. G., Wohlschlegel, J., & Toczyski, D. P. (2010). Damage-Induced Phosphorylation of Sld3 is Important to Block Late Origin Firing. *Nature*, 467(7314), 479–483. <https://doi.org/10.1038/nature09377>
- Lundin, C., North, M., Erixon, K., Walters, K., Jenssen, D., Goldman, A. S. H., & Helleday, T. (2005). Methyl methanesulfonate (MMS) produces heat-labile DNA damage but no detectable in vivo DNA double-strand breaks. *Nucleic Acids Research*, 33(12), 3799–3811. <https://doi.org/10.1093/nar/gki681>
- Lydall, D., Nikolsky, Y., Bishop, D. K., & Weinert, T. (1996). A meiotic recombination checkpoint controlled by mitotic checkpoint genes. *Nature*, 383(6603), Article 6603. <https://doi.org/10.1038/383840a0>
- Lydeard, J. R., Jain, S., Yamaguchi, M., & Haber, J. E. (2007). Break-induced replication and telomerase-independent telomere maintenance require Pol32. *Nature*, 448(7155), 820–823. <https://doi.org/10.1038/nature06047>
- Ma, E., Maloisel, L., Le Falher, L., Guérois, R., & Coïc, E. (2021). Rad52 Oligomeric N-Terminal Domain Stabilizes Rad51 Nucleoprotein Filaments and Contributes to Their Protection against Srs2. *Cells*, 10(6), 1467. <https://doi.org/10.3390/cells10061467>
- Macheret, M., Bhowmick, R., Sobkowiak, K., Padayachy, L., Mailler, J., Hickson, I. D., & Halazonetis, T. D. (2020). High-resolution mapping of mitotic DNA synthesis regions and common fragile sites in the human genome through direct sequencing. *Cell Research*, 30(11), 997–1008. <https://doi.org/10.1038/s41422-020-0358-x>
- MacQueen, A. J., & Hochwagen, A. (2011). Checkpoint mechanisms: The puppet masters of meiotic prophase. *Trends in Cell Biology*, 21(7), 393–400. <https://doi.org/10.1016/j.tcb.2011.03.004>
- Magiera, M. M., Gueydon, E., & Schwob, E. (2014). DNA replication and spindle checkpoints cooperate during S phase to delay mitosis and preserve genome integrity. *The Journal of Cell Biology*, 204(2), 165–175. <https://doi.org/10.1083/jcb.201306023>
- Maguire, M. P. (1962). Pachytene and Diakinesis Behavior of the Isochromosomes 6 of Maize. *Science (New York, N.Y.)*, 138(3538), 445–446. <https://doi.org/10.1126/science.138.3538.445>
- Mailand, N., & Diffley, J. F. X. (2005). CDKs promote DNA replication origin licensing in human cells by protecting Cdc6 from APC/C-dependent proteolysis. *Cell*, 122(6), 915–926. <https://doi.org/10.1016/j.cell.2005.08.013>

- Makarova, K. S., & Koonin, E. V. (2013). Archaeology of eukaryotic DNA replication. *Cold Spring Harbor Perspectives in Biology*, 5(11), a012963. <https://doi.org/10.1101/cshperspect.a012963>
- Malkova, A., & Ira, G. (2013). Break-induced replication: Functions and molecular mechanism. *Current Opinion in Genetics & Development*, 23(3), 271–279. <https://doi.org/10.1016/j.gde.2013.05.007>
- Malkova, A., Ivanov, E. L., & Haber, J. E. (1996). Double-strand break repair in the absence of RAD51 in yeast: A possible role for break-induced DNA replication. *Proceedings of the National Academy of Sciences of the United States of America*, 93(14), 7131–7136. <https://doi.org/10.1073/pnas.93.14.7131>
- Malkova, A., Naylor, M. L., Yamaguchi, M., Ira, G., & Haber, J. E. (2005). RAD51-dependent break-induced replication differs in kinetics and checkpoint responses from RAD51-mediated gene conversion. *Molecular and Cellular Biology*, 25(3), 933–944. <https://doi.org/10.1128/MCB.25.3.933-944.2005>
- Malumbres, M., & Barbacid, M. (2001). To cycle or not to cycle: A critical decision in cancer. *Nature Reviews. Cancer*, 1(3), 222–231. <https://doi.org/10.1038/35106065>
- Mandel, S., Robzyk, K., & Kassir, Y. (1994). IME1 gene encodes a transcription factor which is required to induce meiosis in *Saccharomyces cerevisiae*. *Developmental Genetics*, 15(2), 139–147. <https://doi.org/10.1002/dvg.1020150204>
- Manning, G., Whyte, D. B., Martinez, R., Hunter, T., & Sudarsanam, S. (2002). The protein kinase complement of the human genome. *Science (New York, N.Y.)*, 298(5600), 1912–1934. <https://doi.org/10.1126/science.1075762>
- Marahrens, Y., & Stillman, B. (1992). A yeast chromosomal origin of DNA replication defined by multiple functional elements. *Science (New York, N.Y.)*, 255(5046), 817–823. <https://doi.org/10.1126/science.1536007>
- Maric, M., Maculins, T., De Piccoli, G., & Labib, K. (2014). Cdc48 and a ubiquitin ligase drive disassembly of the CMG helicase at the end of DNA replication. *Science (New York, N.Y.)*, 346(6208), 1253596. <https://doi.org/10.1126/science.1253596>
- Marston, A. L. (2014). Chromosome Segregation in Budding Yeast: Sister Chromatid Cohesion and Related Mechanisms. *Genetics*, 196(1), 31–63. <https://doi.org/10.1534/genetics.112.145144>
- Marston, A. L., & Amon, A. (2004). Meiosis: Cell-cycle controls shuffle and deal. *Nature Reviews Molecular Cell Biology*, 5(12), Article 12. <https://doi.org/10.1038/nrm1526>
- Martínez-Jiménez, F., Muiños, F., Sentís, I., Deu-Pons, J., Reyes-Salazar, I., Arnedo-Pac, C., Mularoni, L., Pich, O., Bonet, J., Kranas, H., Gonzalez-Perez, A., & Lopez-Bigas, N. (2020). A compendium of mutational cancer driver genes. *Nature Reviews Cancer*, 20(10), Article 10. <https://doi.org/10.1038/s41568-020-0290-x>
- Matson, J. P., Dumitru, R., Coryell, P., Baxley, R. M., Chen, W., Twaroski, K., Webber, B. R., Tolar, J., Bielinsky, A.-K., Purvis, J. E., & Cook, J. G. (2017). Rapid DNA replication origin licensing protects stem cell pluripotency. *ELife*, 6, e30473. <https://doi.org/10.7554/eLife.30473>

- Matson, J. P., House, A. M., Grant, G. D., Wu, H., Perez, J., & Cook, J. G. (n.d.). *Intrinsic checkpoint deficiency during cell cycle re-entry from quiescence*. 22.
- Mayle, R., Campbell, I. M., Beck, C. R., Yu, Y., Wilson, M., Shaw, C. A., Bjergbaek, L., Lupski, J. R., & Ira, G. (2015). DNA REPAIR. Mus81 and converging forks limit the mutagenicity of replication fork breakage. *Science (New York, N.Y.)*, 349(6249), 742–747. <https://doi.org/10.1126/science.aaa8391>
- McCarroll, R. M., & Fangman, W. L. (1988). Time of replication of yeast centromeres and telomeres. *Cell*, 54(4), 505–513. [https://doi.org/10.1016/0092-8674\(88\)90072-4](https://doi.org/10.1016/0092-8674(88)90072-4)
- McEachern, M. J., & Haber, J. E. (2006). Break-induced replication and recombinational telomere elongation in yeast. *Annual Review of Biochemistry*, 75, 111–135. <https://doi.org/10.1146/annurev.biochem.74.082803.133234>
- McInerney, P., & O'Donnell, M. (2004). Functional uncoupling of twin polymerases: Mechanism of polymerase dissociation from a lagging-strand block. *The Journal of Biological Chemistry*, 279(20), 21543–21551. <https://doi.org/10.1074/jbc.M401649200>
- McVey, M., Khodaverdian, V. Y., Meyer, D., Cerqueira, P. G., & Heyer, W.-D. (2016). Eukaryotic DNA Polymerases in Homologous Recombination. *Annual Review of Genetics*, 50, 393–421. <https://doi.org/10.1146/annurev-genet-120215-035243>
- Mehta, A., Beach, A., & Haber, J. E. (2017). Homology Requirements and Competition between Gene Conversion and Break-Induced Replication during Double-Strand Break Repair. *Molecular Cell*, 65(3), 515-526.e3. <https://doi.org/10.1016/j.molcel.2016.12.003>
- Mendenhall, M. D. (1993). An inhibitor of p34CDC28 protein kinase activity from *Saccharomyces cerevisiae*. *Science (New York, N.Y.)*, 259(5092), 216–219. <https://doi.org/10.1126/science.8421781>
- Miller, T. C. R., Locke, J., Greiwe, J. F., Diffley, J. F. X., & Costa, A. (2019). Mechanism of head-to-head MCM double-hexamer formation revealed by cryo-EM. *Nature*, 575(7784), 704–710. <https://doi.org/10.1038/s41586-019-1768-0>
- Mimura, S., Komata, M., Kishi, T., Shirahige, K., & Kamura, T. (2009). SCFDia2 regulates DNA replication forks during S-phase in budding yeast. *The EMBO Journal*, 28(23), 3693–3705. <https://doi.org/10.1038/emboj.2009.320>
- Minca, E. C., & Kowalski, D. (2010). Multiple Rad5 activities mediate sister chromatid recombination to bypass DNA damage at stalled replication forks. *Molecular Cell*, 38(5), 649–661. <https://doi.org/10.1016/j.molcel.2010.03.020>
- Minocherhomji, S., Ying, S., Bjerregaard, V. A., Bursomanno, S., Aleliunaite, A., Wu, W., Mankouri, H. W., Shen, H., Liu, Y., & Hickson, I. D. (2015). Replication stress activates DNA repair synthesis in mitosis. *Nature*, 528(7581), 286–290. <https://doi.org/10.1038/nature16139>
- Mirkin, E. V., & Mirkin, S. M. (2007). Replication fork stalling at natural impediments. *Microbiology and Molecular Biology Reviews: MMBR*, 71(1), 13–35. <https://doi.org/10.1128/MMBR.00030-06>

- Mitchison, J. M., & Creanor, J. (1971). Further measurements of DNA synthesis and enzyme potential during cell cycle of fission yeast *Schizosaccharomyces pombe*. *Experimental Cell Research*, 69(1), 244–247. [https://doi.org/10.1016/0014-4827\(71\)90337-5](https://doi.org/10.1016/0014-4827(71)90337-5)
- Mizuno, K., Lambert, S., Baldacci, G., Murray, J. M., & Carr, A. M. (2009). Nearby inverted repeats fuse to generate acentric and dicentric palindromic chromosomes by a replication template exchange mechanism. *Genes & Development*, 23(24), 2876–2886. <https://doi.org/10.1101/gad.1863009>
- Mocanu, C., Karanika, E., Fernández-Casañas, M., Herbert, A., Olukoga, T., Özgürses, M. E., & Chan, K.-L. (2022). DNA replication is highly resilient and persistent under the challenge of mild replication stress. *Cell Reports*, 39(3), 110701. <https://doi.org/10.1016/j.celrep.2022.110701>
- Moreno, S. P., Bailey, R., Campion, N., Herron, S., & Gambus, A. (2014). Polyubiquitylation drives replisome disassembly at the termination of DNA replication. *Science (New York, N.Y.)*, 346(6208), 477–481. <https://doi.org/10.1126/science.1253585>
- Mori, S., & Shirahige, K. (2007). Perturbation of the activity of replication origin by meiosis-specific transcription. *The Journal of Biological Chemistry*, 282(7), 4447–4452. <https://doi.org/10.1074/jbc.M609671200>
- Morin, I., Ngo, H.-P., Greenall, A., Zubko, M. K., Morrice, N., & Lydall, D. (2008). Checkpoint-dependent phosphorylation of Exo1 modulates the DNA damage response. *The EMBO Journal*, 27(18), 2400–2410. <https://doi.org/10.1038/emboj.2008.171>
- Murakami, H., & Keeney, S. (2014a). Temporospatial Coordination of Meiotic DNA Replication and Recombination via DDK Recruitment to Replisomes. *Cell*, 158(4), 861–873. <https://doi.org/10.1016/j.cell.2014.06.028>
- Murakami, H., & Keeney, S. (2014b). DDK links replication and recombination in meiosis. *Cell Cycle*, 13(23), 3621–3622. <https://doi.org/10.4161/15384101.2014.986626>
- Nakano, T., Miyamoto-Matsubara, M., Shoulkamy, M. I., Salem, A. M. H., Pack, S. P., Ishimi, Y., & Ide, H. (2013). Translocation and Stability of Replicative DNA Helicases upon Encountering DNA-Protein Cross-links. *The Journal of Biological Chemistry*, 288(7), 4649–4658. <https://doi.org/10.1074/jbc.M112.419358>
- Nakatani, T., Lin, J., Ji, F., Ettinger, A., Pontabry, J., Tokoro, M., Altamirano-Pacheco, L., Fiorentino, J., Mahammadov, E., Hatano, Y., Van Rechem, C., Chakraborty, D., Ruiz-Morales, E. R., Arguello Pascualli, P. Y., Scialdone, A., Yamagata, K., Whetstine, J. R., Sadreyev, R. I., & Torres-Padilla, M.-E. (2022). DNA replication fork speed underlies cell fate changes and promotes reprogramming. *Nature Genetics*, 54(3), Article 3. <https://doi.org/10.1038/s41588-022-01023-0>
- Nash, P., Tang, X., Orlicky, S., Chen, Q., Gertler, F. B., Mendenhall, M. D., Sicheri, F., Pawson, T., & Tyers, M. (2001). Multisite phosphorylation of a CDK inhibitor sets a threshold for the onset of DNA replication. *Nature*, 414(6863), Article 6863. <https://doi.org/10.1038/35107009>
- Nasheuer, H. P., Moore, A., Wahl, A. F., & Wang, T. S. (1991). Cell cycle-dependent phosphorylation of human DNA polymerase alpha. *The Journal of Biological Chemistry*, 266(12), 7893–7903.

- Nasmyth, K. (1993). Control of the yeast cell cycle by the Cdc28 protein kinase. *Current Opinion in Cell Biology*, 5(2), 166–179. [https://doi.org/10.1016/0955-0674\(93\)90099-c](https://doi.org/10.1016/0955-0674(93)90099-c)
- Noguchi, Y., Yuan, Z., Bai, L., Schneider, S., Zhao, G., Stillman, B., Speck, C., & Li, H. (2017). Cryo-EM structure of Mcm2-7 double hexamer on DNA suggests a lagging-strand DNA extrusion model. *Proceedings of the National Academy of Sciences of the United States of America*, 114(45), E9529–E9538. <https://doi.org/10.1073/pnas.1712537114>
- Nurse, P., Thuriaux, P., & Nasmyth, K. (1976). Genetic control of the cell division cycle in the fission yeast *Schizosaccharomyces pombe*. *Molecular and General Genetics MGG*, 146(2), 167–178. <https://doi.org/10.1007/BF00268085>
- Ogawa, T., Yu, X., Shinohara, A., & Egelman, E. H. (1993). Similarity of the yeast RAD51 filament to the bacterial RecA filament. *Science (New York, N.Y.)*, 259(5103), 1896–1899. <https://doi.org/10.1126/science.8456314>
- Oh, S. D., Jessop, L., Lao, J. P., Allers, T., Lichten, M., & Hunter, N. (2009). Stabilization and electrophoretic analysis of meiotic recombination intermediates in *Saccharomyces cerevisiae*. *Methods in Molecular Biology (Clifton, N.J.)*, 557, 209–234. [https://doi.org/10.1007/978-1-59745-527-5\\_14](https://doi.org/10.1007/978-1-59745-527-5_14)
- Ohta, K., Shibata, T., & Nicolas, A. (1994). Changes in chromatin structure at recombination initiation sites during yeast meiosis. *The EMBO Journal*, 13(23), 5754–5763. <https://doi.org/10.1002/j.1460-2075.1994.tb06913.x>
- Okamoto, Y., Iwasaki, W. M., Kugou, K., Takahashi, K. K., Oda, A., Sato, K., Kobayashi, W., Kawai, H., Sakasai, R., Takaori-Kondo, A., Yamamoto, T., Kanemaki, M. T., Taoka, M., Isobe, T., Kurumizaka, H., Innan, H., Ohta, K., Ishiai, M., & Takata, M. (2018). Replication stress induces accumulation of FANCD2 at central region of large fragile genes. *Nucleic Acids Research*, 46(6), 2932–2944. <https://doi.org/10.1093/nar/gky058>
- Okaz, E., Argüello-Miranda, O., Bogdanova, A., Vinod, P. K., Lipp, J. J., Markova, Z., Zagoriy, I., Novak, B., & Zachariae, W. (2012). Meiotic prophase requires proteolysis of M phase regulators mediated by the meiosis-specific APC/C<sub>Am1</sub>. *Cell*, 151(3), 603–618. <https://doi.org/10.1016/j.cell.2012.08.044>
- O'Neill, B. M., Szyjka, S. J., Lis, E. T., Bailey, A. O., Yates, J. R., Aparicio, O. M., & Romesberg, F. E. (2007). Pph3–Psy2 is a phosphatase complex required for Rad53 dephosphorylation and replication fork restart during recovery from DNA damage. *Proceedings of the National Academy of Sciences of the United States of America*, 104(22), 9290–9295. <https://doi.org/10.1073/pnas.0703252104>
- Örd, M., Möll, K., Agerova, A., Kivi, R., Faustova, I., Venta, R., Valk, E., & Loog, M. (2019). Multisite phosphorylation code of CDK. *Nature Structural & Molecular Biology*, 26(7), 649–658. <https://doi.org/10.1038/s41594-019-0256-4>
- Ortiz-Bazán, M. Á., Gallo-Fernández, M., Saugar, I., Jiménez-Martín, A., Vázquez, M. V., & Tercero, J. A. (2014). Rad5 plays a major role in the cellular response to DNA damage during chromosome replication. *Cell Reports*, 9(2), 460–468. <https://doi.org/10.1016/j.celrep.2014.09.005>

- Osborn, A. J., & Elledge, S. J. (2003). Mrc1 is a replication fork component whose phosphorylation in response to DNA replication stress activates Rad53. *Genes & Development*, *17*(14), 1755–1767. <https://doi.org/10.1101/gad.1098303>
- Osia, B., Twarowski, J., Jackson, T., Lobachev, K., Liu, L., & Malkova, A. (2022). Migrating bubble synthesis promotes mutagenesis through lesions in its template. *Nucleic Acids Research*, *50*(12), 6870–6889. <https://doi.org/10.1093/nar/gkac520>
- Padmore, R., Cao, L., & Kleckner, N. (1991). Temporal comparison of recombination and synaptonemal complex formation during meiosis in *S. cerevisiae*. *Cell*, *66*(6), 1239–1256. [https://doi.org/10.1016/0092-8674\(91\)90046-2](https://doi.org/10.1016/0092-8674(91)90046-2)
- Panizza, S., Mendoza, M. A., Berlinger, M., Huang, L., Nicolas, A., Shirahige, K., & Klein, F. (2011). Spo11-accessory proteins link double-strand break sites to the chromosome axis in early meiotic recombination. *Cell*, *146*(3), 372–383. <https://doi.org/10.1016/j.cell.2011.07.003>
- Pardo, B., Crabbé, L., & Pasero, P. (2017). Signaling pathways of replication stress in yeast. *FEMS Yeast Research*, *17*(2). <https://doi.org/10.1093/femsyr/fow101>
- Pasero, P., Braguglia, D., & Gasser, S. M. (1997a). ORC-dependent and origin-specific initiation of DNA replication at defined foci in isolated yeast nuclei. *Genes & Development*, *11*(12), 1504–1518. <https://doi.org/10.1101/gad.11.12.1504>
- Pasero, P., Braguglia, D., & Gasser, S. M. (1997b). ORC-dependent and origin-specific initiation of DNA replication at defined foci in isolated yeast nuclei. *Genes & Development*, *11*(12), 1504–1518. <https://doi.org/10.1101/gad.11.12.1504>
- Patel, S. S., Pandey, M., & Nandakumar, D. (2011). Dynamic coupling between the motors of DNA replication: Hexameric helicase, DNA polymerase, and primase. *Current Opinion in Chemical Biology*, *15*(5), 595–605. <https://doi.org/10.1016/j.cbpa.2011.08.003>
- Pavlov, Y. I., & Shcherbakova, P. V. (2010). DNA polymerases at the eukaryotic fork-20 years later. *Mutation Research*, *685*(1–2), 45–53. <https://doi.org/10.1016/j.mrfmmm.2009.08.002>
- Petermann, E., & Helleday, T. (2010). Pathways of mammalian replication fork restart. *Nature Reviews Molecular Cell Biology*, *11*(10), Article 10. <https://doi.org/10.1038/nrm2974>
- Phizicky, D. V., Berchowitz, L. E., & Bell, S. P. (2018). Multiple kinases inhibit origin licensing and helicase activation to ensure reductive cell division during meiosis. *ELife*, *7*, e33309. <https://doi.org/10.7554/eLife.33309>
- Piatti, S., Lengauer, C., & Nasmyth, K. (1995). Cdc6 is an unstable protein whose de novo synthesis in G1 is important for the onset of S phase and for preventing a “reductional” anaphase in the budding yeast *Saccharomyces cerevisiae*. *The EMBO Journal*, *14*(15), 3788–3799. <https://doi.org/10.1002/j.1460-2075.1995.tb00048.x>
- Piazza, A., Shah, S. S., Wright, W. D., Gore, S. K., Koszul, R., & Heyer, W.-D. (2019). Dynamic Processing of Displacement Loops during Recombinational DNA Repair. *Molecular Cell*, *73*(6), 1255-1266.e4. <https://doi.org/10.1016/j.molcel.2019.01.005>
- Pike, A. C. W., Gomathinayagam, S., Swuec, P., Berti, M., Zhang, Y., Schneck, C., Marino, F., von Delft, F., Renault, L., Costa, A., Gileadi, O., & Vindigni, A. (2015). Human RECQ1 helicase-driven DNA unwinding, annealing, and branch migration: Insights from DNA complex

- structures. *Proceedings of the National Academy of Sciences*, 112(14), 4286–4291.  
<https://doi.org/10.1073/pnas.1417594112>
- Poli, J., Tsaponina, O., Crabbé, L., Keszthelyi, A., Pantesco, V., Chabes, A., Lengronne, A., & Pasero, P. (2012). DNTP pools determine fork progression and origin usage under replication stress. *The EMBO Journal*, 31(4), 883–894. <https://doi.org/10.1038/emboj.2011.470>
- Pratto, F., Brick, K., Cheng, G., Lam, K.-W. G., Cloutier, J. M., Dahiya, D., Wellard, S. R., Jordan, P. W., & Camerini-Otero, R. D. (2021). Meiotic recombination mirrors patterns of germline replication in mice and humans. *Cell*, 184(16), 4251–4267.e20.  
<https://doi.org/10.1016/j.cell.2021.06.025>
- Priego Moreno, S., Jones, R. M., Poovathumkadavil, D., Scaramuzza, S., & Gambus, A. (2019). Mitotic replisome disassembly depends on TRAIIP ubiquitin ligase activity. *Life Science Alliance*, 2(2), e201900390. <https://doi.org/10.26508/lsa.201900390>
- Pyatnitskaya, A., Andreani, J., Guérois, R., Muyt, A. D., & Borde, V. (2022). The Zip4 protein directly couples meiotic crossover formation to synaptonemal complex assembly. *Genes & Development*, 36(1–2), 53–69. <https://doi.org/10.1101/gad.348973.121>
- Qi, H., & Zakian, V. A. (2000). The *Saccharomyces* telomere-binding protein Cdc13p interacts with both the catalytic subunit of DNA polymerase  $\alpha$  and the telomerase-associated Est1 protein. *Genes & Development*, 14(14), 1777–1788.
- Qiao, R., Weissmann, F., Yamaguchi, M., Brown, N. G., VanderLinden, R., Imre, R., Jarvis, M. A., Brunner, M. R., Davidson, I. F., Litos, G., Haselbach, D., Mechtler, K., Stark, H., Schulman, B. A., & Peters, J.-M. (2016). Mechanism of APC/CCDC20 activation by mitotic phosphorylation. *Proceedings of the National Academy of Sciences*, 113(19), E2570–E2578.  
<https://doi.org/10.1073/pnas.1604929113>
- Raghuraman, M. K., Winzeler, E. A., Collingwood, D., Hunt, S., Wodicka, L., Conway, A., Lockhart, D. J., Davis, R. W., Brewer, B. J., & Fangman, W. L. (2001). Replication Dynamics of the Yeast Genome. *Science*, 294(5540), 115–121. <https://doi.org/10.1126/science.294.5540.115>
- Rao, H., & Stillman, B. (1995). The origin recognition complex interacts with a bipartite DNA binding site within yeast replicators. *Proceedings of the National Academy of Sciences of the United States of America*, 92(6), 2224–2228. <https://doi.org/10.1073/pnas.92.6.2224>
- Rao, P. N., & Johnson, R. T. (1970). Mammalian Cell Fusion: Studies on the Regulation of DNA Synthesis and Mitosis. *Nature*, 225(5228), Article 5228. <https://doi.org/10.1038/225159a0>
- Regairaz, M., Zhang, Y.-W., Fu, H., Agama, K. K., Tata, N., Agrawal, S., Aladjem, M. I., & Pommier, Y. (2011). Mus81-mediated DNA cleavage resolves replication forks stalled by topoisomerase I–DNA complexes. *The Journal of Cell Biology*, 195(5), 739–749.  
<https://doi.org/10.1083/jcb.201104003>
- Reuswig, K.-U., Bittmann, J., Peritore, M., Wierer, M., Mann, M., & Pfander, B. (2021). *Unscheduled DNA replication in G1 causes genome instability through head-to-tail replication fork collisions* (p. 2021.09.06.459115). bioRxiv.  
<https://doi.org/10.1101/2021.09.06.459115>

- Richardson, H. E., Wittenberg, C., Cross, F., & Reed, S. I. (1989). An essential G1 function for cyclin-like proteins in yeast. *Cell*, *59*(6), 1127–1133. [https://doi.org/10.1016/0092-8674\(89\)90768-x](https://doi.org/10.1016/0092-8674(89)90768-x)
- Roseaulin, L. C., Noguchi, C., Martinez, E., Ziegler, M. A., Toda, T., & Noguchi, E. (2013). Coordinated Degradation of Replisome Components Ensures Genome Stability upon Replication Stress in the Absence of the Replication Fork Protection Complex. *PLOS Genetics*, *9*(1), e1003213. <https://doi.org/10.1371/journal.pgen.1003213>
- Rossi, S. E., Ajazi, A., Carotenuto, W., Foiani, M., & Giannattasio, M. (2015). Rad53-Mediated Regulation of Rrm3 and Pif1 DNA Helicases Contributes to Prevention of Aberrant Fork Transitions under Replication Stress. *Cell Reports*, *13*(1), 80–92. <https://doi.org/10.1016/j.celrep.2015.08.073>
- Rouse, J., & Jackson, S. P. (2002). Lcd1p recruits Mec1p to DNA lesions in vitro and in vivo. *Molecular Cell*, *9*(4), 857–869. [https://doi.org/10.1016/s1097-2765\(02\)00507-5](https://doi.org/10.1016/s1097-2765(02)00507-5)
- Rowley, A., Cocker, J. H., Harwood, J., & Diffley, J. F. (1995). Initiation complex assembly at budding yeast replication origins begins with the recognition of a bipartite sequence by limiting amounts of the initiator, ORC. *The EMBO Journal*, *14*(11), 2631–2641.
- Saintigny, Y., Delacôte, F., Varès, G., Petitot, F., Lambert, S., Averbeck, D., & Lopez, B. S. (2001). Characterization of homologous recombination induced by replication inhibition in mammalian cells. *The EMBO Journal*, *20*(14), 3861–3870. <https://doi.org/10.1093/emboj/20.14.3861>
- Sale, J. E., Lehmann, A. R., & Woodgate, R. (2012). Y-family DNA polymerases and their role in tolerance of cellular DNA damage. *Nature Reviews. Molecular Cell Biology*, *13*(3), 141–152. <https://doi.org/10.1038/nrm3289>
- Sanchez, A., Reginato, G., & Cejka, P. (2021). Crossover or non-crossover outcomes: Tailored processing of homologous recombination intermediates. *Current Opinion in Genetics & Development*, *71*, 39–47. <https://doi.org/10.1016/j.gde.2021.06.012>
- Sanchez, Y., Desany, B. A., Jones, W. J., Liu, Q., Wang, B., & Elledge, S. J. (1996). Regulation of RAD53 by the ATM-like kinases MEC1 and TEL1 in yeast cell cycle checkpoint pathways. *Science (New York, N.Y.)*, *271*(5247), 357–360. <https://doi.org/10.1126/science.271.5247.357>
- Saner, N., Karschau, J., Natsume, T., Gierliński, M., Retkute, R., Hawkins, M., Nieduszynski, C. A., Blow, J. J., de Moura, A. P. S., & Tanaka, T. U. (2013). Stochastic association of neighboring replicons creates replication factories in budding yeast. *The Journal of Cell Biology*, *202*(7), 1001–1012. <https://doi.org/10.1083/jcb.201306143>
- Sansregret, L., & Swanton, C. (2017). The Role of Aneuploidy in Cancer Evolution. *Cold Spring Harbor Perspectives in Medicine*, *7*(1), a028373. <https://doi.org/10.1101/cshperspect.a028373>
- Santocanale, C., & Diffley, J. F. (1998). A Mec1- and Rad53-dependent checkpoint controls late-firing origins of DNA replication. *Nature*, *395*(6702), 615–618. <https://doi.org/10.1038/27001>

- Sarbajna, S., & West, S. C. (2014). Holliday junction processing enzymes as guardians of genome stability. *Trends in Biochemical Sciences*, 39(9), 409–419. <https://doi.org/10.1016/j.tibs.2014.07.003>
- Satterwhite, L. L., & Lohka, M. J. (n.d.). *Phosphorylation of Myosin-II Regulatory Light Chain by Cyclin-p34cda: A Mechanism for the Timing of Cytokinesis*. 11.
- Schacherer, J., Ruderfer, D. M., Gresham, D., Dolinski, K., Botstein, D., & Kruglyak, L. (2007). Genome-Wide Analysis of Nucleotide-Level Variation in Commonly Used *Saccharomyces cerevisiae* Strains. *PLoS ONE*, 2(3). <https://doi.org/10.1371/journal.pone.0000322>
- Schatz, D. G., & Swanson, P. C. (2011). V(D)J recombination: Mechanisms of initiation. *Annual Review of Genetics*, 45, 167–202. <https://doi.org/10.1146/annurev-genet-110410-132552>
- Schwob, E., Böhm, T., Mendenhall, M. D., & Nasmyth, K. (1994). The B-type cyclin kinase inhibitor p40SIC1 controls the G1 to S transition in *S. cerevisiae*. *Cell*, 79(2), 233–244. [https://doi.org/10.1016/0092-8674\(94\)90193-7](https://doi.org/10.1016/0092-8674(94)90193-7)
- Schwob, E., & Nasmyth, K. (1993). CLB5 and CLB6, a new pair of B cyclins involved in DNA replication in *Saccharomyces cerevisiae*. *Genes & Development*, 7(7A), 1160–1175. <https://doi.org/10.1101/gad.7.7a.1160>
- Schwob, E., Renty, C. de, Coulon, V., Gostan, T., Boyer, C., Camet-Gabut, L., & Amato, C. (2009). Use of DNA Combing for Studying DNA Replication In Vivo in Yeast and Mammalian Cells. In S. Vengrova & J. Z. Dalgard (Eds.), *DNA Replication: Methods and Protocols* (pp. 673–687). Humana Press. [https://doi.org/10.1007/978-1-60327-815-7\\_36](https://doi.org/10.1007/978-1-60327-815-7_36)
- Sherman, F. (2002). Getting started with yeast. *Methods in Enzymology*, 350, 3–41. [https://doi.org/10.1016/s0076-6879\(02\)50954-x](https://doi.org/10.1016/s0076-6879(02)50954-x)
- Sheu, Y.-J., & Stillman, B. (2006). Cdc7-Dbf4 Phosphorylates MCM Proteins via a Docking Site-Mediated Mechanism to Promote S Phase Progression. *Molecular Cell*, 24(1), 101–113. <https://doi.org/10.1016/j.molcel.2006.07.033>
- Shingu, Y., Mikawa, T., Onuma, M., Hirayama, T., & Shibata, T. (2010). A DNA-binding surface of SPO11-1, an Arabidopsis SPO11 orthologue required for normal meiosis. *The FEBS Journal*, 277(10), 2360–2374. <https://doi.org/10.1111/j.1742-4658.2010.07651.x>
- Shinohara, M., Bishop, D. K., & Shinohara, A. (2019). Distinct Functions in Regulation of Meiotic Crossovers for DNA Damage Response Clamp Loader Rad24(Rad17) and Mec1(ATR) Kinase. *Genetics*, 213(4), 1255–1269. <https://doi.org/10.1534/genetics.119.302427>
- Shirayama, M., Tóth, A., Gálová, M., & Nasmyth, K. (1999). APCCdc20 promotes exit from mitosis by destroying the anaphase inhibitor Pds1 and cyclin Clb5. *Nature*, 402(6758), Article 6758. <https://doi.org/10.1038/46080>
- Shreeram, S., Sparks, A., Lane, D. P., & Blow, J. J. (2002). Cell type-specific responses of human cells to inhibition of replication licensing. *Oncogene*, 21(43), 6624–6632. <https://doi.org/10.1038/sj.onc.1205910>
- Signon, L., Malkova, A., Naylor, M. L., Klein, H., & Haber, J. E. (2001). Genetic Requirements for RAD51- and RAD54-Independent Break-Induced Replication Repair of a Chromosomal

Double-Strand Break. *Molecular and Cellular Biology*, 21(6), 2048–2056.

<https://doi.org/10.1128/MCB.21.6.2048-2056.2001>

Simon, A. C., Zhou, J. C., Perera, R. L., van Deursen, F., Evrin, C., Ivanova, M. E., Kilkenny, M. L., Renault, L., Kjaer, S., Matak-Vinković, D., Labib, K., Costa, A., & Pellegrini, L. (2014). A Ctf4 trimer couples the CMG helicase to DNA polymerase  $\alpha$  in the eukaryotic replisome. *Nature*, 510(7504), 293–297. <https://doi.org/10.1038/nature13234>

Slater, M. L. (1973). Effect of reversible inhibition of deoxyribonucleic acid synthesis on the yeast cell cycle. *Journal of Bacteriology*, 113(1), 263–270. <https://doi.org/10.1128/jb.113.1.263-270.1973>

Smith, H. E., Su, S. S., Neigeborn, L., Driscoll, S. E., & Mitchell, A. P. (1990). Role of IME1 expression in regulation of meiosis in *Saccharomyces cerevisiae*. *Molecular and Cellular Biology*, 10(12), 6103–6113. <https://doi.org/10.1128/mcb.10.12.6103-6113.1990>

Smolka, M. B., Albuquerque, C. P., Chen, S., & Zhou, H. (2007). Proteome-wide identification of in vivo targets of DNA damage checkpoint kinases. *Proceedings of the National Academy of Sciences*, 104(25), 10364–10369. <https://doi.org/10.1073/pnas.0701622104>

So, A., Dardillac, E., Muhammad, A., Chailleux, C., Sesma-Sanz, L., Ragu, S., Le Cam, E., Canitrot, Y., Masson, J. Y., Dupaigne, P., Lopez, B. S., & Guirouilh-Barbat, J. (2022). RAD51 protects against nonconservative DNA double-strand break repair through a nonenzymatic function. *Nucleic Acids Research*, 50(5), 2651–2666. <https://doi.org/10.1093/nar/gkac073>

Sonneville, R., Bhowmick, R., Hoffmann, S., Mailand, N., Hickson, I. D., & Labib, K. (n.d.). TRAIIP drives replisome disassembly and mitotic DNA repair synthesis at sites of incomplete DNA replication. *ELife*, 8, e48686. <https://doi.org/10.7554/eLife.48686>

Sonneville, R., Moreno, S. P., Knebel, A., Johnson, C., Hastie, C. J., Gartner, A., Gambus, A., & Labib, K. (2017). CUL-2LRR-1 and UBXN-3 drive replisome disassembly during DNA replication termination and mitosis. *Nature Cell Biology*, 19(5), 468–479. <https://doi.org/10.1038/ncb3500>

Sorger, P. K., & Murray, A. W. (1992). S-phase feedback control in budding yeast independent of tyrosine phosphorylation of p34cdc28. *Nature*, 355(6358), 365–368. <https://doi.org/10.1038/355365a0>

Sparks, J. L., Chistol, G., Gao, A. O., Räschle, M., Larsen, N. B., Mann, M., Duxin, J. P., & Walter, J. C. (2019). The CMG Helicase Bypasses DNA-Protein Cross-Links to Facilitate Their Repair. *Cell*, 176(1), 167–181.e21. <https://doi.org/10.1016/j.cell.2018.10.053>

Speck, C., Chen, Z., Li, H., & Stillman, B. (2005). ATPase-dependent, cooperative binding of ORC and Cdc6p to origin DNA. *Nature Structural & Molecular Biology*, 12(11), 965–971. <https://doi.org/10.1038/nsmb1002>

Spies, J., Lukas, C., Somyajit, K., Rask, M.-B., Lukas, J., & Neelsen, K. J. (2019). 53BP1 nuclear bodies enforce replication timing at under-replicated DNA to limit heritable DNA damage. *Nature Cell Biology*, 21(4), Article 4. <https://doi.org/10.1038/s41556-019-0293-6>

Stinchcomb, D. T., Struhl, K., & Davis, R. W. (1979). Isolation and characterisation of a yeast chromosomal replicator. *Nature*, 282(5734), 39–43. <https://doi.org/10.1038/282039a0>

- Storer, M., Mas, A., Robert-Moreno, A., Pecoraro, M., Ortells, M. C., Di Giacomo, V., Yosef, R., Pilpel, N., Krizhanovsky, V., Sharpe, J., & Keyes, W. M. (2013). Senescence Is a Developmental Mechanism that Contributes to Embryonic Growth and Patterning. *Cell*, 155(5), 1119–1130. <https://doi.org/10.1016/j.cell.2013.10.041>
- Stuart, D. (2013). *The Mechanisms of DNA Replication*. <https://doi.org/10.5772/3433>
- Stuart, D., & Stuart, D. (2013). *The Mechanisms of DNA Replication*. <https://doi.org/10.5772/3433>
- Subramanian, V. V., & Hochwagen, A. (2014). The Meiotic Checkpoint Network: Step-by-Step through Meiotic Prophase. *Cold Spring Harbor Perspectives in Biology*, 6(10), a016675. <https://doi.org/10.1101/cshperspect.a016675>
- Sun, J., Shi, Y., Georgescu, R. E., Yuan, Z., Chait, B. T., Li, H., & O'Donnell, M. E. (2015). The architecture of a eukaryotic replisome. *Nature Structural & Molecular Biology*, 22(12), Article 12. <https://doi.org/10.1038/nsmb.3113>
- Sun, S., & Gresham, D. (2021). Cellular Quiescence in Budding Yeast. *Yeast (Chichester, England)*, 38(1), 12–29. <https://doi.org/10.1002/yea.3545>
- Sundin, O., & Varshavsky, A. (1980). Terminal stages of SV40 DNA replication proceed via multiply intertwined catenated dimers. *Cell*, 21(1), 103–114. [https://doi.org/10.1016/0092-8674\(80\)90118-x](https://doi.org/10.1016/0092-8674(80)90118-x)
- Sung, P., & Roberson, D. L. (1995). DNA strand exchange mediated by a RAD51-ssDNA nucleoprotein filament with polarity opposite to that of RecA. *Cell*, 82(3), 453–461. [https://doi.org/10.1016/0092-8674\(95\)90434-4](https://doi.org/10.1016/0092-8674(95)90434-4)
- Suzuki, K., Sako, K., Akiyama, K., Isoda, M., Senoo, C., Nakajo, N., & Sagata, N. (2015). Identification of non-Ser/Thr-Pro consensus motifs for Cdk1 and their roles in mitotic regulation of C2H2 zinc finger proteins and Ect2. *Scientific Reports*, 5(1), 7929. <https://doi.org/10.1038/srep07929>
- Swaney, D. L., Beltrao, P., Starita, L., Guo, A., Rush, J., Fields, S., Krogan, N. J., & Villén, J. (2013). Global analysis of phosphorylation and ubiquitylation cross-talk in protein degradation. *Nature Methods*, 10(7), 676–682. <https://doi.org/10.1038/nmeth.2519>
- Sweeney, F. D., Yang, F., Chi, A., Shabanowitz, J., Hunt, D. F., & Durocher, D. (2005). *Saccharomyces cerevisiae* Rad9 acts as a Mec1 adaptor to allow Rad53 activation. *Current Biology: CB*, 15(15), 1364–1375. <https://doi.org/10.1016/j.cub.2005.06.063>
- Szyjka, S. J., Viggiani, C. J., & Aparicio, O. M. (2005). Mrc1 is required for normal progression of replication forks throughout chromatin in *S. cerevisiae*. *Molecular Cell*, 19(5), 691–697. <https://doi.org/10.1016/j.molcel.2005.06.037>
- Talarek, N., Petit, J., Gueydon, E., & Schwob, E. (2015). EdU Incorporation for FACS and Microscopy Analysis of DNA Replication in Budding Yeast. *Methods in Molecular Biology (Clifton, N.J.)*, 1300, 105–112. [https://doi.org/10.1007/978-1-4939-2596-4\\_7](https://doi.org/10.1007/978-1-4939-2596-4_7)
- Tanaka, H., Katou, Y., Yagura, M., Saitoh, K., Itoh, T., Araki, H., Bando, M., & Shirahige, K. (2009). Ctf4 coordinates the progression of helicase and DNA polymerase  $\alpha$ . *Genes to Cells*, 14(7), 807–820. <https://doi.org/10.1111/j.1365-2443.2009.01310.x>

- Tanaka, S., & Diffley, J. F. X. (2002). Deregulated G1-cyclin expression induces genomic instability by preventing efficient pre-RC formation. *Genes & Development*, *16*(20), 2639–2649. <https://doi.org/10.1101/gad.1011002>
- Tanaka, T., Knapp, D., & Nasmyth, K. (1997). Loading of an Mcm protein onto DNA replication origins is regulated by Cdc6p and CDKs. *Cell*, *90*(4), 649–660. [https://doi.org/10.1016/s0092-8674\(00\)80526-7](https://doi.org/10.1016/s0092-8674(00)80526-7)
- Técher, H., Koundrioukoff, S., Azar, D., Wilhelm, T., Carignon, S., Brison, O., Debatisse, M., & Le Tallec, B. (2013). Replication Dynamics: Biases and Robustness of DNA Fiber Analysis. *Journal of Molecular Biology*, *425*(23), 4845–4855. <https://doi.org/10.1016/j.jmb.2013.03.040>
- Tercero, J. A., Longhese, M. P., & Diffley, J. F. X. (2003). A central role for DNA replication forks in checkpoint activation and response. *Molecular Cell*, *11*(5), 1323–1336. [https://doi.org/10.1016/s1097-2765\(03\)00169-2](https://doi.org/10.1016/s1097-2765(03)00169-2)
- Thangavel, S., Berti, M., Levikova, M., Pinto, C., Gomathinayagam, S., Vujanovic, M., Zellweger, R., Moore, H., Lee, E. H., Hendrickson, E. A., Cejka, P., Stewart, S., Lopes, M., & Vindigni, A. (2015). DNA2 drives processing and restart of reversed replication forks in human cells. *The Journal of Cell Biology*, *208*(5), 545–562. <https://doi.org/10.1083/jcb.201406100>
- Theulot, B., Lacroix, L., Arbona, J.-M., Millot, G. A., Jean, E., Cruaud, C., Pellet, J., Proux, F., Hennion, M., Engelen, S., Lemainque, A., Audit, B., Hyrien, O., & Le Tallec, B. (2022). Genome-wide mapping of individual replication fork velocities using nanopore sequencing. *Nature Communications*, *13*(1), 3295. <https://doi.org/10.1038/s41467-022-31012-0>
- Thorpe, P. H., Bruno, J., & Rothstein, R. (2009). Kinetochore asymmetry defines a single yeast lineage. *Proceedings of the National Academy of Sciences of the United States of America*, *106*(16), 6673–6678. <https://doi.org/10.1073/pnas.0811248106>
- Ticau, S., Friedman, L. J., Champasa, K., Corrêa, I. R., Gelles, J., & Bell, S. P. (2017). Mechanism and timing of Mcm2-7 ring closure during DNA replication origin licensing. *Nature Structural & Molecular Biology*, *24*(3), 309–315. <https://doi.org/10.1038/nsmb.3375>
- Ticau, S., Friedman, L. J., Ivica, N. A., Gelles, J., & Bell, S. P. (2015). Single-molecule studies of origin licensing reveal mechanisms ensuring bidirectional helicase loading. *Cell*, *161*(3), 513–525. <https://doi.org/10.1016/j.cell.2015.03.012>
- Tittel-Elmer, M., Alabert, C., Pasero, P., & Cobb, J. A. (2009). The MRX complex stabilizes the replisome independently of the S phase checkpoint during replication stress. *The EMBO Journal*, *28*(8), 1142–1156. <https://doi.org/10.1038/emboj.2009.60>
- Tittel-Elmer, M., Lengronne, A., Davidson, M. B., Bacal, J., François, P., Hohl, M., Petrini, J. H. J., Pasero, P., & Cobb, J. A. (2012). Cohesin association to replication sites depends on rad50 and promotes fork restart. *Molecular Cell*, *48*(1), 98–108. <https://doi.org/10.1016/j.molcel.2012.07.004>
- Torres-Rosell, J., De Piccoli, G., Cordon-Preciado, V., Farmer, S., Jarmuz, A., Machin, F., Pasero, P., Lisby, M., Haber, J. E., & Aragón, L. (2007). Anaphase Onset Before Complete DNA Replication with Intact Checkpoint Responses. *Science*, *315*(5817), 1411–1415. <https://doi.org/10.1126/science.1134025>

- Tourrière, H., & Pasero, P. (2007). Maintenance of fork integrity at damaged DNA and natural pause sites. *DNA Repair*, 6(7), 900–913. <https://doi.org/10.1016/j.dnarep.2007.02.004>
- Toyn, J. H., Johnson, A. L., Donovan, J. D., Toone, W. M., & Johnston, L. H. (1997). The Swi5 transcription factor of *Saccharomyces cerevisiae* has a role in exit from mitosis through induction of the cdk-inhibitor Sic1 in telophase. *Genetics*, 145(1), 85–96. <https://doi.org/10.1093/genetics/145.1.85>
- Trujillo, K. M., & Sung, P. (2001). DNA structure-specific nuclease activities in the *Saccharomyces cerevisiae* Rad50\*Mre11 complex. *The Journal of Biological Chemistry*, 276(38), 35458–35464. <https://doi.org/10.1074/jbc.M105482200>
- Tsabar, M., Waterman, D. P., Aguilar, F., Katsnelson, L., Eapen, V. V., Memisoglu, G., & Haber, J. E. (2016). Asf1 facilitates dephosphorylation of Rad53 after DNA double-strand break repair. *Genes & Development*, 30(10), 1211–1224. <https://doi.org/10.1101/gad.280685.116>
- Uzunova, S. D., Zarkov, A. S., Ivanova, A. M., Stoyanov, S. S., & Nedelcheva-Veleva, M. N. (2014). The subunits of the S-phase checkpoint complex Mrc1/Tof1/Csm3: Dynamics and interdependence. *Cell Division*, 9(1), 4. <https://doi.org/10.1186/1747-1028-9-4>
- VanHulle, K., Lemoine, F. J., Narayanan, V., Downing, B., Hull, K., McCullough, C., Bellinger, M., Lobachev, K., Petes, T. D., & Malkova, A. (2007). Inverted DNA repeats channel repair of distant double-strand breaks into chromatid fusions and chromosomal rearrangements. *Molecular and Cellular Biology*, 27(7), 2601–2614. <https://doi.org/10.1128/MCB.01740-06>
- Villa, F., Simon, A. C., Ortiz Bazan, M. A., Kilkenny, M. L., Wirthensohn, D., Wightman, M., Matak-Vinković, D., Pellegrini, L., & Labib, K. (2016). Ctf4 Is a Hub in the Eukaryotic Replisome that Links Multiple CIP-Box Proteins to the CMG Helicase. *Molecular Cell*, 63(3), 385–396. <https://doi.org/10.1016/j.molcel.2016.06.009>
- Viret, J. F., Bravo, A., & Alonso, J. C. (1991). Recombination-dependent concatemeric plasmid replication. *Microbiological Reviews*, 55(4), 675–683. <https://doi.org/10.1128/mr.55.4.675-683.1991>
- Visintin, R., Craig, K., Hwang, E. S., Prinz, S., Tyers, M., & Amon, A. (1998). The phosphatase Cdc14 triggers mitotic exit by reversal of Cdk-dependent phosphorylation. *Molecular Cell*, 2(6), 709–718. [https://doi.org/10.1016/s1097-2765\(00\)80286-5](https://doi.org/10.1016/s1097-2765(00)80286-5)
- Voitenleitner, C., Rehfuess, C., Hilmes, M., O’Rear, L., Liao, P.-C., Gage, D. A., Ott, R., Nasheuer, H.-P., & Fanning, E. (1999). Cell Cycle-Dependent Regulation of Human DNA Polymerase  $\alpha$ -Primase Activity by Phosphorylation. *Molecular and Cellular Biology*, 19(1), 646–656.
- Waizenegger, I. C., Hauf, S., Meinke, A., & Peters, J. M. (2000). Two distinct pathways remove mammalian cohesin from chromosome arms in prophase and from centromeres in anaphase. *Cell*, 103(3), 399–410. [https://doi.org/10.1016/s0092-8674\(00\)00132-x](https://doi.org/10.1016/s0092-8674(00)00132-x)
- Wan, L., Niu, H., Fitcher, B., Zhang, C., Shokat, K. M., Boulton, S. J., & Hollingsworth, N. M. (2008). Cdc28-Clb5 (CDK-S) and Cdc7-Dbf4 (DDK) collaborate to initiate meiotic recombination in yeast. *Genes & Development*, 22(3), 386–397. <https://doi.org/10.1101/gad.1626408>

- Wang, G., Tong, X., Weng, S., & Zhou, H. (2012). Multiple phosphorylation of Rad9 by CDK is required for DNA damage checkpoint activation. *Cell Cycle*, *11*(20), 3792–3800. <https://doi.org/10.4161/cc.21987>
- Wang, Y., & Burke, D. J. (1995). Checkpoint genes required to delay cell division in response to nocodazole respond to impaired kinetochore function in the yeast *Saccharomyces cerevisiae*. *Molecular and Cellular Biology*, *15*(12), 6838–6844. <https://doi.org/10.1128/MCB.15.12.6838>
- Warren, E. M., Vaithiyalingam, S., Haworth, J., Greer, B., Bielinsky, A.-K., Chazin, W. J., & Eichman, B. F. (2008). Structural Basis for DNA Binding by Replication Initiator Mcm10. *Structure*, *16*(12), 1892–1901. <https://doi.org/10.1016/j.str.2008.10.005>
- Wassing, I. E., Graham, E., Saayman, X., Rampazzo, L., Ralf, C., Bassett, A., & Esashi, F. (2021). The RAD51 recombinase protects mitotic chromatin in human cells. *Nature Communications*, *12*(1), Article 1. <https://doi.org/10.1038/s41467-021-25643-y>
- Weinert, T. A., & Hartwell, L. H. (1988). The RAD9 gene controls the cell cycle response to DNA damage in *Saccharomyces cerevisiae*. *Science (New York, N.Y.)*, *241*(4863), 317–322. <https://doi.org/10.1126/science.3291120>
- Williams, R. S., Shohet, R. V., & Stillman, B. (1997). A human protein related to yeast Cdc6p. *Proceedings of the National Academy of Sciences of the United States of America*, *94*(1), 142–147. <https://doi.org/10.1073/pnas.94.1.142>
- Williams RS et al. (1997), A human protein related to yeast Cdc6p. - Paper. (n.d.). Retrieved August 23, 2022, from <https://www.xenbase.org/literature/article.do?method=display&articleId=17055>
- Wilson, M. A., Kwon, Y., Xu, Y., Chung, W.-H., Chi, P., Niu, H., Mayle, R., Chen, X., Malkova, A., Sung, P., & Ira, G. (2013). Pif1 helicase and Polδ promote recombination-coupled DNA synthesis via bubble migration. *Nature*, *502*(7471), 393–396. <https://doi.org/10.1038/nature12585>
- Winter, E. (2012). The Sum1/Ndt80 transcriptional switch and commitment to meiosis in *Saccharomyces cerevisiae*. *Microbiology and Molecular Biology Reviews: MMBR*, *76*(1), 1–15. <https://doi.org/10.1128/MMBR.05010-11>
- Winzeler, E. A., Castillo-Davis, C. I., Oshiro, G., Liang, D., Richards, D. R., Zhou, Y., & Hartl, D. L. (2003). Genetic diversity in yeast assessed with whole-genome oligonucleotide arrays. *Genetics*, *163*(1), 79–89.
- Wu, P.-Y. J., & Nurse, P. (2014). Replication origin selection regulates the distribution of meiotic recombination. *Molecular Cell*, *53*(4), 655–662. <https://doi.org/10.1016/j.molcel.2014.01.022>
- Wu, T. C., & Lichten, M. (1994). Meiosis-induced double-strand break sites determined by yeast chromatin structure. *Science (New York, N.Y.)*, *263*(5146), 515–518. <https://doi.org/10.1126/science.8290959>
- Xu, L., Ajimura, M., Padmore, R., Klein, C., & Kleckner, N. (1995). NDT80, a meiosis-specific gene required for exit from pachytene in *Saccharomyces cerevisiae*. *Molecular and Cellular Biology*, *15*(12), 6572–6581. <https://doi.org/10.1128/MCB.15.12.6572>

- Yeeles, J. T. P., Deegan, T. D., Janska, A., Early, A., & Diffley, J. F. X. (2015). Regulated eukaryotic DNA replication origin firing with purified proteins. *Nature*, *519*(7544), 431–435. <https://doi.org/10.1038/nature14285>
- Yeeles, J. T. P., Janska, A., Early, A., & Diffley, J. F. X. (2017). How the Eukaryotic Replisome Achieves Rapid and Efficient DNA Replication. *Molecular Cell*, *65*(1), 105–116. <https://doi.org/10.1016/j.molcel.2016.11.017>
- Yekezare, M., Gómez-González, B., & Diffley, J. F. X. (2013). Controlling DNA replication origins in response to DNA damage—Inhibit globally, activate locally. *Journal of Cell Science*, *126*(Pt 6), 1297–1306. <https://doi.org/10.1242/jcs.096701>
- Yoshizawa-Sugata, N., & Masai, H. (2007). Human Tim/Timeless-interacting protein, Tipin, is required for efficient progression of S phase and DNA replication checkpoint. *The Journal of Biological Chemistry*, *282*(4), 2729–2740. <https://doi.org/10.1074/jbc.M605596200>
- Youds, J. L., & Boulton, S. J. (2011). The choice in meiosis – defining the factors that influence crossover or non-crossover formation. *Journal of Cell Science*, *124*(4), 501–513. <https://doi.org/10.1242/jcs.074427>
- Yuan, Z., Schneider, S., Dodd, T., Riera, A., Bai, L., Yan, C., Barbon, M., Magdalou, I., Ivanov, I., Stillman, B., Li, H., & Speck, C. (2020). Structural mechanism of helicase loading onto replication origin DNA by ORC-Cdc6. *Proceedings of the National Academy of Sciences*, *117*(30), 17747–17756. <https://doi.org/10.1073/pnas.2006231117>
- Zechiedrich, E. L., & Osheroff, N. (1990). Eukaryotic topoisomerases recognize nucleic acid topology by preferentially interacting with DNA crossovers. *The EMBO Journal*, *9*(13), 4555–4562. <https://doi.org/10.1002/j.1460-2075.1990.tb07908.x>
- Zellweger, R., Dalcher, D., Mutreja, K., Berti, M., Schmid, J. A., Herrador, R., Vindigni, A., & Lopes, M. (2015). Rad51-mediated replication fork reversal is a global response to genotoxic treatments in human cells. *The Journal of Cell Biology*, *208*(5), 563–579. <https://doi.org/10.1083/jcb.201406099>
- Zeman, M. K., & Cimprich, K. A. (2014). Causes and consequences of replication stress. *Nature Cell Biology*, *16*(1), 2–9. <https://doi.org/10.1038/ncb2897>
- Zwerschke, W., Rottjakob, H. W., & Küntzel, H. (1994). The *Saccharomyces cerevisiae* CDC6 gene is transcribed at late mitosis and encodes a ATP/GTPase controlling S phase initiation. *The Journal of Biological Chemistry*, *269*(37), 23351–23356.



**Chapter vii: Determination of S-Phase  
Duration Using 5-Ethynyl-2'-deoxyuridine  
Incorporation in *Saccharomyces cerevisiae*  
(Publication)**

# Determination of S-Phase Duration Using 5-Ethynyl-2'-deoxyuridine Incorporation in *Saccharomyces cerevisiae*

Juan de Dios Barba Tena<sup>1</sup>, Etienne Schwob<sup>1</sup>, Nicolas Talarek<sup>1</sup>

<sup>1</sup> Institut de Génétique Moléculaire de Montpellier, Université de Montpellier, CNRS

## Corresponding Authors

Etienne Schwob

etienne.schwob@igmm.cnrs.fr

Nicolas Talarek

nicolas.talarek@igmm.cnrs.fr

## Citation

Barba Tena, J.d.D., Schwob, E., Talarek, N. Determination of S-Phase Duration Using 5-Ethynyl-2'-deoxyuridine Incorporation in *Saccharomyces cerevisiae*. *J. Vis. Exp.* (), e64490, doi:10.3791/64490 (2022).

## Date Published

October 8, 2022

## DOI

10.3791/64490

## URL

jove.com/t/64490

## Introduction

Genome stability through mitotic division is ensured by the transmission of a complete and equal set of chromosomes to the two produced cell progenies. This relies on the accurate completion of a series of events occurring in a given time in each phase of the cell cycle. In G<sub>1</sub>, the replication origins are licensed upon the recruitment of several licensing factors, including Cdc6<sup>1</sup>. In the S phase, whole-genome duplication is initiated from multiple active replication origins and performed by replication machineries

that gather in microscopically visible foci named replication factories<sup>2</sup>. In the M phase, duplicated sister chromatids are attached and bioriented on the mitotic spindle to allow their segregation to the opposite poles of the mitotic cell<sup>3</sup>. The regulation, proper completion, and duration of each phase are key to ensure genome stability. Indeed, premature exit from any of these phases leads to genome instability. For instance, a shorter G<sub>1</sub> induced by deletion of the budding yeast CDK inhibitor Sic1 or by the overexpression of G<sub>1</sub>

## Abstract

Eukaryotic DNA replication is a highly regulated process that ensures that the genetic blueprint of a cell is correctly duplicated prior to chromosome segregation. As DNA synthesis defects underlie chromosome rearrangements, monitoring DNA replication has become essential to understand the basis of genome instability. *Saccharomyces cerevisiae* is a classical model to study cell cycle regulation, but key DNA replication parameters, such as the fraction of cells in the S phase or the S-phase duration, are still difficult to determine. This protocol uses short and non-toxic pulses of 5-ethynyl-2'-deoxyuridine (EdU), a thymidine analog, in engineered TK-hENT1 yeast cells, followed by its detection by Click reaction to allow the visualization and quantification of DNA replication with high spatial and temporal resolution at both the single-cell and population levels by microscopy and flow cytometry. This method may identify previously overlooked defects in the S phase and cell cycle progression of yeast mutants, thereby allowing the characterization of new players essential for ensuring genome stability.

cyclins will alter the subsequent S phase<sup>4,5,6</sup>. Consequently, these deregulations, associated or not with replication stress, result in chromosome breaks, rearrangements, and mis-segregation<sup>4,5,6</sup>. Therefore, monitoring the duration of the S phase and, more broadly, the duration of the other phases of the cell cycle may be crucial to identify the defects occurring in different mutants and in different stressful conditions.

A traditional method for measuring cell cycle phase duration includes simple DNA content flow cytometry (**Figure 1A**) and relies on a fitting algorithm (available in most cytometry software) used to separate the population into G<sub>1</sub>, S, and G<sub>2</sub> + M phase fractions from the 1C and 2C peaks. The fractions are then multiplied by the population doubling time<sup>7</sup>. However, this method gives only estimated values, requires a homogeneous cell size distribution within a given fraction, and is not applicable to synchronized cultures. To study the S-phase duration in mammalian cells, several thymidine analogs have been developed and widely used, including EdU. Their uptake from the extracellular medium and phosphorylation by thymidine kinase (hereafter referred to as TK) make them available for DNA polymerases to incorporate them at sites of DNA synthesis (replication, recombination, repair). To bypass the absence of the TK gene in *Saccharomyces cerevisiae* cells, yeast strains have been engineered to allow stable and constitutive expression of the herpes simplex virus TK<sup>8</sup> and the human equilibrative nucleoside transporter (hENT1)<sup>9</sup>. Once incorporated into DNA, EdU is detected *via* the selective Click reaction, which chemically couples its alkyne moiety to azide-modified fluorochromes<sup>10</sup>.

This paper provides two optimized comprehensive protocols to pulse-label asynchronous and synchronous TK-hENT1 engineered cells with EdU in order to precisely visualize and

measure DNA replication duration and dynamics, as well as the duration of the other phases of the cell cycle, with high spatial and temporal resolution at both the single-cell and population levels by microscopy and flow cytometry.

## Protocol

### 1. *S. cerevisiae* cell culture

**NOTE:** The yeast strains used are listed in **Table 1**

**NOTE:** The S-phase duration can be monitored in different ways. Depending on the question to be addressed, the cells can be grown asynchronously or synchronously following G<sub>1</sub> arrest.

1. From asynchronously growing *S. cerevisiae* cells

**NOTE:** This method allows for the determination of the percentage of cells in the S phase in an asynchronously growing cell population. By determining the doubling time, the duration of the S phase (and the other phases) can be extrapolated.

1. Inoculate *S. cerevisiae* cells in 10 mL of synthetic complete (SC) medium at a low cell concentration ( $5 \times 10^4$  cells/mL) for an overnight culture at 30 °C with orbital agitation at 130 rpm.

**NOTE:** The concentration is measured with a cell counter. To efficiently calculate the doubling times, it is recommended to inoculate the culture from an overnight culture that is still in the exponential phase (i.e., ideally below  $2 \times 10^7$  cells/mL). Growing cells in rich medium (YPD) is not recommended, as EdU detection is not efficient.

2. The following day, dilute the cells in 20 mL of fresh SC medium at the final concentration of  $5 \times 10^5$  cells/mL.
  3. Culture the cells at 30 °C in a shaking water bath with horizontal shaking at 120 rpm.
  4. Measure the cell concentration every hour until it reaches  $1 \times 10^7$  cells/mL.  
**NOTE:** This step allows for making a graphical representation of the cell concentration increase over time. The formula used to calculate the doubling times is explained in the legend of **Table 2**.
  5. Proceed in parallel to step 2 for EdU labeling when the cell concentration is about  $2 \times 10^6$ - $5 \times 10^6$  cells/mL.
2. From G<sub>1</sub>-synchronized *S. cerevisiae* cells  
**NOTE:** This method allows for the determination of when the S phase starts and finishes by means of flow cytometry and/or microscopy analyses.
    1. Inoculate *S. cerevisiae* cells in 10 mL of SC medium at a low cell concentration ( $5 \times 10^4$  cells/mL) for an overnight culture at 30 °C with orbital agitation at 130 rpm.  
**NOTE:** See the notes after step 1.1.1.
    2. The following day, dilute the cells in 20 mL of fresh SC medium at a final concentration of  $2 \times 10^6$ - $3 \times 10^6$  cells/mL.
    3. Add 40 µL of 1 mg/mL α-factor diluted in water.
    4. Culture the cells at 30 °C with orbital agitation at 130 rpm for 1 h.
    5. Add again 40 µL of 1 mg/mL α-factor diluted in water.
    6. Culture the cells at 30 °C with orbital agitation at 130 rpm for 1 h.
    7. Visualize the cells under a light microscope to monitor G<sub>1</sub> arrest. Proceed if more than 90% of the cells display a shmoo and the others are rounded, unbudded cells.  
**NOTE:** Depending on the background used, it is recommended to sonicate the cells before shmoo visualization. For the W303 background, sonicate 2x, for 2 s each time, at an amplitude of 40-50.
    8. Centrifuge for 3 min at  $1,500 \times g$ . Discard the supernatant with a vacuum pipette.
    9. Resuspend the cells in 20 mL of SC medium.
    10. Repeat steps 1.2.8-1.2.9 once.  
**NOTE:** The α-factor is washed away with these steps, and the cells are released in the cell cycle. Alternatively, the α-factor may be washed away by filtering the yeast cells with a 1.2 µm nitrocellulose filter using a funnel set on a side-arm flask connected to a vacuum pump.
    11. Collect 1 mL of cells 2x every 5 min and proceed to step 2 for EdU labeling.  
**NOTE:** Pulse-label the cells from only one of the two tubes with EdU. The non-pulse-labeled cells are used to distinguish EdU-positive from EdU-negative cells on a bivariate propidium iodide (PI)-EdU graph.
    12. Add 400 µL of 1 mg/mL α-factor diluted in water 30 min after the release.  
**NOTE:** This high dose of α-factor is required to arrest the cells in the G<sub>1</sub> phase of the next cell cycle and to prevent the cells from re-entering the subsequent S phase.

## 2. EdU labeling

1. Transfer 1 mL of cell culture to a 2.0 mL microfuge tube containing 1  $\mu$ L of 10 mM EdU. Mix well by inversion.

**NOTE:** To discriminate the EdU-positive cells from the EdU-negative cells on a PI-EdU bivariate FACS, transfer another 1 mL of cell culture to a 2.0 mL microfuge tube containing 1  $\mu$ L of DMSO.

2. Incubate for 3-5 min at 30 °C under agitation in a shaking water bath.

**NOTE:** Three minutes are sufficient for EdU detection with a microscope; 5 min are required for optimal EdU detection on a flow cytometer.

3. Stop the reaction with the addition of 100  $\mu$ L of 100% ethanol.

1. Stop the reaction with the addition of 100  $\mu$ L of 20% paraformaldehyde if cell size measurement is required.

**NOTE:** If the nuclear architecture of the mitotic cells is to be kept intact for further analyses following the Click reaction, we recommend fixing cells with 2% paraformaldehyde at room temperature (RT) rather than putting the cells on ice, since the latter causes microtubule depolymerization.

2. Leave the cells for 20 min at RT under mild agitation on a variable speed rocker at 20 tilts/min to fix the cells before the addition of 100  $\mu$ L of 100% ethanol.

## 3. Cell fixation and permeabilization

1. Pellet the cells for 2 min at 10,000  $\times g$  in a microfuge. Remove the supernatant using a vacuum pipette.
2. Resuspend the cell pellet in 500  $\mu$ L of 70% ethanol. Mix well by vortexing.

3. Leave for  $\geq 1$  h at RT at 20 tilts/min on a variable speed rocker to permeabilize the cells.

**NOTE:** Cells grown in SC medium do not pellet well as they tend to stick to the microfuge walls. The addition of ethanol improves pelleting and reduces cell loss. The cells may be stored at 4 °C overnight or for longer periods at -20 °C.

4. Pellet the cells for 2 min at 10,000  $\times g$  in a microcentrifuge. Discard the supernatant with a vacuum pipette.

5. Wash the cells 2x with 500  $\mu$ L of 10% ethanol in PBS.

**NOTE:** The washes are crucial to remove unincorporated EdU from the cells.

## 4. Click-it reaction

1. For cytometry analysis

1. Pellet the cells for 2 min at 10,000  $\times g$  in a microfuge. Discard the supernatant with a vacuum pipette.

2. Resuspend the pellet in 200  $\mu$ L of PBS containing 0.1 mg/mL RNase A and 0.2 mg/mL proteinase K.

3. Incubate for 1-2 h at 50 °C with occasional shaking (or overnight at 37 °C).

4. Pellet the cells for 2 min at 10,000  $\times g$  in a microcentrifuge. Discard the supernatant with a vacuum pipette.

5. Wash the cells with 500  $\mu$ L of PBS.

6. Pellet the cells for 2 min at 10,000  $\times g$  in a microfuge. Discard the supernatant with a vacuum pipette.

7. Resuspend the cell pellet in 200  $\mu$ L of PBS + 1% bovine serum albumin (BSA). Incubate for 30 min at RT.

**NOTE:** Longer times are not necessary and are even detrimental to the efficiency of Click reactions.

8. Pellet the cells for 2 min at  $10,000 \times g$  in a microcentrifuge. Discard the supernatant with a vacuum pipette.
9. Resuspend the pellet in 300  $\mu\text{L}$  of PBS + 1% BSA.
10. Distribute the cells between two tubes: 200  $\mu\text{L}$  in a 1.5 mL microcentrifuge tube for the Click reaction and 100  $\mu\text{L}$  in another 1.5 mL microcentrifuge tube for Sytox Green staining.
11. Pellet the cells for 2 min at  $10,000 \times g$  in a microcentrifuge. Discard the supernatant with a vacuum pipette.

12. For Sytox Green staining

**NOTE:** We highly recommend taking an aliquot for Sytox Green staining (without Click) in order to obtain high-quality DNA content reference profiles. Indeed, the Click reaction strongly quenches intercalant fluorescence, including the Sytox Green and PI fluorescence. Consequently, the Click reaction can distort the reading of DNA content.

1. Resuspend the cell pellet in 100  $\mu\text{L}$  of PBS.
2. Transfer 10-30  $\mu\text{L}$  (depending on the cell concentration) to a flow cytometer tube containing 300  $\mu\text{L}$  of 50 mM Tris-HCl, pH 7.5, and 0.5  $\mu\text{M}$  Sytox Green.
3. Sonicate 2x, for 2 s each time, at an amplitude of 40-50.
4. Leave in the dark until processing the samples on a flow cytometer.

**NOTE:** The cells can be kept at this stage at 4  $^{\circ}\text{C}$  for a few days.

13. For the Click reaction

1. Prepare fresh Azide Dye buffer by mixing the reagents in the following order (quantity for one tube): 36  $\mu\text{L}$  of PBS, 2  $\mu\text{L}$  of 0.2 M  $\text{CuSO}_4$ , 0.2  $\mu\text{L}$  of 2 mM Cy5 Azide, and 2  $\mu\text{L}$  of 1 M ascorbic acid.

**NOTE:** It is possible to prepare a master mix of the Azide Dye buffer. The reagents have to be mixed in the same order as that mentioned above.

2. Resuspend the cell pellet with 40  $\mu\text{L}$  of freshly made Azide Dye mix. Incubate at RT in the dark for 60 min.
3. Pellet the cells for 2 min at  $10,000 \times g$  in a microcentrifuge. Discard the supernatant with a vacuum pipette.
4. Wash the cells 3x with 300  $\mu\text{L}$  of 10% ethanol in PBS.

**NOTE:** The washes are crucial to eliminate all the soluble EdU-Cy5 azide.

5. Resuspend the cells in 100  $\mu\text{L}$  of 50  $\mu\text{g}/\text{mL}$  PI in PBS. Leave for 10 min in the dark.
6. Transfer 10-30  $\mu\text{L}$  of the cell suspension (depending on the cell concentration) to a flow cytometer tube containing 300  $\mu\text{L}$  of 50 mM Tris-HCl, pH 7.5.
7. Sonicate 2x, for 2 s each time, at an amplitude of 40-50.
8. Leave in the dark until processing the samples on a cytometer.

**NOTE:** The cells can be kept at this stage at 4  $^{\circ}\text{C}$  for a few days.

14. Read the Sytox Green samples using an excitation blue laser at 488 nm and a 530/30 BP filter. See **Figure 1A** for typical results. Read the bivariate PI-Edu samples on a dot plot using an excitation blue laser at 488 nm and a 615/20 BP filter for the PI (x-axis) and an excitation red laser at 640 nm and a 660/20 BP filter (y-axis). See **Figure 1B** for typical results.

**NOTE:** **Figure 1C** represents the typical PI-Edu bivariate FACS result for Edu-negative cells. It allows for the discrimination of the Edu-negative cells from the Edu-positive cells.

2. For microscopy analysis

1. Pellet the cells for 2 min at 10,000 × g in a microcentrifuge. Discard the supernatant with a vacuum pipette.
2. Resuspend the pellet in 200 µL of PBS + 1% BSA. Incubate for 30 min at RT.
3. Pellet the cells for 2 min at 10,000 × g in a microfuge. Discard the supernatant with a vacuum pipette.
4. Prepare fresh Azide Dye buffer by mixing the reagents in the following order (quantity for one tube): 36 µL of PBS, 2 µL of 0.2 M CuSO<sub>4</sub>, 0.2 µL of 2 mM Dy-530 azide, 2 µL of 1 M ascorbic acid.  
**NOTE:** A master mix of the Azide Dye buffer can be prepared fresh by mixing the reagents in the aforementioned order.
5. Resuspend the pellet with 40 µL of freshly made Azide Dye buffer. Incubate at RT in the dark for 60 min.
6. Pellet the cells for 2 min at 10,000 × g in a microfuge. Discard the supernatant with a vacuum pipette.

7. Wash the cells 2x with 300 µL of 10% ethanol in PBS.

**NOTE:** The washes are crucial to eliminate all soluble Dy-530 azide.

8. Pellet the cells for 2 min at 10,000 × g in a microcentrifuge. Discard the supernatant with a vacuum pipette.
9. Resuspend the cells in 100 µL of 0.5 µg/mL 4',6-diamidino-2-phenylindole (DAPI) in PBS. Leave for 30 min in the dark at room temperature.
10. Pellet the cells for 2 min at 10,000 × g in a microcentrifuge. Discard the supernatant with a vacuum pipette.
11. Wash with 300 µL of PBS to remove excess DAPI.
12. Pellet the cells for 2 min at 10,000 × g in a microfuge. Discard the supernatant with a vacuum pipette.
13. Resuspend the pellet with 10-50 µL of PBS depending on the cell concentration.
14. Sonicate 2x, for 2 s each time, at an amplitude of 40-50.  
**NOTE:** The cells can be kept at this stage at 4 °C for a few days.
15. Pipette 1.7 µL of the cells onto a glass microscope slide and cover with a clean coverslip.
16. Immediately observe under a fluorescence microscope with DAPI and TexasRed or Cy3 filters.

## Representative Results

To determine the S-phase duration and, more broadly, the duration of G<sub>1</sub> and G<sub>2</sub> + M (protocol step 1.1), *S. cerevisiae* W303 wild-type cells (WT, **Table 1**) were grown asynchronously in SC medium for 7 h. Every hour, the

cell concentration was monitored to determine the doubling time (**Figure 2B**). In these growth conditions, the calculated doubling time was  $120 \text{ min} \pm 13 \text{ min}$  at  $25 \text{ }^\circ\text{C}$  (**Table 2**). When the cells were in the exponential phase ( $2 \times 10^6$ - $5 \times 10^6$  cells/mL), an aliquot of cells was pulse-labeled with EdU ( $10 \text{ } \mu\text{M}$ ) for 5 min to single out the cells in the S phase and determine the percentage of cells that were in the G<sub>1</sub>, S, and G<sub>2</sub> + M phases. Three populations of cells were observed in a bivariate EdU-PI cytometer analysis (**Figure 1B**). The discrimination between the EdU-negative and EdU-positive populations was made using a control experiment in which the cells were not pulse-labeled with EdU but the Click reaction was carried out (**Figure 1C**). The two EdU-negative populations in the bottom-left and the bottom-right areas that differed in PI intensity two-fold corresponded to G<sub>1</sub> and G<sub>2</sub> + M, respectively (**Figure 1B,C**). Therefore, the upper population (with an intensity  $>1 \times 10^4$ - $2 \times 10^4$ ) corresponded to the EdU-positive cells that were in the S phase at the time of the pulse (**Figure 1B**). Hence,  $27\% \pm 5\%$  of the cell population was in the G<sub>1</sub> phase,  $29\% \pm 3\%$  was in the S phase, and  $44\% \pm 2\%$  was in G<sub>2</sub> + M. As the doubling time was  $120 \text{ min} \pm 13 \text{ min}$  in these conditions, we extrapolated that the G<sub>1</sub>, S, and G<sub>2</sub> + M phases lasted  $32 \text{ min} \pm 4 \text{ min}$ ,  $35 \text{ min} \pm 6 \text{ min}$ , and  $53 \text{ min} \pm 7 \text{ min}$ , respectively, at  $25 \text{ }^\circ\text{C}$  (**Table 2** and **Table 3**).

Next, we aimed to validate this method and show that it is sensitive enough to identify mutants with DNA replication defects that have been overlooked so far. We reasoned that tunable loss-of-function alleles of the factors involved in DNA replication would be ideal validation controls. Hence, we used a yeast strain containing a temperature-sensitive *cdc6-1* mutant (**Table 1**)<sup>11</sup>. Cdc6 is an essential licensing factor that is expressed in late M and G<sub>1</sub> to assemble prereplication complexes (preRC) on ORC-bound chromosome sites that may later be used as replication origins. Therefore, at

a permissive temperature, its S-phase duration should be the same as that of the WT, while at a restrictive temperature, no DNA replication should occur as no origin is licensed<sup>12</sup>. However, at a semi-permissive temperature, where fewer origins are licensed but there are enough to confer cell viability (our unpublished data; Barba Tena et al., in preparation), we anticipated different durations for each phase. As expected, based on drop tests, the *cdc6-1* cells grew the same as WT cells at a permissive temperature (i.e.,  $25 \text{ }^\circ\text{C}$ , **Figure 2A**), displaying the same doubling time (**Figure 2B** and **Table 2**), but were dead at or above  $34 \text{ }^\circ\text{C}$  (**Figure 2A**). Of interest, at a semi-permissive temperature (i.e.,  $28 \text{ }^\circ\text{C}$ ), *cdc6-1* was viable ( $28 \text{ }^\circ\text{C}$ , **Figure 2A**). However, the doubling time was longer than for WT (**Figure 2B** and **Table 2**), and the duration of each phase was different. Indeed, in *cdc6-1*, G<sub>1</sub> was slightly shorter ( $12 \text{ min} \pm 1 \text{ min}$  vs.  $16 \text{ min} \pm 2 \text{ min}$ ), while the S phase was slightly extended ( $34 \text{ min} \pm 4 \text{ min}$  vs.  $29 \text{ min} \pm 5 \text{ min}$ ), and the G<sub>2</sub> + M phase was significantly longer ( $77 \text{ min} \pm 4 \text{ min}$  vs.  $45 \text{ min} \pm 3 \text{ min}$ ) compared to WT (**Figure 2C,D** and **Table 3**). The S phase was, surprisingly, not extended very much, but the mean intensity of the EdU signal was decreased by 25% (**Figure 2C,D**), which is consistent with an S phase initiated from fewer origins. Moreover, while the EdU-positive WT cells were homogeneously distributed between the early (S1) and late S (S2) phases (**Figure 2C**, **Supplemental Figure S1A**, early [S1] and late S [S2] phases delimited with a vertical dashed line in the upper gate), 65% of the EdU-positive *cdc6-1* cells accumulated in the late S phase (**Figure 2D**, **Supplemental Figure S1B**). There was even no clear distinction between the S and G<sub>2</sub> + M populations (**Figure 2D**), suggesting that the cells struggled to complete the S phase before entering G<sub>2</sub> phase. Therefore, this method is suitable and sensitive to

identify mutants with defects in the S phase (duration and/or distribution) and in cell cycle phase duration.

A complementary method was devised to determine when cells start and finish their DNA replication and estimate the S-phase duration using synchronized cells (protocol step 1.2).

To this end, using  $\alpha$ -factor with synchronized cells in G<sub>1</sub>, cells were released in SC medium and collected every 5 min. The duration of the S phase may be about 25 min based on the time when the DNA content changed from 1C to 2C on the Sytox Green flow cytometer profile (**Figure 3A**). However, this estimation depends on when a significant cell fraction of the population has incorporated enough Sytox Green to be seen in the FACS profile. The early and late replication events cannot be detected with this method. To define accurately when the S phase starts and finishes and how long it lasts, S-phase cells were singled out from an aliquot of cells upon pulse-labeling with EdU (10  $\mu$ M) for 5 min every 5 min after the G<sub>1</sub> release. As expected, within the first 10 min after the release, all the cells were in the bottom-left area (i.e., in G<sub>1</sub>, **Figure 3B**, **Supplemental Figure S2**). Fifteen minutes after the release, a fraction of EdU-positive cells was already detected (compare the first two rows in **Supplemental Figure S2** and **Supplemental Figure S3**, EdU-treated and EdU-free cells, respectively), indicating that the S phase had started (**Figure 3C**). The progression through the S phase was seen by the cell cloud first moving upward and then rightward in the bivariate PI-EdU graph (**Figure 3D-F**). Finally, 35 min from the release, a fraction of cells was EdU-negative but with twice the amount of DNA, indicating that those cells had completed the S phase and were in the G<sub>2</sub> + M phase (**Figure 3G**). Thus, the S phase lasts 20 min in these conditions. Of note, despite the high synchrony observed with the overlay of DNA content detected with Sytox Green, suggesting that the S phase was over in

the whole population 40 min after the release, the bivariate analyses showed that some cells finished the S phase 60 min after the release and that the S phase was complete for the whole population 65 min after the release (**Figure 3H,I** and **Supplemental Figure S2**).

Additionally, the S phase and DNA synthesis can be monitored by microscopy. From each activated replication origin, DNA synthesis is carried out by two tethered replisomes, forming a nuclear replication focus that may be followed by microscopy by imaging a tagged version of a replication factor and/or operators array and their corresponding repressor fused to a fluorescent protein<sup>2,13</sup>. Alternatively, DNA synthesis can be detected by microscopy using thymidine analogues<sup>14,15</sup>. We used EdU to monitor the subnuclear DNA regions that undergo DNA synthesis. To this end, we pulse-labeled asynchronous WT and *cdc6-1* cells with EdU (10  $\mu$ M) for 3 min at 28 °C and imaged them after the Click reaction. We were expecting to detect variations in the EdU signal intensities depending on the DNA synthesis rate and on the cell progression in the cell cycle during the 3 min EdU pulse (i.e., cells spending the whole 3 min in the S phase will display a stronger signal than those entering or exiting S phase during the pulse). Accordingly, WT S-phase cells displayed an EdU signal in their nucleus that varied in intensity (**Figure 4A**). The S-phase duration can be readily extrapolated from this analysis. Indeed, it was determined from two biological replicates (at least 150 cells were counted), that 34%  $\pm$  3% and 38%  $\pm$  3% of WT and *cdc6-1* cells were EdU positive, respectively. As in these growth conditions, the doubling time was 90 min and 123 min for the WT and *cdc6-1* cells, respectively (**Table 2**), we extrapolated that the S phase lasted 31 min and 47 min, respectively. The former result is in line with that obtained from our FACS analyses (**Table 3**), indicating that

the detection of EdU-positive cells by microscopy allows the determination of the S-phase duration. Of note, the latter is higher than the S-phase duration extrapolated from our FACS analyses because there was no clear distinction between the S and G<sub>2</sub> + M populations (**Figure 2D**). The EdU foci were readily observed in the WT cells (**Figure 4B**) but were dimmer and fewer in the *cdc6-1* cells (**Figure 4C**). To rule out the possibility that the EdU signal intensity difference between the WT and *cdc6-1* cells depended on the step of the S phase, the intensity was quantified from synchronized cells. As expected, the mean EdU signal intensity was three-fold lower in the *cdc6-1* cells (**Figure 4D**), consistent with DNA

replication initiated from fewer replication origins. The EdU signal was restricted to the nucleus, colocalizing with a strong DAPI signal, and organized in globular patterns, consistent with the organization of DNA replication in nuclear regions or replication factories. Importantly, EdU was only detected in unbudded or small-budded cells and never present in cells with large buds, indicating that the WT yeast cells had finished replication by the time they entered mitosis. This method is, therefore, sensitive for visualizing DNA replication at a high spatial resolution, as well as for detecting and quantifying mild DNA replication defects.

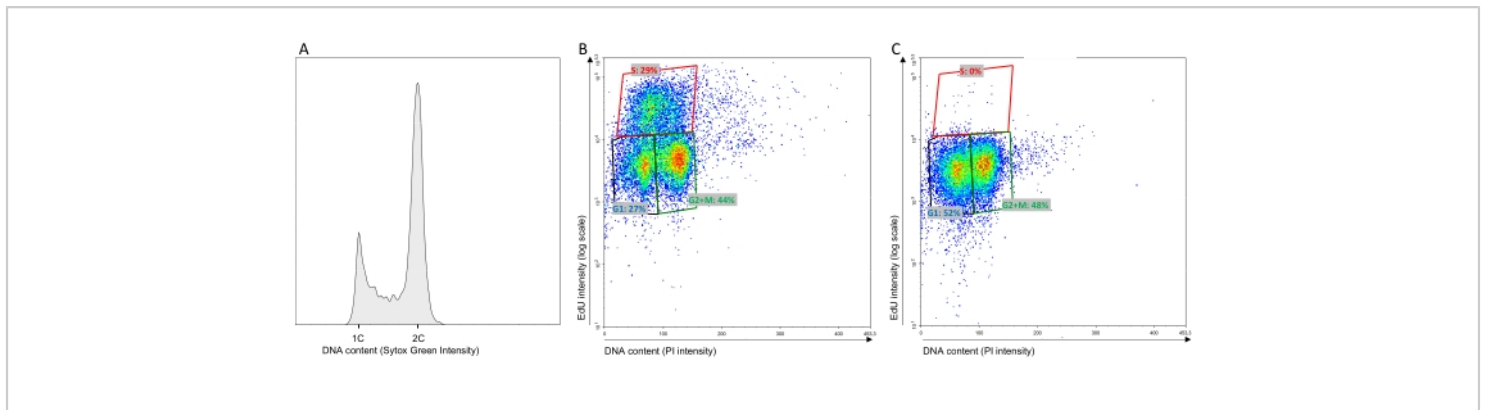


**Figure 1: Representative FACS analyses.** (A) Representative Sytox Green FACS analyses for WT cells grown at 25 °C. (B,C) Representative EdU-PI bivariate FACS analyses for WT cells grown at 25 °C and pulse-labeled for 5 min with EdU (10 μM) or 1 μL of DMSO. The polygons were the same in both analyses. C was used to delineate the EdU-negative from the EdU-positive cells (generally, the limit is set at an intensity  $>1 \times 10^4$ - $2 \times 10^4$ ). The top polygon gate delineated the EdU-positive cells (S-phase fraction). [Please click here to view a larger version of this figure.](#)

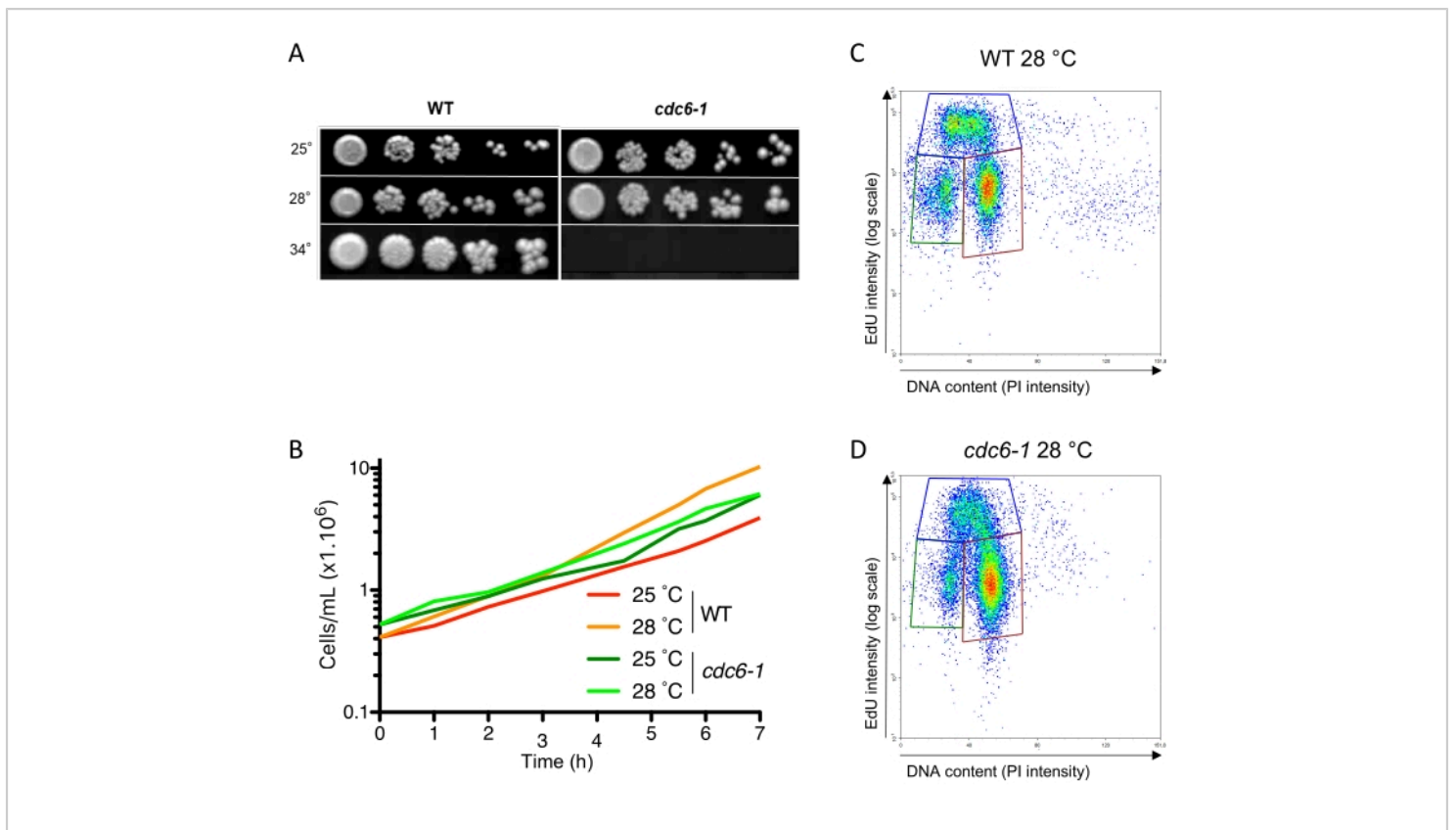


**Figure 2: Fraction of cells in the G<sub>1</sub>, S, and G<sub>2</sub> + M cell cycle phases in asynchronous cell populations. (A)** WT and *cdc6-1* strains were spotted at serial five-fold dilutions on rich medium and grown either at 25 °C, 28 °C, or 34 °C. **(B)** Population doubling time. Asynchronous WT and *cdc6-1* cells were grown at 25 °C or 28 °C, and the cell concentration was measured every hour for 7 h. **(C,D)** EdU-PI bivariate FACS analysis of WT and *cdc6-1* cells grown at 28 °C and pulse-labeled for 5 min with EdU (10 μM). Multiplying the population doubling time by the S-phase fraction provides the S-phase duration. The mean intensities of the EdU-positive and EdU-negative cells were calculated as the mean of the intensity of each value in the corresponding polygon. The mean intensities of the WT and *cdc6-1* EdU-negative cells (5,077 and 4,454, respectively) were normalized to 1. The mean intensities of the WT and *cdc6-1* EdU-positive cells (52,604 and 36,141, respectively) were divided by the normalization factor used for each strain. The obtained values were 10.4 and 8.1, respectively (i.e., a 25% decrease, as mentioned in the text). Abbreviations: WT = wild-type; EdU = 5-ethynyl-2'-deoxyuridine; FACS = fluorescence-activated cell sorting; PI = propidium iodide. [Please click here to view a larger version of this figure.](#)

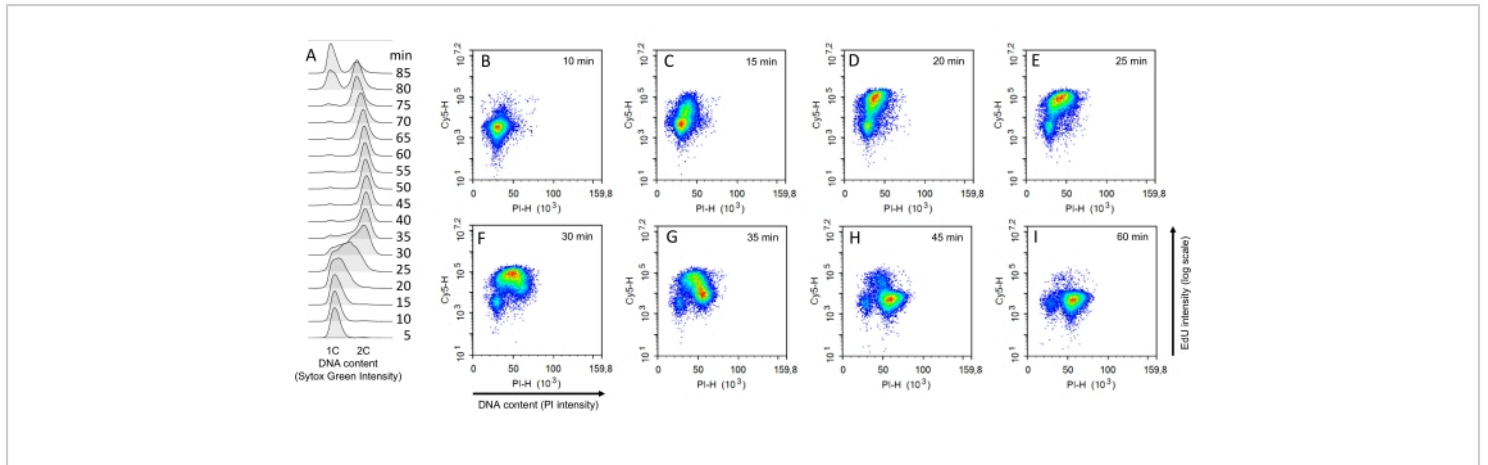


**Figure 3: Determination of the S-phase duration on synchronized cells.** (A) Time course analysis of the DNA content of WT cells after  $\alpha$ -factor release at 28 °C. The indicated time takes into account the duration of the EdU pulse (5 min). (B-I) EdU-PI bivariate FACS analyses for synchronized WT cells pulse-labeled for 5 min with EdU (10  $\mu$ M) and collected at the indicated times after the release from G<sub>1</sub> arrest. Abbreviations: WT = wild-type; EdU = 5-ethynyl-2'-deoxyuridine; FACS = fluorescence-activated cell sorting; PI = propidium iodide. [Please click here to view a larger version of this figure.](#)

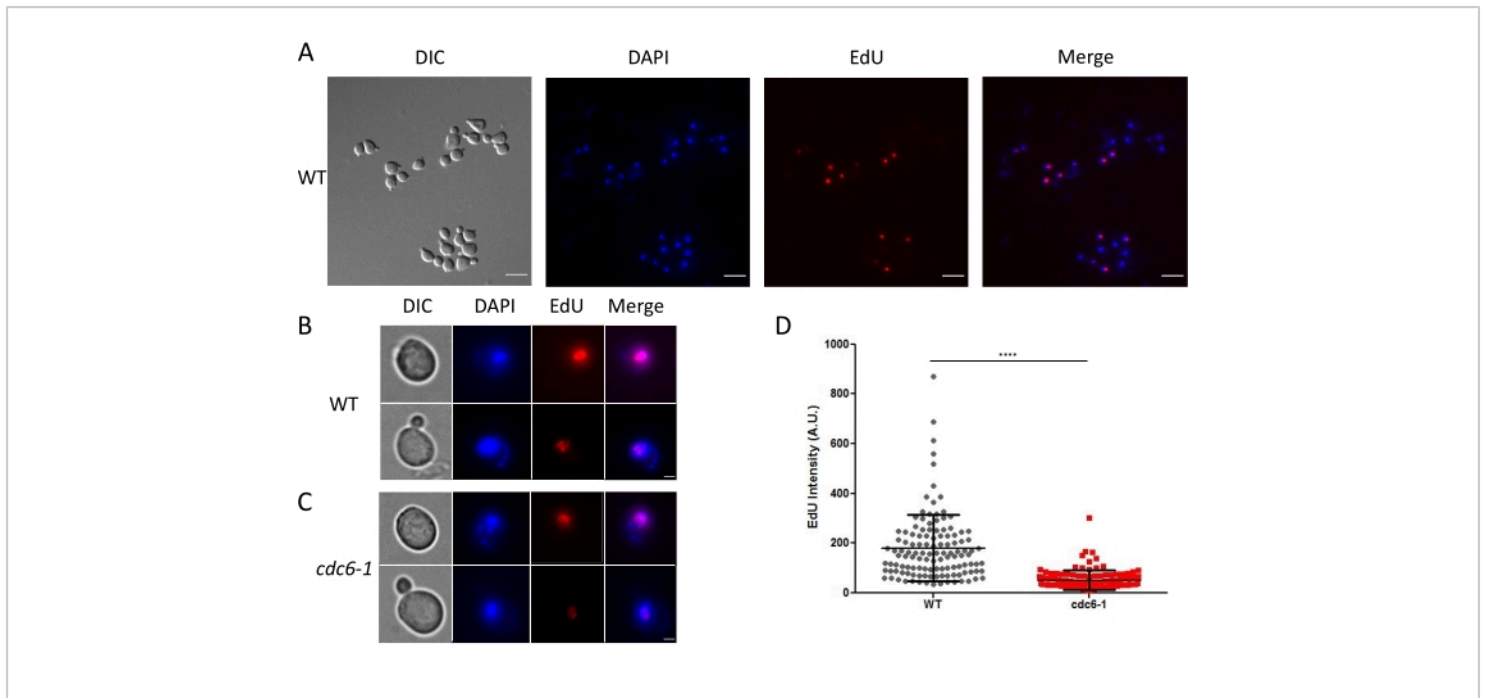


**Figure 4: EdU detection and quantification by microscopy.** Asynchronous WT and *cdc6-1* strains were grown for 2 h at 28 °C, and then pulse-labeled for 3 min with EdU (10  $\mu\text{M}$ ) and imaged by wide-field microscopy using adequate excitation/ emission filters. **(A)** Representative images from wide-field microscopy for WT and **(B,C)** individual cells for WT and *cdc6-1* visualized by DIC and stained with DAPI or for EdU, as indicated. The scale bars in **(A)** and **(B,C)** are 10  $\mu\text{m}$  and 2  $\mu\text{m}$ , respectively. **(D)** EdU intensity measurements on synchronous WT and *cdc6-1* cells grown at 28 °C 30 min after the release from G<sub>1</sub> arrest. The graph represents the pooling of three biological replicates (at least 50 cells were counted in each biological replicate). Mean  $\pm$  SD are displayed on the graph. An unpaired two-tailed t-test between WT and *cdc6-1* cells is indicated by \*\*\*\* ( $p < 0.0001$ ). Abbreviations: WT = wild-type; EdU = 5-ethynyl-2'-deoxyuridine; DIC = differential interference contrast; DAPI = 4',6-diamidino-2-phenylindole; A.U. = arbitrary units. [Please click here to view a larger version of this figure.](#)

Name	Genotype	Figures and tables
WT (E3087):	MATa, <i>ade2-1, trp1-1, can1-100, leu2-3,112, his3-11,15, RAD5, ura3::URA3/GPD-TK(5x), AUR1c::ADH-hENT1</i>	Fig.1, Fig.2A,B,C, Fig3, Fig.4A,B,D, Supp Fig.1,2,3 Tables2,3
<i>cdc6-1</i> (E5956):	MATa, <i>ade2-1, trp1-1, can1-100, leu2-3,112, his3-11,15, cdc6-1, RAD5, ura3::URA3/GPD-TK(5x), AUR1c::ADH-hENT1</i>	Fig.2A,B,D, Fig.4 C,D, Supp Fig.1, Tables2,3
TK+ (E1000):	MATa, <i>ade2-1, trp1-1, can1-100, leu2-3,112, his3-11,15, RAD5, ura3::URA3/GPD-TK(7x)</i>	Supp Fig.4
TK+ hENT+ (E2031):	MATa, <i>ade2-1, trp1-1, can1-100, leu2-3,112, his3-11,15, RAD5, ura3::URA3/GPD-TK(7x), AUR1c::ADH-hENT1</i>	Supp Fig.4
hENT+ (E2031):	MATa, <i>ade2-1, trp1-1, can1-100, leu2-3,112, his3-11,15, RAD5, AUR1c::ADH-hENT1, RAD52-GFP, URA3::mCherry-TUB1</i>	Supp Fig.4
<i>cdc6-1</i> TK+ hENT+ (E3968):	MATa, <i>ade2-1, trp1-1, can1-100, leu2-3,112, his3-11,15, cdc6-1, RAD5, ura3::URA3/GPD-TK(7x), AUR1c::ADH-hENT1</i>	Supp Fig.4
W303-1A (E001):	MATa, <i>ade2-1, trp1-1, can1-100, leu2-3,112, his3-11,15, RAD5, ura3-1</i>	Supp Fig.4

**Table 1: List of the strains used in this study.**

	WT		<i>cdc6-1</i>	
	25 °C	28 °C	25 °C	28 °C
Doubling time (min)	120	90	118	123
SD	± 13 min	± 3 min	± 10 min	± 6 min

**Table 2: Mean doubling times of WT and *cdc6-1* strains grown at 25 °C and 28 °C.** The doubling times were calculated from three biological replicates (four technical replicates for each biological replicate) using the following formula:  $\Delta t \times \ln(2) / \ln(C_f/C_i)$ , where  $C_f$  and  $C_i$  correspond to the final and initial cell concentrations, respectively, and  $\Delta t$  corresponds to the difference in minutes between  $t_f$  and  $t_i$ , when  $C_f$  and  $C_i$  were measured, respectively.

	WT				<i>cdc6-1</i>			
	25 °C		28 °C		25 °C		28 °C	
	Percent	Duration (min)	Percent	Duration (min)	Percent	Duration (min)	Percent	Duration (min)
G <sub>1</sub>	27	32	18	16	13	16	10	12
S	29	35	32	29	28	34	28	34
G <sub>2</sub> +M	44	53	50	45	59	71	62	77
SD G <sub>1</sub>	±5	±4	±3	±2	±2	±1	±1	±1
SD S	±3	±6	±5	±5	±5	±7	±4	±4
SD G <sub>2</sub> +M	±2	±7	±4	±3	±4	±4	±6	±4

**Table 3: Mean fractions of cells and duration of the G<sub>1</sub>, S, and G<sub>2</sub> + M phases in WT and *cdc6-1* cells grown at 25 °C and 28 °C.** The fractions of cells were determined from three biological replicates (two technical replicates for each biological replicate). The differences in G<sub>1</sub>, S, and G<sub>2</sub> + M duration between the WT and *cdc6-1* cells grown at 28 °C were statistically significant (unpaired two-tailed t-test,  $p < 0.1$ ).

**Supplemental Figure S1: Fraction of cells in the early and late S phases in WT and *cdc6-1* cells grown at 28 °C.** Two identical polygons named S1 and S2 for the early and late S phases, respectively, were drawn in the fraction of EdU-positive cells to split it into two halves on the EdU-PI bivariate FACS analyses for (A) WT cells grown at 28 °C and (B) *cdc6-1* cells grown at 28 °C. [Please click here to download this File.](#)

**Supplemental Figure S2: Cell cycle progression of EdU pulse-labeled cells after release from G<sub>1</sub> arrest visualized by EdU-PI bivariate FACS.** An aliquot of cells was pulse-labeled for 5 min with 10 μM EdU every 5 min after release from α-factor arrest at 28 °C and until 80 min, as indicated. Abbreviations: EdU = 5-ethynyl-2'-deoxyuridine; FACS =

fluorescence-activated cell sorting; PI = propidium iodide. [Please click here to download this File.](#)

**Supplemental Figure S3: Cell cycle progression of DMSO-treated cells after release from G<sub>1</sub> arrest visualized by EdU-PI bivariate FACS.** This is the same as Supplemental Figure 2, but the cells were incubated for 5 min with 1 μL DMSO (dimethyl sulfoxide). [Please click here to download this File.](#)

**Supplemental Figure S4: BrdU and EdU toxicity in TK hENT1 yeast cells.** Cells of the indicated genotype were spotted in five-fold serial dilutions on YPD plates containing increasing concentrations of BrdU or EdU and grown for 40 h at 30 °C. Abbreviations: DMSO = dimethyl sulfoxide; BrdU = bromodeoxyuridine; Edu = 5-ethynyl-2'-deoxyuridine; TK =

thymidine kinase; hENT1 = human equilibrative nucleoside transporter. [Please click here to download this File.](#)

## Discussion

Yeast is a prime model organism for cell cycle studies, yet the characterization of its S phase has long been hampered by its inability to incorporate exogenous nucleosides, such as BrdU, which are used as tracers of DNA replication. Equipping yeast with a high expression of herpes simplex thymidine kinase (TK) and the addition of a human nucleoside transporter (hENT) has largely solved this problem<sup>15,16</sup>. EdU is more versatile than BrdU as its detection with small fluorescent azide and Click chemistry is amenable to permeabilized yeast cells and FACS analysis, unlike anti-BrdU antibodies<sup>17</sup>. Here, we optimized the conditions of EdU labeling and detection in this TK-hENT1 strain and showed that previously undetected replication defects can be quantified using this protocol by FACS or microscopy.

Studying a biological mechanism using tools that may interfere with the same mechanism is a common issue in biology. As EdU has a known cytotoxic effect, we searched for EdU concentrations that are not toxic in chronic exposure to the engineered TK-hENT1 strain and found 10  $\mu\text{M}$  to be a suitable dose. TK-hENT1 cells fail to proliferate at 25  $\mu\text{M}$  EdU, while TK-alone or hENT1-alone cells easily withstand 100  $\mu\text{M}$  EdU (**Supplemental Figure S4**). Although yeast cells are considerably more sensitive to EdU than BrdU, we found that proliferation decreased only after the second cell cycle after EdU exposure, suggesting that it needs to be incorporated on both strands to impact cell proliferation (data not shown). To remain on the safe side, we used 10  $\mu\text{M}$  EdU throughout this protocol, with short pulses only (3 min for microscopy; 5

min for FACS), and found this was suitable for good detection using this optimized protocol.

Subtle defects in DNA replication may have a strong impact on chromosome rearrangements<sup>4</sup>. Therefore, the development of techniques and protocols capable of detecting these subtle defects is key for uncovering the etiology of chromosomal aberrations. Here, we show that this optimized protocol of EdU incorporation and detection can measure up to a three-fold reduction in signal intensity (**Figure 2** and **Figure 4**), indicating that the rate of DNA synthesis is reduced in temperature-sensitive *cdc6-1* cells grown at 28 °C, which, as of yet, show no defects on plate viability assays (**Figure 2A**). This protocol of EdU incorporation and quantification can, thus, be used to screen other mutants for which replication defects are not suspected initially. Additionally, it may be useful to detect mitotic DNA synthesis (MiDAS), meiotic recombination-dependent DNA synthesis, or other long-tract DNA synthesis.

One drawback is that EdU detection can be performed on fixed cells only, precluding live analysis as with PCNA-GFP or other fluorescent readouts of DNA replication, which suffer themselves from the high phototoxicity of the laser beams used for imaging. Growing cells in a synthetic medium is crucial for best detection, as YPD remnants appear to significantly quench the Click reaction. Interestingly, singling out the S-phase cells using bivariate EdU-PI FACS analysis on synchronized populations allows the estimation of the duration of the S phase to 20 min in single cells (**Figure 3**, **Supplemental Figure S2**, and **Supplemental Figure S3**). However, even when synchrony after  $\alpha$ -factor release appears as near-perfect as in classical Sytox Green FACS analysis (**Figure 3A**), it becomes clear from bivariate EdU-

PI FACS analysis that cells enter the S phase relatively asynchronously (**Figure 3B-I**).

Here, we describe three methods to determine S-phase duration using flow cytometry and microscopy on synchronous and asynchronous cells at both the single-cell and population levels. The average S-phase durations determined in asynchronous WT cells at the population level are similar using flow cytometry and microscopy, at 29 min and 31 min, respectively, whereas our synchronized single cell-based approach shows that the duration can be as short as 20 min (**Figure 2, Figure 3, Figure 4, and Table 3**). The discrepancy between these values is surprising but can be readily explained. Indeed, with our single cell-based approach, S-phase duration was determined based on the earliest events (i.e., the first cells entering and exiting the S phase, **Figure 3C,G**), but it does not imply that the S phase lasts 20 min in every cell within a population. These data would support the unexpected notion that there is a certain level of heterogeneity in S-phase duration between cells.

Improved protocols or new techniques can overthrow long-standing dogmas or novel ideas. There are three that these data challenge. First, it is believed that DNA synthesis is concomitant with bud emergence in *S. cerevisiae*. **Figure 4A-C** shows that EdU staining is strongest in unbudded and small-budded cells, despite the 3 min labeling lag, indicating that the S phase clearly starts before budding, as shown previously<sup>16</sup>. Second, it is reported that yeast cells do not have a G<sub>2</sub> phase, with mitotic spindles forming at the same time as DNA synthesis. The very short pulses combined with sensitive EdU detection by FACS (**Figure 3, Supplemental Figure S2, and Supplemental Figure S3**) or microscopy (**Figure 4**) allows for determining precisely when the S phase begins and finishes in single cells. By doing so, we found

that bulk DNA synthesis finishes 40 min after  $\alpha$ -factor release (**Figure 3, Supplemental Figure S2, and Supplemental Figure S3**), while short mitotic spindles only form 20 min later (data not shown). We conclude that yeast cells have a G<sub>2</sub> phase. Third, it was proposed recently that up to 30% of yeast cells complete DNA synthesis in anaphase-telophase<sup>18</sup>. Using this optimized protocol, we did not detect EdU incorporation in cells displaying an anaphase/telophase spindle (data not shown), but we cannot rule out that this second wave of DNA synthesis is below the used threshold of detection. Given the strong signal/noise ratio, we consider the latter option unlikely.

## Disclosures

The authors declare that they have no competing financial interests.

## Acknowledgments

The authors wish to acknowledge Agence Nationale de la Recherche (ANR) and Association pour la Recherche sur le Cancer (ARC) for the PhD fellowships to J.d.D.B.T. and the Agence Nationale pour la Recherche (ANR) for financial support (grant ANR-18-CE12-0018-01). Cytometry and microscopy were performed at the Montpellier MRI BioCampus imaging facility.

## References

1. Bell, S. P., Labib, K. Chromosome duplication in *Saccharomyces cerevisiae*. *Genetics*. **203** (3), 1027-1067 (2016).
2. Kitamura, E., Blow, J. J., Tanaka, T. U. Live-cell imaging reveals replication of individual replicons in eukaryotic replication factories. *Cell*. **125** (7), 1297-1308 (2006).

3. Marston, A. L. Chromosome segregation in budding yeast: Sister chromatid cohesion and related mechanisms. *Genetics*. **196** (1), 31-63 (2014).
4. Lengronne, A., Schwob, E. The yeast CDK inhibitor Sic1 prevents genomic instability by promoting replication origin licensing in late G1. *Molecular Cell*. **9** (5), 1067-1078 (2002).
5. Tanaka, S., Diffley, J. F. X. Deregulated G<sub>1</sub>-cyclin expression induces genomic instability by preventing efficient pre-RC formation. *Genes & Development*. **16** (20), 2639-2649 (2002).
6. Teixeira, L. K. et al. Cyclin E deregulation promotes loss of specific genomic regions. *Current Biology*. **25** (10), 1327-1333 (2015).
7. Slater, M. L., Sharrow, S. O., Gart, J. J. Cell cycle of *Saccharomyces cerevisiae* in populations growing at different rates. *Proceedings of the National Academy of Sciences of the United States of America*. **74** (9), 3850-3854 (1977).
8. McNeil, J. B., Friesen, J. D. Expression of the herpes simplex virus thymidine kinase gene in *Saccharomyces cerevisiae*. *Molecular and General Genetics*. **184** (3), 386-393 (1981).
9. Vernis, L. Reconstitution of an efficient thymidine salvage pathway in *Saccharomyces cerevisiae*. *Nucleic Acids Research*. **31** (19), e120 (2003).
10. Salic, A., Mitchison, T. J. A chemical method for fast and sensitive detection of DNA synthesis *in vivo*. *Proceedings of the National Academy of Sciences of the United States of America*. **105** (7), 2415-2420 (2008).
11. Bruschi, C. V., McMillan, J. N., Coglievina, M., Esposito, M. S. The genomic instability of yeast *cdc6-1/cdc6-1* mutants involves chromosome structure and recombination. *Molecular and General Genetics*. **249** (1), 8-18 (1995).
12. Feng, L., Wang, B., Wu, L., Jong, A. Loss control of Mcm5 interaction with chromatin in *cdc6-1* mutated in CDC-NTP motif. *DNA and Cell Biology*. **19** (7), 447-457 (2000).
13. Saner, N. et al. Stochastic association of neighboring replicons creates replication factories in budding yeast. *Journal of Cell Biology*. **202** (7), 1001-1012 (2013).
14. Pasero, P., Braguglia, D., Gasser, S. M. ORC-dependent and origin-specific initiation of DNA replication at defined foci in isolated yeast nuclei. *Genes & Development*. **11** (12), 1504-1518 (1997).
15. Lengronne, A. Monitoring S phase progression globally and locally using BrdU incorporation in TK<sup>+</sup> yeast strains. *Nucleic Acids Research*. **29** (7), 1433-1442 (2001).
16. Magiera, M. M., Gueydon, E., Schwob, E. DNA replication and spindle checkpoints cooperate during S phase to delay mitosis and preserve genome integrity. *The Journal of Cell Biology*. **204** (2), 165-175 (2014).
17. Talarek, N., Petit, J., Gueydon, E., Schwob, E. EdU incorporation for FACS and microscopy analysis of DNA replication in budding yeast. *Methods in Molecular Biology*. **1300**, 105-112 (2015).
18. Ivanova, T. et al. Budding yeast complete DNA synthesis after chromosome segregation begins. *Nature Communications*. **11** (1), 2267 (2020).